Mixing and Compaction Temperatures of Asphalt Binders in Hot-Mix Asphalt

DETAILS

147 pages | | PAPERBACK

ISBN 978-0-309-11825-5 | DOI 10.17226/14367

AUTHORS

Donald E Watson; Randy C West; Pamela A Turner; John R Casola; Transportation Research Board

NATIONAL COOPERATIVE HIGHWAY RESEARCH PROGRAM

NCHRP REPORT 648

Mixing and Compaction Temperatures of Asphalt Binders in Hot-Mix Asphalt

Randy C. West
Donald E. Watson
Pamela A. Turner
National Center for Asphalt Technology
Auburn, AL

John R. Casola
Malvern Instruments Inc.
Westborough, MA

Subscriber Categories
Materials

Research sponsored by the American Association of State Highway and Transportation Officials
in cooperation with the Federal Highway Administration

TRANSPORTATION RESEARCH BOARD

WASHINGTON, D.C.
2010
www.TRB.org

NATIONAL COOPERATIVE HIGHWAY RESEARCH PROGRAM

Systematic, well-designed research provides the most effective approach to the solution of many problems facing highway administrators and engineers. Often, highway problems are of local interest and can best be studied by highway departments individually or in cooperation with their state universities and others. However, the accelerating growth of highway transportation develops increasingly complex problems of wide interest to highway authorities. These problems are best studied through a coordinated program of cooperative research.

In recognition of these needs, the highway administrators of the American Association of State Highway and Transportation Officials initiated in 1962 an objective national highway research program employing modern scientific techniques. This program is supported on a continuing basis by funds from participating member states of the Association and it receives the full cooperation and support of the Federal Highway Administration, United States Department of Transportation.

The Transportation Research Board of the National Academies was requested by the Association to administer the research program because of the Board's recognized objectivity and understanding of modern research practices. The Board is uniquely suited for this purpose as it maintains an extensive committee structure from which authorities on any highway transportation subject may be drawn; it possesses avenues of communications and cooperation with federal, state and local governmental agencies, universities, and industry; its relationship to the National Research Council is an insurance of objectivity; it maintains a full-time research correlation staff of specialists in highway transportation matters to bring the findings of research directly to those who are in a position to use them.

The program is developed on the basis of research needs identified by chief administrators of the highway and transportation departments and by committees of AASHTO. Each year, specific areas of research needs to be included in the program are proposed to the National Research Council and the Board by the American Association of State Highway and Transportation Officials. Research projects to fulfill these needs are defined by the Board, and qualified research agencies are selected from those that have submitted proposals. Administration and surveillance of research contracts are the responsibilities of the National Research Council and the Transportation Research Board.

The needs for highway research are many, and the National Cooperative Highway Research Program can make significant contributions to the solution of highway transportation problems of mutual concern to many responsible groups. The program, however, is intended to complement rather than to substitute for or duplicate other highway research programs.

NCHRP REPORT 648

Project 9-39
ISSN 0077-5614
ISBN 978-0-309-11825-5
Library of Congress Control Number 2010923478

COPYRIGHT INFORMATION

NOTICE

The project that is the subject of this report was a part of the National Cooperative Highway Research Program conducted by the Transportation Research Board with the approval of the Governing Board of the National Research Council. Such approval reflects the Governing Board's judgment that the program concerned is of national importance and appropriate with respect to both the purposes and resources of the National Research Council.

The members of the technical committee selected to monitor this project and to review this report were chosen for recognized scholarly competence and with due consideration for the balance of disciplines appropriate to the project. The opinions and conclusions expressed or implied are those of the research agency that performed the research, and, while they have been accepted as appropriate by the technical committee, they are not necessarily those of the Transportation Research Board, the National Research Council, the American Association of State Highway and Transportation Officials, or the Federal Highway Administration, U.S. Department of Transportation.

Each report is reviewed and accepted for publication by the technical committee according to procedures established and monitored by the Transportation Research Board Executive Committee and the Governing Board of the National Research Council.

The Transportation Research Board of the National Academies, the National Research Council, the Federal Highway Administration, the American Association of State Highway and Transportation Officials, and the individual states participating in the National Cooperative Highway Research Program do not endorse products or manufacturers. Trade or manufacturers' names appear herein solely because they are considered essential to the object of this report.

Published reports of the

NATIONAL COOPERATIVE HIGHWAY RESEARCH PROGRAM

are available from:

Transportation Research Board
Business Office
500 Fifth Street, NW
Washington, DC 20001

and can be ordered through the Internet at:

http://www.national-academies.org/trb/bookstore

Printed in the United States of America

THE NATIONAL ACADEMIES
Advisers to the Nation on Science, Engineering, and Medicine

The **National Academy of Sciences** is a private, nonprofit, self-perpetuating society of distinguished scholars engaged in scientific and engineering research, dedicated to the furtherance of science and technology and to their use for the general welfare. On the authority of the charter granted to it by the Congress in 1863, the Academy has a mandate that requires it to advise the federal government on scientific and technical matters. Dr. Ralph J. Cicerone is president of the National Academy of Sciences.

The **National Academy of Engineering** was established in 1964, under the charter of the National Academy of Sciences, as a parallel organization of outstanding engineers. It is autonomous in its administration and in the selection of its members, sharing with the National Academy of Sciences the responsibility for advising the federal government. The National Academy of Engineering also sponsors engineering programs aimed at meeting national needs, encourages education and research, and recognizes the superior achievements of engineers. Dr. Charles M. Vest is president of the National Academy of Engineering.

The **Institute of Medicine** was established in 1970 by the National Academy of Sciences to secure the services of eminent members of appropriate professions in the examination of policy matters pertaining to the health of the public. The Institute acts under the responsibility given to the National Academy of Sciences by its congressional charter to be an adviser to the federal government and, on its own initiative, to identify issues of medical care, research, and education. Dr. Harvey V. Fineberg is president of the Institute of Medicine.

The **National Research Council** was organized by the National Academy of Sciences in 1916 to associate the broad community of science and technology with the Academy's purposes of furthering knowledge and advising the federal government. Functioning in accordance with general policies determined by the Academy, the Council has become the principal operating agency of both the National Academy of Sciences and the National Academy of Engineering in providing services to the government, the public, and the scientific and engineering communities. The Council is administered jointly by both the Academies and the Institute of Medicine. Dr. Ralph J. Cicerone and Dr. Charles M. Vest are chair and vice chair, respectively, of the National Research Council.

The **Transportation Research Board** is one of six major divisions of the National Research Council. The mission of the Transportation Research Board is to provide leadership in transportation innovation and progress through research and information exchange, conducted within a setting that is objective, interdisciplinary, and multimodal. The Board's varied activities annually engage about 7,000 engineers, scientists, and other transportation researchers and practitioners from the public and private sectors and academia, all of whom contribute their expertise in the public interest. The program is supported by state transportation departments, federal agencies including the component administrations of the U.S. Department of Transportation, and other organizations and individuals interested in the development of transportation. **www.TRB.org**

www.national-academies.org

COOPERATIVE RESEARCH PROGRAMS

CRP STAFF FOR NCHRP REPORT 648

Christopher W. Jenks, *Director, Cooperative Research Programs*
Crawford F. Jencks, *Deputy Director, Cooperative Research Programs*
Edward T. Harrigan, *Senior Program Officer*
Melanie Adcock, *Senior Program Assistant*
Eileen P. Delaney, *Director of Publications*
Margaret B. Hagood, *Editor*
Andréa Briere, *Editor*

NCHRP PROJECT 09-39 PANEL
Field of Materials and Construction—Area of Bituminous Materials

Rita B. Leahy, *Asphalt Pavement Association of California, Sacramento, CA* (Chair)
John H. Tenison, *AMEC Earth & Environmental, Albuquerque, NM*
Paul J. Hoelscher, *Texas DOT, Abilene, TX*
Gayle N. King, *GHK, Inc., The Woodlands, TX*
Michael W. Longshaw, *Kansas DOT, El Dorado, KS*
Louay N. Mohammad, *Louisiana State University, Baton Rouge, LA*
Allen H. Myers, *Kentucky Transportation Cabinet, Frankfort, KY*
Nelio J. Rodrigues, *Connecticut DOT, Rocky Hill, CT*
John D'Angelo, *FHWA Liaison*
Nelson H. Gibson, *FHWA Liaison*
Frederick Hejl, *TRB Liaison*

AUTHOR ACKNOWLEDGMENTS

The research reported herein was performed under NCHRP Project 9-39 by the National Center for Asphalt Technology, Auburn University. Randy C. West, Director, was the principal investigator and Donald E. Watson, Lead Research Engineer at the National Center for Asphalt Technology, was the co-principal investigator. John Casola, Product Sales Manager at Malvern Instruments, and Pamela Turner, Assistant Research Engineer at the National Center for Asphalt Technology, were key contributors to the research and preparation of this report. The authors thank Fred Mazzeo of Malvern Instruments for providing rheological testing and analysis and Saeed Maghsoodloo, Auburn University, for experimental design and statistical analysis. The authors thank Jason Moore and all of the staff of the National Center for Asphalt Technology who worked on this project. The authors thank the Federal Highway Administration Turner-Fairbank Highway Research Center for binder testing and the asphalt binder suppliers who provided materials and information for this project.

FOREWORD

By Edward Harrigan
Staff Officer
Transportation Research Board

This report identifies improved test methods for determining laboratory mixing and compaction temperatures of modified and unmodified asphalt binders. The report will be of immediate interest to materials engineers in state highway agencies and the hot-mix asphalt (HMA) construction industry.

The Asphalt Institute (AI) procedure for determining mixing and compaction temperatures of asphalt binders was developed for penetration- and viscosity-graded asphalt cements used in the United States until the 1990s. Since that time, the use of modified, performance-graded asphalt binders in HMA paving has increased significantly, especially on high-volume traffic routes. The AI procedure often requires heating of modified binders to unrealistically high temperatures that can potentially damage the asphalt binder. To overcome this problem, highway agencies usually rely on the modifier suppliers to recommend mixing and compaction temperatures, a circumstance that can produce mixed results.

The objective of this research was to identify or develop a simple, rapid, and accurate laboratory procedure—suitable for routine use—for determining the mixing and compaction temperatures of both unmodified and modified asphalt binder. The research was performed by the National Center for Asphalt Technology, Auburn University, Auburn, Alabama with the support of Malvern Instruments Inc., Westborough, Massachusetts.

In the course of the research, the project team evaluated existing and emerging methods to determine temperatures that will provide satisfactory aggregate coating during laboratory mixing and appropriate laboratory specimen compaction without degrading the asphalt binder and identified two improved, equally effective test methods. These tests, termed (1) the phase angle method and (2) the steady shear flow viscosity (SSFV) method, provide reasonable, consistent mixing and compaction temperatures that correlate well with the results of HMA coating, workability, and compactability tests for both binder types. The phase angle and SSFV measurements are made with the dynamic shear rheometer (DSR), already widely used in asphalt laboratories for measuring binder stiffnesses over a range of temperatures and frequencies.

This report includes four appendices as follows:

- Appendix A: Responses of Survey on Agency Specifications Regarding Mixing and Compaction Temperatures;
- Appendix B: Mix Design Data for Base Mix and Other Compaction Experiment Mixes;
- Appendix C: Draft AASHTO Standard for Steady Shear Flow and Phase Angle Methods; and
- Appendix D: Statistical Analyses of the Steady Shear Flow and Phase Angle Methods.

The draft standard methods of test are under consideration for possible adoption by the AASHTO Highway Subcommittee on Materials.

CONTENTS

SUMMARY

Mixing and Compaction Temperatures of Asphalt Binder in Hot-Mix Asphalt

Background

The use of modified asphalt binders in hot-mix asphalt has steadily increased over the past several decades. Modified asphalt binders currently make up over 20% of paving grade asphalt sales in the United States, and the percentage continues to grow. However, selecting appropriate temperatures for handling these binders has been an issue with the use of modified asphalt binders. The traditional method of determining appropriate mixing and compaction temperatures for an asphalt binder is based on relatively simple viscosity measurements of the asphalt. However, this method often yields excessively high temperatures for many modified binders that have caused concerns with degradation of the binder's properties and emission problems in laboratories during preparation of samples and during production and placement of asphalt mixtures in the field. In the absence of a reliable method for selecting mixing and compaction temperatures for modified asphalt binders, many agencies have written their specifications to simply allow the binder supplier to set an appropriate mixing temperature for each modified binder. In some cases, agencies or binder suppliers have based mixing and compaction temperature ranges on the Superpave® performance grades (PGs), and in other cases the mixing and compaction temperatures have been established based on field experience. Clearly, a standardized method or more formal process was needed for selecting mixing and compaction temperatures for asphalt mixtures.

Research Approach

The goal of this research was to identify or develop a simple, reliable, and accurate procedure for determining the mixing and compaction temperatures that is applicable for both modified and unmodified asphalt binders in hot-mix asphalt (HMA). An examination of available literature on the subject identified several possible methods for determining mixing and compaction temperatures. With the input from the project panel and the desire for this research to ultimately recommend a practical method for possible implementation, three candidate methods were selected for the laboratory evaluation. Each of the candidate methods was based only on measurements of binder properties using common equipment used in asphalt binder laboratories.

Candidate Method A, developed by Yildirim Soaimanian, and Kennedy in Texas, was based on proof that most modified binders exhibit shear thinning behavior. This method, referred to as High Shear Rate Viscosity, used measurements from a rotational viscometer at shear rates ranging from 0.1 1/s to 93 1/s at 135 and 165°C. The Cross-Williams model was used to extrapolate the measured shear rate versus viscosity data to the higher shear rate of 500 1/s. The extrapolated viscosity data were plotted on a conventional log viscosity versus

log temperature chart to obtain temperatures corresponding to the traditional viscosity criteria of 0.17 ± 0.02 Pa·s for mixing, and 0.28 ±0.03 Pa·s for compaction.

Candidate Method B, developed by Reinke, is called the Steady Shear Flow test. This method uses a Dynamic Shear Rheometer (DSR) with a 25-mm-diameter parallel plate geometry and a 500-micron gap. The viscosities of binders were measured in a constant shear mode over a range of shear stresses at temperatures ranging from 76 to 94°C. At higher shear stresses, around 500 Pa, viscosities of most modified binders approach a steady state. Using a log viscosity versus log temperature chart, viscosity results at 500 Pa shear were extrapolated to 180°C. The mixing temperature was selected at a viscosity of 0.17 ± 0.02 Pa·s, which is consistent with conventional practice. However, as recommended by Reinke, compaction temperature from the Steady Shear Flow method was selected at a viscosity of 0.35 ± 0.03 Pa·s.

Candidate Method C, developed by Casola, is referred to as the Phase Angle method, which is based on the observation that the Phase Angle from dynamic shear rheology is a binder consistency property that takes into account the visco-elastic nature of asphalt binders. This method uses a DSR with 25 mm parallel plate geometries and a 1-mm gap set up in oscillatory shear at angular frequencies from of 0.001 to 100 rad/s. The frequency sweep data is used to construct a Phase Angle versus frequency master curve at a reference temperature of 80°C. The binder's transition point from viscous behavior to viscoelastic behavior was represented by the Phase Angle of 86°. The frequency corresponding to this transition point was correlated to the temperatures where binders provide good aggregate coating during mixing and lubrication during compaction.

The research approach included two series of experiments. The first series involved tests with the candidate methods and other methods to assess emissions potential and binder degradation due to exposure of binders to high temperatures. Modified and unmodified binders used in the experiments were obtained from several binder suppliers across the United States to include a range of crude sources, refining processes, and modification systems. The second series of experiments were laboratory mixture tests to assess how temperatures affect the coating of aggregates during mixing, workability, compactability, and low temperature properties of asphalt mixtures with the different binders. The primary purpose of the mixture tests was to provide validation of the predicted mixing and compaction temperatures from the candidate methods. A few additional mixture test experiments also were conducted to evaluate how other factors affect coating and compactability results.

Findings

The High Shear Rate Viscosity method resulted in mixing temperatures for all of the modified binders well above 177°C, which are widely considered in the asphalt paving industry to be too high and likely to result in emissions problems. Results from the high shear rate viscosity method were very similar to the traditional equiviscous method and therefore provided no improvement to the current procedure.

The Steady Shear Flow method yielded mixing and compaction temperatures lower than those from the traditional equiviscous method for modified and unmodified binders. Temperature differences between the two methods were greater for modified binders, which confirmed shear thinning behavior for the modified binders. The Steady Shear Flow method also yielded lower mixing and compaction temperatures for the unmodified binders; in most cases, the mixing temperatures are more than 6°C lower than the equiviscous mixing temperatures. Correlation of the mixing temperatures from the Steady Shear Flow method with the binder producers' recommended mixing temperatures was reasonable, yielding a coefficient of determination (R^2) of 70.1%.

The Phase Angle method also resulted in lower mixing and compaction temperatures than did the equiviscous method for modified binders. However, for unmodified binders, some of mixing and compaction temperatures from the Phase Angle method were lower and some were higher than from the equiviscous method. The coefficient of determination for correlation of the Phase Angle results with the binder producers' recommended temperatures was 58.2%, which is lower than for the Steady Shear Flow method. However, the regression equation between the Phase Angle method and producers' recommendations was closer to the line of equality than for the Steady Shear Flow method.

Results from the smoke and emissions test (SEP) showed that emissions increased with higher temperatures for some binders much more than for others. However, with the limited set of binders from different crudes, different refineries, different modification types, and different grades, it was not possible to identify what factors may cause some binders to smoke more than others. Test results for various binder properties before and after the SEP test did show that binders increased in stiffness with exposure to higher temperatures, but there was no strong evidence of polymer degradation for the modified binders.

Although the results of the mixture coating tests at different temperatures generally followed expected trends for each binder, using the data to estimate mixing temperatures to achieve specific coating percentages did not always provide reasonable results. Therefore, the validation of the candidate methods with mixture coating test results by direct correlation yielded poor goodness-of-fit statistics, even when a few outlier coating test results were removed from the dataset. The same was true for the results of the workability tests and their correlations with the results from the Steady Shear Flow and Phase Angle methods. Compaction tests with the binders over a range of four temperatures did indicate that both the binder and temperature had significant effects on specimen density at 25 gyrations. A separate experiment showed that a mixture's aggregate components have a greater affect on compaction behavior than do the binder characteristics. Maximum shear ratio was not a useful indicator of compactability. Reasonable correlation statistics were obtained for regressions between the compaction temperatures from the Steady Shear Flow and the Phase Angle method and the predicted compaction temperatures to reach a set level of density from the lab experiments.

Compaction temperatures also significantly affected the low temperature properties of mixtures. Higher mixing temperatures stiffened mixtures (reduced the creep compliance), which will reduce the ability of the pavement to dissipate thermal stresses. The stiffening effect was more evident for binders with lower PG grades.

Conclusions

Both the Steady Shear Flow method and the Phase Angle method provide lower mixing and compaction temperatures for modified asphalt binders compared with the traditional equiviscous method. Both methods also appear to provide reasonable temperatures for mixing and compaction temperatures for a variety of modified and unmodified asphalt binders being used across the United States.

An advantage of both methods is that they can be set up and performed using existing standard DSR equipment used in most asphalt binder labs in the United States. Limitations of both methods include the restrictions normally applicable to parallel plate DSR testing, such as the binder test sample, must be homogenous and free of particulate matter (e.g., ground rubber particles) that may interfere with or distort the rheological response of the instrument. Correlations of the mixing and compaction temperatures with laboratory coating, workability, and compactability were similar for both methods. Although the Steady Shear

Flow and Phase Angle methods are based on different binder properties, both methods use a standard DSR and common parallel plate geometries for testing of the binder. Therefore, they have some practical limitations including the test temperatures at which the properties are measured and particulate matter begins to have an effect. Results from the two methods are well correlated. Differences in results exist primarily for unmodified binders where the Steady Shear Flow method generally yields lower mixing and compaction temperatures.

No links were evident between opacity (i.e., smoking) of a binder and its grade, crude source, or whether the binder was modified. Performance grading of the binders after SEP tests showed that the critical high and critical low temperatures increased slightly with higher SEP temperatures. However, there was no evidence of degradation of the binders due to exposure at elevated temperatures in the SEP test. The lack of evidence of degradation does not mean that it is not possible; rather, it may mean that the conditions in the SEP test are not sufficiently severe to cause breakdown of polymer modifiers. Although the SEP test may have value in identifying binders with opacity problems, it does not appear that it is suitable for establishing maximum mixing temperatures.

Recommendations

Both the Phase Angle method and the Steady Shear Flow method are recommended for further evaluation. Draft AASHTO format procedures for both methods are provided. Mixing and compaction temperatures determined by these methods are only applicable to the laboratory setting for mix design work, quality assurance testing of HMA, and fabricating HMA samples for laboratory performance tests. The mixing and compaction temperatures determined by these methods should *not* be used to control plant production or pavement construction temperatures. Greater latitude in mixing temperatures is necessary in the field to allow for different ambient conditions, haul distances, and other mix characteristics that affect coating and compactability.

Four additional steps are recommended to validate, refine, and assist the implementation of the Steady Shear Flow and/or Phase Angle methods:

1. Independent validation of the methods by asphalt suppliers with a much broader range of binders;
2. Refinement of the methods by developing standard DSR control and computer analysis routines, possibly eliminating steps to reduce testing times, and evaluation of alternate instrument geometries to avoid issues with temperatures and some filled binders;
3. Interlaboratory studies to establish precision information for the procedures; and
4. Training on the method(s) for full implementation by the asphalt paving industry.

CHAPTER 1

Background

Introduction

The use of modified asphalt binders in hot-mix asphalt (HMA) has steadily increased over the past several decades. The Association of Modified Asphalt Producers (AMAP) estimates that modified asphalt binders currently make up approximately 20% of paving grade asphalt sales (*1*), and the quantity of modified binders used in HMA is increasing at an annual rate of about 4%. However, a suitable method for determining mixing and compaction temperatures for these binders has not been established. The traditional equiviscous principle used to determine mixing and compaction temperatures was developed using unmodified binders having Newtonian behavior. However, using this method with many modified asphalt binders often results in excessively high mixing temperatures that have caused concerns with emission problems and degradation of the binder's properties.

The objective of this research was to identify or develop a simple, reliable, and accurate procedure for determining the mixing and compaction temperatures applicable for modified and unmodified asphalt binders in HMA. The research project consisted of six tasks:

- Task 1-Literature Search,
- Task 2-Design of Experiments,
- Task 3-Interim Report,
- Task 4-Conduct Experiments and Analyze Results,
- Task 5-Prepare Procedure in AASHTO Format and Field Validation Plan, and
- Task 6-Final Report.

Literature Search

A review of available literature was conducted on the subject of mixing and compaction temperatures for asphalt mixtures. The purpose of the literature review was to gain an understanding of the historical development of the current method, identify shortcomings of this method, and identify potential new methods that may be evaluated or explored. A survey of state highway agencies and materials suppliers also was conducted to evaluate the current practices for determining mixing and compaction in the United States and abroad.

The literature review is organized into the following topics:

- A note on the units of viscosity.
- Background on the development of mixing and compaction temperature criteria.
- Effect of temperature on degradation of asphalt binders.
- Mixing and compaction temperatures for modified asphalts.
- Survey on current practices for selecting mixing and compaction temperatures.
- Recent research on proposed new methods for determining mixing and compaction temperatures.
- Shear rates during mixing and compaction.
- Summary of key findings.

A Note on Units of Viscosity

Viscosity may be expressed in several different ways, and this often leads to some confusion. One of the early methods for measuring asphalt viscosity was the Saybolt Furol viscosity test, which measured the time for a given volume of asphalt to flow through an orifice of specific dimensions. Thus the results of this test were reported as seconds Saybolt Furol (SSF).

Another expression of viscosity is kinematic viscosity, which is actually the viscosity divided by the material's density. The most commonly used unit of kinematic viscosity is the centistokes, which is written as mm^2/s. The original equiviscous criteria in AASHTO T 312 used ranges of kinematic viscosity to define mixing and compaction temperatures. These criteria were 170 ± 20 mm^2/s and 280 ± 30 mm^2/s for mixing and compaction, respectively.

The measurement of viscosity using a rotational viscometer is often recorded in units of centipoise (cP). However, the SI

unit of viscosity is the Pascal-second (Pa·s). The conversion from centipoises to Pa·s is made by multiplying by 0.001.

In some references cited in this report, the viscosity units used by the original author(s) were retained for clarity.

It is much less confusing to use a single unit of viscosity for the test measurement and the specification criteria. Since it is more convenient to use Pa·s and not have to worry about temperature-density corrections for asphalt binders, this unit will be used in this report for both measurements and criteria. This requires the conversion of the kinematic viscosity to absolute viscosity. If the density of an asphalt is assumed to be 1.000 g/mm^3, the equiviscous criteria convert to 0.17 ± 0.02 Pa·s and 0.28 ± 0.03 Pa·s for mixing and compaction, respectively. Although most asphalts have densities between 0.93 and 0.98 g/mm^3 at temperature ranges used for mixing and compaction, the small error due to the assumed density of 1.000 g/mm^3 is not considered to be significant. The Asphalt Institute (AI) has used this practice in its Superpave mix design manual, SP-2. In 2009, AASHTO balloted a revision for T 312 to include viscosity criteria for mixing and compaction as 0.17 ± 0.02 Pa·s and 0.28 ± 0.03 Pa·s.

Background on the Development of Mixing and Compaction Temperature Criteria

The origin of the equiviscous concept, which has been the standard method for determining appropriate temperatures for mixing and compacting asphalt mixtures for many decades, was a logical place to begin. However, there is scarce documentation of the origin of this technique. It is clear that the AI guided its development and evolution through several decades in the mid 1900s.

The first mention of equiviscous temperatures found in the literature was a 1951 paper titled "Viscosity Effects in the Marshall Stability Test" (*2*) by Fink and Lettier of the Shell Laboratories in Wood River, Illinois. They conducted research aimed at evaluating the influence of type and consistency of asphalt binders on Marshall stability values. Experimental factors included compaction temperature and the test temperature for measuring Marshall stability. A variety of types and grades of asphalt binders was incorporated in the mixes. They reported that compaction temperature had little effect on the density of the specimens. However, stability values increased with increasing compaction temperature. Flow values were influenced almost entirely by asphalt content, but not affected by compaction temperature. They concluded that, "neither stability nor flow was influenced by the consistency or source of the asphaltic binder if compaction temperature is carried out at equiviscous temperatures above the softening point of the binder."

However, different results were obtained by Parker. In his 1950 paper titled "Use of Steel-Tired Rollers," (*3*) Parker describes an experiment in which Marshall specimens were compacted at temperatures ranging from 100°F to 350°F. Eleven sets of samples were compacted over the range at 25°F increments. Results show that specimen densities were similar for temperatures of 275°F and above, but decreased in a linear fashion for temperatures down to 150°F. Below 150°F, specimen density dropped significantly.

Another reference dating to work in the mid 1950s alluded to specific ranges for Saybolt Furol viscosity as the basis for plant mixing temperature. In the description of constructing the Michigan Test Road in 1954, Serafin et al. (*4*) state that mixing temperatures were set so that the asphalts would have Saybolt Furol viscosities of 75 to 200 SSF. Six asphalts were used in the test road. At the midpoint of the viscosity range, mixing temperatures for the asphalts ranged from 290°F to about 312°F. Therefore, it is apparent that a recommended range for plant mixing viscosity was established prior to 1954. According to Vyt Puzinauskas, former AI chief chemist, the viscosity range cited above was essentially based on the field experience of AI's field engineers.

These studies may have provided the impetus for establishing the equiviscous criterion for laboratory compaction. The first edition of the AI's *Mix Design Methods for Hot-Mix Asphalt Paving* (*5*) in 1956 does not include viscosity criteria for mixing and compaction temperatures. In the 1960 paper titled "The Effect of Compaction Temperature on the Properties of Bituminous Concrete," (*6*) Kiefer states that "a mixing viscosity of about 100 seconds Saybolt Furol (SSF) was chosen in accordance with the recommendations of the Asphalt Institute which advised a mixing viscosity of between 75 and 150 sec Saybolt Furol." The reference cited in Kiefer's work was an informal paper by John W. Griffith, "The Effects of Viscosity of Asphalt Cement at the Temperature of Mixing on the Properties of Bituminous Materials," presented at the 38th annual meeting of the Highway Research Board in 1959. Kiefer's work (*6*) with the Hveem mix design procedure also concluded that compaction temperature also should be standardized. Samples were compacted in a Hveem kneading compactor at temperatures of 150, 190, 230, 270, 310, and 350°F. The range of temperatures was shown to affect sample density, air voids, Hveem stabilometer value, and cohesiometer value.

The second edition of the AI's Manual Series No. 2 *Mix Design Methods for Asphalt Concrete* (*7*) includes the equiviscous criteria for mixing and compaction of laboratory samples. The publication states: "The temperature to which the asphalt must be heated to produce 85 ± 10 seconds Saybolt Furol and 140 ± 15 seconds Saybolt Furol shall be established as the mixing temperature and compaction temperature respectively."

In 1965, Bahri and Rader reported on experiments with the recommended mixing and compaction viscosities for the Marshall method (*8*). The recommended ranges in ASTM D

1559 were the same as the MS-2 criteria. Effects of temperature and mineral filler content were studied. The results showed that variations in mixing and compaction viscosities produced significant changes in Marshall stability, flow, specific gravity, and voids. They concluded that the mixing and compaction viscosities recommended by ASTM were satisfactory for the mixture with 8.6% mineral filler (bitumen filler ratio 1.81). For the mixture with 11.3% mineral filler (bitumen filler ratio 2.38), an optimum mixing viscosity of 54 SSF and an optimum compaction viscosity of 250 SSF were recommended.

In 1984, Kennedy et al. (*9*) conducted a study to analyze the effect of lower compaction temperatures on the engineering properties of HMA. The study was prompted by an investigation of premature rutting of a recycled asphalt concrete overlay that had met in-place density specifications even though unusually low compaction temperatures had been used. Field records showed that the average delivery temperature to the roadway was 93°C (200°F). Laboratory experiments involved compacting samples over the range of temperatures during construction and determining the tensile strengths of the samples. They concluded that the low compaction temperature had an adverse effect on the properties of the HMA and thus contributed to the early pavement failure.

In 1985, Crawley (*10*) conducted a field evaluation of lower compaction temperatures and reached a different conclusion. This research evaluated engineering properties of HMA placed on a field project in which about half the asphalt base and binder courses were produced at the normal temperature of 149°C (300°F) and half were produced at 107°C (225°F). After 3.5 years, cores were taken from the project, and it was found that there was no significant difference in mixture properties or performance, although mixtures were placed at the different temperatures. The study further quantified a reduction of 20.6% in energy consumption by using the lower production mixing temperatures.

Other studies have demonstrated the effects of laboratory compaction temperature on the results of mechanical tests. Newcomb et al. (*11*) conducted a lab and field study to evaluate asphalt mixtures with plastic and latex modifiers. Part of their work examined the effect of compaction temperature on air voids and resilient modulus. Compaction was accomplished with a California kneading compactor at four temperatures: 79, 116, 154, and 191°C (175, 240, 310, and 375°F). The lowest air voids were achieved when compaction temperature was 154°C (310°F). Resilient moduli increased linearly with increasing temperature. Aschenbrener and Far (*12*) evaluated the influence of compaction temperature on results of the Hamburg Wheel Tracking Device. They reported that a higher compaction temperature improved the resistance to deformation in the Hamburg test. Azari et al. (*13*) compacted samples of an HMA mixture in a Superpave Gyratory Compactor (SGC) over a wide range of compaction temperatures and found that except for strain-controlled fatigue testing using a Superpave shear tester, the shear properties of the mixture improved with increasing compaction temperature. The strain-controlled fatigue results were not significantly affected by mixing temperature.

A number of studies have shown that laboratory compaction temperature has little to no influence on the volumetric properties of samples compacted in a SGC. Findings of NCHRP Project 9-10 (*14*) indicated very minor changes in density of SGC samples when compaction temperature varied from 80° to 155°C (176° to 311°F). Over this same temperature range, the binder viscosity increased by three orders of magnitude. It is interesting to note, however, that when the mixtures were compacted with a U.S. Army Corps of Engineers gyratory testing machine and with a Marshall hammer, the air voids increased by 56% and 44%, respectively, over the same temperature range. Huner and Brown (*15*) investigated the effect of reheating HMA and the effect of varying compaction temperature over a range of 28°C (50°F) on volumetric properties for mixtures compacted in the SGC. Their work included eight mixtures using two aggregate types, two gradation types, and two binders. None of the mixtures were affected by changing the compaction temperature. In a ruggedness study of the SGC compaction procedure, McGennis et al. (*16*) also found that compaction temperature was not a significant factor on the compacted density of mixtures for unmodified asphalts, but it was a significant factor for mixtures containing modified binders.

De Sombre et al. (*17*) conducted research to determine the range of temperatures over which the compactive effort of HMA is maximized. In this study, an Intensive Compaction Tester (ICT) gyratory compactor produced in Finland was used to compact samples at different temperatures. Density data were recorded at several points during compaction. The density data, the change in height of the sample during compaction, the size of the sample, and the pressure used to compact the sample were used to calculate the total work energy during compaction. By plotting the shear stress and power used during compaction against the number of gyrations for each temperature, the compactability of the mixtures was evaluated. By testing samples at several temperatures, it was possible to determine a desirable range of compaction temperature for a given mixture. Six laboratory mixes using three binder grades and two aggregate gradations, dense-graded and Stone Matrix Asphalt (SMA), as well as five field mixes were used in the study. For both the laboratory and field mixes, there was an attempt to establish a relationship between temperature and shear stress during compaction at different temperatures for each mix. A comparison of shear stress versus temperature showed that there was very little change in shear stress although the temperature changed

significantly. It appeared that aggregate type, angularity, and gradation had a greater effect on the energy required for compaction than did the compaction temperature. A difference in the type of polymer used also was found to be important, even though the binders met the same PG specifications.

In the field, however, temperature is considered one of the primary factors to affect the compactability of HMA. Leiva and West (*18*) found that field compactability of HMA was dominated by mat temperature and mat thickness relative to mixture characteristics such as gradation, aggregate type, and binder grade. Willoughby et al.(*19*), in a study of temperature segregation during placement of HMA, found significant differences for in-place density resulting from localized temperature differentials of only 14°C (25°F). In the field validation of the Pavecool program for estimating cooling rates of HMA during compaction, Chadbourn et al. (*20*) showed that almost no increase in mat density changes with continued passes of rollers as the mat temperature dropped below 100°C. Many industry references (*20–23*) cite 79°C (175°F) as the cessation temperature for compaction of HMA in the field. However, it is probable that the cessation temperature limit is a general rule of thumb and will vary from mix to mix depending to a large degree on the grade or consistency of the binder.

Effect of Temperature on Degradation of Asphalt Binders

A significant amount of research during the 1950s and 1960s also investigated asphalt aging. Some studies focused on the hardening of asphalts that occurs during manufacturing of asphalt mixtures. In the 1958 AAPT symposium on asphalt hardening, Clark (*24*) summarized that the mechanisms involved in age deterioration of asphalts are volatilization, oxidation, action of water, action of light, and chemical changes. He stated that volatilization was the primary cause of hardening and that oxidation assumes a secondary role in aging of asphalt. Fink's paper (*25*) stated that "most oxidation reactions approximately double for each 10°C increase." Serafin (*26*) discussed ways of minimizing binder hardening during the manufacture of asphalt mixtures. The discussion touched on topics such as oven aging procedures, recovery procedures, temperature control charts, and penalties. Of interest for this research was how Michigan dealt with temperature control at plants. The Michigan specification at the time required the "mixture be delivered at the temperature, between 275°F and 375°F, as directed by the Engineer, and shall not vary more than 20°F, plus or minus, from that temperature, except that no mixture shall exceed a temperature of 375°F." The discussion says that normal mix temperature was in the range of 285°F to 325°F.

Lottman et al. (*27*) investigated the effect of mixing temperature on viscosity changes (hardening) of asphalt binders. They found "a linear relationship between the dependent variable of final asphalt viscosity (after mixing) and the independent variables of aggregate temperatures and initial asphalt viscosity." However, they concluded that mixing temperature was not a significant factor on asphalt hardening. The discussions of the paper drew several criticisms of the analysis and points of view disagreeing with the conclusions.

Excessive temperatures during processing and storage of binders as well as during HMA production have several serious consequences. Airey and Brown (*28*) reported that storage of binders at elevated temperatures can cause breakdown of long chain polymers in modified asphalts, thereby negating the benefits of modified binders. Linde and Johansson also examined the effect of processing and storage temperature on degradation of polymer modified binders (*29*). Tests were conducted with size exclusion chromatography (SEC) to detect changes in molecular sizes in the bitumen and the polymer phase of the binders. Binders were stored at 200°C (392°F), and aliquots taken periodically for SEC testing and analysis. After just a few hours, the polymer degradation occurred as evidenced by a decrease in molecular size. The bitumen phase showed increases in molecular size most likely the result of oxidation and polymerization reactions. However, in an inert atmosphere, the polymer phase did not show changes in molecular size. The changes in molecular size were correlated to changes in mechanical properties of the binders. Tensile properties dropped significantly for the binders showing polymer degradation.

Stroup-Gardiner and Lange demonstrated environmental concerns associated with excessive HMA temperatures (*30*). They reported greater volatile loss, emissions, and concentrations of odor-causing compounds with increasing temperatures for a range of asphalt binders. They conducted a number of studies on fumes and odors that can be released from asphalts and asphalt additives at different temperatures (*31, 32*). They used gas chromatography (GC) analyses to identify specific compounds that can be linked to nuisance odors. They also developed a practical method of quantifying smoke and emissions potential from asphalt binders, called the SEP test. They demonstrated that the release of volatile organic compounds (VOCs), SEP mass loss rates, and opacity for asphalt binders are strongly influenced by temperature and crude source.

One of the most widely used references for asphalt around the world is *The Shell Bitumen Handbook* (*33*). This handbook provides useful guidance on handling of asphalt binders. Several specific recommendations are worth noting:

> Bitumen should always be stored and handled at the lowest temperature possible, consistent with efficient use . . . to prevent auto-ignition of the bitumen 230°C (446°F) must never be exceeded. . . . During mixing the hot bitumen must be readily able to coat the dried and heated mineral aggregate, given the shearing conditions employed, in a relatively short period of time (typically 30 to 90 seconds); this determines the lowest mixing

> temperature. Whilst the mixing temperature must be sufficiently high to allow rapid distribution of the bitumen on the aggregate, the use of the minimum mixing time at the lowest temperature possible should be advocated. The higher the mixing temperature the greater will be the oxidation of the bitumen exposed in thin films on the aggregate surface. . . . There are, therefore, upper and lower limits to mixing temperature. . . . These different considerations combine to give an optimal bitumen viscosity of 0.2 Pa·s (2 poise) at mixing temperatures. . . .When materials are being laid at low ambient temperatures, or if haulage over long distances is necessary, mixing temperatures are often increased to offset these two factors. However, increasing the mixing temperature will considerably accelerate the rate of bitumen oxidation which will increase the viscosity of the bitumen. Thus a significant proportion of the reduction in viscosity achieved by increasing the mixing temperature will be lost because of additional oxidation of the bitumen. . . . Once the mat has been spread it must still be sufficiently workable to enable the material to be satisfactorily compacted with the available 30 Pa · s (300 poise). At viscosities lower than 5 Pa · s the material will probably be too mobile to compact and at viscosities greater than 30 Pa · s the material will be too stiff to allow any further compaction.

Mixing and Compaction Temperatures for Modified Asphalt Binders

The use of polymer-modified asphalt binders has become much more common over the past two decades. Many types of polymers have been used in paving asphalts to enhance the performance of asphalt pavements in a wide range of climates and loading conditions. The AMAP now estimates that modified asphalt binders make up about 20% of paving grade asphalt sales in the United States (*1*).

Most modified binders require higher temperatures for mixing and compaction in the field and the laboratory to achieve the same workability as mixes with unmodified binders. In "Using Additives and Modifiers in Hot Mix Asphalt," Terrel and Epps (*34*) include construction guidelines for a number of specific modifiers. The guidelines regarding temperatures for mixing and placing vary widely for the several specific HMA polymers. For example, mixing information for Butonal NS 175, a styrene/butadiene latex, states that "the temperature of the aggregate, when introduced into the mixture should not exceed 182°C (360°F), and the temperature of the mixture when discharged from the hauling unit shall be 149°C (300°F) minimum." Another polymer required much higher temperatures. Rosphalt 50®, a virgin polymeric additive, primarily used as an additive to HMA for bridge deck sealing, recommended the discharge temperature be at least 199°C (390°F).

For Kraton®, a block copolymer, mix preparation instructions simply state that "it may be necessary to adjust the mixing and compaction temperatures when conducting laboratory work." For plant operations, asphalt mixtures containing Kraton® should be as workable as a typical asphalt mixture because of "the relatively high shear forces seen at the manufacturing level compared to the lower shear forces used in laboratory viscosity measurements." Shuler et al. (*35*) showed that viscosities increased with higher polymer contents for Kraton® and Styrelf® modified binders. Based on the viscosity tests, significantly higher mixing and compaction temperatures would be required. However, experience with these binders on previous construction projects indicated that the extremely high mixing and compaction temperatures were not necessary. For environmental reasons, they considered the upper limit for field mixing to be 160°C (320°F). Newcomb et al. (*11*) conducted laboratory and field studies of mixtures containing polyolefin and styrene-butadiene latex. In the field, normal construction procedures were used, and they noted that the only modified mixtures that created any handling difficulty were mixtures with 3% latex that tended to cause sticking problems in the trucks and screeds. Otherwise, modified mixtures behaved similar to conventional unmodified mixtures.

Shenoy (*36*) studied the temperature-viscosity relationships of two polymer modified asphalts, Styrelf® and Novophalt®. Both of these binders have been studied extensively at the FHWA Turner Fairbank Research Center's Accelerated Loading Facility and laboratories. The Novophalt® binder used in this study was an AC-10 modified with about 6.5% low-density polyethylene. The Styrelf® binder was an AC-20, which was air blown to AC-40 and then modified with styrene-butadiene. Sulfur was also added as a cross-linking agent. Testing utilized a Brookfield viscometer with three spindles to generate a wide range of shear rates. Arrhenius plots for the binders showed that the viscosity-temperature relationships are influenced by the melting points of the polymers. For the Novophalt®, the polyethylene has a melting point around 125°C (257°F). For the Styrelf®, the melting point of the polystyrene occurs in the range of 115°C to 150°C (239 to 302°F) and the polybutadiene melts between 150°C and 163°C (302°F and 325°F). Evidence of polymer degradation also was presented. Aging of the binders and breakdown of the polymers occurred in the same temperature range. Aging tended to cause the viscosity to increase whereas polymer degradation caused viscosity to decrease.

In a field trial of various modified binders and one unmodified control binder, Albritton et al. (*37*) used a rotational viscometer to determine viscosity of the different modified binders. At the lower temperature of 135°C (275°F), the viscosities of the binders range from a high viscosity value of 2.60 Pa · s for the multigrade binder to a lower value of 0.50 Pa · s for the unmodified binder control section. At the higher temperature of 190°C (374°F), the viscosities of the modified binders grouped closer together, ranging from a high value of 0.40 Pa · s for the Novophalt® modified binder to a lower value less than 0.10 Pa · s for the control and multigrade

binders. The study showed that mixing and compaction temperatures for polymer modified mixes were higher than for conventional unmodified binders. Mixing temperature ranged from 160°C to 177°C (320°F to 351°F). They noted that the linear temperature-viscosity relationship assumed for unmodified binders may not be valid for modified asphalt binders.

Recognizing the potential problems with using the equiviscous method with modified asphalts, a note was added to AASHTO T 312 in the section on preparation of specimens:

> Note 4 – Modified asphalts may not adhere to the equiviscosity requirements notes, and the manufacturer's recommendation should be used to determine mixing and compaction temperatures.

In 2000, the Asphalt Pavement Environmental Council published an industry guidance document titled *Best Management Practices to Minimize Emissions During Construction* also known as EC 101 (*38*). This document includes several important recommendations regarding mixing and compaction temperatures. It states that the equiviscous method is meant to be used only for laboratory purposes and should not be used as a starting point for plant mixing and field compaction temperatures. For modified binders, it is advised to use the binder supplier's recommendation for proper laboratory and plant mix production and field compaction temperatures.

Table 1, reproduced from this publication, serves as a guide for the industry on suitable temperatures for field operations. These recommended HMA plant temperature ranges were considered as practical guidelines for mixing temperatures in this study.

Table 1. Recommended plant temperatures for different binder grades (*38*).

Asphalt Pavement Environmental Council Best Practices				
Typical Asphalt Binder Temperatures				
Binder Grade	HMA Plant Asphalt Tank Storage Temperature (ºF)		HMA Plant Mixing Temperature (ºF)	
	Range	Midpoint	Range	Midpoint
PG 46-28	260 – 290	275	240 – 295	264
PG 46-34	260 – 290	275	240 – 295	264
PG 46-40	260 – 290	275	240 – 295	264
PG 52-28	260 – 295	278	240 – 300	270
PG 52-34	260 – 295	278	240 – 300	270
PG 52-40	260 – 295	278	240 – 300	270
PG 52-46	260 – 295	278	240 – 300	270
PG 58-22	280 – 305	292	260 – 310	285
PG 58-28	280 – 305	292	260 – 310	285
PG 58-34	280 - 305	292	260 – 310	285
PG 64-22	285 – 315	300	265 – 320	292
PG 64-28	285 – 315	300	265 – 320	292
PG 64-34	285 - 315	300	265 – 320	292
PG 67-22	295 – 320	320	275 – 325	300
PG 70-22	300 – 325	312	280 – 330	305
PG 70-28	295 – 320	308	275 – 325	300
PG 76-22	315 – 330	322	285 – 335	310
PG 76-28	310 – 325	318	280 – 330	305
PG 82-22	315 – 335	325	290 – 340	315

Survey of Current Practices for Determining Mixing and Compaction Temperatures

A survey was conducted to examine procedures used by highway agencies to determine mixing and compacting temperatures for mix design and construction operations. Survey results were obtained from 65 agencies including the highway agencies for all 50 states and the U.S. Army Corps of Engineers. Survey responses also were received from highway agencies in Canada, Australia, China, Denmark, India, Japan, and Malaysia. A table listing each agency's responses is included in Appendix A.

In the survey summary, the survey responses add up to more than 100% for each of the questions because some agencies used more than one method for determining mixing and compaction temperatures. For example, an agency may generally follow AASHTO T 245 and T 312 to determine mixing and compaction temperatures, but if the temperatures exceed a certain value then the supplier's recommendation would be used. Likewise, for setting production and placement temperatures, some agencies may follow AASHTO T 245 and T 312, but allow the contractor some flexibility to change those temperatures depending on ambient temperature, haul distance, and layer thickness.

The survey questions, along with a summary of responses, are as follows:

1. What procedure does your agency/organization currently use to determine mixing and compaction temperature for asphalt binders used in unmodified hot-mix asphalt?

   As shown in Figure 1, the largest response (46%) indicated that the guidelines in AASHTO T 245 and T 312 were used to determine mixing and compaction temperatures for unmodified asphalt. Several agencies reported using the AASHTO procedures unless the temperature exceeded a certain limit, such as 166°C (325°F), and if that limit were exceeded, they would use the binder supplier's recommendation. A few agencies reported that they avoided the mixing and compaction temperature issue altogether

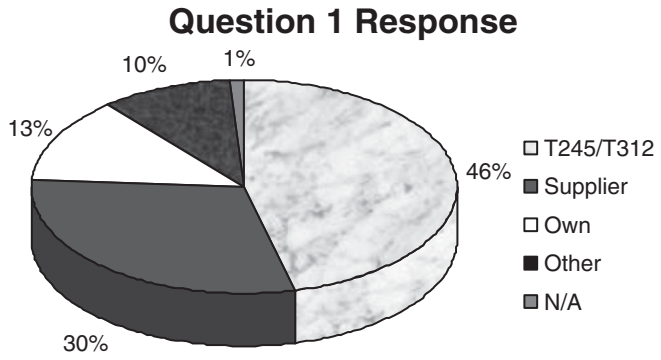

Figure 1. Survey responses to Question 1.

by using the supplier's recommendation for all binders. A few agencies also reported that they have established a standard mixing and compacting temperature based on their own experience and use those temperatures for all unmodified binders. Nevada indicated that they no longer use unmodified asphalt binders.

Of those using other methods, ASTM D2493 was the procedure most often used. The ASTM procedure is a method for determining the standard viscosity-temperature chart but does not specify mixing and compacting temperatures.

The Japan Road Association uses a procedure that is similar to AASHTO T 245 and T 312, but allows a slightly higher temperature. The mixing temperature range is that which gives a viscosity of 180 ±20 mm^2/s, and the compaction temperature range is that which gives a viscosity of 300 ± 30 mm^2/s.

2. What procedure does your agency/organization currently use to determine mixing and compaction temperatures for asphalt binders used in polymer-modified hot-mix asphalt?

The overwhelming response to Question 2 (Figure 2) was that binder supplier recommendations are used for determining mixing and compacting temperatures for polymer-modified asphalt mixtures. Fifty-six percent of the agencies responding stated they use supplier recommendations. A few of those indicated they use AASHTO T 245 and T 312 unless unusually high temperatures are needed, and in that case, they would use supplier recommendations. Even though supplier recommendations were used most often, some agencies also established a maximum mixing and compaction temperature. Four agencies (British Columbia, Canada; Hawaii; New York State Thruway Authority; and Puerto Rico) reported that they do not currently use polymer-modified asphalt.

Since supplier recommendations are typically used for polymer-modified asphalts, an obvious question is, "What procedures do suppliers use?" For answers to this question, 17 surveys were sent to representatives of the modified asphalt industry. Unfortunately, no responses were received to the surveys. However, Gaylon Baumgardner of Paragon Technical Services, Inc., (a division of Ergon) and Frank Fee of NuStar Energy, L.P., were very helpful in providing information by telephone and e-mail in regard to industry procedures.

Suppliers most often use temperature-viscosity charts based on AASHTO T 245 and T 312 for determining mixing and compacting temperatures for unmodified asphalt. Some suppliers of modified asphalt use a rough adjustment of 10°F for each grade increase with polymer modification. Other suppliers set mixing and compaction temperatures solely based on experience with the particular binder and modification system. It was stated that prior experience has shown that a mixing temperature in the range of 160°C to 171°C (320°F to 340°F) and a compaction temperature in the range of 143°C to 155°C (290°F to 310°F) are adequate for most mixes with polymer-modified binders. Suppliers also may allow some flexibility in adjusting those temperatures depending on project conditions such as ambient temperature, haul distance, layer thickness, etc. For highly modified binders such as PG 82-22, the temperatures may need to be increased slightly. However, suppliers generally recommend that mixing temperatures never exceed 190°C (375°F), which is consistent with EC 101.

3. What procedure does your agency/organization currently use to determine mixing and compaction temperatures for asphalt binders used in crumb rubber-modified hot-mix asphalt?

Sixty-four percent of agencies responded that they do not use crumb rubber modifiers (Figure 3). Of those that use crumb rubber, most rely on supplier recommendations that are generally based on experience. Some states supplement the supplier recommendations with a maximum mixing temperature of their own. From the responses, the highest mixing temperature allowed in the United States and Canada is 176°C (350°F). Asian countries generally allow slightly

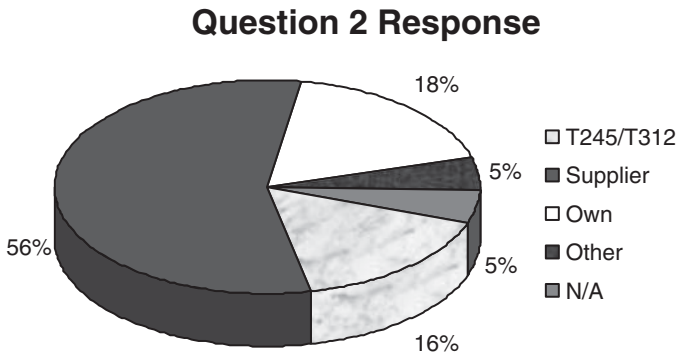

Figure 2. Survey responses to Question 2.

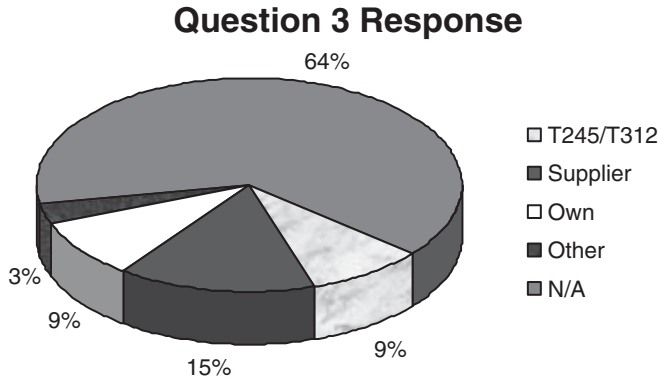

Figure 3. Survey responses to Question 3.

higher temperatures. For example, India uses a mixing temperature range of 165°C to 185°C (330°F to 365°F) and Japan has a maximum mixing temperature of 185°C (365°F) for all types of modified asphalts.

4. Does your agency/organization have experience with air-blown or chemically modified asphalt? If so, what procedure is currently used to determine mixing and compaction temperatures for asphalt binders used in hot-mix asphalt modified in this manner?

Fifty-nine percent of the agencies responded that they do not have experience with or do not allow air-blown or chemically modified asphalt (Figure 4). Most of the agencies that allow these modifiers use supplier recommendations or a combination of AASHTO T 245 and T 312 and supplier recommendations. The Quebec Ministry of Transportation uses a combination of AASHTO T 245 and T 312 and specification limits. If the temperature that corresponds to 0.17 Pa · s exceeds 170°C (338°F), then 170°C (338°F) becomes the maximum temperature and a mixing temperature range of 156°C to 170°C (313°F to 338°F) is used.

5. Are the same procedures used to determine plant production and laydown temperatures?

Most agencies (61%) responded that they use the same procedures for establishing mixing and compaction temperatures in the field as they do for laboratory work (Figure 5). Fifteen percent of the responding agencies allow the contractor flexibility to set the temperatures for construction (or to adjust temperatures to account for ambient temperature, haul distance, layer thickness, etc.) so long as a maximum temperature such as 177°C (350°F) is not exceeded. Four agencies vary production temperature based on PG grade, and two others vary production temperatures depending on whether the binder is virgin or modified.

In Denmark, the maximum mixing temperature is regulated by legislation with the Danish Working Environment Authority. Based on those guidelines, contractors must not exceed 190°C (375°F) for polymer-modified mixtures. If the maximum mixing temperature is exceeded, the contractor is required to provide special safety precautions (such as "space suits") for workers. In order to keep from being associated with hazardous materials, contractors avoid going over the maximum limit. For unmodified asphalt, the maximum mixing temperature is 180°C (355°F).

Where polymer-modified asphalt is used in China, the agency has set temperatures for heating the aggregate and the modified binder, and if the combined mixture exceeds 195°C (383°F), the mixture is discarded. A minimum compaction temperature is also established depending on surface temperature and layer thickness as indicated in Table 2.

The Japanese method for determining mixing and compaction temperatures for mixes with polymer-modified binders is interesting and rather straightforward. A 13-mm maximum aggregate size mix using the same aggregates as will be used in the project is mixed with straight-run unmodified asphalt and compacted using their standard temperature-viscosity curves. The density of the samples are determined and used as the standard density. Using the same mix with the modified asphalt specified for the project, mixture is compacted at three to five incremental temperature levels up to a compaction temperature of 185°C (365°F). The density of each set of samples is determined

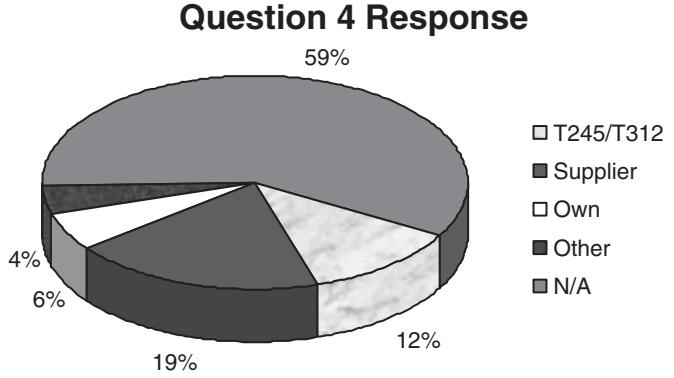

Figure 4. Survey responses to Question 4.

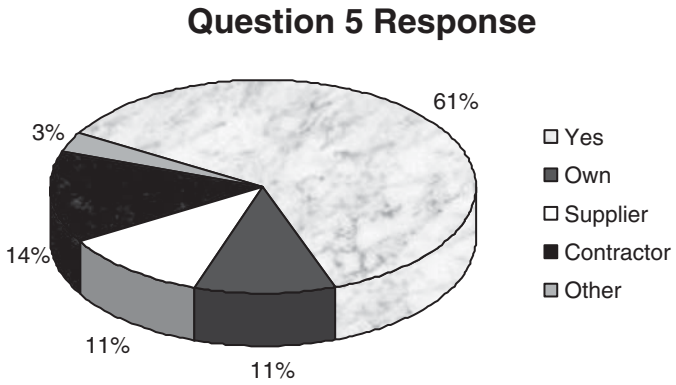

Figure 5. Survey responses to Question 5.

Table 2. Minimum compaction temperatures of HMA in China.

Surface Temperature of Existing Layer (°C)	Minimum Compaction Temperature Related to the Following Thickness (°C)					
	Unmodified			Modified or SMA		
	<50mm	50-80	>80mm	<50mm	50-80	>80mm
<5	NA	NA	140	NA	NA	NA
5 - 10	NA	140	135	NA	NA	NA
10 - 15	145	138	132	165	155	150
15 - 20	140	135	130	158	150	145
20 - 25	138	132	128	153	147	143
25 - 30	132	130	126	147	145	141
>30	130	125	124	145	140	139

and compared with the standard density. The temperature that results in the same density for modified samples as obtained in the standard unmodified samples becomes the minimum compaction temperature. An increment of 10°C (18°F) is added to the minimum compaction temperature to determine the maximum compaction temperature. An increment of 10°C (18°F) is added to the maximum compaction temperature to determine the minimum mixing temperature. Another increment of 10°C (18°F) is added to the minimum mixing temperature to obtain the maximum mixing temperature. However, the maximum mixing temperature cannot exceed 185°C (365°F).

Responses from each agency that replied to the questionnaire are provided in Appendix A. Although AASHTO T 245 (Marshall method) and T 312 (Superpave Gyratory Compaction) are similar with regard to establishing mixing and compaction temperatures, some agencies specified one over the other. In those cases, the specified AASHTO procedure is underlined.

Recent Research on Proposed New Methods for Determining Mixing and Compaction Temperatures

Over the past decade, several studies have specifically addressed the issue of mixing and compaction temperatures for modified binders. Several of these research projects proposed new approaches for determining mixing and compaction temperatures.

Zero Shear Viscosity

In *NCHRP Report 459: Characterization of Modified Asphalt Binders in Superpave Mix Design,* Bahia et al. (*39*) determined that the equiviscous requirements in AASHTO T 312 did not give practical results for 17 out of the 38 modified binders tested. For these modified binders, mixing temperatures of over 165°C (329°F) were calculated. The researchers hypothesized that this was due to the fact that most of the modified binders were sensitive to shear rate and therefore did not meet the current assumption that all binders are Newtonian fluids. They introduced the concept of Zero Shear Viscosity (ZSV) and recommended its use for determining mixing and compaction temperatures for modified asphalt binders. They reasoned that since the vertical compression rate during most of the SGC compaction process is very low, the measurement of the viscosity for the binder should be made at a very low shear rate. They also found that low shear viscosity data for the binders correlated better to air voids in SGC-compacted specimens compared with high shear (300 1/s) viscosity measurements. Initially, the viscosity corresponding to a shear rate of 0.001 1/s was estimated with a curve-fitting model. The criteria at this shear rate were set at 3.0 Pa·s and 6.0 Pa·s, for mixing and compaction, respectively.

Laboratory compaction in an SGC at the ZSV compaction temperature for four mixtures and five binders yielded very similar air void contents for two of the mixes, but the other two mixtures had increased air voids of 0.7% to 1.1% for the modified binders compared with results with the unmodified binder. To simplify the approach so that the Brookfield rotational viscometer could be used, low shear rate viscosity criteria were set at 0.75 ± 0.05 Pa·s and 1.4 ± 0.10 Pa·s respectively, for mixing and compaction. The shear rate for the Brookfield rotational viscometer, as currently used in AASHTO T 316, is 6.8 1/s. This resulted in about a 40°C (72°F) reduction in mixing and compaction temperatures compared with the standard equiviscous temperatures. Laboratory mix coating tests at the low shear rate mixing temperature with four mixtures and five binders yielded good coating for most mix-binder combinations in a restaurant-type mixer and a bucket-type mixer.

A couple of independent studies evaluated the ZSV method. Grover (*40*) presented research and discussion of mixing and compaction temperatures based on the ZSV method and the equiviscous temperature method. Included in the presentation were several different definitions of ZSV and a description of Bahia's method of determining a value for Low Shear Viscosity. Data for both the equiviscous temperature method and the ZSV method were presented for several modified and unmodified asphalt binders. The data showed that the equiviscous temperature method required excessive heating of the modified binders. The ZSV method yielded mixing and compaction temperatures that were 35°C to 40°C lower than those calculated by the equiviscous method.

Tang and Haddock (*41*) evaluated seven Superpave mixtures and one SMA mixture obtained from Indiana DOT projects. Three projects utilized a PG 64-22, two projects utilized a PG 70-22, and three projects used a PG 76-22. Raw materials from the projects were obtained and used in the laboratory research. Since four of the binders were not shear rate dependent (Newtonian), their mixing and compaction temperatures were determined by the traditional equiviscous technique. All binders also were tested to determine their ZSV mixing and compaction temperatures using the procedure described by Khatri et al. (*42*). Mix designs were performed in accordance with Superpave procedures. They found that the ZSV mixing and compaction temperatures yielded the same optimum asphalt content as was used on the project. The paper did not state how the mixing and compaction temperatures were determined for the original mix designs. Field mixing and compaction temperature for the modified binders were based on "experience." Correlations of mixing and compaction temperature from the equiviscous technique and the ZSV principle showed that the ZSV

temperatures were about 40°C below the equiviscous temperatures. They recommended that the equiviscous method be used to determine mixing and compaction temperatures for Newtonian binders and the ZSV method be used for modified binders.

Extrapolated High Shear Rate Viscosity

Yildirim et al. (*43*) presented an approach that estimates high shear rate binder viscosity from rotational viscosity measurements for the determination of mixing and compaction temperatures. The shear rate of 490 1/s was selected from experimental work with mixtures compacted in a SGC. The same mixtures were prepared with four different binders and then compacted in the SGC over a range of relatively low temperatures (between 50°C and 95°C) to amplify the effect of temperature on mix density. It was hypothesized that equivalent mix densities would occur when the viscosities of binders were the same. To find the point where binder viscosities were the same, the binders were tested in a Brookfield viscometer at shear rates ranging from 0.1 1/s to 93 1/s. These viscosity data were extrapolated to find the shear rate where the unmodified asphalt and the modified asphalts had the same viscosity. The hypothesis was that the shear rate at which the viscosities of binders intersect is equivalent to the shear rate that the mix experiences in the gyratory mold during compaction. The average equiviscous shear rate for the eight pairs of mixtures was 487 1/s, which was rounded to 490 1/s. The extrapolated viscosity of binders at 490 1/s was referred to as the high shear rate viscosity. Using a shear rate of 490 1/s, the traditional viscosity criteria of 0.17 ± 0.02 Pa·s for mixing, and 0.28 ± 0.03 Pa·s for compaction, they determined mixing and compaction temperatures for the four modified binders to be 10°C to 40°C (18°F to 72°F) below the respective temperatures from AASHTO T 312.

This method was criticized on several points (*44*). One issue with this approach was the use of unrealistically low compaction temperatures and then using viscosity measurements at those temperatures to extrapolate viscosity-shear rate data. The accuracy of the estimates for viscosities at the recommended shear rate of 490 1/s was questioned. At higher temperatures typical of the range normally used in the laboratory, the binders would have exhibited less shear thinning behavior and thus the extrapolations would be different.

Steady Shear Flow

Reinke (*45*) presented another concept, which he called the steady shear flow test, to determine mixing and compaction temperatures. This approach uses a DSR with a 500-micron gap and a 25-mm-diameter plate geometry. The viscosities of binders are tested over a range of shear stresses at temperatures ranging from 76°C to 94°C (169°F to 201°F). At high shear stresses, around 500 Pa, the viscosities of modified binders approach a steady state (i.e., very small change in viscosity with increasing shear stress). This is illustrated in Figure 6. Using a log-log temperature-viscosity chart, the viscosities from the 500-Pa shear flow tests are extrapolated out to 180°C (356°F). As with unmodified binder using the equiviscous principle, the recommended mixing temperature is based on a viscosity of 0.17 ± 0.02 Pa·s. The recommended compaction temperature from the steady shear flow technique is 0.35 ± 0.03 Pa·s, which is higher than the equiviscous compaction range of 0.28 ± 0.03 Pa·s. Reinke indicated that the mixing and compaction temperatures derived from the steady shear flow method for the few polymer-modified binders evaluated matched well to the temperature ranges successfully used in practice.

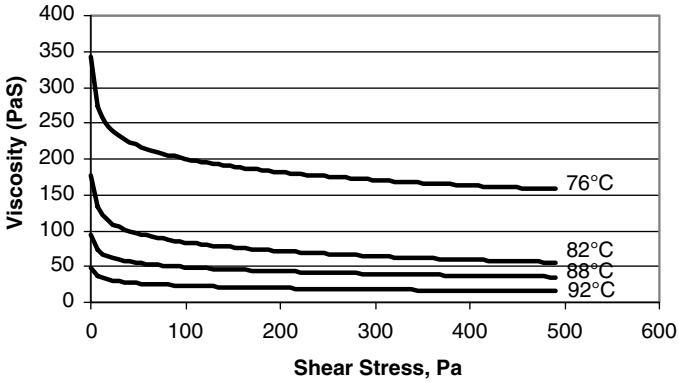

Figure 6. Steady shear viscosity over a range of shear stresses.

Shear Rate Dependency

As noted previously, Shenoy (*36*) proposed a technique of selecting mixing temperatures based on shear rate dependency and other factors. The study included only two polymer-modified asphalts, Styrelf® and Novophalt®. The binders and a diabase filler were mixed at four temperatures ranging from 150 to 200°C (302 to 392°F) and tested in the Brookfield viscometer with three spindles to generate viscosities over a range of shear rates. The ratio of viscosities for the filled binder divided by the unfilled binder showed a pessimum point for the Novophalt® around 180°C (356°F). For the Styrelf®, the viscosity ratio was at an apparent minimum around 163°C. Shenoy selected the mixing temperature range for the binders based on a table of pass/fail criteria for shear-rate dependency, fluidity, Arrhenius plot smoothness, degradation, aging, and viscosity ratio. This yielded mixing temperatures of 180°C (356°F) for the Novophalt® binder and a range of 163°C to 180°C (325°F to 356°F) for the Styrelf® binder.

Extensional Viscosity

Sudduth et al. (*46*) evaluated eight polymer additives used to modify an AC-20 asphalt binder using a technique referred to as "Pseudo Extensional Viscosity, η_{ext}." η_{ext} is defined as the difference in the viscosity measured using the Rotational Viscometer for the smaller 27 spindle and the viscosity measured using the larger 21 spindle. The asphalts were evaluated at strain rates of 1 1/sec and 100 1/sec. It was concluded that a positive value for η_{ext} was most desirable for roadway paving, and a negative value would be undesirable as it would indicate a softer asphalt pavement.

Equivalent Mixture Properties

Stuart (*47*) used an SGC to compact three mixtures with an unmodified binder over a range of compaction temperatures, then substituted the unmodified binder with two different modified binders (Novophalt® and Styrelf®) at the same asphalt contents and repeated the SGC compaction tests. The temperature range that yielded the same volumetric properties as the unmodified binder was determined for each modified binder. Rheological properties of the binders and mastics were measured to determine which property provided the same temperature ranges given by the compaction process. The results of the compaction tests indicated that a compaction temperature of 145°C (293°F) could be used for each of the binders and achieve the same air void content. The allowable compaction temperature range was found to be 20°C to 40°C (36°F to 72°F), which indicates that compaction was insensitive to temperature. The temperature at which smoking was observed for each of the binders during mixing or short-term oven aging was used to set the maximum compaction temperature. Stuart concluded that a single binder viscosity range could not be used to select the laboratory compaction range for all binders. He also commented that the viscosity range of 1.4 ± 0.10 Pa · s, as recommended by the NCHRP Project 9-10 study, was too low for the unmodified binder.

Azari et al. (*13*) conducted a follow up study to the work by Stuart. They tested mechanical properties and physical characteristics of the limestone-Novophalt® mixture from Stuart's study compacted at four different compaction temperatures. Mixture specimens were fabricated by mixing at 145°C (293°F) and then short-term oven-aged and compacted at the following temperatures: 119°C, 139°C, 159°C, and 179°C (246°F, 282°F, 318°F, and 354°F). The samples were analyzed using computer-aided tomography to study the distribution of air voids and aggregate orientation. The shear testing conducted was repeated load at constant height and frequency sweep at constant height at 25 and 50°C. The compaction temperature affected the total air void content and the distribution of the air voids within specimens. The vertical gradient of the air voids was higher than the lateral gradient in the gyratory-compacted specimens. The vertical air void gradients (top to bottom) in the SGC specimens were lowest for samples compacted at 139°C. Lateral air void gradients (side to side) were of a much smaller magnitude but were lowest at the highest compaction temperature of 179°C. Aggregate orientation, measured as vector magnitude, peaked at 159°C. A stepwise regression was performed to relate the physical properties (air voids, air void distribution, aggregate orientation, and binder shear stiffness) to the mix shear properties $\sin\delta/G^*$, $G^*\sin\delta$, and permanent shear strain. Binder stiffness and the distribution of the air voids were important factors that affected the mechanical properties. All shear properties except $G^*\sin\delta$ improved with increasing compaction temperature. For this binder, they recommended an optimum compaction temperature in the range of 139°C to 159°C (282 to 318°F).

Workability

One of the earliest attempts to evaluate workability of HMA was performed in 1979. Marvillet and Bougalt (*48*) developed a prototype stirring device for loose mixtures to evaluate the factors that affect workability. They defined workability as the inverse of the torque required to rotate the stirring blade through a sample of mixture. The prototype device was used to test various combinations of materials and it was found that

- Workability increased as viscosity decreased.
- Workability was unaffected by changes in asphalt content.
- Workability was reduced as the dust content (percent passing the No. 200 sieve) was increased.
- Mixes with angular aggregate particles were less workable than mixes with rounded particles.

Their work showed that an increase in workability resulted in a corresponding increase in compactability. However, they cautioned that just because two different mixes have the same workability does not necessarily mean the mixes will have the same compactability. It was pointed out in the discussion of the paper that two mixes can start out with the same density and reach the same final density but have different compaction slopes. The steeper the compaction slope, which was referred to as coefficient of compactability, the easier the material would be to compact.

Gudimettla et al. (*49, 50*) developed another prototype workability device similar to the French workability machine. The first study evaluated several operational parameters such as paddle configuration and speed of rotation and their effect on torque measurements with a few mix factors. This work

indicated that the prototype workability device could effectively differentiate the effects of mixture gradations and binder grades. This led to development of the current workability device by Instrotek, Inc.

Further research with the Instrotek workability device studied additional materials factors including three aggregate types (granite, crushed gravel, limestone); two NMAS (19 mm, 12.5 mm); five gradations; and three binder types (PG 64-22, 70-22, 76-22). The research found that each mix has a range of workability as the mix temperature decreases. When the same binder grade was used with three different aggregate types, each mix had different workability levels. This indicates that binder properties alone may not be the best measure of the compactability of an asphalt mixture. When compared with the equiviscous method for determining mixing and compacting temperatures, the workability tests resulted in compaction temperatures 9°C to 28°C (16°F to 50°F) lower for modified asphalts and about the same temperature for unmodified asphalt. The data were examined to determine the temperatures at which mixtures with different binders had the same workability. The study also evaluated an approach to define compaction temperatures for each mixture based on the workability versus temperature data. The research concluded that every mix has a unique relationship between temperature and workability based on aggregate type, binder type, gradation, and NMAS.

Table 3 provides a summary of methods in use or proposed by researchers for determining mixing and compaction temperatures of hot-mix asphalt.

Shear Rates During Mixing and Compaction

If viscosity is the binder parameter used to establish mixing and compaction temperatures, the shear rate(s) used to determine the viscosity should approximate the shear rates that occur during mixing and compaction. However, very little information was found in the literature regarding the shear rates that exist during mixing and compaction in the laboratory or during plant production and construction. The maximum shear rate that exists in a rotating shaft mixer can be approximated using Equation 1 and substituting tangential velocity of the mixing tip for the relative velocity, V:

$$\gamma' = \frac{V}{d} \tag{1}$$

where

γ' = the shear rate;
V = the relative velocity of the solid elements shearing the fluid; and
d = distance between solids.

$$v_t = r\omega$$

where

v_t = the tangential velocity;
r = the radius; and
ω = the angular velocity.

The rotation speed for a popular model of continuous mix plant (Astec 400 ton/hr double barrel plant) is 7.68 rpm (0.8 rad/s). This plant has a drum radius of 1.69 m (5.56 ft). The tangential velocity at the point of mixing for this plant is 1,352 mm/s. In a popular size batch plant, the pugmill is driven at a rate of 33.6 rpm (3.52 rad/s). The length of the mixing arms from the center of the mixer shaft is 0.47 m (1.55 ft). Therefore, the maximum tangential velocity during mixing in this pugmill is 1,654 mm/s. If the nominal thickness of the asphalt coating on an aggregate particle during the initial mixing is approximated as 10 microns (0.01 mm), then the instantaneous shear rate of the binder film on a particle in contact with the pugmill tip can be estimated with Equation 1.

Using this approach, the pugmill will yield a maximum instantaneous shear rate of 165,400 1/s, and for the drum plant, the maximum instantaneous shear rate is estimated to be 135,200 1/s. These estimated shear rates for mixing represent the high end of a range of shearing that occurs during mixing. In reality, the mixing process in a plant or in laboratory mixers produce a turbulent mass mixing action with an extremely wide range in shear rates.

For comparison, the shear rates for several laboratory mixers and binder test methods are shown in Table 4. These estimates also reveal how different the conditions may be in routine laboratory binder tests versus an HMA plant.

For estimating shear rates during compaction, it is necessary at this point to only be concerned with laboratory compaction since that is the issue at hand. Although the conditions of laboratory compaction are much more controlled than in the field, there are still numerous complications in estimating shear rates during compaction.

In *NCHRP Report 459,* Bahia et al. (*39*) reasoned that the shear rate during compaction in the SGC was very low. This logic was based on the observation that the change in specimen heights is very low during most of the compaction, especially after the first 10 or so gyrations. However, the one-dimensional vertical strain rate of the mixture and the shear rate of the binder films coating the aggregate particles during compaction are not the same thing. Since the aggregate particles are essentially nondeformable rigid bodies, the strain or deformation only occurs due to manipulation of aggregate particles around one another, thus shearing the asphalt films during those movements. One valid point is that the strain rate changes throughout the compaction process. The early part of compaction is where the binder consistency plays a greater role.

Table 3. Summary of researched methods for determining mixing and compaction temperatures.

Method	Description	Advantages	Disadvantages
Equiviscous Temperatures	The rotational viscometer is used to determine the viscosity at 2 temperatures and 1 shear rate. The viscosities are plotted vs. temperature and a temperature range corresponding to 0.17±0.02 Pa·s is chosen for mixing and a temperature range corresponding to 0.28±0.03 Pa·s is chosen for compaction.	• Simple to obtain and analyze results • Can be completed in less than 1 hour	• Assumes linear relationship between viscosity and temperature • Assumes that all asphalt binders are Newtonian liquids; does not account for shear rate dependency • Can result in unnecessarily high mixing and compacting temperature for some modified asphalt binders
High Shear Rate Viscosity	Uses the rotational viscometer to determine the shear rate dependency of an asphalt binder at 2 temperatures (135°C, 165°C). For each temperature, the data is fit to an inverse power curve and extrapolated to estimate the viscosity at a shear rate of 490 1/s. The high shear viscosities are plotted versus temperature, and mixing and compaction temperature ranges are determined at target values of 0.17±0.02 Pa·s and 0.28±0.03 Pa·s, respectively.	• Takes into account the shear rate dependency of modified asphalt binders • Testing is simple to perform • Does not require complicated modeling	• Requires extrapolation of results to a high shear rate
Steady Shear Flow	Uses a DSR Steady State Flow test at 76°C, 82°C, 88°C, and 94°C. Measurements of steady state viscosity are made over a range of 0.16 to 500 Pa stress. The viscosity values at 500 Pa are plotted versus temperature and mixing and compaction temperature ranges are determined at target values of 0.17±0.02 Pa·s and 0.35±0.03 Pa·s, respectively.	• Simple to perform, uses standard DSR equipment and testing procedures	• Can be time consuming for modified asphalts • Not all modified asphalts reach a state of steady shear by 500 Pa • Requires extrapolation of viscosity to much higher temperatures
Zero (Low) Shear Viscosity	Uses the rotational viscometer to determine the shear rate dependency of an asphalt binder at 3 temperatures (120, 135, 165°C). The Cross-Williams model is used to fit a curve to the data at each temperature from which the viscosity at a shear rate of 0.001 1/s is estimated. The low shear viscosities are plotted versus temperature and mixing and compaction temperature ranges are determined at target values of 3.0 Pa·s and 6.0 Pa·s, respectively.	• Takes into account the shear rate dependency of modified asphalt binders • Testing is simple to conduct • Results in lower mixing and compaction temperatures for modified asphalt binders	• May not accurately represent the shear thinning behavior of modified asphalt binders • Requires extrapolation of results to a low shear rate • Cross-Williams regression model is complicated • No clear agreement on definition of zero shear viscosity • Results for some binders yield unrealistically low mixing and compaction temperatures

(continued on next page)

Table 3. (Continued).

Method	Description	Advantages	Disadvantages
Mixture Workability	Uses a large stirring device to measure the torque required to stir a mix as it cools. Torque is inversely proportional to workability. The relationship between workability and temperature can be used to help establish temperature range where a mix is easiest to work.	• Considers the effects of aggregate particle shapes and size on compactability of mixtures	• New equipment • Time-consuming procedure • Not practical for routine use • Aggregate characteristics and gradation may overwhelm binder effects
Compaction Test	A standard mix is compacted with an unmodified "control" binder to establish a baseline density. The modified binder is then added to the standard mix and samples are compacted at temperature intervals. The temperature that provides the same density as the control binder is the compaction temperature for the modified binder.	• Easy to analyze based on density and volumetric properties	• Time-consuming procedure • SGC is insensitive to binder consistency • Only provides results for compaction temperature • Results are dependent on the "standard" mixture. Other mixes may provide different results.

As the aggregates compact more closely together, the compaction resistance and mixture strain is dominated more by the aggregate texture, shapes, and gradation. In a typical gyratory compaction record, the height change during the first gyration is 2.8 mm, and by the tenth gyration the height change is down to about 0.4 mm. The speed of gyration for SGC compactors is specified to be 30 gyrations per minute or 0.5 gyrations/sec. Multiplying the height changes by the gyration rate gives an approximate instantaneous vertical velocity within the compacting mixture. For the first gyration, it is 1.4 mm/s and for the tenth gyration, 0.2 mm/s. However, due to the fixed tilting angle, there is also a rotational shear. Using a 2-D approximation of this 3-D problem, the horizontal displacement for a 120-mm tall specimen gyrated at 1.16° is 2.43 mm. Figure 7 illustrates the shear movement during SGC compaction. As the specimen is compacted, the shear moves in the opposite direction for a total displacement of 4.86 mm within one-half of a gyration, which occurs in 1 second. Thus, at the top of the specimen, there is an approximate horizontal shear rate of 4.86 mm/s.

Resolving the vertical and horizontal shear movements yields

$$\sqrt{(1.4)^2+(4.86)^2}=5.06 mm/s.$$

Dividing this velocity by a nominal film thickness of 10 microns yields estimated shear rate of 506 1/s for the first gyration, with a slight reduction in shear rates as the compaction process continues. Note that this is very similar to the shear rate estimated for gyratory compaction by Yildirim et al. (*43*, *44*) based on experimental analyses.

Table 4. Summary of shear rates for some field and lab equipment.

Laboratory Device	Model #	RPM	Radius (in.)	Tangential velocity (mm/s)	shear rate (1/s)
Bucket mixer	KOL M-60	65	5.6	961	96,100
Pugmill mixer	7590-H	128	3.9	1341	134,100
Workability device	Instrotek	20	6.0	319	31,919
Bowl mixer	Hobart A200	48	4.0	425	42,558
Rotational viscometer	Brookfield DV-II+	20	8.4 mm	17.5	6.8
Dynamic Shear Rheometer		10rad/s	25 mm 8 mm		125 20

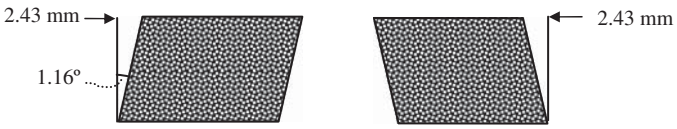

Figure 7. Illustration of horizontal strain during SGC compaction.

These are only estimates of shear rates at specific moments and locations during mixing and compaction. However, they show that shear rates during mixing and compaction are likely to be very different in the lab and in the field. It is also apparent that high rates occur at short instances of time. In reality, it is not reasonable to select a single shear rate that is representative of the extreme range of shear and flow of binder films on aggregate particles during mixing and compaction operations.

Summary of Key Findings from the Literature Review

Key findings from the literature search and state of practice survey for mixing and compaction temperatures are listed here.

1. The equiviscous concept for selecting mixing and compaction temperatures was established by the Asphalt Institute between 1956 and 1962 (*5, 7*). However, the methods used to establish the viscosity criteria are not known. Several studies in the 1950s reference mixing temperatures based on asphalt viscosity ranges (*2, 3, 4, 6*).
2. Criteria for mixing and compaction temperatures were initially based on viscosity measurements made with a Saybolt Furol viscometer (*4, 5, 6, 7, 8*).
3. Numerous studies have demonstrated that compaction temperatures have a significant effect on the mechanical properties of the fabricated specimens (*2, 3, 4, 6, 8, 13).*
4. Volumetric properties of asphalt mixtures compacted with SGC, on the other hand, appear to be insensitive to compaction temperature (*15, 16, 17*).
5. The use of the equiviscous concept for many polymer-modified asphalts results in excessively high mixing and compaction temperatures (*34, 35, 36*).
6. High mixing temperatures cause asphalt binders to harden, primarily through mechanisms of volatilization and oxidation (*24*). Most oxidation reactions approximately double as temperature increases by 10°C (*25*). Polymer additives in asphalt can break down at excessively high temperatures. However, the temperatures where these changes become detrimental are not clearly established (*28, 29, 36*).
7. High temperatures also cause emission and odor problems for some asphalt binders (*30, 31, 32*).
8. Most modified asphalt binders are shear rate dependent and exhibit shear thinning behavior (reduced viscosity at high shear rates).
9. In some cases, mixtures with polymer modified asphalts can be more difficult to work with in the field (*34*). However, in other cases, some mixtures with modified binders have been reported to be as workable as mixes with unmodified binders (*11*).
10. Most agencies use the equiviscous mixing and compaction criteria cited in AASHTO T 245 and T 312 (e.g., 0.17 ± 0.02 Pa·s for mixing and 0.28 ± 0.03 Pa·s for compaction) for unmodified asphalt binders. However, many agencies refer instead to the binder supplier for recommended mixing and compaction criteria even for unmodified binders.
11. Some countries use slightly higher viscosity ranges than given in AASHTO T 312 for setting mixing and compaction temperatures.
12. Supplier recommendations are most often used for setting mixing and compaction temperatures for polymer modified binders. Some agencies set their own criteria for modified binders.
13. Field experience (i.e., trial and error) has generally been used to determine appropriate mixing and compaction temperatures for modified binders.
14. For many agencies and suppliers, mixing and compaction temperature ranges are based on the Superpave PG of the binder.
15. Most agencies use the same mixing and compaction temperature ranges for laboratory testing and field operations of HMA production and construction. Some agencies specify a temperature range for plant produced HMA and reject mix outside of that range.
16. The Zero (or Low) Shear Viscosity concept has been shown to yield unrealistically low mixing and compaction temperatures for some binders.
17. Yildirim's method of estimating binder viscosities at high shear rates from rotational viscosity data attempts to take the shear rate dependency of modified binders into account. Although this method requires extrapolation of viscosity-shear rate data, reasonable mixing and compaction temperatures for a limited number of modified binders were demonstrated in the study.
18. Reinke's method of using a DSR steady shear flow test uses viscosity measurements taken at shear stress levels where binders appear to have Newtonian behavior. However, this method relies on extrapolating viscosity data to much higher temperature ranges.
19. Research has yet to clearly identify a reliable method of determining mixing and compaction temperatures for modified and unmodified asphalt binders.

CHAPTER 2

Research Approach

Experimental Plan

Approach

In developing the research approach for this study, several principles helped guide the plan for how and what should be investigated. As stated in the objective for this study, the desired outcome was the development of a *simple* and effective method for determining mixing and compaction temperatures for asphalt binders. The researchers have taken the approach that for the procedure to be simple, it should be based only on binder properties and not involve aggregates or mineral filler. It is recognized that this is a significant practical limitation, but to include interactions of asphalt and aggregate would complicate the matter greatly. The researchers also constrained the evaluation to candidate tests that utilize existing equipment found in typical asphalt binder labs.

Several candidate methods for determining mixing and compaction temperatures were examined in the experimental plan. An expectation was that some measure of binder consistency would be a good indicator of how well binders coat and lubricate aggregate particles during mixing and compacting. One concern was that there also may need to be a maximum mixing temperature to protect against overheating and damaging the binder during mixing. Therefore, some additional experimentation was conducted to evaluate binder degradation due to exposure to elevated temperatures.

However, in order to validate any simple binder procedure, a variety of mixture tests was considered necessary to characterize when the consistency of the binders is suitable for mixing with aggregates and subsequent handling and compacting of the mixtures. Since volumetric properties of asphalt mixtures compacted in SGC are insensitive to changes in binder consistency, other mix characteristics were examined to help identify temperatures that cause significant changes in the mixtures.

Since experience is an excellent guide for what has worked and what has caused problems with regard to mixing and compaction temperatures, consideration was given to such information. Accordingly, the equiviscous principle has worked well for unmodified binders. For modified binders, producers and users have found reasonable mixing and compaction temperatures for a wide variety of asphalt binders. These practical temperature ranges developed through field experience were used to check the reasonableness of the laboratory results.

Overview of the Experimental Research Plan

Based on the literature review and the guidance from the research panel, three candidate methods for selecting mixing and compacting temperatures were explored:

1. High shear rate viscosity,
2. Steady shear rate viscosity, and
3. A new approach based on the phase angle of binders.

The high shear rate viscosity approach is based on the hypothesis that modified binders are shear thinning and that the reason SGC compaction is insensitive to binder viscosity or moduli is because the compaction process is a high shear domain for asphalt coatings on aggregates. The viscosity data generated with this method are easy to obtain and indicate the shear rate dependency of binders through typical mixing and compaction temperature ranges.

The steady shear flow approach also takes into account the shear rate dependency of binders. Flow profiles for shear dependent binders show that viscosities tend to stabilize with increasing shear. The target shear stress of 490 Pascals was chosen by Reinke as a value where the viscosity measurements appeared more stable and within the capabilities of standard asphalt DSR. Although this approach requires viscosity-temperature data to be extrapolated to high temperatures outside of the range of most DSRs, the method is fairly simple and, based on a limited set of binders, appears to yield reasonable results for mixing and compaction temperatures.

The third candidate procedure was developed during this project. This technique considers the non-Newtonian viscoelastic behavior of binders as measured using standard asphalt DSR equipment. In dynamic testing, the phase angle is the measure of the time lag between the applied stress and the resulting measured strain. For dynamic shear rheology, the phase angle identifies the relative elastic and viscous response to shear and can be easily measured over a range of temperatures and frequencies. Therefore, it was logical to explore the phase angle as an alternate consistency parameter that could be used to establish mixing and compaction temperatures. Although phase angle is a fundamental material property, its relationship to coating and lubricating aggregate particles is empirical. However, this is also the case for viscosity at any shear rate.

Binders also were analyzed with regard to their potential for emissions and thermal degradation over a range of temperatures normally used for storage and mixing. The results from these were anticipated to aid in establishing upper limits for mixing temperatures in the field and the lab.

Mixture tests were performed to analyze the effects of temperature and binder consistency on aggregate coating, mix workability, lubrication and shear resistance during laboratory compaction, and the mechanical properties creep compliance and indirect tensile strength. The results of these tests were used to identify temperatures at which each binder provides similar mixture responses or where properties change significantly with temperature. The minimum temperature suitable for mixing should be based on how well the binder coats the aggregate in simulated plant mixing conditions. Two types of laboratory mixers were used to evaluate coating of binders on a base aggregate material at four temperatures. Coating percentages were evaluated by the Ross count method (ASTM D 2489).

Mix workability tests were included in the test plan to characterize how binder consistency affects the reaction of HMA mixtures to manipulation by equipment and manual tools. Workability is considered to be an intermediate state between mixing and compaction. The simple workability test was anticipated to show how different binders change how easy or how difficult a mixture is to handle.

Mix compaction tests were conducted with a SGC. Since many studies have shown that the densities of mixtures compacted in an SGC to a high number of gyrations are insensitive to binder consistency, compaction tests in this study used 25 gyrations. It was believed that differences due to binder consistency may be more apparent in the early part of the compaction process before aggregates lock up and dominate mixture shear resistance.

A diagram illustrating the experimental plan is shown in Figure 8. Part 1 included the series of binder tests that included testing of the 14 binders described in the following section using the candidate methods for determining mixing and compaction temperatures. Also included in Part 1 were the

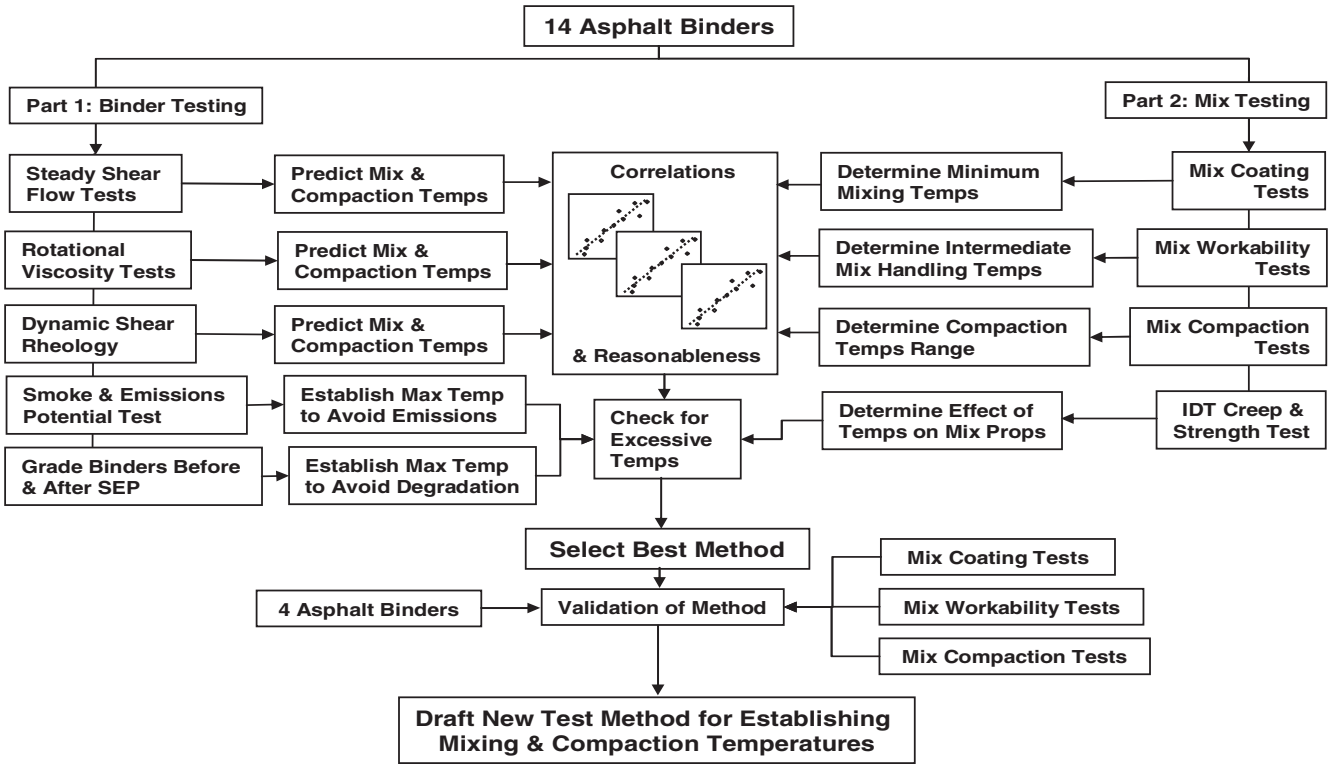

Figure 8. Diagram illustrating experimental test plan.

analyses of emissions and degradation potential of the 14 binders using the SEP test. Part 2 of the testing plan included conducting the series of mixture tests with the 14 binders. Selection of the best method for determining mixing and compaction temperatures would be based on how well the temperatures predicted using the candidate methods from Part 1 correlated with the temperatures needed for good coating, workability, and compaction as determined with the mixture tests in Part 2. Analysis of the SEP results and the change in binder properties before and after the SEP test were expected to provide information to be used for establishing maximum mixing temperatures so that emissions and/or binder degradation would not be a problem. Indirect tensile mixture tests also would be used to assess the need for upper limits for mixing temperatures.

A small validation experiment was planned using a set of four new binders with a range of grades and modification types. The validation testing of the binders would include testing of the binders with the selected candidate method and performing mix coating tests, workability tests, and compaction tests to see whether the predicted mixing and compaction temperatures provided reasonable results.

Materials

The experimental plan included 14 different binders that represent a range of commonly used U.S. binder grades, crude sources, and modifiers as well as a few more unique modifications systems. The list of binders with their reported grades, crude source, and modification systems is shown in Table 5. Throughout this report, data for modified binders are identified with shaded rows in tables. Also shown in Table 5 are the recommended mixing and compaction temperatures that the producers have provided to their customers. Inconsistencies in the recommended temperatures are apparent. Some suppliers recommend a single temperature, whereas others give a range of temperatures as wide as 18°F (10°C). Also, Binders B and C are different PG, but have the same exact recommended mixing and compaction temperatures. Binders G and H, which are both PG 76-22, have recommended mixing temperatures that differ by at least 10°F (6°C).

A set of four different binders were selected for validation testing of the method selected for establishing mixing and compaction temperatures. The validation binders set is shown in Table 6.

Organization of the Test Plan

As previously noted, the overall testing plan was divided into two parts. The first part dealt with testing binders and the second part involved testing those binders in aggregate mixtures. The mixture tests included in the experimental plan were not candidate procedures for establishing mixing and compaction temperatures. They were used in the experimental plan to eval-

Table 5. Binders included in the research.

Binder I.D.	Producer's Reported Binder Grade	Producer's Recommended Mixing Temperatures	Producer's Recommended Compaction Temperatures	Modification Type	Crude Source
B	**PG 64-40**	**302-320**	**284-311**	**SBS**	**Canada**
C	**PG 70-34**	**302-320**	**284-311**	**SBS**	**Canada**
D	PG 58-28	295-309	275-284	None	Alaskan Slope /Canada
E	PG 58-34	293-308	273-284	Air Blown	Canada
F	PG 64-22	315	295	None	North Sea
G	**PG 76-22**	**335**	**315**	**SBS + PPA**	**North Sea**
H	**PG 76-22**	**315-325**	**305-315**	**SBS**	**Venezuela**
I	PG 70-28	322-336	302-313	Air Blown	Alaskan Slope /Canada
J	PG 64-16	307-313	267-273	None	West Texas
K	PG 64-16	285-305	265-285	None	California Valley
L	**PG 76-22**	**320-330**	**290-300**	**18% Crumb Rubber**	**California Valley**
M	**PG 82-22**	**285-300**	**250-260**	**SBS + Sasobit®**	**Venezuela**
N	**PG 82-22**	**325-340**	**300-320**	**SBS**	**Mexico**
O	PG 64-28	313-324	291-300	None	Venezuela

Table 6. Binders for validation of proposed new method for establishing mixing and compaction temperatures.

Binder I.D.	Producer's Reported Binder Grade	Producer's Recommended Mixing Temperature	Producer's Recommended Compaction Temperature	Modification Type	Crude Source
W	**PG 82-22**	**345**	**325**	**SBS**	**Venezuela**
X	**PG 70-28**	**308-315**	**279-285**	**Elvaloy**	**North Sea**
Y	PG 64-22	314-327	293-302	None	Venezuela
Z	**PG 76-22**	**347-353**	**317-322**	**SBS + Air Blown**	**West Texas**

uate how the consistency of the binders affects mixing and compaction behavior. The mixture tests were a means to an end, the end being an independent set of measurements on the coatability and compactability to assess the predicted mixing and compaction temperatures from the candidate binder test methods. Unless noted otherwise, all testing was conducted at the National Center for Asphalt Technology (NCAT) laboratory.

Part 1: Binder Tests

For each binder, a series of tests or experiments were used to characterize properties of the binder and evaluate changes in high temperature binder properties. These tests were performed at temperatures that span typical mixing and compaction temperatures used for asphalt mixtures. The binder tests include the candidate procedures and additional tests to assess binder degradation.

The binder tests were

- Viscosity measurements using AASHTO T 316 to estimate traditional equiviscous temperatures.
- Steady shear flow viscosity from a DSR extrapolated to higher temperatures.
- Viscosity at various shear rates from a rotational viscometer extrapolated to high shear rates.
- Phase angle master curve from oscillation frequency sweeps using a DSR.
- Opacity (smoke) and mass loss measurements from the SEP test.
- Binder grading in accordance with AASHTO M 320 and Multiple Stress Creep Recovery (MSCR) tests following AASHTO TP 70 on binder samples before and after the SEP test to evaluate degradation.

Part 2: Mixture Tests

Mixture tests were included in the experimental plan to validate the predicted mixing and compaction temperatures from the candidate binder tests. For each of the study binders, mixture tests were used to establish relationships among temperature and coating, workability, and compactability. The mixture experiments included

- Mix coating tests using a laboratory bucket mixer and a laboratory pugmill mixer.
- Mix workability tests with the Instrotek workability device.
- Mix compaction tests using a specially equipped Pine Instruments SGC model AFG1A (i.e., baby Pine).
- Indirect tensile creep compliance and strength tests in accordance with AASHTO T 322.

Most of the mixture tests were based on a fine-graded Superpave mix design containing a blend of NCAT's lab standard granite aggregate. The mix design for this baseline mix is included in Appendix B. To further evaluate the effects of aggregate type, aggregate gradation, and RAP content, an additional compaction experiment was conducted with a subset of four binders. The subset of four binders selected for this mixture effects experiment were based on binders that exhibited distinctly different behaviors. A description of the mixtures used in this subset of tests is shown in Table 7. Fine and coarse gradations were to assess how aggregate particle size distributions affect mixing and compaction. The two aggregate types (granite and gravel) are distinctively different with respect to texture, shape, and absorption. Recycled asphalt pavement (RAP) also was included to evaluate the interaction of new asphalt and aged RAP binder.

Table 7. Mixture variations used in Compaction Experiment B.

Aggregate Type	Gradation Type	RAP Content
Granite	Fine	none
Granite	Fine	15%
Granite	Coarse	15%
Gravel	Fine	15%
Gravel	Coarse	15%

Description of Tests

Binder Tests

Equiviscous Tests. Rotational viscosity tests were conducted to establish the traditional equiviscous temperatures for mixing and compaction. These tests were performed at 135°C and 165°C with a Brookfield model DV-II+ Rotational Viscometer using a shear rate of 6.8 1/s.

High Shear Rate Viscosity. Following the method developed by Yildirim, viscosity measurements were also made with the Brookfield rotational viscometer at temperatures ranging from 120°C to 180°C (248°F to 356°F) in 15°C increments using as much of the range of shear rates possible with the instrument as each individual binder and temperature combination would allow. Example data are shown in Figure 9 and Figure 10. For binders that exhibit non-Newtonian behavior, a Cross-Williams model was fit to the viscosity-shear rate data to estimate viscosity of each binder corresponding at a shear rate of 500 1/s. High shear rate viscosities were plotted on a log viscosity versus log temperature chart, as shown in Figure 11, to determine mixing and compaction temperatures corresponding to 1.7 ± 0.02 Pa·s and 2.8 ± 0.03 Pa·s, respectively.

Steady Shear Flow. Steady shear flow viscosity measurements were made with a TA Model CSA DSR using parallel plate geometry and following the procedure recommended by Reinke (*45*). Steady shear flow tests with a DSR utilize a one directional turning action of the top plate with a constant stress. Viscosities were measured at three temperatures (76°C, 82°C, and 88°C) over a series of stress levels from 0.33 Pa to 500 Pa to evaluate shear dependency of the binders. Figure 12 shows example data obtained using Binder Y. The viscosities at 500 Pa measured for each temperature are then plotted using a log viscosity versus log temperature chart as seen in Figure 13 and extrapolated to obtain temperatures corresponding to 0.17 ± 0.02 Pa·s and 0.35 ± 0.03 Pa·s for mixing and compaction, respectively.

Phase Angle Method. This method, conceived and developed by John Casola as part of the study, is based on the observation that the phase angle from dynamic shear rheology is a consistency measure that takes into account the viscoelastic nature of asphalt binders. The development and testing of the Phase Angle method for this project was conducted at the Malvern Instruments facility in Southborough, MA.

The procedure consists of performing a frequency sweep on unaged binder using a DSR meeting Superpave PG binder testing requirements and employing the same geometries and temperatures used in routine PG binder grading. Tests were conducted at four temperatures, typically 50°C, 60°C, 70°C, and 80°C, and at frequencies from 0.001 to 100 rad/s with 10 points/decade. Strain was maintained at 12%. Data collected included

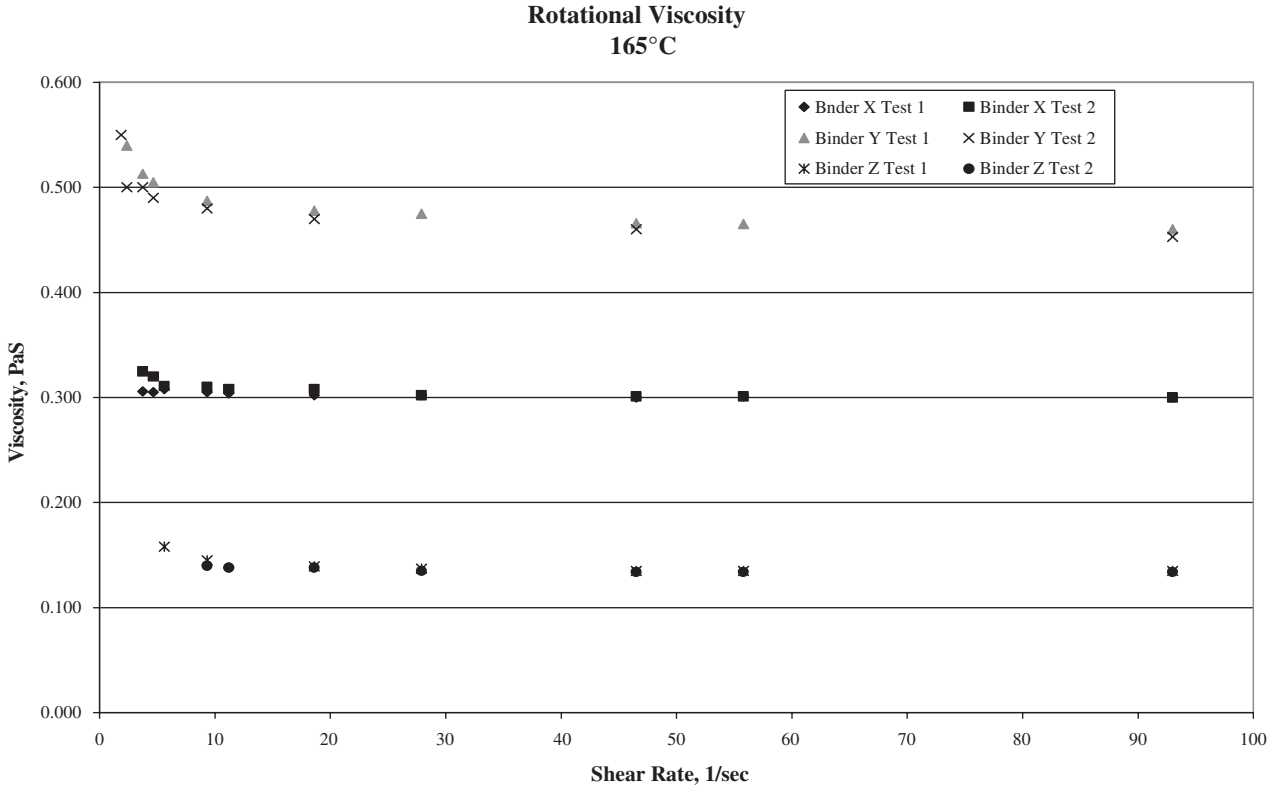

Figure 9. Example data from rotational viscosity test, viscosity at 165°C versus shear rate for three binders.

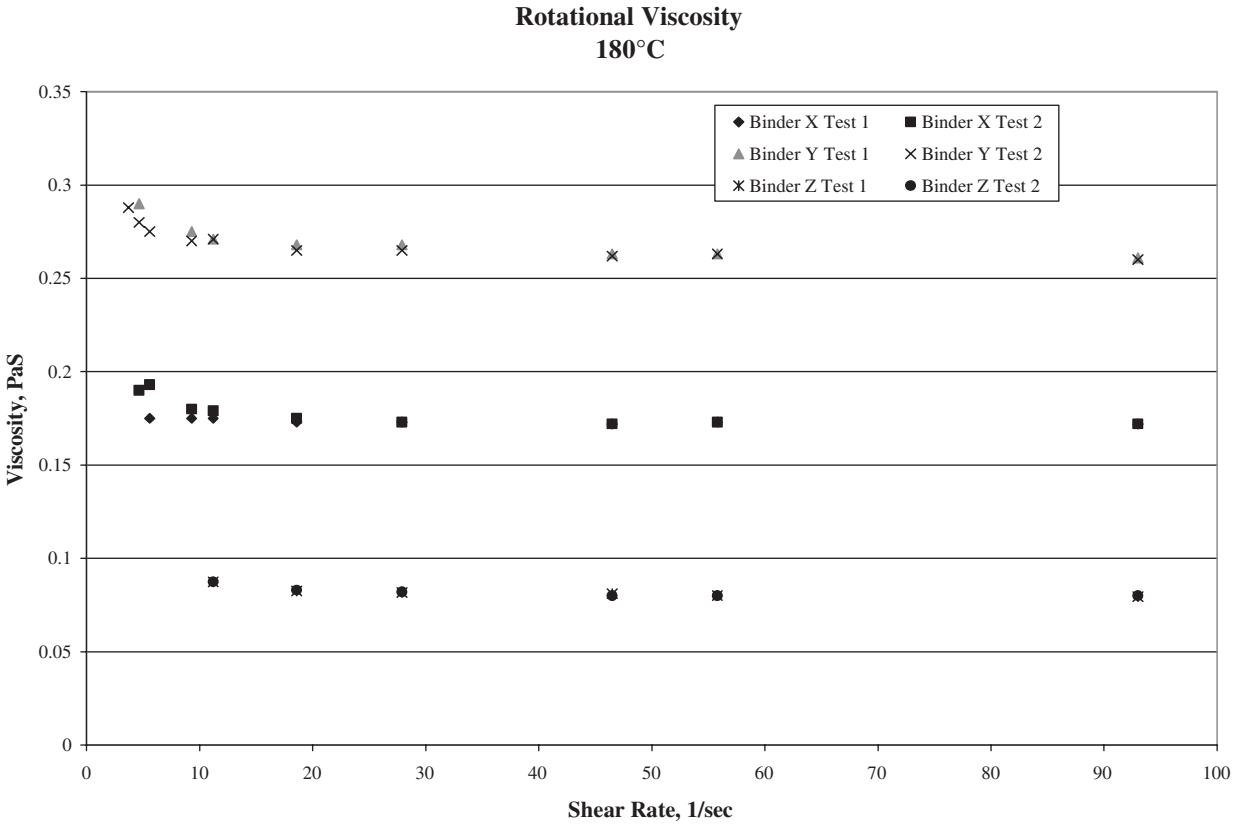

Figure 10. Example data from rotational viscosity test, viscosity at 180°C versus shear rate for three binders.

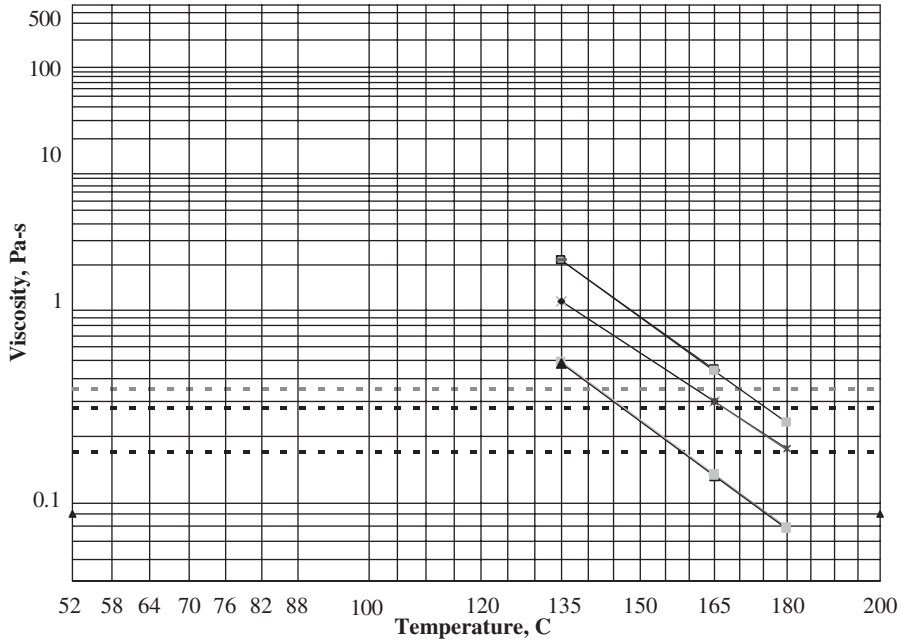

Figure 11. Temperature viscosity plot showing mixing and compaction temperatures for high shear viscosity method.

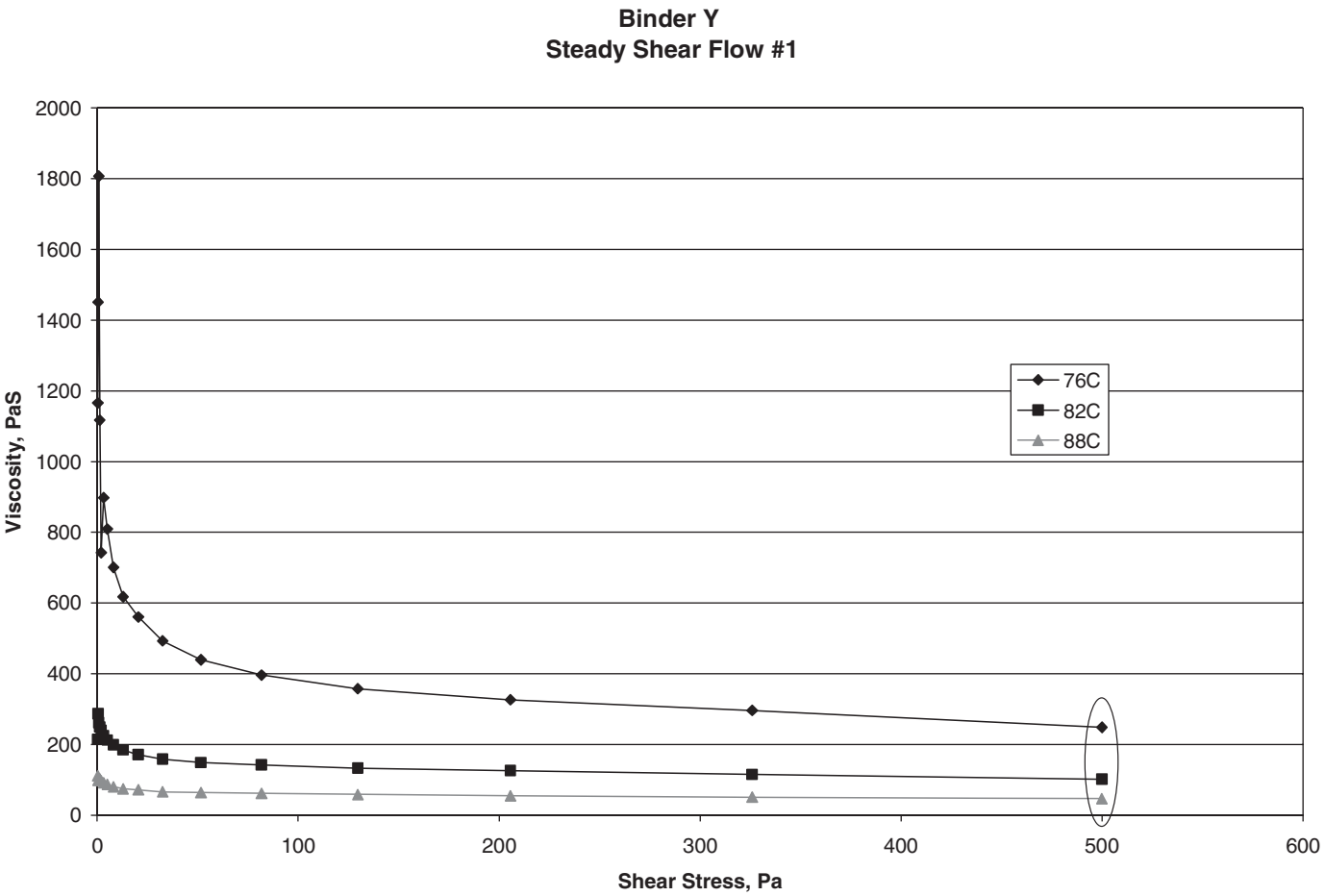

Figure 12. Example data of steady shear flow method, viscosity versus shear stress at three test temperatures.

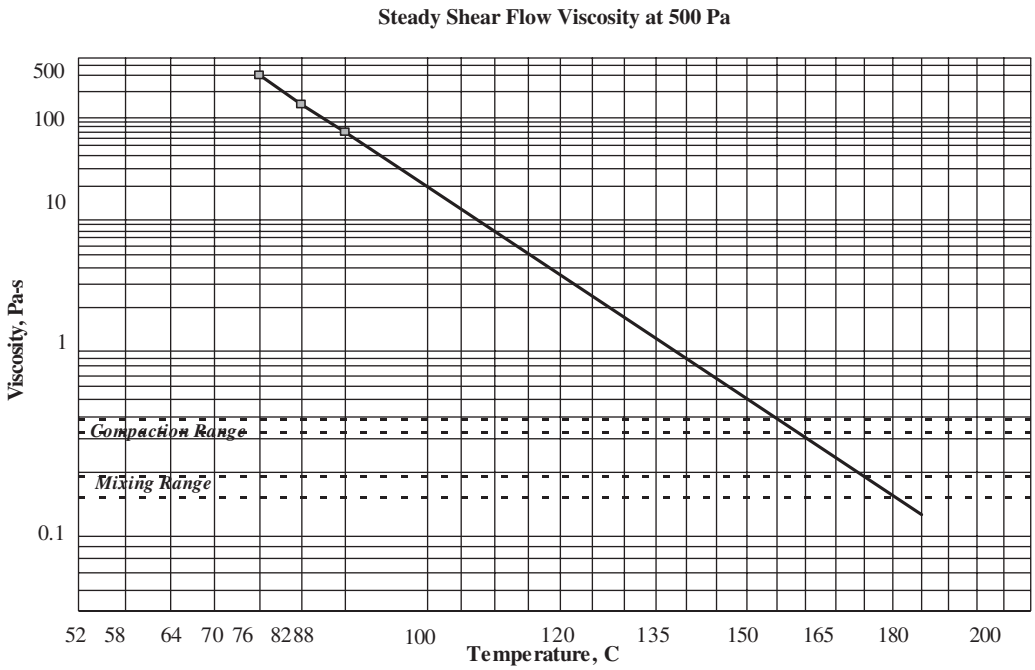

Figure 13. Example results of steady shear flow method, viscosity data from Figure 12 at 500 Pa shear stress extrapolated to determine mixing and compaction temperatures.

standard values of shear moduli, temperature, frequency, and phase angle. Phase angle master curves were developed from the data using a reference temperature of 80°C. This temperature range provides reliable phase angle resolution. Rheological testing of a wide variety of asphalt binders at temperatures above 135°C generally yields Newtonian behavior (phase angles at or very near 90°). The selection of 80°C as the reference temperature was also to avoid confusion with standard-grade high temperatures (e.g., 76°C, 82°C). Figure 14 shows phase angle and shear modulus master curves for a typical modified binder. The shear modulus is shown simply to verify the shifting of the data to construct the phase angle master curve. A smooth and straight shear modulus master curve illustrates a good data shift. The region of the phase angle master curve between $\delta = 90°$ and 85° represents the transition from purely viscous to visco-elastic behavior. Therefore, this is a region that can easily differentiate rheological behaviors among binders. The frequency corresponding to $\delta = 86°$ was selected as a reasonable reference point for this technique.

Casola established an initial relationship between this frequency and mixing temperature using the recommended plant mixing temperatures for each binder grade from the EC 101. A curve-fitting program was used to establish a preliminary power-law regression to fit the data:

$$\text{Mixing Temperature } (^\circ\text{F}) = 310\omega^{-0.01} \quad (2)$$

where the frequency, ω, is in radians/sec. Since the midpoints of recommended plant mixing temperatures in EC 101 are conservative toward lower temperatures, the preliminary frequency-temperature relationship yielded mixing temperatures that were considered lower than what are typically used in practice, particularly for modified binders. The frequency-mixing temperature regression equation was adjusted to balance the desire to increase the mixing temperatures, particularly for modified binders, with the aim to minimize differences with equiviscous mixing temperatures for unmodified binders. The resulting adjusted equation for mixing temperature using the Phase Angle method was

$$\text{Mixing Temperature } (^\circ\text{F}) = 325\omega^{-0.0135} \quad (3)$$

Figure 15 shows a plot of the EC 101 plant mixing temperature ranges and midpoints with the Phase Angle method results based on the preliminary and the adjusted frequency-mixing temperature relationships for the eight binders that have PG that are provided in the EC 101 guide. It can be seen that the preliminary equation yielded results closer to the EC 101 midpoint and the adjusted equation yielded results closer to the maximum of the EC 101 range. A correlation of the mixing temperatures using the adjusted Phase Angle method and the corresponding EC 101 maximum mixing temperature yielded the following regression:

Phase Angle method

$$T_M = 1.1 \times (EC\ 101\ T_{\max}) - 33, \quad R^2 = 0.92$$

Establishing a relationship between frequency and compaction temperature began with the observation that compaction temperatures for unmodified binders were typically 20°F to 25°F lower than the mixing temperature based on the equiviscous method. Using this simple offset, a similar power function to the one for mixing temperature was developed

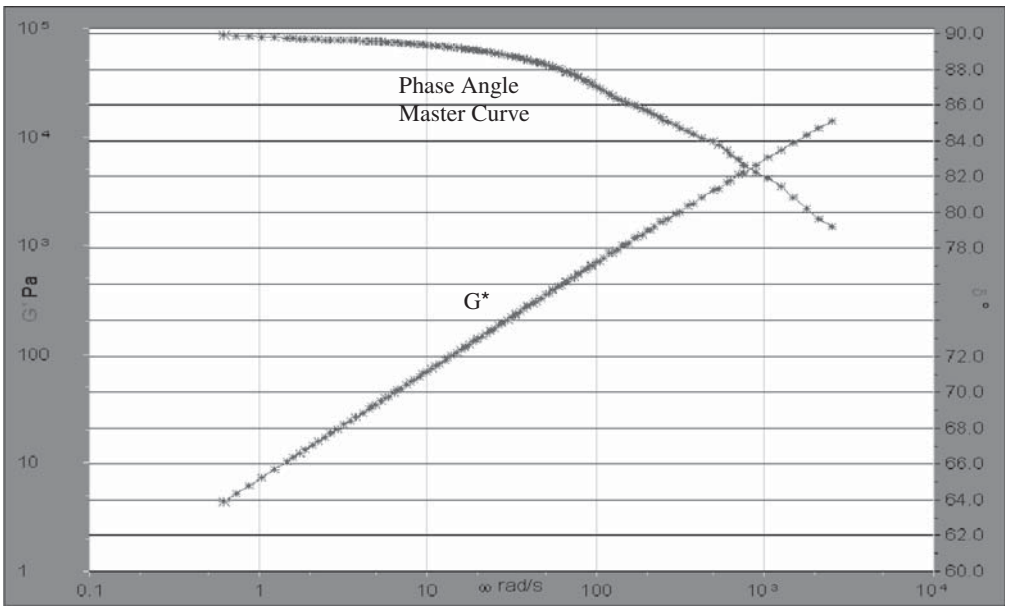

Figure 14. Phase Angle master curve of a typical modified asphalt.

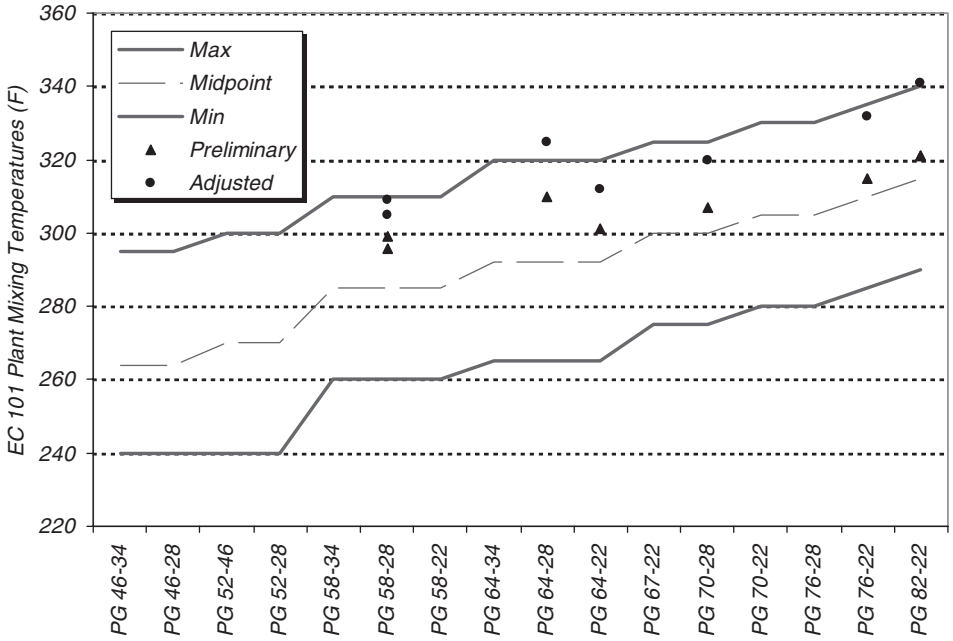

Figure 15. Plot showing results of the preliminary and adjusted Phase Angle mixing temperatures to the recommended mixing range from EC 101.

for compaction temperature. This relationship is shown as Equation 4:

$$\text{Compaction Temperature } (°\text{F}) = 300\omega^{-0.012} \quad (4)$$

Example results for two binders are used to illustrate the Phase Angle method for selecting mixing and compaction temperatures. Figure 16 shows the results of frequency sweep testing for an unmodified PG 52-34 and an SBS-modified PG 64-40. The figure shows that the PG 52-34 binder reached a phase angle of 86 at a frequency of 158.5 rad/sec, whereas the PG 64-40 binder crossed the reference phase angle at a frequency of 1.1 rad/sec. Using the temperature-frequency relationships in Equations 3 and 4, the mixing and compaction temperatures for the two binders are

- PG 52-34:
  - Mixing temperature = $325(158.5)^{-0.0135} = 303.5°\text{F}$
  - Compaction temperature = $300(158.5)^{-0.012} = 282.3°\text{F}$
- PG 64-40:
  - Mixing temperature = $325(1.1)^{-0.0135} = 324.6°\text{F}$
  - Compaction temperature = $300(1.1)^{-0.012} = 299.7°\text{F}$

SEP Test. All binders were tested using the SEP test developed by Stroup-Gardiner and Lange (*30*). All of the SEP tests except for those on the validation binders were performed by Stroup-Gardiner at Auburn University. This test utilized a Thermolyne moisture content oven equipped with an internal scale for measuring mass loss during heating. To quantify the amount of smoke emitted from the binders, an opacity meter was added to the oven's flue to continuously record the opacity. Asphalt samples were placed in thin film oven pans and loaded in a rack placed on the balance in the oven. The rack held five pans, each filled with 50 grams of asphalt binder. Tests were run for 2 hours at 130°C, 150°C, 170°C, and 190°C (266°F, 302°F, 338°F, and 374°F). Opacity, mass loss, and temperature were recorded versus time and temperature for each binder. Figure 17 illustrates opacity data for a binder tested at four temperatures.

Following the SEP tests, the binders were re-graded in accordance with AASHTO M 320 and also tested with the MSCR test following AASHTO TP 70-07. The binder properties of the original binders and binders recovered from the SEP tests were used to evaluate changes due to thermal degradation. The MSCR tests on the original unaged binders were conducted by the Turner-Fairbank Highway Research Center. Post SEP test binders were graded and tested at NCAT.

The MSCR test consists of a series of 1-second creep loading (constant stress) times followed by 9-second rest periods. The samples were loaded for 10 cycles each at creep loads of 25, 50, 100, 200, 400, 800, 1600, 3200, 6400, and 12,800 Pa. Test temperatures were 58°C, 64°C, 70°C, and 76°C.

An unmodified binder typically has low elasticity and, consequently, does not recover most of the deformation caused by the loading stress during the 9-second rest period. This results in a plot that resembles stair steps, with vertical rises during the 1-second loading period, and horizontal plateaus during the 9-second rest time. Unmodified binders accumulate unrecovered strain during the MSCR test. Binders that have been modified with elastomeric modifiers, on the other hand,

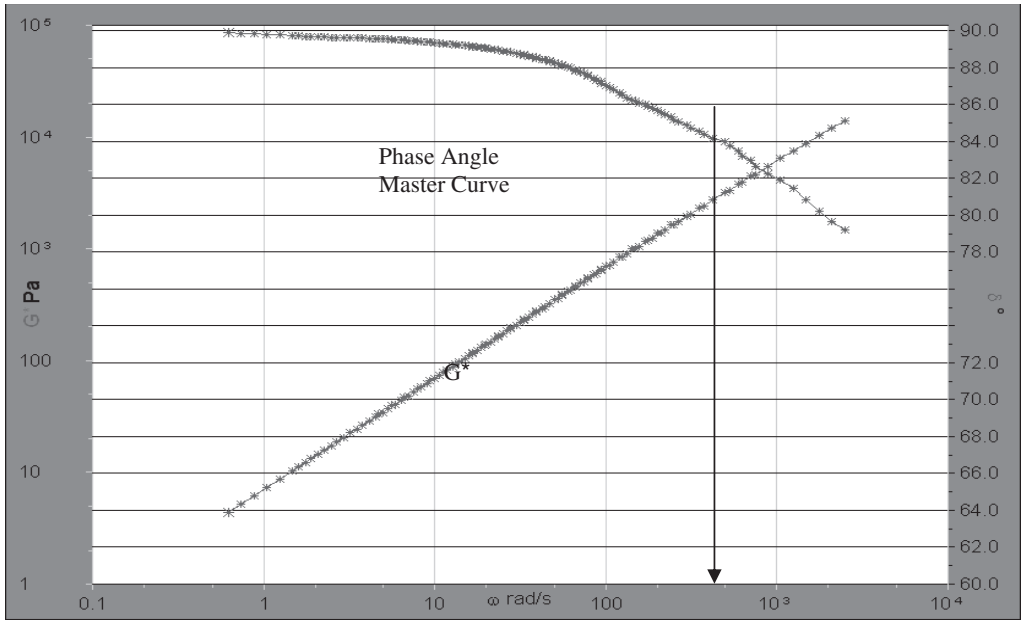

(a)

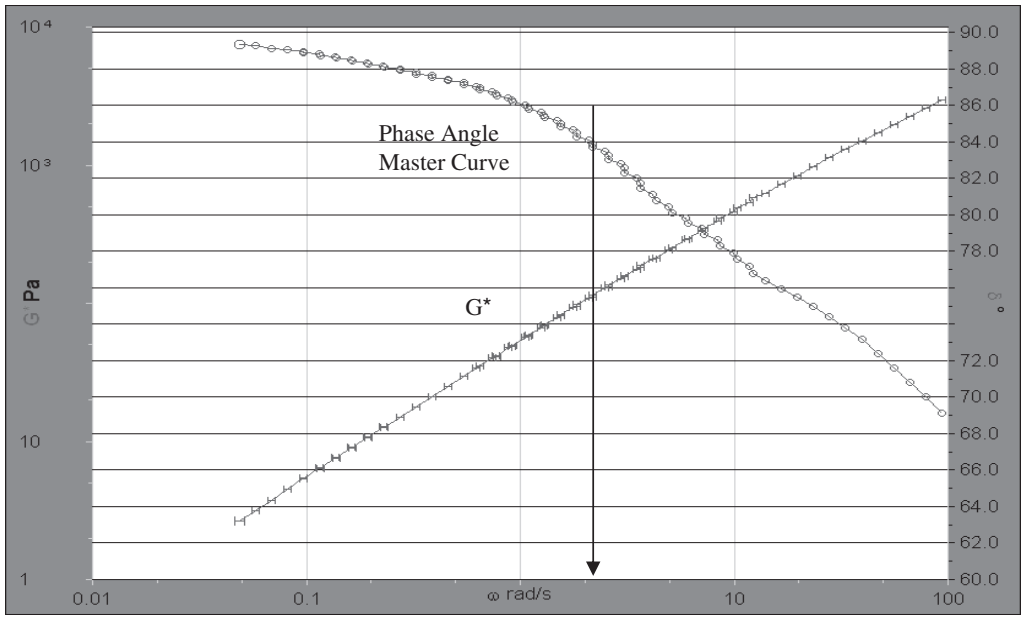

(b)

Figure 16. (a) Comparison of a PG 52-34 and (b) a PG 64-40 (bottom graph) at a Threshold Phase Angle of 86.

typically recover nearly all of the shear strain under the same conditions during the rest periods.

The output of the MSCR test is the nonrecovered compliance, Jnr, of the binder at each level of applied stress. For each stress level, the total amount of unrecovered strain is calculated using Equation 5:

$$\gamma_u = \varepsilon_{10} - \varepsilon_0 \quad (5)$$

where ε_{10} is strain at end of 10th cycle and ε_0 is strain at beginning of first cycle.

For each stress level, Jnr is calculated using Equation 6:

$$J_{nr} = \frac{\gamma_u}{\tau} \quad (6)$$

where γ_u is unrecovered strain and τ = applied stress, Pa.

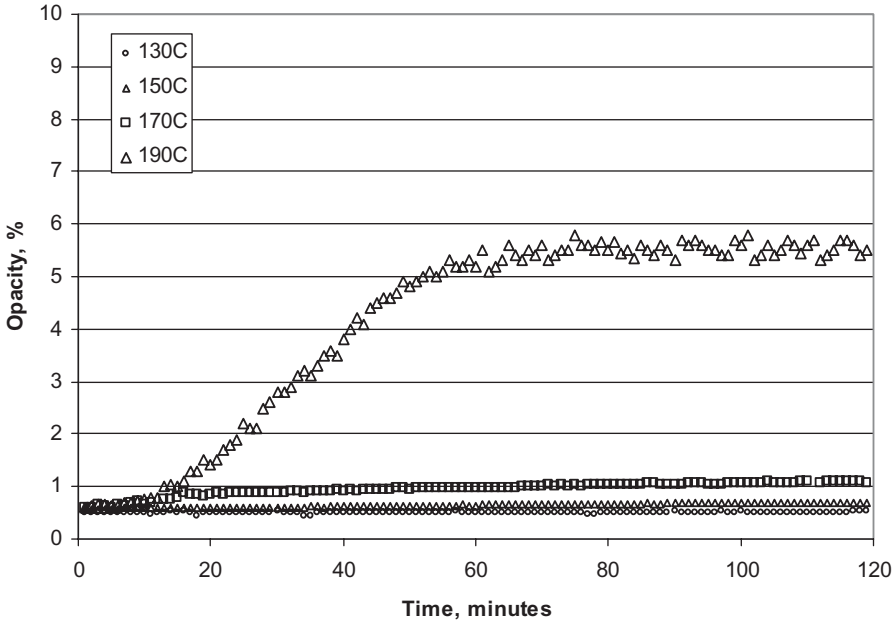

Figure 17. Example data from a SEP test, opacity measurements versus time for four temperatures.

Mixture Tests

Mix Coating Tests. Each of the binders was mixed with the baseline mix using a common bucket-type mixer and a laboratory pugmill mixer at four temperatures to evaluate coating of the binder on the aggregates. The two mixer types (bucket and pugmill) were selected because they provide reasonable simulations of the mixing action occurring in drum mix plants and batch plants. Ratings of mix coating were determined using the Ross count method, ASTM D 2489. Results of the coating tests for both mixer types were analyzed by developing regression equations based on a Sigmoid function of the form:

$$C = \frac{1}{1 + ae^{-b\,T}} \tag{7}$$

where C is the percentage coating at any temperature T, and a and b are regression constants. The regressions were used to estimate the coating percentage of the binders at any temperature. Using the equiviscous mixing temperatures of the unmodified binders, baseline coating percentages for the bucket mixer and the pugmill mixer were determined to be 98% and 89%, respectively. The temperatures to achieve these coating percentages for the modified binders were then estimated with the regression equations. Results of the coating percentages for both mixer types were correlated to mixing temperatures from the candidate methods.

An additional coating experiment was conducted to assess the effect of residual aggregate moisture on how well asphalt binders coat the aggregate. The motivation for this experiment was that in the field, aggregate stockpiles are often wet and the plant's drier may not completely dry the moisture from the coarse aggregate before mixing with the asphalt binder. As residual moisture escapes the aggregate and expands to steam, the asphalt binder can be foamed, which greatly increases it volume and enhances the coating process. The procedure used for this experiment was as follows:

1. The baseline mix with granite aggregate was batched to 4,600 grams and then split into coarse (+4.75 mm) and fine fractions.
2. The coarse aggregate fraction was placed in a deep pan, covered with water, then placed in an oven overnight at 210°F. The fine aggregate fraction was heated in a separate oven at about 20°F above the target mixing temperature, either 248°F, 284°F, 320°F, or 356°F.
3. The heated coarse and fine aggregate were combined in the pugmill mixer, and the combined blend was heated with a propane blowtorch until the blend reached the target mixing temperature. For higher mixing temperatures, the blowtorch heating took as much as 20 minutes.
4. The asphalt was added (161.2 grams) to the aggregate in the mixer and mixing continued for 1 minute.
5. The mixture was discharged from the pugmill and immediately sieved on a 2.36-mm sieve, and the coarse aggregate particles were retained for later assessment of percentage coating in accordance with the Ross count method.

This experiment included four binders selected following the main coating experiment as having a wide range of coating results.

Mixture Workability Test. Initially, the workability tests were to be performed with each of the binders and the baseline mixture containing granite aggregate. After several early workability test trials, a decision was made to change from the granite mix to a standard 0.6-mm silica sand to reduce raw data noise that could possibly have been due to binding of aggregate particles between the paddle tips and the workability bowl. An asphalt content of 5.1% was used for the sand mixtures used in the workability tests.

The sand-binder mixtures were short-term oven aged at 180°C (356°F), then transferred to the NCAT workability device to measure the resistance to shearing in the loose state as it cools to approximately 120°C (248°F). The workability device is a large fixed bucket with a two-pronged paddle that is rotated at a constant speed. Twenty-kilogram mix samples were prepared and then dumped into the heated workability bucket. The torque required to turn the paddle through the binder-sand mix as it cooled in the bucket was automatically recorded every second along with the binder-sand temperature.

The raw torque data was filtered to remove extraneous instrument noise in a three-step process using Microsoft Excel. A 60-second running average and standard deviation of the raw torque values were calculated in the first step. Then, at each second, a moving range was calculated as the 60-second average torque plus and minus the 60-second standard deviation. Finally, raw torque data outside of this 1-sigma range were removed. The filtered torque versus temperature data were plotted, and a second-order polynomial equation was fitted to the data with a least-squares regression. An example of the workability test data is shown in Figure 18.

Mix Compaction Tests. Two compaction experiments were conducted. The main compaction experiment consisted of testing the 13 binders mixed with the baseline mixture. This experiment examined the effect of the main experimental factors, binder type and compaction temperature, on changes in the lab compacted density and shear resistance of a single mixture. The second, smaller compaction experiment consisted of testing four unique binders mixed with four other mix designs. Selection of the four unique binders was based on materials that provided a range of binder properties. The additional mix designs include different aggregate types, particle shapes, gradations, and RAP contents. The results from this experiment provide an indication of the range of compaction temperatures necessary to provide good compactability for different mix types. All mix compaction samples were mixed at 150°C (302°F), then short-term oven aged and compacted in an SGC at four temperatures: 110°C, 130°C, 150°C, and 170°C (230°F, 266°F, 302°F, and 338°F).

Indirect Tensile Creep Compliance/Strength Tests. Since indirect tensile creep compliance and strength are highly dependent on binder properties, this test was used to assess how compaction temperatures affect tensile properties of two mixtures. Specimens were prepared with each of the binders mixed in the baseline mix design and tested in accordance with AASHTO T 322 and the recommendations from *NCHRP Report 530* (*51*). The effect of compaction temperature on compliance and strength was analyzed.

Summary of Research Plan

The experimental plan involved testing and analysis of a variety of binders to characterize their visco-elastic responses over the range of temperatures for typical field operations. The testing utilized DSR and rotational viscosity equipment

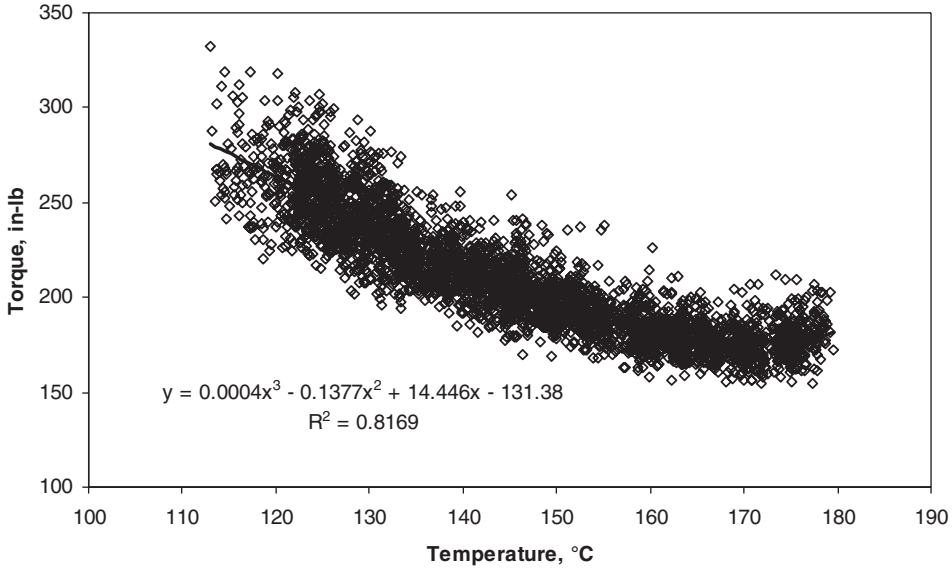

Figure 18. Example results from a workability test, torque versus temperature.

common to Superpave binder laboratories. Binders were also analyzed with regard to their potential for emissions and thermal degradation.

Mixture tests were performed to analyze how temperature and different binders affect aggregate coating, mix workability, shear resistance during laboratory compaction, and mechanical properties. The results from these mix tests were used to identify appropriate mixing and compaction temperatures for each binder. These temperatures were then correlated to predicted mixing and compaction temperatures from the candidate binder tests. The study recommends a new method for establishing mixing and compaction temperatures based on the simplest method that provides the best correlation statistics. A small validation experiment with an independent set of binders from a range of crude sources and with a range of properties and modification types was used to verify the selected method as a viable new procedure for determining mixing and compaction temperatures of asphalt binders.

CHAPTER 3

Findings and Applications

Experimental Results

Binder Testing

This section summarizes the results from all of the binder tests including Superpave performance grading of the binders, mixing temperatures from the equiviscous method and the three candidate methods, SEP tests, multi-stress creep recovery tests, and analyses of binder degradation following the SEP test.

Binder Grading

Table 8 lists the Superpave performance grades of the binders as reported by the supplier/producer and the results of the grading conducted by NCAT. In this table and in all subsequent tables showing the study binders, the binders are sorted by their high temperature true grade as a simple way of putting the binders in a rational order. Modified binders are identified by shaded rows.

Binder L, which contained ground tire rubber as a modifier, was not able to be graded or tested in DSR equipment due to apparent incompatibility of the rubber particles and the asphalt. Therefore, binder L was not included in the results or analysis.

Based on NCAT's binder grading results, nearly half of the binders did not meet the requirements for the Superpave binder grade as reported by the supplier. The discrepancies between the producer's grades and the results from NCAT were mostly due to low temperature properties. Binder G actually met a higher grade than the supplier reported. However, the differences between the reported grade and NCAT results are generally fairly small and probably not significant considering lab variability of the tests. The NCAT results are used throughout the analysis to sort the binders and to serve as a baseline for evaluating changes due to heating the binders to elevated temperatures.

High Shear Rate Viscosity Method

Table 9 shows the mixing and compaction temperature results from the high shear rate viscosity tests performed using Yildirim's approach. The table also shows the mixing and compaction temperatures from the equiviscous method for comparison. It can be seen from these data that the temperatures from the high shear rate viscosity method are very similar to the equiviscous method for most of the binders. Mixing temperatures for all of the modified binders are greater than 350°F, with most above 360°F. Since modified binder results from the high shear viscosity method are excessive and the method provides essentially no improvement compared with the equiviscous method, further analysis of the high shear rate viscosity method is not included in this report.

Steady Shear Flow Method

Table 10 shows the results from the Steady Shear Flow method. These mixing and compaction temperatures are substantially lower than the equiviscous mixing and compaction temperatures. The differences between the two methods are greater for modified binders, which indicates that many of these binders exhibit shear thinning (i.e., lower viscosity at higher shear rates) behavior. The steady shear flow method also yields lower mixing and compaction temperatures for the unmodified binders: in most cases, the mixing temperatures are more than 10°F lower than the equiviscous mixing temperatures.

Phase Angle Method

Mixing and compaction temperatures determined using the Phase Angle method are shown in Table 11. For the modified binders, the mixing and compaction temperatures using the Phase Angle method are substantially lower than from the equiviscous method. For the unmodified binders,

Table 8. True grades of the research binders as determined by NCAT.

Binder ID	Producer's Reported Binder Grade	NCAT results True Grade	Grade Confirmed? Yes/No	Comments
M	**PG 82-22**	**85.5 -19.5**	**No**	**Failed BBR**
N	**PG 82-22**	**84.3 -25.5**	**Yes**	
G	**PG 76-22**	**82.5 -24.2**	**No**	**Met higher grade**
H	**PG 76-22**	**78.3 -26.1**	**Yes**	
C	**PG 70-34**	**75.1 -38.9**	**Yes**	
I	PG 70-28	71.8 -29.2	Yes	
B	**PG 64-40**	**69.3 -37.3**	**No**	**Failed BBR**
F	PG 64-22	67.8 -21.3	No	Failed DTT
O	PG 64-28	65.6 -29.7	Yes	
K	PG 64-16	65.3 -13.0	No	Failed BBR & DTT
J	PG 64-16	64.3 -20.7	Yes	
E	PG 58-34	60.9 -33.1	No	Failed BBR
D	PG 58-28	60.3 -26.0	No	Failed DTT

some of the mixing and compaction temperatures from the Phase Angle method are lower and some are higher than from the equiviscous method.

SEP Tests

Table 12 shows a summary of the opacity results from the SEP tests on the binders. Although these data show that emissions increase with higher temperatures, the amount and rate of emissions increase differs among the binders.

In order to properly compare the SEP opacity results for the binders in the experiment, the midpoint of the producer's recommended mixing temperature range for each respective binder was determined and opacity was interpolated at this temperature. This, in effect, normalized the opacity data to an appropriate reference temperature for each binder. These opacity values were then ranked and graphed in Figure 19.

It can be observed from the SEP opacity data there is no apparent link between opacity and binder high grade, binder low grade, grade spread, or whether the binder is modified. Even binders from the same crude source—such as Binders B, C, and E, which were refined from the same Canadian crude—had markedly different opacity results. This finding

Table 9. Mixing and compaction temperatures from the high shear rate viscosity method.

Binder ID	True Grade	Mixing Temperature °F (°C)		Compaction Temperature °F (°C)	
		Equiviscous Method	High Shear Rate Viscosity	Equiviscous Method	High Shear Rate Viscosity
M	**85.5 -19.5**	**372 (189)**	**363 (184)**	**343 (173)**	**336 (169)**
N	**84.3 -25.5**	**433 (223)**	**433 (223)**	**401 (205)**	**401 (205)**
G	**82.5 -24.2**	**379 (193)**	**372 (189)**	**352 (178)**	**349 (176)**
H	**78.3 -26.1**	**365 (185)**	**363 (184)**	**338 (170)**	**338 (170)**
C	**75.1 -38.7**	**388 (198)**	**385 (196)**	**355 (179)**	**352 (178)**
I	71.8 -29.2	333 (167)	333 (167)	311 (155)	311 (155)
B	**69.3 -37.3**	**354 (179)**	**352 (178)**	**325 (163)**	**325 (163)**
F	67.8 -21.3	320 (160)	318 (159)	298 (148)	297 (147)
O	65.6 -29.7	318 (159)	318 (159)	293 (145)	297 (147)
K	65.3 -13.0	295 (146)	295 (146)	271 (132)	275 (135)
J	64.3 -20.7	295 (146)	295 (146)	275 (135)	273 (134)
E	60.9 -33.1	293 (145)	293 (145)	273 (134)	297 (147)
D	60.3 -31.7	295 (146)	297 (147)	275 (135)	279 (137)

Table 10. Mixing and compaction temperatures from the steady shear viscosity method.

Binder ID	True Grade	Mixing Temperature °F (°C)		Compaction Temperature °F (°C)	
		Equiviscous Method	Steady Shear Flow Viscosity	Equiviscous Method	Steady Shear Flow Viscosity
M	**85.5 -19.5**	**372 (189)**	**296 (147)**	**343 (173)**	**275 (135)**
N	**84.3 -25.5**	**433 (223)**	**337 (169)**	**401 (205)**	**311 (155)**
G	**82.5 -24.2**	**379 (193)**	**340 (171)**	**352 (178)**	**312 (156)**
H	**78.3 -26.1**	**365 (185)**	**333 (167)**	**338 (170)**	**304 (151)**
C	**75.1 -38.7**	**388 (198)**	**320 (160)**	**355 (179)**	**291 (144)**
I	71.8 -29.2	333 (167)	316 (158)	311 (155)	289 (143)
B	**69.3 -37.3**	**354 (179)**	**325 (163)**	**325 (163)**	**295 (146)**
F	67.8 -21.3	320 (160)	309 (154)	298 (148)	281 (138)
O	65.6 -29.7	318 (159)	309 (154)	293 (145)	280 (138)
K	65.3 -13.0	295 (146)	280 (138)	271 (132)	257 (125)
J	64.3 -20.7	295 (146)	289 (143)	275 (135)	263 (128)
E	60.9 -33.1	293 (145)	293 (145)	273 (134)	269 (132)
D	60.3 -31.7	295 (146)	289 (143)	275 (135)	262 (128)

does not agree with the conclusion from Stroup-Gardiner and Lange (*31*). Another example is the set of binders refined from the blend of Alaskan slope and Canadian crudes, D and I. These two binders also have substantially different opacity results at the producer's recommended mixing temperature.

Another measurement from the SEP test is the mass loss of the binders due to exposure to high temperatures. A summary of the mass loss results are shown in Table 13. Mass loss also increased with higher SEP test temperatures for all of the binders. As with opacity, there does not appear to be a relationship between mass loss and binder high grade, low grade, grade spread, modified versus unmodified, or crude source.

Mass loss and opacity are not strongly correlated, as shown in Figure 20. The trend shows that higher mass loss generally corresponds to higher opacity, but the relationship is not suitable to use one measurement to predict the other. For some binder samples, mass loss may include the loss of molecular water rather than purely a loss of volatile organic components that would be better associated with opacity and changes in physical properties of the binder.

Table 11. Mixing and compaction temperatures from the Phase Angle Method.

Binder ID	True Grade	Freq. at δ =86° T=80°C	Mixing Temp. °F (°C)		Compaction Temp. °F (°C)	
			Equiviscous Method	Phase Angle Method	Equiviscous Method	Phase Angle Method
M	**85.5 -19.5**	**0.07**	**372 (189)**	**337 (169)**	**343 (173)**	**310 (154)**
N	**84.3 -25.5**	**0.03**	**433 (223)**	**341 (172)**	**401 (205)**	**313 (156)**
G	**82.5 -24.2**	**0.03**	**379 (193)**	**341 (172)**	**352 (178)**	**313 (156)**
H	**78.3 -26.1**	**0.22**	**365 (185)**	**332 (167)**	**338 (170)**	**305 (152)**
C	**75.1 -38.7**	**0.21**	**388 (198)**	**332 (167)**	**355 (179)**	**306 (152)**
I	71.8 -29.2	2.98	333 (167)	320 (160)	311 (155)	296 (147)
B	69.3 -37.3	1.10	354 (179)	325 (163)	325 (163)	300 (149)
F	67.8 -21.3	75.00	320 (160)	307 (153)	298 (148)	285 (141)
O	65.6 -29.7	21.12	318 (159)	312 (156)	293 (145)	289 (143)
K	65.3 -13.0	800	295 (146)	297 (147)	271 (132)	277 (136)
J	64.3 -20.7	580	295 (146)	298 (148)	275 (135)	278 (137)
E	60.9 -33.1	37.85	293 (145)	309 (154)	273 (134)	287 (142)
D	60.3 -31.7	122.56	295 (146)	305 (152)	275 (135)	283 (139)

Table 12. Opacity results from SEP test.

ID	True Grade	Avg. opacity (%) at test temp.				Std. dev. of opacity at test temp.			
		130°C 266°F	150°C 302°F	170°C 338°F	190°C 374°F	130°C 266°F	150°C 302°F	170°C 338°F	190°C 374°F
M	**85.5 -19.5**	**0.28**	**4.80**	**4.80**	**11.63**	**0.07**	**0.06**	**0.06**	**0.13**
N	**84.3 -25.5**	**0.35**	**0.39**	**0.42**	**0.79**	**0.09**	**0.05**	**0.04**	**0.05**
G	**82.5 -24.2**	**0.00**	**1.16**	**1.45**	**2.13**	**0.14**	**0.06**	**0.05**	**0.06**
H	**78.3 -26.1**	**0.22**	**2.83**	**5.27**	**13.21**	**0.11**	**0.08**	**0.4**	**0.78**
C	**75.1 -38.7**	**3.11**	**8.68**	**8.68**	**16.46**	**0.12**	**0.11**	**0.11**	**0.68**
I	71.8 -29.2	0.23	4.41	10.21	16.62	0.08	0.22	0.54	1.09
B	**69.3 -37.3**	**0.51**	**1.39**	**4.92**	**8.45**	**0.08**	**0.08**	**0.31**	**0.61**
F	67.8 -21.3	0.00	1.09	1.16	2.12	0.09	0.07	0.05	0.05
O	65.6 -29.7	0.26	0.14	5.35	11.84	0.12	0.17	0.34	0.76
K	65.3 -13.0	0.00	3.17	7.02	19.26	0.09	0.06	0.26	0.48
J	64.3 -20.7	0.22	3.37	8.94	12.94	0.09	0.07	0.14	0.36
E	60.9 -33.1	0.55	2.48	8.50	27.40	0.08	0.12	0.56	0.87
D	60.3 -31.7	0.07	2.53	5.23	7.53	0.05	0.11	0.24	0.64

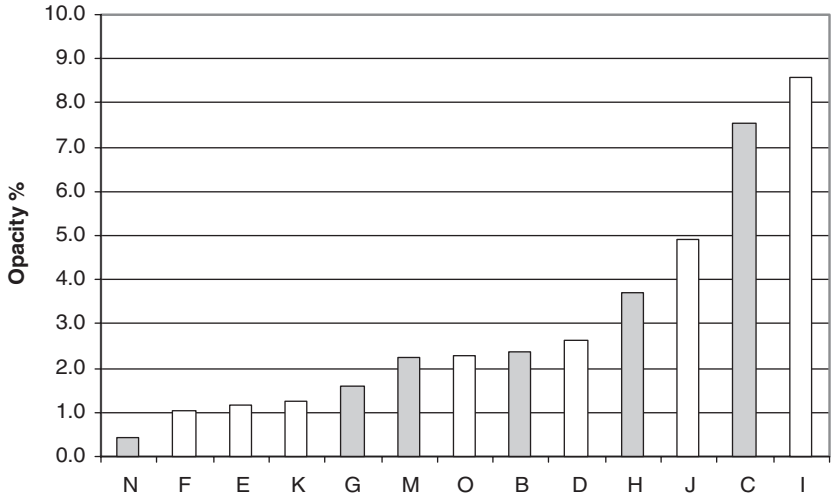

Figure 19. Ranked opacity results after normalizing to the midpoint of the producer's recommended mixing temperature.

Table 13. Mass loss results from SEP Test.

ID	True Grade	Avg. Mass Loss (%)				Std. Dev. of Mass Loss (%)			
		130°C 266°F	150°C 302°F	170°C 338°F	190°C 374°F	130°C 266°F	150°C 302°F	170°C 338°F	190°C 374°F
M	**85.5 -19.5**	**0.09**	**0.18**	**0.11**	**0.43**	**0.02**	**0.03**	**0.03**	**0.02**
N	**84.3 -25.5**	**0.31**	**0.55**	**1.99**	**2.76**	**0.09**	**0.06**	**0.06**	**0.06**
G	**82.5 -24.2**	**0.01**	**0.11**	**0.15**	**0.35**	**0.03**	**0.02**	**0.03**	**0.02**
H	**78.3 -26.1**	**0.02**	**0.23**	**0.23**	**0.20**	**0.03**	**0.03**	**0.02**	**0.02**
C	**75.1 -38.7**	**0.12**	**0.01**	**0.12**	**1.07**	**0.04**	**0.02**	**0.02**	**0.05**
I	71.8 -29.2	0.12	0.23	0.63	1.09	0.03	0.02	0.03	0.04
B	**69.3 -37.3**	**0.31**	**0.01**	**0.34**	**0.95**	**0.07**	**0.02**	**0.04**	**0.05**
F	67.8 -21.3	0.12	0.09	0.06	0.09	0.04	0.03	0.04	0.02
O	65.6 -29.7	0.23	0.41	0.65	0.73	0.02	0.03	0.02	0.03
K	65.3 -13.0	0.06	0.20	0.20	0.51	0.04	0.03	0.02	0.03
J	64.3 -20.7	0.00	0.00	0.69	1.16	0.01	0.01	0.02	0.07
E	60.9 -33.1	0.00	0.12	0.56	1.11	0.01	0.03	0.02	0.06
D	60.3 -31.7	0.00	0.28	0.39	1.07	0.03	0.05	0.04	0.05

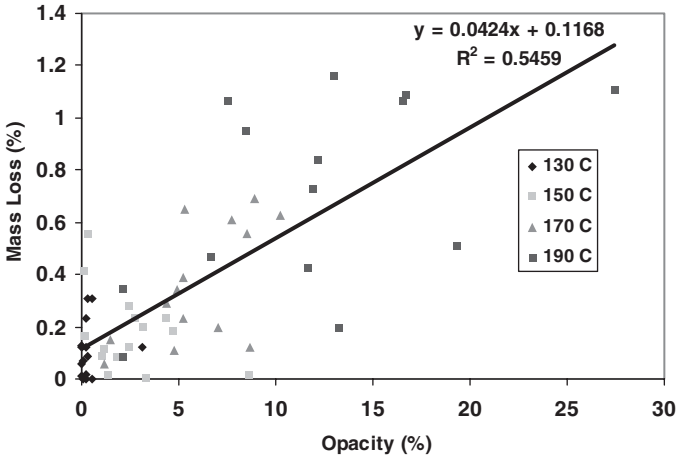

Figure 20. Comparison of mass loss and opacity data.

Results of Re-Graded Binders

Binder grading results for the original binder materials and the residues from the SEP tests are shown in Table 14. True grades for the samples are shown based on the critical low temperatures determined from the bending beam rheometer (BBR) test and the direct tension test (DTT). Also shown are the phase angles for each binder at the high PG temperature. These results are discussed in a later section regarding analysis of binder degradation.

MSCR Tests

Table 15 is a summary of the results from the MSCR tests. The information shown in this table is the non-recoverable creep compliance results that indicate the degree to which a binder recovers shear strains resulting from a range of stresses. Binders that are modified with elastomeric polymers will typically exhibit a high degree of recovery or, inversely, have very low values of non-recoverable compliance. Following the AASHTO TP 70 protocol, binders are normally tested after rolling-thin-film oven (RTFO) conditioning at the binder's high PG temperature. However, initial MSCR tests on RTFO-aged samples after the SEP procedure showed that the RTFO aging masked the effects of the SEP tests. Therefore, no RTFO conditioning was performed on the SEP-conditioned binders to better assess the effects of the SEP temperatures on the binders. For this study, the binders were tested after four temperatures (58°C, 64°C, 70°C, and 76°C) in the SEP test. MSCR tests were conducted on the original and SEP conditioned binder samples. Results are reported as non-recoverable creep compliance, Jnr, at two standard levels of stress, 100 and 3200 Pa.

Example plots of the change in Jnr with increasing test temperature and SEP conditioning are shown in Figures 21 and 22. Results for a modified Binder, H, are shown in Figure 21, and the results of an unmodified Binder, E, are shown in Figure 22. Note that the y-axis (Jnr) scales of these graphs are different. For all of the modified binders, the maximum Jnr was less than 20 1/Pa. However, for the unmodified binders, much of the data was above this level and, in one case (as shown in Figure 22), exceeded 100 1/Pa. Further analysis of these results is provided in the next section.

Analysis of Binder Degradation

Four binder characteristics were examined for evidence of binder degradation due to exposure to high temperatures:

- Changes in the true grade critical high temperature of the binders;
- Changes in the true grade critical low temperature of the binders;
- Changes in the phase angle of the binders at their respective grade temperatures; and
- Changes in the MSCR non-recoverable creep compliance.

Table 16 shows the change in the critical high temperatures, that is, the change in critical high temperature from the original, unaged binder to the re-graded binder after SEP conditioning at each temperature (i.e., SEP residue T_c – Original T_c). The data show that the critical high temperatures increased with higher SEP temperatures. Increases in high temperature grades are considered beneficial to rutting resistance. This trend is expected since exposure to high temperatures increases molecular size through oxidation and polymerization and therefore stiffens the binders. The three binders with the greatest increase in the critical high temperature were I, O, and H. The high temperature grade for the air-blown Binder I changed the most with a two-grade increase. Those that changed the least were unmodified Binder K and modified Binder C, with an increase in critical high temperature of 4.6°C and 4.4°C, respectively. Although there are differences among the binders in the magnitude of change of the high temperature grade due to the SEP conditioning, there is no evidence of binder degradation from this data.

Table 17 shows the change in the critical low temperature for the binders. For most binders, the critical low temperature after the SEP testing was based on the DTT. Overall, the low critical temperatures typically increased several degrees from the original binders, but not enough to change the grade for most binders. This indicates that pavements with these binders would be only slightly more likely to experience thermal cracking after exposure to the temperatures in the SEP test. Binders that had the greatest increase in critical low temperature were I, J, N and O. Of these, J, N, and O barely had a one-grade change at the low temperature end; Binder I did not change low temperature grade. There was no general trend of increasing critical low temperature with higher temperatures, and most modified binders increased slightly less than the unmodified binders. Therefore, there is no strong evidence of

Table 14. Results of grading of binders before and after SEP testing.

		SEP Test Temperature, °C				
Binder	Test	Original	130	150	170	190
M	**Original DSR**	**85.4**	**91.7**	**89.6**	**92.1**	**95.6**
	Phase Angle @ 82°C	**65.8**	**64.1**	**65.2**	**65.8**	**62.4**
	RTFO DSR	**65.8**	**64.1**	**65.2**	**65.8**	**62.4**
	PAV DSR	**24.1**	**23.0**	**25.4**	**26.7**	**26.9**
	BBR Stiffness	**-26.4**	**-27.3**	**-26.1**	**-28.7**	**-27.7**
	BBR *m*-value	**-19.5**	**-17.7**	**-16.4**	**-17.3**	**-17.3**
	DTT	**-24.8**	**-17.7**	**-17.3**	**-19.6**	**-21.5**
	True Grade - BBR	**85.4 -19.5**	**88.4 -17.7**	**89.6 -16.4**	**90.8 -17.3**	**92.2 -17.3**
	True Grade - DTT	**85.4 -24.8**	**88.4 -17.7**	**89.6 -17.3**	**90.8 -19.6**	**92.2 -21.5**
N	**Original DSR**	**96.6**	**88.9**	**94.6**	**98.7**	**97.7**
	Phase Angle @ 82°C	**70.0**	**69.6**	**71.4**	**66.5**	**66.1**
	RTFO DSR	**84.3**	**83.0**	**85.7**	**88.9**	**91.0**
	PAV DSR	**15.0**	**25.7**	**23.2**	**20.2**	**24.3**
	BBR Stiffness	**-33.1**	**-23.5**	**-24.4**	**-30.0**	**-30.5**
	BBR *m*-value	**-25.5**	**-22.3**	**-24.1**	**-23.8**	**-27.0**
	DTT	**-27.8**	**-18.4**	**-20.3**	**-20.5**	**-20.8**
	True Grade - BBR	**84.3 -25.5**	**83.0 -22.3**	**85.7 -24.1**	**88.9 -23.8**	**91.0 -19.5**
	True Grade - DTT	**84.3 -27.8**	**83.0 -18.4**	**85.7 -20.3**	**88.9 -20.5**	**91.0 -20.8**
G	**Original DSR**	**82.5**	**89.9**	**90.6**	**90.4**	**89.9**
	Phase Angle @ 76°C	**67.1**	**64.0**	**63.3**	**61.8**	**63.1**
	RTFO DSR	**85.5**	**94.3***	**87.9**	**88.7**	**89.8**
	PAV DSR	**20.3**	**22.5**	**22.2**	**18.6**	**20.9**
	BBR Stiffness	**-27.1** °	**-27.2**	**-25.8**	**-28.1**	**-26.7**
	BBR *m*-value	**-24.2**	**-24.3**	**-23.4**	**-23.5**	**-22.3**
	DTT	**-25.6**	**-23.9**	**-22.3**	**-24.3**	**-21.2**
	True Grade - BBR	**82.5 -24.2**	**89.9 -24.3**	**87.9 -23.4**	**88.7 -23.5**	**89.8 -22.3**
	True Grade - DTT	**82.5 -25.6**	**89.9 -23.9**	**87.9 -22.3**	**88.7 -24.3**	**89.8 -21.2**
H	**Original DSR**	**78.7**	**81.5**	**85.9**	**86.3**	**88.4**
	Phase Angle @ 76°C	**72.3**	**70.2**	**68.4**	**67.7**	**66.7**
	RTFO DSR	**78.3**	**82.3**	**79.7**	**75.3**	**88.0**
	PAV DSR	**20.3**	**22.0**	**22.7**	**25.3**	**26.3**
	BBR Stiffness	**-27.9**	**-28.0**	**-26.9**	**-26.8**	**-27.3**
	BBR *m*-value	**-27.7**	**-28.0**	**-27.3**	**-26.0**	**-26.4**
	DTT	**-26.1**	**-23.7**	**-22.4**	**-21.0**	**-22.7**
	True Grade - BBR	**78.3 -27.7**	**81.5 -28.0**	**79.7 -26.9**	**86.3 -26.0**	**88.0 -26.4**
	True Grade - DTT	**78.3 -26.1**	**81.5 -23.7**	**79.7 -22.4**	**86.3 -21.0**	**88.0 -22.7**
C	**Original DSR**	**77.8**	**79.3**	**85.3**	**80.0**	**91.3**
	Phase Angle @ 70°C	**62.4**	**64.0**	**63.6**	**63.3**	**57.2**
	RTFO DSR	**75.1**	**76.2**	**76.6**	**77.9**	**79.5**
	PAV DSR	**6.7**	**6.7**	**9.0**	**7.0**	**12.6**
	BBR Stiffness	**-39.6**	**-39.0**	**-41.0**	**-42.7**	**-41.0**
	BBR *m*-value	**-38.9**	**-38.1**	**-38.1**	**-40.3**	**-38.1**
	DTT	**-34.9**	**-36.8**	**-36.1**	**-37.7**	**-28.2**
	True Grade - BBR	**75.1 -38.9**	**76.2 -38.1**	**76.6 -38.1**	**77.9 -40.3**	**79.5 -38.1**
	True Grade - DTT	**75.1 -34.9**	**76.2 -36.8**	**76.6 -36.1**	**77.9 -37.7**	**79.5 -28.2**
I	Original DSR	71.8	77.3	76.5	81.9	84.6
	Phase Angle @ 70°C	80.2	78.2	77.8	74.8	73.4
	RTFO DSR	74.8	78.3	79.9	80.6	83.9
	PAV DSR	17.5	20.1	18.9	22.1	22.6
	BBR Stiffness	-34.8	-33.9	-39.0	-30.8	-35.9
	BBR *m*-value	-29.2	-28.3	-27.8	-28.0	-23.3
	DTT	-25.8	-27.0	-25.4	-23.8	-23.2
	True Grade - BBR	71.8 -29.2	77.3 -28.3	76.5 -27.8	80.6 -28.0	83.9 -23.3
	True Grade - DTT	71.8 -25.8	77.3 -27.0	76.5 -25.4	80.6 -23.8	83.9 -23.2

Table 14. (Continued).

B	**Original DSR**	**69.3**	**72.8**	**72.6**	**74.4**	**75.7**
	Phase Angle @ 64°C	**71.8**	**68.7**	**68.9**	**67.1**	**65.6**
	RTFO DSR	**69.8**	**71.1**	**71.6**	**72.4**	**74.5**
	PAV DSR	**10.4**	**10.9**	**10.9**	**11.1**	**12.4**
	BBR Stiffness	**-37.3**	**-37.8**	**-38.5**	**-38.5**	**-38.3**
	BBR *m*-value	**-37.9**	**-37.7**	**-36.5**	**-36.2**	**-36.6**
	DTT	**-34.1**	**-34.9**	**-35.1**	**-33.0**	**-34.1**
	True Grade - BBR	**69.3 -37.3**	**71.1 -37.7**	**71.6 -36.5**	**72.4 -36.2**	**74.5 -36.6**
	True Grade - DTT	**69.3 -34.1**	**71.1 -34.9**	**71.6 -35.1**	**72.4 -33.0**	**74.5 -34.1**
F	Original DSR	68.4	71.6	72.4	74.3	73.6
	Phase Angle @ 64°C	83.5	85.4	85.2	83.6	83.6
	RTFO DSR	67.8	70.2	71.1	76.5	74.3
	PAV DSR	30.5	31.5	25.4	26.0	33.1
	BBR Stiffness	-24.9	-23.4	-24.0	-23.6	-23.9
	BBR *m*-value	-23.5	-22.8	-22.7	-25.0	-22.2
	DTT	-21.3	-18.7	-18.2	-15.9	-18.5
	True Grade - BBR	67.8 -23.5	70.2 -22.8	71.1 -22.7	74.3 -14.1	73.6 -22.2
	True Grade - DTT	67.8 -21.3	70.2 -18.7	71.1 -18.2	74.3 -15.9	73.6 -18.5
O	Original DSR	65.6	69.1	70.2	74.1	76.0
	Phase Angle @ 64°C	79.2	83.5	82.9	80.3	78.8
	RTFO DSR	68.2	70.5	71.0	73.6	77.7
	PAV DSR	19.2	20.1	20.6	20.2	22.1
	BBR Stiffness	-29.7	-27.9	-28.0	-27.7	-27.3
	BBR *m*-value	-30.1	-27.5	-27.5	-27.5	-26.8
	DTT	-30.2	-23.8	-23.6	-22.8	-22.0
	True Grade - BBR	65.6 -29.7	69.1 -27.5	70.2 -27.5	73.6 -27.5	76.0 -26.8
	True Grade - DTT	65.6 -30.2	69.1 -23.8	70.2 -23.6	73.6 -22.8	76.0 -22.0
K	Original DSR	66.1	68.9	69.8	70.8	71.3
	Phase Angle @ 64°C	89.1	88.0	86.7	88.1	88.3
	RTFO DSR	65.3	67.1	67.3	68.3	69.9
	PAV DSR	32.4	32.1	32.2	32.3	33.7
	BBR Stiffness	-13.0	-11.6	-13.8	-11.7	-11.0
	BBR *m*-value	-15.8	-15.8	-15.8	-15.0	-14.1
	DTT	-14.5	-9.0	-12.0	-10.9	-11.5
	True Grade - BBR	65.3 -13.0	67.1 -11.6	67.3 -13.8	68.3 -11.7	69.9 -11.0
	True Grade - DTT	65.3 -14.5	67.1 -9.0	67.3 -12.0	68.3 -10.9	69.9 -11.5
J	Original DSR	64.3	69.1	71.6	72.0	74.8
	Phase Angle @ 64°C	89.4	86.9	88.4	88.2	86.6
	RTFO DSR	64.7	69.2	69.4	71.2	72.4
	PAV DSR	27.0	31.1	27.9	29.1	30.0
	BBR Stiffness	-21.2	-19.0	-23.9	-22.2	-29.8
	BBR *m*-value	-20.7	-19.7	-21.2	-20.5	-19.5
	DTT	-21.0	-14.3	-14.5	-13.6	-13.4
	True Grade - BBR	64.3 -20.7	69.1 -19.0	69.4 -21.2	71.2 -20.5	72.4 -19.5
	True Grade - DTT	64.3 -21.0	69.1 -14.3	69.4 -14.5	71.2 -13.6	72.4 -13.4
E	Original DSR	63.2	62.8	63.4	66.0	69.5
	Phase Angle @ 58°C	83.0	82.7	82.4	81.1	78.6
	RTFO DSR	60.9	63.9	65.6	65.9	71.3
	PAV DSR	13.2	13.0	12.7	14.9	14.3
	BBR Stiffness	-36.7	-35.2	-35.1	-34.8	-35.0
	BBR *m*-value	-33.1	-35.2	-32.5	-34.4	-31.2
	DTT	-34.7	-30.6	-29.4	-30.0	-29.2
	True Grade - BBR	60.9 -33.1	62.8 -32.5	63.4 -32.5	65.9 -34.4	69.5 -31.2
	True Grade - DTT	60.9 -34.7	62.8 -30.6	63.4 -29.4	65.9 -30.0	69.5 -29.2
D	Original DSR	60.3	62.4	64.8	65.2	67.6
	Phase Angle @ 58°C	86.7	85.5	84.3	84.0	83.1
	RTFO DSR	61.5	62.7	63.2	64.7	65.9
	PAV DSR	15.5	15.2	14.8	15.1	15.1
	BBR Stiffness	-31.7	-32.3	-31.8	-32.4	-31.1
	BBR *m*-value	-32.5	-33.1	-29.6	-31.9	-32.7
	DTT	-26.0	-29.2	-29.4	-29.0	-28.7
	True Grade - BBR	60.3 -31.7	62.4 -32.3	63.2 -29.6	64.7 -31.9	65.9 -31.1
	True Grade - DTT	60.3 -26.0	62.4 -29.2	63.2 -29.4	64.7 -29.0	65.9 -28.7

Table 15. Summary of non-recoverable creep compliance (Jnr, 1/Pa) results from the MSCR tests.

Binder ID	Temp, °C	100 Pa Stress					3200 Pa Stress				
		Unaged	130	150	170	190	Unaged	130	150	170	190
M	**58**	**0.0500**	**0.0474**	**0.3260**	**0.1727**	**0.0801**	**0.1000**	**0.1385**	**0.1326**	**0.1034**	**0.0685**
	64	**0.0790**	**0.0906**	**0.1581**	**0.3835**	**0.0677**	**0.3200**	**0.2146**	**0.4109**	**0.3815**	**0.1955**
	70	**0.1200**	**0.2653**	**0.5203**	**0.7644**	**0.4954**	**1.1600**	**0.9883**	**1.2364**	**1.0724**	**0.7160**
	76	**0.1900**	**1.2122**	**2.9427**	**1.8101**	**0.8002**	**4.3400**	**3.5709**	**3.7888**	**3.2963**	**2.2566**
N	**58**	**0.0700**	**0.1168**	**0.0626**	**0.0898**	**0.0830**	**0.1000**	**0.1721**	**0.1075**	**0.0752**	**0.0650**
	64	**0.1400**	**0.2719**	**0.1100**	**0.2053**	**0.4125**	**0.2600**	**0.4889**	**0.2553**	**0.2035**	**0.2313**
	70	**0.3200**	**1.6612**	**0.4064**	**0.1997**	**1.8000**	**0.8100**	**3.2819**	**0.5446**	**0.4046**	**0.9200**
	76	**0.6400**	**1.3371**	**0.1698**	**1.2114**	**3.8847**	**2.5100**	**4.2000**	**3.4903**	**1.0648**	**2.3238**
G	**58**	**0.1212**	**0.6695**	**0.9805**	**0.1026**	**0.0795**	**0.1380**	**0.1643**	**0.2130**	**0.0738**	**0.0892**
	64	**0.2216**	**0.2820**	**0.4007**	**0.2440**	**0.0710**	**0.2766**	**0.2127**	**0.3105**	**0.2366**	**0.1446**
	70	**0.3761**	**0.4049**	**0.6539**	**0.5106**	**0.5207**	**0.5261**	**0.5818**	**0.7040**	**0.4514**	**0.4505**
	76	**0.6632**	**1.5013**	**0.9277**	**0.7518**	**0.6698**	**1.3357**	**1.2024**	**1.8758**	**1.3503**	**0.9594**
H	**58**	**0.4600**	**0.6478**	**0.4793**	**0.2325**	**0.2693**	**0.5900**	**0.3988**	**0.2392**	**0.2360**	**0.2935**
	64	**1.0500**	**1.0481**	**1.0372**	**0.5652**	**0.8394**	**1.5800**	**0.8867**	**0.7175**	**0.6685**	**0.5154**
	70	**2.6800**	**0.6555**	**2.2746**	**1.5635**	**0.7825**	**4.5700**	**2.2220**	**1.7273**	**2.0313**	**1.1710**
	76	**5.7200**	**3.8550**	**4.2959**	**3.4807**	**2.0714**	**10.4800**	**5.4825**	**5.1347**	**5.2013**	**3.2522**
C	**58**	**1.0137**	**0.9253**	**0.3740**	**0.2232**	**0.2759**	**1.0075**	**0.5853**	**0.3754**	**0.3605**	**0.2803**
	64	**0.3326**	**1.2603**	**0.7737**	**0.9677**	**0.4490**	**1.7533**	**1.3344**	**1.1739**	**1.8443**	**0.7928**
	70	**0.3690**	**2.8768**	**2.1784**	**2.2559**	**1.8240**	**5.5538**	**4.8275**	**3.5356**	**3.9806**	**2.5025**
	76	**5.4942**	**7.1843**	**4.3437**	**4.5098**	**2.7163**	**13.2738**	**12.5172**	**7.7141**	**11.6331**	**7.5678**
I	58	2.4612	1.2553	1.0379	0.5284	0.0386	2.8189	1.0503	1.2532	0.7221	0.4895
	64	3.6981	2.2093	1.6739	0.9204	0.1364	5.8972	2.9856	2.5595	1.6446	1.4043
	70	14.5110	4.8845	4.4979	2.8155	1.7774	15.4491	7.3369	7.4084	4.8200	2.9999
	76	17.6200	11.6020	6.4407	1.7802	9.4055	27.6559	16.3003	14.7119	8.3325	10.0338
B	**58**	**1.1572**	**1.4219**	**0.2614**	**0.7081**	**0.6351**	**2.3519**	**0.9589**	**0.7046**	**0.7697**	**0.7519**
	64	**2.5669**	**0.3968**	**0.9438**	**1.2274**	**1.5359**	**6.6602**	**2.7654**	**2.6778**	**1.8109**	**2.3599**
	70	**6.4338**	**1.5680**	**2.0909**	**3.5332**	**3.8034**	**16.4549**	**6.7619**	**5.0541**	**5.5288**	**6.5341**
	76	**18.4670**	**3.5533**	**6.7418**	**5.7535**	**0.3094**	**34.8406**	**12.4888**	**11.9631**	**10.7913**	**11.4966**
F	58	2.9939	1.1228	2.2369	1.5380	2.1366	3.5428	2.7608	2.7867	2.5458	2.5664
	64	7.1896	6.1727	5.6663	3.7491	4.5189	8.6328	7.5444	6.9656	6.0781	5.8350
	70	15.5393	13.3200	12.2410	9.0157	10.6770	18.7640	16.4963	15.0584	12.9425	13.4653
	76	32.0430	27.0610	24.8970	23.0810	23.8840	38.9281	33.0313	30.3894	30.4113	27.9788
O	58	6.0360	3.5217	2.8005	1.1717	0.4555	5.6938	4.5128	3.6350	2.3061	1.9970
	64	10.3100	7.2912	2.4976	2.9879	2.0882	12.2366	10.3097	7.4744	5.7025	4.6595
	70	21.7490	14.6570	12.8270	8.1640	2.7960	28.1559	22.5944	17.2275	13.2616	11.6398
	76	27.2230	27.5810	24.8370	18.0570	8.1853	40.2125	41.9750	32.6094	25.0438	19.3758
K	58	4.8934	3.6084	1.8297	0.4587	1.6453	5.7784	4.4663	4.2838	3.3775	2.6775
	64	10.9300	5.4157	4.8001	6.5832	3.4524	12.1772	9.5750	9.9984	9.2616	6.8888
	70	22.3350	17.0770	16.5430	15.0000	13.2470	32.8875	24.7503	24.4169	21.0691	17.9931
	76	35.2620	41.5150	34.8630	13.1870	14.8320	59.6625	53.2031	53.8750	38.6406	35.0313
J	58	5.4921	3.5265	2.7391	2.4878	0.7402	6.2943	4.5581	4.0203	3.3891	3.2017
	64	13.8943	7.1120	6.4143	4.6326	0.6629	16.1071	10.9047	7.8103	7.3150	7.2913
	70	29.3687	19.7640	11.8350	10.7630	9.2671	34.1458	26.0844	19.8675	16.7050	14.5859
	76	58.7047	39.6080	12.1270	25.2900	16.7150	67.6948	51.0125	40.7594	36.2156	35.7234
E	58	11.3737	7.9921	3.0642	4.3426	2.2957	14.3829	10.7188	7.8388	8.2328	3.9384
	64	23.5373	16.9930	13.4830	6.4829	4.7986	29.4433	22.8119	18.1700	15.7816	8.7728
	70	46.0083	21.6180	22.2620	16.4600	9.0460	57.6240	47.0094	39.0000	27.7828	19.0259
	76	92.1573	79.8670	64.1290	38.6380	28.6420	114.3906	92.6563	75.8344	56.0125	39.7531
D	58	10.1716	3.7658	6.0801	4.0700	4.9074	12.1819	8.7575	8.5525	7.0372	6.3491
	64	22.0473	14.0720	10.7090	11.4250	9.5916	26.5592	19.2153	18.1231	12.6216	14.0603
	70	44.5693	32.5280	23.3700	12.6540	17.1720	53.3438	41.9750	40.8813	30.4881	26.8969
	76	83.0037	34.6660	48.3080	47.1410	40.3310	99.6958	45.4875	74.5125	63.8688	56.8281

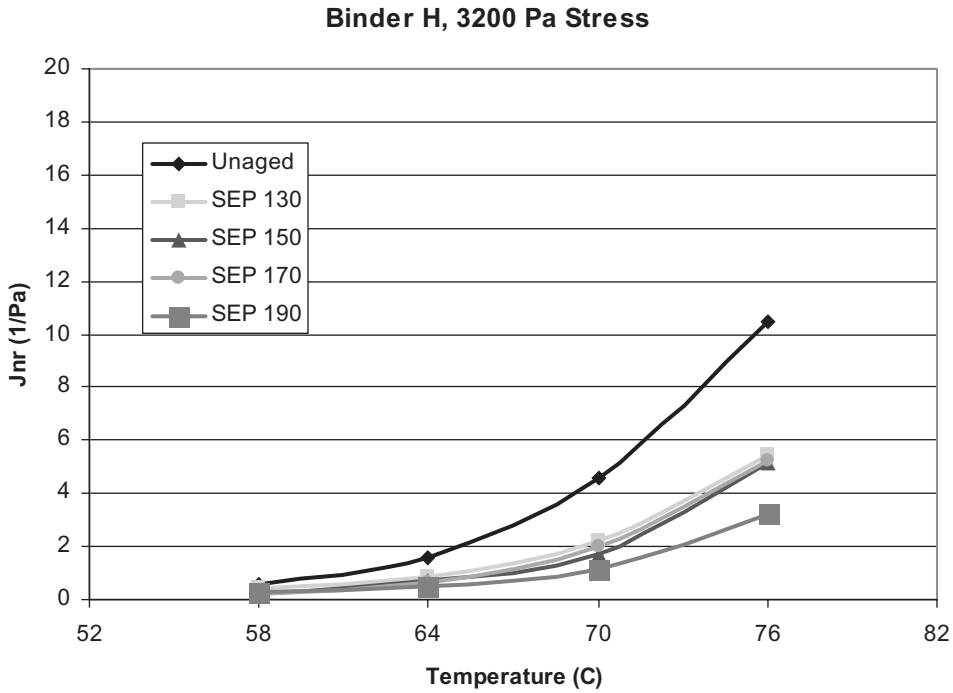

Figure 21. Plot of Jnr for modified Binder H from MSCR tests.

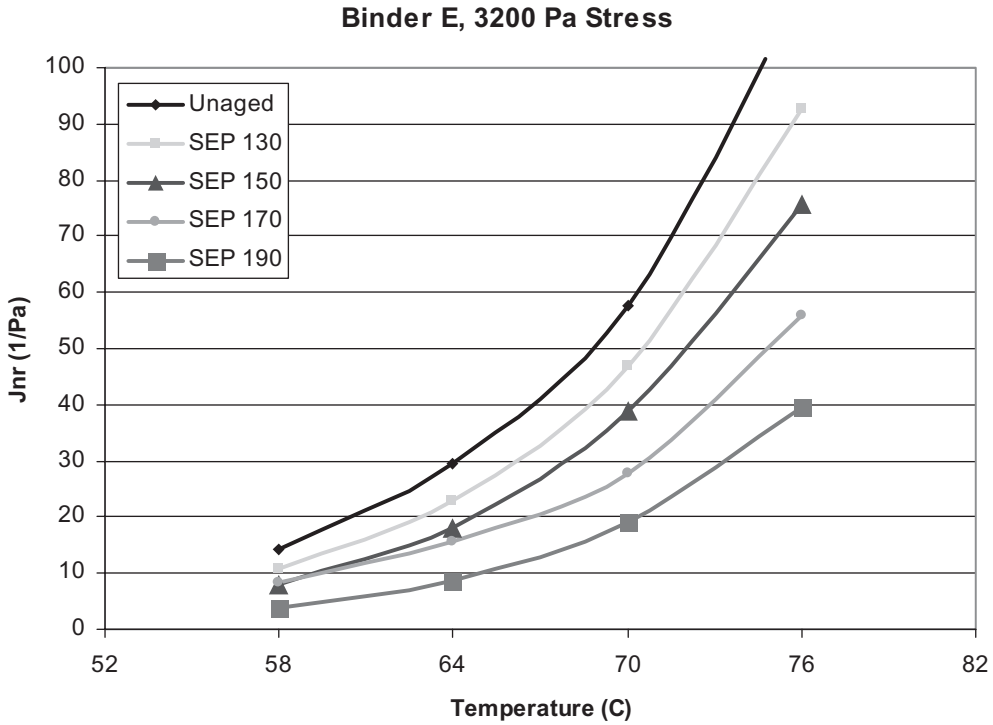

Figure 22. Plot of Jnr for unmodified Binder E from MSCR tests.

Table 16. Changes to high temperature grade (°C) after SEP test.

Binder ID	True Grade	SEP Temperature (°C)			
		130	150	170	190
M	**85.5 -19.5**	**3.0**	**4.2**	**5.4**	**6.8**
N	**84.3 -25.5**	**-1.3**	**1.4**	**4.6**	**6.7**
G	**82.5 -24.2**	**7.4**	**5.4**	**6.2**	**7.3**
H	**78.3 -26.1**	**3.2**	**1.4**	**8.0**	**9.7**
C	**75.1 -38.7**	**1.1**	**1.5**	**2.8**	**4.4**
I	71.8 -29.2	5.5	4.7	8.8	12.1
B	**69.3 -37.3**	**1.8**	**2.3**	**3.1**	**5.2**
F	67.8 -21.3	2.4	3.3	6.5	5.8
O	65.6 -29.7	3.5	4.6	8.0	10.4
K	65.3 -13.0	1.8	2.0	3.0	4.6
J	64.3 -20.7	4.8	5.1	6.9	8.1
E	60.9 -33.1	1.9	2.5	5.0	8.6
D	60.3 -31.7	2.1	2.9	4.4	5.6
Avg. of Modified Binders		**2.5**	**2.7**	**5.0**	**6.7**
Avg. of Unmodified Binders		3.1	3.6	6.1	7.9

Table 18. Changes to Phase Angle (degrees) after SEP tests.

Binder ID	True Grade	SEP Temperature (°C)			
		130	150	170	190
M	**85.5 -19.5**	**-1.73**	**-0.62**	**0.05**	**-3.34**
N	**84.3 -25.5**	**-0.40**	**1.40**	**-3.50**	**-3.90**
G	**82.5 -24.2**	**-3.07**	**-3.76**	**-5.32**	**-4.02**
H	**78.3 -26.1**	**-2.10**	**-3.83**	**-4.57**	**-5.54**
C	**75.1 -38.7**	**1.66**	**1.18**	**0.97**	**-5.21**
I	71.8 -29.2	-2.03	-2.44	-5.43	-6.80
B	**69.3 -37.3**	**-3.18**	**-2.93**	**-4.73**	**-6.22**
F	67.8 -21.3	1.89	1.70	0.12	0.13
O	65.6 -29.7	4.29	3.67	1.06	-0.42
K	65.3 -13.0	-1.06	-2.40	-1.03	-0.84
J	64.3 -20.7	-2.50	-1.00	-1.20	-2.80
E	60.9 -33.1	-0.31	-0.58	-1.96	-4.45
D	60.3 -31.7	-1.23	-2.35	-2.68	-3.57
Avg. of Modified Binders		**-1.5**	**-1.4**	**-2.9**	**-4.7**
Avg. of Unmodified Binders		-0.1	-0.5	-1.6	-2.7

low temperature degradation due to exposure to higher temperatures for most binders.

Table 18 shows the change in phase angle as measured in PG grading of the binders. These data show that generally, phase angles tend to decrease with increasing SEP temperatures for both modified and unmodified binders. However, a few binders had unusual results. Binders C, F, and O exhibited an initial increase in phase angle at an SEP temperature of 130°C, then decreased with higher SEP temperatures. A decrease in phase angle indicates that the binders became stiffer and more elastic after they were exposed to higher temperatures. As observed by Airey and Brown (*28*), had the polymers in the modified binders been damaged by the increased temperatures, the phase angles should have increased, indicating a loss of elastic behavior. Therefore, the phase angle data indicates that there are no signs of polymer degradation in the binders.

Figure 23 shows the effect of SEP temperature on non-recoverable creep compliance, Jnr, for the unmodified binders. The data shown in this graph are from the binder high grade temperatures and a stress level of 3200 Pa. The trend evident from this chart is that the non-recoverable compliance values decrease with higher SEP temperatures. Conversely, the

Table 17. Changes to low temperature grade (°C) after SEP test.

Binder ID	True Grade	SEP Temperature (°C)			
		130	150	170	190
M	**85.5 -19.5**	**1.8**	**3.1**	**2.2**	**2.2**
N	**84.3 -25.5**	**7.1**	**5.2**	**5.0**	**6.0**
G	**82.5 -24.2**	**0.3**	**1.9**	**0.7**	**3.0**
H	**78.3 -26.1**	**2.4**	**3.7**	**5.1**	**3.4**
C	**75.1 -38.7**	**2.1**	**2.8**	**1.2**	**0.8**
I	71.8 -29.2	2.2	3.8	5.4	6.0
B	**69.3 -37.3**	**-0.4**	**0.8**	**1.1**	**0.7**
F	67.8 -21.3	2.6	3.1	5.4	2.8
O	65.6 -29.7	5.9	6.1	6.9	7.7
K	65.3 -13.0	5.5	2.5	3.6	3.0
J	64.3 -20.7	6.7	6.5	7.4	7.6
E	60.9 -33.1	2.5	3.7	3.1	3.9
D	60.3 -31.7	2.5	2.3	2.7	3.0
Avg. of Modified Binders		**2.9**	**2.2**	**2.7**	**2.6**
Avg. of Unmodified Binders		4.0	4.0	4.9	4.9

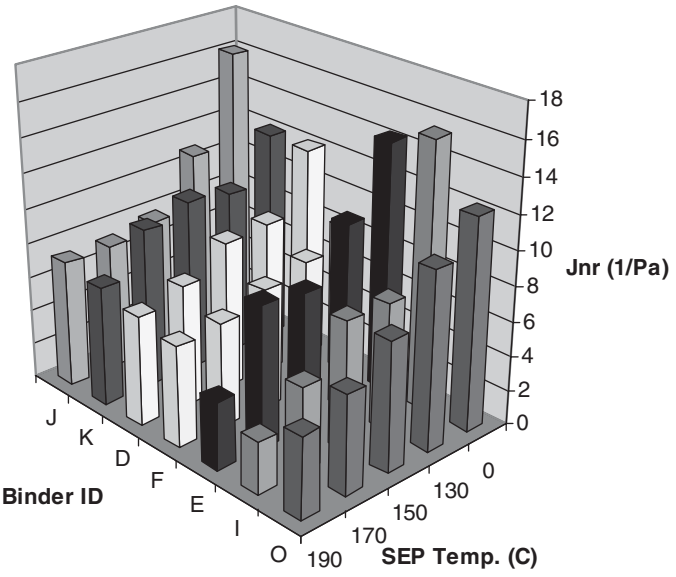

Figure 23. MSCR Jnr results at 3200 Pa stress for unmodified binders.

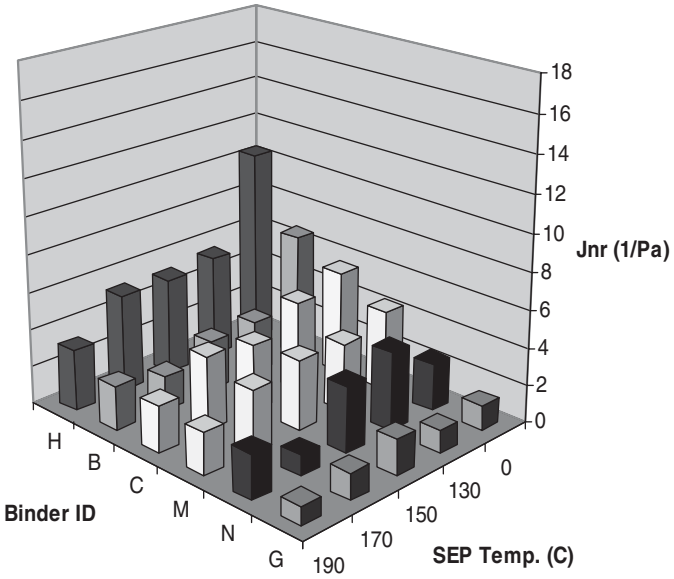

Figure 24. MSCR Jnr results at 3200 Pa stress for modified binders.

binders exhibit more recoverable strain (i.e., are more elastic) after exposure to higher temperatures. The unmodified binder that has the greatest change in Jnr with higher SEP temperatures is Binder I, the air-blown PG 70-28 using an Alaskan Slope/Canadian crude blend. This binder was consistently among the binders with the greatest property changes due to the SEP conditioning. It was also the binder with the highest opacity and, therefore, it may have lost some volatile components that caused a substantial increase in stiffness.

Figure 24 shows the effect of SEP temperature on Jnr for modified binders. As with the unmodified binders, the Jnr data used to evaluate degradation were from the high grade temperature, except for the PG 82 binders (M, N, and G). For these three binders, the creep recovery tests were not performed at 82°C, so the data shown is from the test temperature of 76°C. This graph is shown with the same Jnr scale as for the unmodified binders to illustrate the lower compliance results for the modified binders. As with the unmodified binders, the modified binders show a trend of decreasing Jnr as the SEP temperature was increased. However, there is no evidence of degradation of the binders due to the exposure to the elevated temperatures in the SEP test.

In summary, the assessment of changes in binder properties due to the conditioning of the samples to elevated temperatures in the SEP test indicates that all binders increase in stiffness with higher temperatures. The magnitudes of the property changes differ among the binders in the experiment, but with the limited data set there does not appear to be any consistent trend that binders from particular crude sources are more temperature susceptible than others. Also, modified and unmodified binders generally appear to be affected by high temperatures to similar magnitudes. The results do not provide any evidence that high temperatures cause degradation of the binders. However, this finding may only indicate that the conditions of the SEP test are not severe enough to cause significant damage to the binders.

Mixture Testing

This section presents the results of the tests with the binders in mixture tests over a range of mixing and compaction temperatures. Results are given for the coating tests, the workability tests, the compaction tests, and the indirect tensile creep compliance and strength tests.

Mixture Coating Tests

Results of the coating tests are summarized in Table 19. The table shows the percentage of coated particles determined

Table 19. Summary of coating test results.

		Percentage of Coated Aggregate Particles by ASTM D2489							
Mixer Type		Pugmill				Bucket			
Mixing Temp. °C		120	140	160	180	120	140	160	180
Mixing Temp. °F		248	284	320	356	248	284	320	356
M	**85.5 -19.5**	**52.6**	**59.0**	**90.1**	**89.6**	**63.0**	**98.0**	**99.3**	**99.3**
N	**84.3 -25.5**	**21.5**	**60.7**	**68.2**	**88.3**	**57.3**	**70.9**	**90.4**	**99.5**
G	**82.5 -24.2**	**19.5**	**65.4**	**83.3**	**82.1**	**79.6**	**91.4**	**93.9**	**97.4**
H	**78.3 -26.1**	**37.4**	**74.8**	**91.7**	**83.0**	**73.0**	**94.5**	**88.5**	**92.9**
C	**75.1 -38.7**	**40.8**	**74.9**	**85.3**	**86.4**	**81.0**	**88.4**	**92.5**	**96.0**
I	71.8 -29.2	53.1	72.3	87.1	91.7	83.6	98.2	99.2	100
B	**69.3 -37.3**	**72.4**	**71.9**	**82.5**	**87.2**	**82.2**	**95.9**	**99.4**	**98.9**
F	67.8 -21.3	51.9	89.3	88.0	90.3	77.3	98.2	99.0	99.4
O	65.6 -29.7	57.2	83.9	86.5	92.0	90.1	89.2	99.8	99.7
K	65.3 -13.0	81.0	87.7	90.7	95.5	78.5	96.7	99.9	99.9
J	64.3 -20.7	81.8	83.8	90.3	92.1	75.0	96.4	99.1	99.9
E	60.9 -33.1	91.2	86.7	92.5	95.9	85.6	97.8	98.4	100
D	60.3 -31.7	89.4	91.2	95.0	98.1	91.0	97.3	99.2	99.6

Table 20. ANOVA results for mix coating experiment.

Factor	Type	Levels	Values
Binder	fixed	13	B,C,D,E,F,G,H,I,J,K,M,N,O
Temp	fixed	4	120,140,160,180
Mixer	fixed	2	Bucket,Pugmill

Analysis of Variance for %Coating, using Adjusted SS for Tests

Source	DF	Seq SS	Adj SS	Adj MS	F	P
Binder	12	9507.79	10437.15	869.76	39.04	0.000
Temp	3	23859.07	23195.39	7731.80	347.06	0.000
Mixer	1	10341.81	9827.25	9827.25	441.12	0.000
Binder*Temp	36	5421.71	5917.35	164.37	7.38	0.000
Binder*Mixer	12	2627.86	2565.34	213.78	9.60	0.000
Temp*Mixer	3	1287.80	1159.38	386.46	17.35	0.000
Binder*Temp*Mixer	36	4483.41	4483.41	124.54	5.59	0.000
Error	118	2628.77	2628.77	22.28		
Total	221	60158.22				

by the Ross count method as mixing temperatures were increased from 248°F to 356°F (120°C to 180°C).

Analysis of variance (ANOVA) is a common method of analyzing data from a statistical experimental design to assess differences associated with experimental treatments. Output from the ANOVA for the coating experiment is shown in Table 20. From these results, it can be seen that all three of the main factors (binder ID, mixing temperature, and mixer type) were highly significant. The interactions of these factors were also statistically significant, however, based on the *F* values, not nearly to the same degree as the main factors by themselves.

The main effects plots for the coating test experiment are shown in Figure 25. All of the modified binders, except Binder B, plot below the overall mean for percent coating, which indicates that aggregates are harder to coat with the modified binders under the same conditions. The temperature effect on coating percentage follows the expected trend of increased coating at higher temperatures, but that the effect is not linear. The results also show that the bucket mixer provided better coating than the pugmill. This seems to conflict with the hypothesis that the bucket mixer would be less efficient than the pugmill due to its lower mixing speed (slower shear rate). However, besides mixing speed, the action of the two mixers is very different. The tumbling action of the bucket mixer, like that of a drum mix plant, allows aggregate particles to stay in contact with the binder and other coated particles. This could be a more efficient coating process than a pugmill, which is a more violent churning action with aggregate particles tossed into space, especially when the pugmill is under filled.

For each binder, the coating percentages were related to mixing temperatures using Sigmoid functions of the form:

$$C = \frac{1}{1 + ae^{-bT}} \tag{8}$$

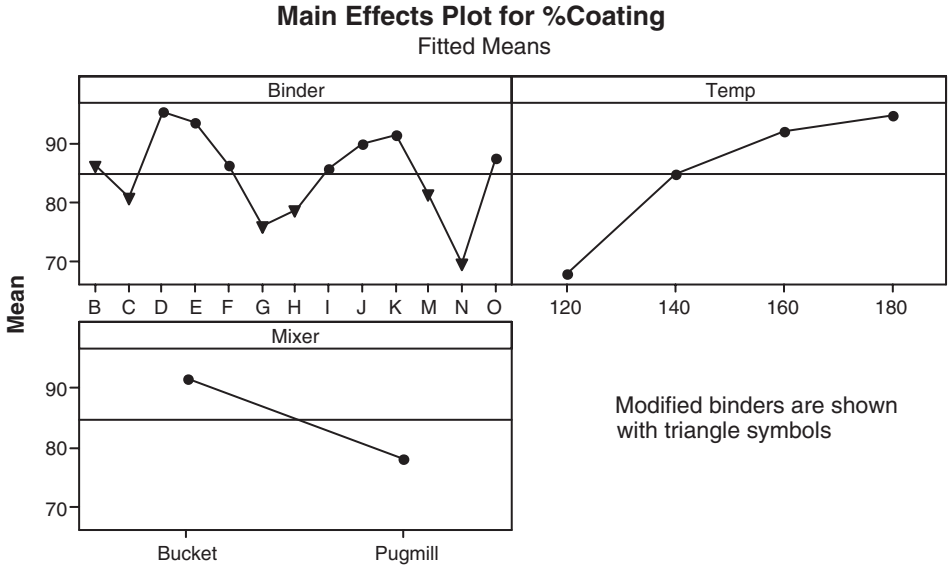

Figure 25. Effects of binder, temperature, and mixer on coating percentage.

Table 21. Coating test regression model results.

ID	True Grade	Bucket Mixer			Pugmill Mixer		
		a	*b*	T for 98% Coating °F (°C)	*a*	*b*	T for 89% Coating °F (°C)
M	85.5-19.5	24590795	0.146	289 (143)	117	0.039	345 (174)
N	84.3-25.5	3518845	0.113	334 (168)	1911	0.053	361 (183)
G	82.5-24.2	146	0.051	347 (175)	8990	0.067	333 (167)
H	78.3-26.1	14	0.031	412 (211)	3183	0.064	318 (159)
C	75.1-38.7	30688	0.078	360 (182)	876	0.055	324 (162)
I	71.8-29.2	134998	0.112	284 (140)	130	0.042	333 (167)
B	69.3-37.3	3514	0.081	300 (149)	7	0.021	374 (190)
F	67.8-21.3	715	0.066	318 (159)	2902	0.068	298 (148)
O	65.6-29.7	404	0.056	347 (175)	130	0.044	318 (159)
K	65.3-13.0	58144	0.102	293 (175)	4	0.024	297 (147)
J	64.3-20.7	131832	0.107	295 (146)	2	0.017	318 (159)
E	60.9-33.1	9177	0.091	289 (143)	0.4	0.010	222 (106)
D	60.3-31.7	182	0.063	293 (145)	2	0.023	250 (121)

where C is the percentage coating at any temperature T, and a and b are regression constants. Regression results for each binder are summarized in Table 21. The relationships were used to estimate the coating percentage of the binders at any temperature. The equiviscous mixing temperatures for the unmodified binders were used to establish reference coating percentages for the bucket mixer and the pugmill mixers. These reference coating percentages were 98% (bucket) and 89% (pugmill mixer). The temperatures to achieve these coating percentages for each binder were then estimated with the Sigmoid function regression equations. These predicted mixing temperatures for equivalent coating are included in Table 21.

It is evident from these results that the predicted temperatures from the two laboratory mixers are different and neither consistently provides reasonable mixing temperatures. With the bucket mixer, the temperature to achieve the baseline coating percentage for Binder H was 412°F (211°C). This result is much higher than most asphalt technologists consider reasonable. At the other extreme, the lowest predicted temperature to achieve the baseline coating percentage was for Binder I, which is not consistent with the rank of the binder grades. Binder M, modified with SBS and Sasobit®, is somewhat lower than the other highly modified binders, but this may be due to the beneficial effect of the Fischer Tropsch wax. For the pugmill mixer, the predicted temperature for modified Binder B is excessive, and the temperatures for the lowest-graded binders, D and E, are lower than expected. Overall, the inconsistent coating test results for several binders demonstrate the challenge of using this method to predict mixing temperatures and to use this approach to validate the candidate methods.

Mixture Coating Tests with Incompletely Dried Aggregate

A second small coating experiment was conducted to assess the effect of residual aggregate moisture on the coating of the aggregates with four binders. One of the challenges with this limited experiment was preparing the samples with residual moisture to specific mixing temperatures. The granite aggregate used in this experiment had a low water absorption (0.7%) and although the coarse aggregates were saturated at the start of the final heating step by combining with hot, dry fine aggregate and using a blow torch, the amount of moisture remaining in the aggregate at the time the asphalt was added had certainly decreased substantially.

A paired t-test was used to compare the results of the coating test with and without incompletely dried aggregates. The experimental hypothesis was that the coating percentages were the same (difference = 0) for partially wet and dry aggregates. The results, provided in Table 22, show that there is a high probability (P-value = 0.469) that the coating percentages of dry samples and incompletely dry samples were not statistically different. Some asphalt technologists have suggested that

Table 22. Results of paired T-test for %coating using wet and dry aggregates.

Paired T for Wet %Coated - Dry %Coated				
	N	Mean	St Dev	SE Mean
Wet %Coated	32	66.0219	27.8339	4.9204
Dry %Coated	32	63.0844	31.3435	5.5408
Difference	32	2.93750	22.66805	4.00718

95% CI for mean difference: (–5.23520, 11.11020)
T-Test of mean difference = 0 (vs not = 0): T-Value = 0.73 P-Value = 0.469

moisture escaping from aggregate pores during mixing with binder may cause the asphalt film to foam and significantly expand, which would enhance the coating process. Although steam was evident during the mixing, foaming of the asphalt was not observed during the tests with the incompletely dried aggregates.

Workability Tests

The raw torque data from each workability test was processed and a least-squares regression was used to fit a quadratic equation to the processed torque versus temperature data. The temperature-torque regressions for each replicate sample are shown in Table 23. Initially, a reference torque based on the midpoints between the equiviscous mixing and compaction temperatures of the unmodified binders was considered. This yielded a reference torque value of 9.7 N-m. However, results with some modified binders did not quite reach this value even at the highest temperature. One of the challenges with analysis of the workability data was finding a single torque value to use as a reference point for comparing the binders. In the temperature range that the workability tests span, typically from about 180°C to 120°C, the results for all binders did not cross any given torque value, which required an extrapolation for some results beyond the experimental range. 10 N-m was selected as a reasonable reference torque value because it was close to the average equiviscous midpoint torque and required small extrapolations. Therefore, using the temperature-torque regressions, the temperatures at which the binder-sand mixture reached 10 N-m of torque were determined. These results also are summarized in Table 23. It can be seen that for over half of the binders tested, the difference between replicates was more than 25°F. Some samples had very shallow temperature-torque relationships, which meant that the torque only changed by a relatively small amount over a wide temperature range. Replicate results that had similar but shallow and nearly parallel temperature-torque regressions had large differences between the temperatures to reach the reference torque value.

Table 23. Workability experiment — temperatures to yield equivalent torque.

ID	Run	Regression Equation	R^2	°C	°F	°F Avg.
M	**1**	**$y = 0.0035x^2 - 1.2027x + 111.88$**	**0.67**	**152**	**305**	**328**
	2	**$y = 0.0045x^2 - 1.5717x + 147.32$**	**0.80**	**177**	**351**	
N	**1**	**$y = 0.0044x^2 - 1.4866x + 135.3$**	**0.63**	**177**	**351**	**347**
	2	**$y = 0.0032x^2 - 1.1296x + 110.27$**	**0.50**	**173**	**343**	
G	**1***	**$y = 0.0135x^2 - 4.2228x + 339.19$**	**0.39**	**134**	**272**	**289**
	2	**$y = 0.0046x^2 - 1.554x + 139.94$**	**0.89**	**152**	**306**	
H	**1**	**$y = 0.002x^2 - 0.834x + 95.567$**	**0.89**	**182**	**360**	**358**
	2	**$y = 0.0041x^2 - 1.5494x + 158.01$**	**0.96**	**180**	**356**	
C	**1**	**$y = 0.0021x^2 - 0.8114x + 88.106$**	**0.61**	**181**	**358**	**352**
	2	**$y = 0.0012x^2 - 0.5356x + 67.004$**	**0.56**	**175**	**347**	
I	1	$y = 0.0039x^2 - 1.3958x + 136.84$	0.74	180	356	361
	2	$y = 0.0029x^2 - 1.1313x + 120.13$	0.75	186	367	
B	**1**	**$y = 0.0018x^2 - 0.6268x + 62.533$**	**0.23**	**141**	**285**	**307**
	2	**$y = 0.0011x^2 - 0.3908x + 44.778$**	**0.19**	**165**	**328**	
F	1	$y = 0.0019x^2 - 0.6247x + 60.037$	0.59	138	280	295
	2	$y = 0.002x^2 - 0.7276x + 74.616$	0.59	154	309	
O	1	$y = 0.0027x^2 - 0.8801x + 78.499$	0.51	129	263	251
	2	$y = 0.0021x^2 - 0.6556x + 57.564$	0.15	115	238	
K	1	$y = 0.001x^2 - 0.3593x + 37.633$	0.39	112	233	257
	2	$y = 0.0013x^2 - 0.4528x + 47.712$	0.56	138	280	
J	1	$y = 0.0028x^2 - 0.927x + 82.634$	0.64	128	262	257
	2	$y = 0.0016x^2 - 0.5354x + 51.654$	0.47	123	253	
E	1	$y = 0.0001x^2 - 0.1246x + 25.015$	0.42	135	275	294
	2	$y = 0.002x^2 - 0.7656x + 80.762$	0.78	156	313	
D	1	$y = 0.001x^2 - 0.4073x + 47.171$	0.47	138	280	305
	2	$y = 0.002x^2 - 0.6858x + 68.707$	0.46	165	329	

* Incomplete data set.

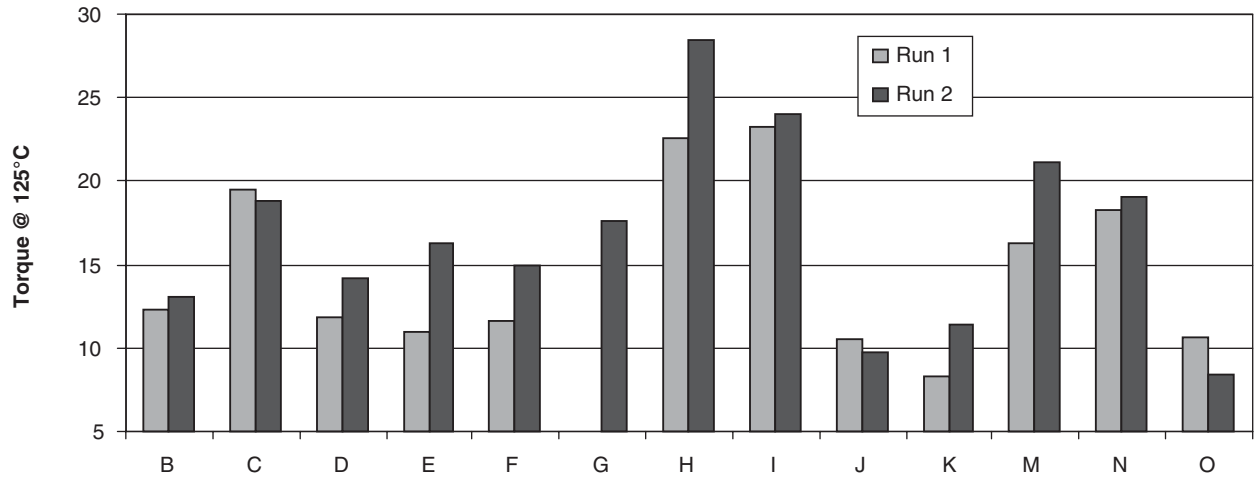

Figure 26. Torque calculated at 125°C from workability test results.

Unfortunately, the poor repeatability and the low R^2 for several of the regressions indicate that this test may not be a dependable test to evaluate specific relationships between temperature and workability for binders.

Another way to analyze the workability results was to compare the torque values at specific temperatures. Figure 26 through Figure 28 show a series of plots of torque values calculated at three temperatures spanning 40°C (72°F). Although the differences in torque values between replicates are evident, relative to the range of torque values among the binders, the replicate differences are in the order of 10% to 15%. The average difference between replicates at 125°C is 2.2 N-m, and the range in torque among the different binders is 20 N-m. At 165°C, the average difference between replicates is 1.3 N-m with an overall range of about 9 N-m.

It also can be seen from these plots that the second run yielded higher torque results for most binders. The procedure was reviewed to determine whether the second sample was aged longer and stiffened in the oven before testing. Each replicate sample was individually mixed and placed in the oven until it reached 180°C to start the workability test. The systematic pattern that caused the second sample to be less workable could have been due to a longer time in the oven for the second sample due to opening the oven to retrieve the first sample and the workability bowl and paddle. The one binder that does not follow that trend was Binder O. This was the only case where the second sample was run on a different day from the first sample. In this review, it was discovered that the data for the first sample for Binder G was incomplete: data was only recorded from about 165°C to 135°C. Therefore results for this replicate were excluded in the analyses.

Compaction Tests

The mix compaction experiments were conducted to assess the effect of compaction temperature on the compacted specimen density and resistance to compaction based on the maximum shear ratio obtained from the specially equipped Pine Instruments SGC, model AFG1A. In order to better differentiate the binder stiffness effects (i.e., binder ID

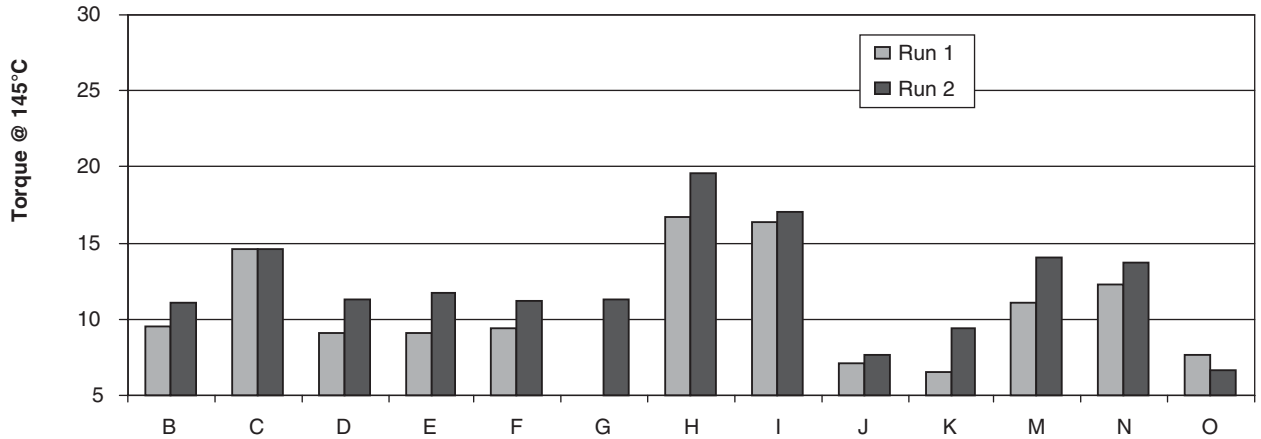

Figure 27. Torque calculated at 145°C from workability test results.

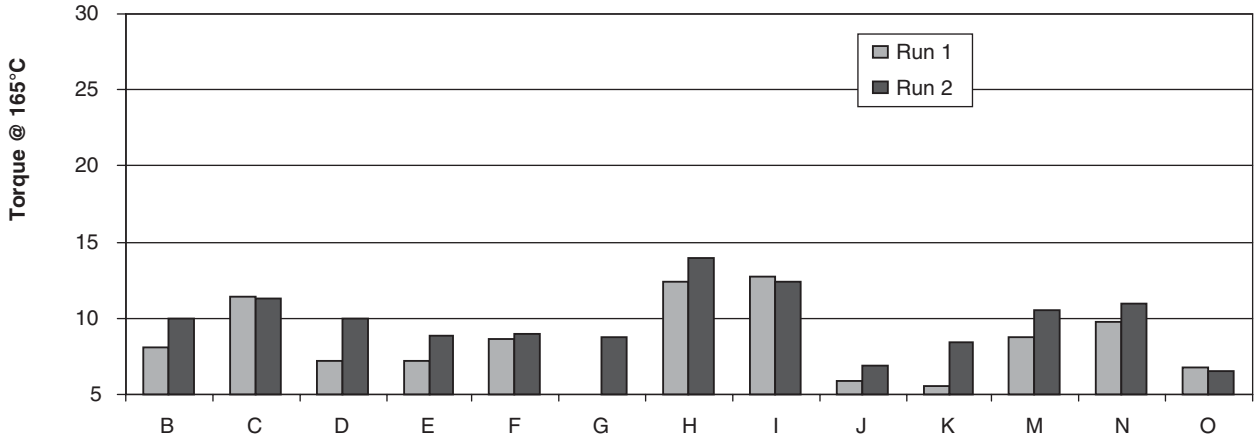

Figure 28. Torque calculated at 165°C from workability test results.

and temperatures), the specimens were compacted to only 25 gyrations. A summary of the main compaction experiment is shown in Table 24.

Table 25 provides the Minitab ANOVA output for relative density, %Gmm, as the dependent variable. The main effects (binder and compaction temperature) were statistically significant (P-value <0.05). Surprisingly however, the ANOVA results indicate that the interaction of the main effects was not significant (P-value >0.05). This suggests that within each binder set, increasing the compaction temperature did not have a statistically significant impact on the mixture density.

Table 24. Summary of Compaction Experiment A results.

		%Gmm				Max. Shear Ratio			
Comp. Temp. °C		110	130	150	170	110	130	150	170
Comp. Temp. °F		230	266	302	338	230	266	302	338
M	**85.5 -19.5**	**92.5**	**92.7**	**92.7**	**93.1**	**0.912**	**0.881**	**0.888**	**0.888**
N	**84.3 -25.5**	**91.7**	**92.0**	**92.3**	**92.9**	**0.782**	**0.788**	**0.744**	**0.793**
G	**82.5 -24.2**	**91.6**	**92.1**	**92.5**	**93.0**	**0.848**	**0.888**	**0.872**	**0.906**
H	**78.3 -26.1**	**92.4**	**92.8**	**92.6**	**93.0**	**0.860**	**0.821**	**0.861**	**0.871**
C	**75.1 -38.7**	**92.3**	**92.4**	**93.5**	**93.1**	**0.852**	**0.823**	**0.827**	**0.875**
I	71.8 -29.2	92.4	92.1	92.5	92.7	0.812	0.732	0.854	0.786
B	**69.3 -37.3**	**92.6**	**93.0**	**93.1**	**93.3**	**0.819**	**0.883**	**0.827**	**0.908**
F	67.8 -21.3	92.7	92.9	92.5	93.5	0.863	0.837	0.979	0.961
O	65.6 -29.7	92.7	93.1	93.3	93.3	0.820	0.800	0.936	0.942
K	65.3 -13.0	92.5	93.3	93.3	93.6	0.802	0.832	1.000	0.983
J	64.3 -20.7	92.2	92.5	92.4	92.8	0.852	0.843	0.889	0.790
E	60.9 -33.1	92.8	92.7	93.3	93.6	0.832	0.872	0.881	0.862
D	60.3 -31.7	92.7	93.0	93.2	93.2	0.821	0.830	0.837	0.873

Table 25. ANOVA for relative density from Compaction Experiment A.

Factor	Type	Levels	Values
Binder	fixed	13	B,C,D,E,F,G,H,I,J,K,M,N,O
Temperature	fixed	4	230,266,302,338

Analysis of Variance for %Gmm, using Adjusted SS for Tests

Source	DF	Seq SS	Adj SS	Adj MS	F	P
Binder	12	9.80846	9.80846	0.81737	10.93	0.000
Temperature	3	8.11731	8.11731	2.70577	36.17	0.000
Binder*Temperature	36	3.57769	3.57769	0.09938	1.33	0.172
Error	52	3.89000	3.89000	0.07481		
Total	103	25.39346				

S = 0.273510 R-Sq = 84.68% R-Sq (adj) = 69.66%

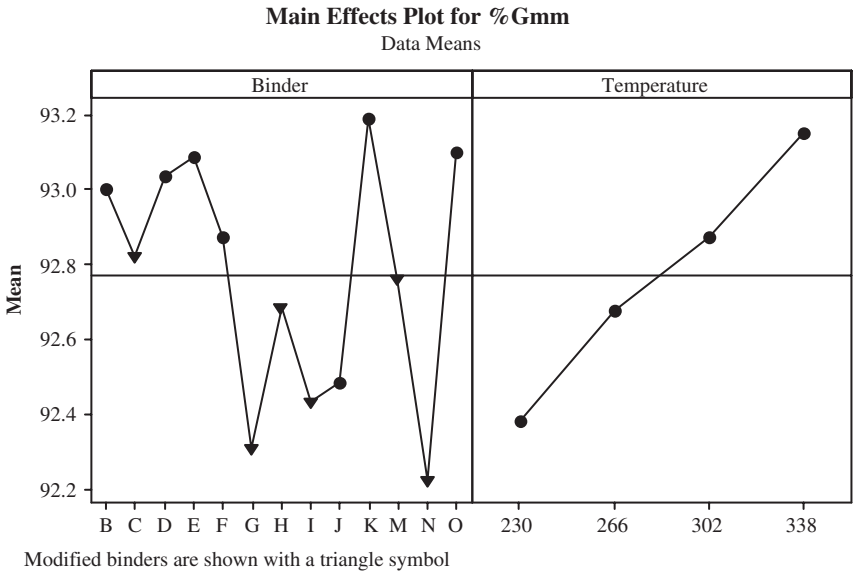

Figure 29. Main effects plot for %Gmm from Compaction Experiment A.

Figure 29 is a plot of the main effects that shows as compaction temperature increased, the relative density increased for the relatively low compactive effort used in this experiment. The mean densities (averaged over all compaction temperatures) for each of the unmodified binders (D, E, F, J, K, and O) plot above the grand mean except for Binder J. This provides a level of confidence that binder stiffness or consistency has some effect on compacted density.

Figure 30 summarizes a Tukey's pair-wise comparison analysis of just the binder effect. This figure shows a cross matrix of the binders shown in rows and columns. Black cells identify binder pairs that had %Gmm results that were not statistically different. For example, the average density for Binder M (85.5-19.5) was statistically different only with Binder N. This indicates that the warm asphalt additive Sasobit® used in Binder M improved the compactability of the mix compared to the similarly graded Binder N. Other comparisons associated with Binders H, C, and J were unexpected. Compacted density results for modified Binders H (78.8-26.1) and C (75.1-38.7) compared more favorably with most of the unmodified binders than with the other modified binders. On the other hand, unmodified Binder J (64.3-20.7) compared favorably with all of the modified binders and was statistically different than the two unmodified binders with the closest true grades, Binders O and K. As with the coating test results and the workability test results, there are several compaction test results that seem inconsistent with the binder grades. Unfortunately there does not appear to be a pattern with the inconsistencies attributed to certain binders.

Linear regressions were established between %Gmm and compaction temperature for each binder. The regressions are shown in Table 26. Given that the equiviscous compaction

		M	N	G	H	C	I	B	F	O	K	J	E	D
M	**85.5-19.5**	■		■	■	■	■	■	■	■	■	■	■	■
N	**84.3-22.5**		■	■	■		■					■		
G	**82.5-24.2**			■	■		■					■		
H	**78.3-26.1**				■	■	■	■	■	■		■	■	■
C	**75.1-38.7**					■	■	■	■	■	■	■	■	■
I	71.8-29.2						■		■			■		
B	**69.3-37.3**							■	■	■	■	■	■	■
F	67.8-21.3								■	■	■	■	■	■
O	65.6-29.7									■	■		■	■
K	65.3-13.0										■		■	■
J	64.3-20.7											■		
E	60.9-33.1												■	■
D	60.3-31.7													■

Figure 30. Matrix chart showing binder pairs that had statistically different compacted densities.

Table 26. Compaction experiment regressions.

ID	True Grade	Regression Equation (T is Temperature ºC)	R^2	Compaction Temperature for 92.9%Gmm, ºF (ºC)
M	**85.5 -19.5**	**%Gmm = 0.0087T + 91.527**	**0.75**	**317 (159)**
N	**84.3 -25.5**	**%Gmm = 0.0193T + 89.510**	**0.85**	**349 (176)**
G	**82.5 -24.2**	**%Gmm = 0.0228T + 89.085**	**0.78**	**334 (168)**
H	**78.3 -26.1**	**%Gmm = 0.0085T + 91.495**	**0.47**	**331 (166)**
C	**75.1 -38.7**	**%Gmm = 0.0182T + 90.260**	**0.59**	**293 (145)**
I	71.8 -29.2	%Gmm = 0.0066T + 91.496	0.30	417 (214)
B	**69.3 -37.3**	**%Gmm = 0.0119T + 91.319**	**0.65**	**272 (133)**
F	67.8 -21.3	%Gmm = 0.0098T + 91.508	0.27	289 (143)
O	65.6 -29.7	%Gmm = 0.0098T + 91.718	0.44	284 (140)
K	65.3 -13.0	%Gmm = 0.0151T + 91.060	0.54	257 (125)
J	64.3 -20.7	%Gmm = 0.0098T + 91.097	0.57	354 (179)
E	60.9 -33.1	%Gmm = 0.0140T + 91.119	0.71	262 (128)
D	60.3 -31.7	%Gmm = 0.0085T + 91.852	0.51	264 (129)

temperatures for unmodified binders are considered reasonable and satisfactory, they were used to establish a reference density. The relative density for the mixtures with the five unmodified binders at their respective equiviscous compaction temperatures ranged from 92.4 to 93.1%, with an average density of 92.9 %Gmm. Using the linear regressions equations for each binder in Table 26, the compaction temperature to achieve 92.9 %Gmm was predicted for each binder. These results are also summarized in Table 26. These results are generally consistent with the binder grades with a few exceptions. The predicted compaction temperature for Binder I is extremely high as a result of the low slope term in the regression. The R^2 of the linear regression for this binder was not as good as for most other binders, and the predicted temperature is well outside of the experimental range of the data. The predicted compaction temperature for Binder J is also very high, considering that it is an unmodified binder.

Another output of the main compaction experiment was the maximum shear ratio developed during the compaction process. According to Pine Instrument Company (*52*), maximum shear ratio is a parameter that indicates the resistance of the mixture to compaction as measured with the specially equipped AFG1 Pine SGC. The ANOVA results with shear ratio as the dependent variable are shown in Table 27. This analysis also shows that the main factors, binder and compaction temperature, as well as their interaction are statistically significant. However, the main effects and interactions plots, shown in Figure 31 and Figure 32, do not follow any reasonable trends for individual binders such as decreasing shear ratio with increasing compaction temperatures, or higher shear ratios for mixtures with modified binders compared with unmodified binders. For this reason, the maximum shear ratio does not appear to be a useful indicator of compactability.

Compaction Experiment B was a ½ factorial experiment designed to evaluate the factors binder, temperature, aggregate, and gradation. Since binder and temperature effects were analyzed in Compaction Experiment A, the factors of primary interest in this analysis were gradation (coarse versus fine) and

Table 27. ANOVA for maximum compaction shear ratio from Compaction Experiment A.

Factor	Type	Levels	Values
Binder	fixed	13	B,C,D,E,F,G,H,I,J,K,M,N,O
Temperature	fixed	4	230,266,302,338

Analysis of Variance for Shear Ratio, using Adjusted SS for Tests

Source	DF	Seq SS	Adj SS	Adj MS	F	P
Binder	12	0.138555	0.131887	0.010991	10.83	0.000
Temperature	3	0.046824	0.047087	0.015696	15.46	0.000
Binder*Temperature	36	0.132823	0.132823	0.003690	3.63	0.000
Error	50	0.050751	0.050751	0.001015		
Total	101	0.368952				

S = 0.0318592 R-Sq = 86.24% R-Sq(adj) = 72.21%

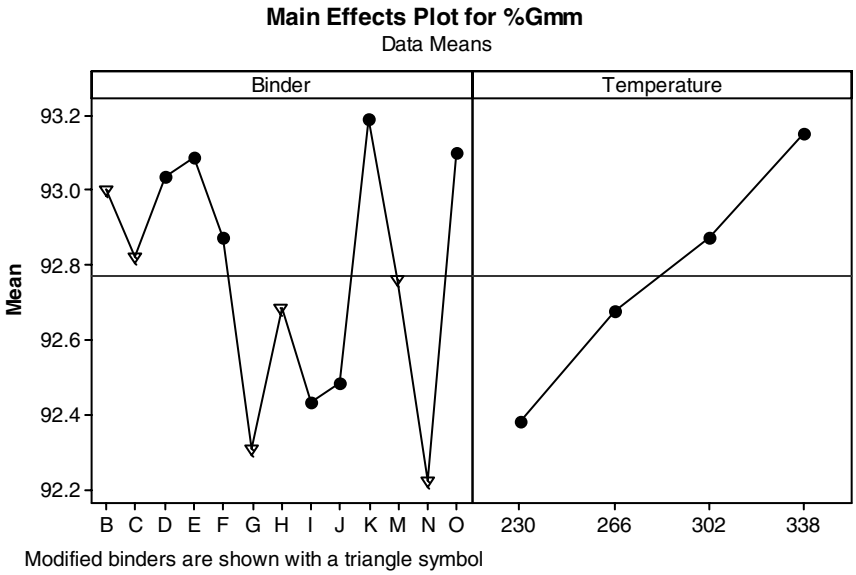

Figure 31. Main effects plot for maximum shear ratio from Compaction Experiment A.

aggregate type (low absorption and angular granite compared with a high absorption, more rounded gravel). In the experimental design, binder and temperature had four levels, and aggregate and gradation had two levels. Binder and temperature were reduced to two 2-level factors for the design. This resulted in a 2^6 design, which was reduced to a ½ factorial, yielding 32 observations. Since the experiment was replicated, a total of 63 observations were made. The ANOVA table for this experiment is shown in Table 28. Due to the ½ factorial design, some of the interactions of the factors were sacrificed. The ANOVA table shows the effects of the main effects and the two-way interactions. These results show that gradation has the largest affect on relative density, followed by aggregate type. Recall that each of these mixtures was, in effect, normalized by designing them with a single binder to 96% Gmm at 75 gyrations. These experimental results indicate that a mixture's aggregate components (gradation, particle shapes, texture, absorption, etc.) have a greater affect on compaction behavior than the binder characteristics. This finding is consistent with other research at NCAT (*18*).

Although it has little significance to the primary objective of this project, data from the compaction experiments also made

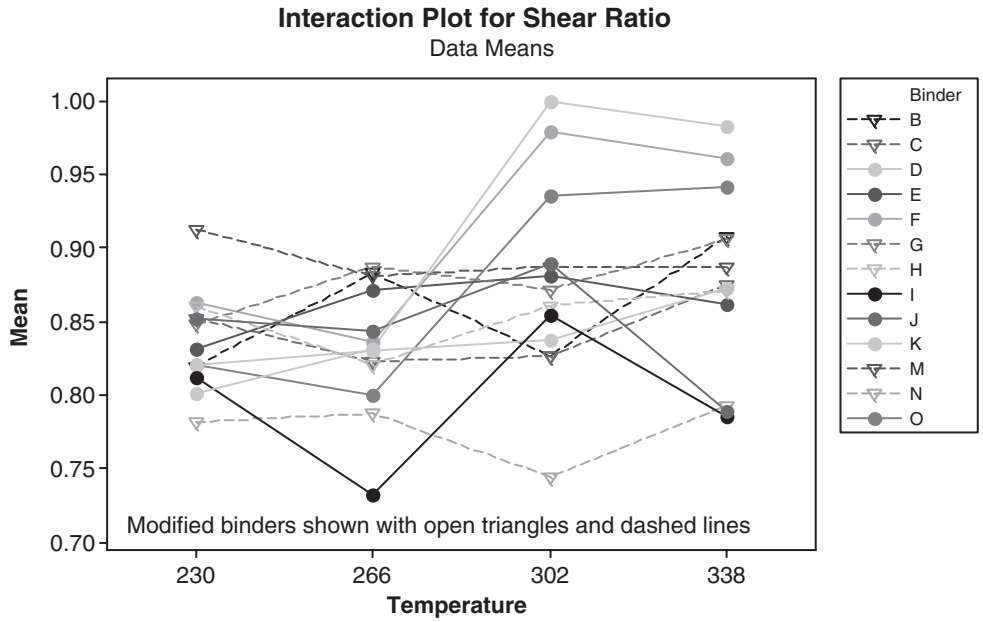

Figure 32. Interaction plot for binder and temperature on maximum shear ratio.

Table 28. ANOVA for Compaction Experiment B.

Factor	Type	Levels	Values
Aggregate	fixed	2	Granite,Gravel
Grad.	Fixed	2	Coarse,Fine
Binder	fixed	4	B,E,G,M
Temperature	fixed	4	230,266,302,338

Analysis of Variance for %Gmm, using Adjusted SS for Tests

Source	DF	Seq SS	Adj SS	Adj MS	F	P
Agg.	1	15.8006	15.8006	15.8006	238.50	0.0000
Grad.	1	40.6406	40.6406	40.6406	613.44	0.0000
Binder	3	16.7987	16.7987	5.5996	84.59	0.0000
Temp.	3	5.4162	5.4162	1.8054	27.27	0.0000
Agg.*Grad.	1	11.5600	11.5600	11.5600	174.49	0.0000
Agg.*Binder	2	1.5781	1.5780	0.7890	11.92	0.0001
Agg.*Temp.	2	0.3931	0.3931	0.1966	2.97	0.0658
Grad.*Binder	2	0.8406	0.8406	0.4203	6.35	0.0048
Grad.*Temp	2	0.2356	0.2356	0.1178	1.78	0.1852
Temp.*Binder	8	2.2199	2.2199	0.2775	4.19	0.0016
AB1B2=GT1T2	1	0.0400	0.0400	0.0400	0.60	0.4428
AT1T2=B1B2G	1	0.3600	0.3600	0.3600	5.44	0.0262
AB1T1=B2GT2	1	0.0303	0.0306	0.0306	0.46	0.5016
AB1T2=B2GT1	1	0.8100	0.8100	0.8100	12.23	0.0014
AB2T1=B1GT2	1	0.0400	0.0400	0.0400	0.60	0.4428
AB2T2+B1GT1	1	0.0156	0.0156	0.0156	0.24	0.6308
Error	32	2.1200	2.1200	0.0662		
Total	63	98.9000				

it possible to assess the effect of RAP on the compactability of HMA in an SGC. This limited analysis examined the effects of three factors on the density (% of Gmm) of the compacted specimens at 25 gyrations. RAP content was the variable of primary interest and was evaluated at two levels, 0 and 15%. Both mixtures used a fine-graded blend of granite aggregates. Two binders were also included in the analysis: B (64-34) and M (82-16). The third variable was compaction temperature, which was tested at four levels.

The ANOVA on this data set is shown in Table 29. These results indicate that each of the main factors, including RAP content, have a statistically significant effect on the compactability of the mixtures. The interaction plot from this analysis is shown in Figure 33. This diagram shows that densities increased as compaction temperatures increased and also that the densities for the samples with the softer-grade Binder B were higher than the samples with the stiffer Binder M at equivalent temperatures. The right side of the interaction plot shows that the mixtures with 15% RAP had higher densities than the virgin mixtures. These results do not support the hypothesis that aged binder from the RAP makes the mix stiffer and harder to compact. The interaction of RAP and

Table 29. ANOVA for compaction %Gmm including RAP.

Factor	Type	Levels	Values
Binder	fixed	2	B,M
Temp	fixed	4	110,130,150,170
RAP	fixed	2	0,15

Analysis of Variance for %Gmm, using Adjusted SS for Tests

Source	DF	Seq SS	Adj SS	Adj MS	F	P
Binder	1	2.20500	2.20500	2.20500	47.68	0.000
Temp	3	5.44500	5.44500	1.81500	39.24	0.000
RAP	1	3.00125	3.00125	3.00125	64.89	0.000
Binder*Temp	3	0.65500	0.65500	0.21833	4.72	0.015
Binder*RAP	1	0.66125	0.66125	0.66125	14.30	0.002
Temp*RAP	3	1.21375	1.21375	0.40458	8.75	0.001
Binder*Temp*RAP	3	0.29375	0.29375	0.09792	2.12	0.138
Error	16	0.74000	0.74000	0.04625		
Total	31	14.21500				

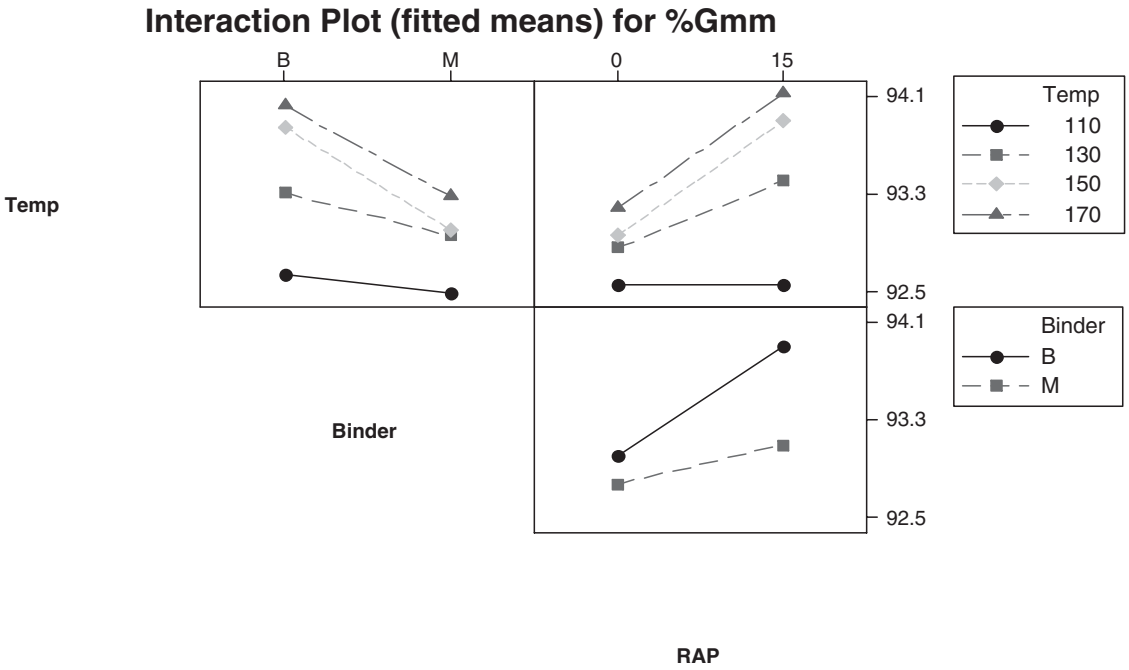

Figure 33. Interaction plot of RAP, binder, and temperature on %Gmm.

temperature also shows that the effect of the RAP was greater at higher compaction temperatures.

Indirect Tensile Creep Compliance and Strength

Gyratory specimens compacted at the four compaction temperatures were tested to determine indirect tensile creep compliance in accordance with AASHTO T 322. Creep compliance is the inverse of stiffness. Therefore, at very low temperatures, a mixture with lower compliance is able to strain more and avoid thermal fracture. The goal of this testing and analysis was to determine whether the low temperature mix properties were affected by the compaction temperature. If an effect was detected, then the results would be analyzed to assess the potential that the change was due to binder degradation.

Creep compliance results are summarized in Table 30. Since compliance values are greatly affected by test temperature, separate analyses were performed at each temperature. Figure 34 through Figure 36 show the change in compliance values for the modified binders at test temperatures −20°C, −10°C, and 0°C, respectively. Similarly, Figure 37 through

Table 30. Summary of creep compliance results (Dt_{90} 1 x 10^{-6} 1/kPa) for different compaction temperatures.

Test Temp. °C		-20				-10				0			
Comp. Temp. °C		110	130	150	170	110	130	150	170	110	130	150	170
Comp. Temp. °F		230	266	302	338	230	266	302	338	230	266	302	338
M	**85.5 -19.5**	**0.0770**	**0.0716**	**0.0717**	**0.0661**	**0.1244**	**0.1111**	**0.1340**	**0.1088**	**0.3090**	**0.3001**	**0.2177**	**0.1997**
N	**84.3 -25.5**	**0.1416**	**0.1284**	**0.1077**	**0.1088**	**0.3447**	**0.2106**	**0.2106**	**0.1895**	**0.9503**	**0.7135**	**0.4367**	**0.4355**
G	**82.5 -24.2**	**0.1049**	**0.0834**	**0.0704**	**0.0688**	**0.1595**	**0.1302**	**0.1332**	**0.1006**	**0.4937**	**0.3711**	**0.3191**	**0.2160**
H	**78.3 -26.1**	**0.0851**	**0.0929**	**0.0792**	**0.0706**	**0.1702**	**0.1450**	**0.1678**	**0.1401**	**0.5753**	**0.5835**	**0.4825**	**0.2819**
C	**75.1 -38.7**	**0.1383**	**0.1394**	**0.1682**	**0.1509**	**0.3424**	**0.3527**	**0.4028**	**0.3221**	**1.3254**	**1.1280**	**1.1655**	**0.8607**
I	71.8 -29.2	0.2295	0.1712	0.1792	0.1324	0.3237	0.3525	0.3516	0.1324	0.8144	1.0476	0.7209	0.4414
B	**69.3 -37.3**	**0.1847**	**0.1808**	**0.1937**	**0.1926**	**0.4525**	**0.2987**	**0.4698**	**0.3873**	**1.6037**	**1.2855**	**1.4417**	**1.0198**
F	67.8 -21.3	0.0728	0.0725	0.0527	0.0723	0.1978	0.1881	0.1598	0.1221	0.4417	0.3788	0.3420	0.2619
O	65.6 -29.7	0.1136	0.0737	0.0934	0.0869	0.2123	0.2077	0.1615	0.1493	0.8818	0.5780	0.4572	0.4249
K	65.3 -13.0	0.0580	0.0445	0.0439	0.0407	0.0668	0.0588	0.0551	0.0478	0.1755	0.1288	0.2243	0.1473
J	64.3 -20.7	0.0584	0.0529	0.0509	0.0581	0.0955	0.0795	0.0693	0.0738	0.2154	0.1886	0.1546	0.1691
E	60.9 -33.1	0.1678	0.1341	0.1237	0.1257	0.4213	0.1034	0.4169	0.3110	1.4816	1.2073	1.2343	0.6301
D	60.3 -31.7	0.1130	0.1001	0.0970	0.1034	0.2527	0.2488	0.2022	0.2209	1.1238	0.7832	0.6618	0.6020

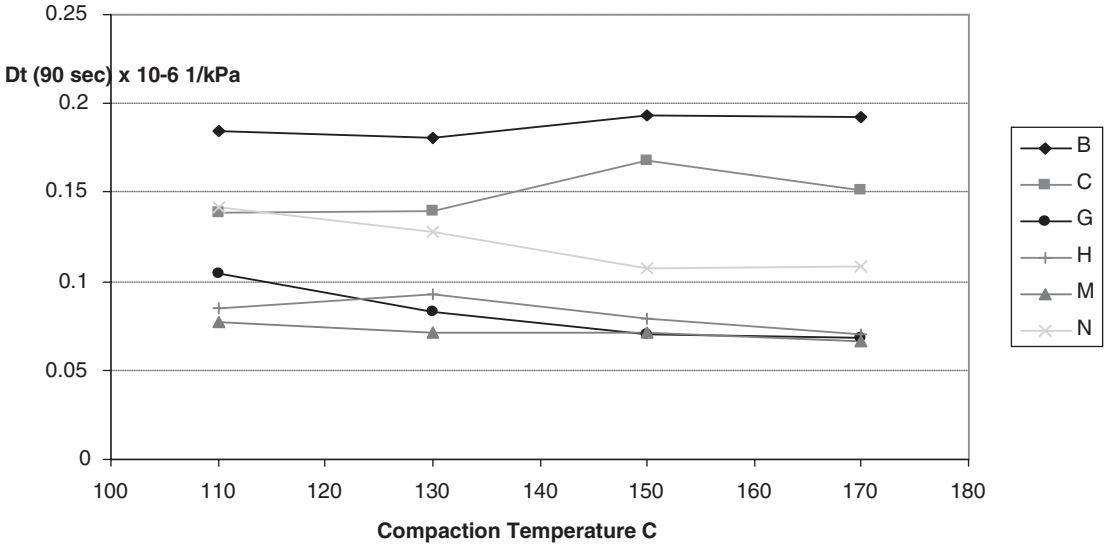

Figure 34. Creep compliance results for modified binders tested at −20°C.

Figure 39 show the change in compliance for the set of unmodified binders. The compliance results generally follow the expected trends:

- Lower test temperatures yield lower creep compliance results (higher stiffness), which means that the mixes lose their ability to relax thermal strains as the temperature decreases.
- Higher compliance values are generally observed for mixes having binders with lower low-temperature grades. For example, Mix B, which has a low PG true grade of −37.3°C, is more compliant than Mix M, which has a low PG true grade of −19.5. This observation confirms that a binder's low PG number controls thermal cracking performance.

From Figure 34 [the lowest test temperature (−20°C)], the modified binders are so stiff that compaction temperature appears to have a negligible effect. However, for the unmodified binders, shown in Figure 37, most have a slight trend indicating that lower compaction temperatures resulted in slightly higher creep compliance values.

From Figure 36 and Figure 39, which are plots of the creep compliance results at 0°C for the modified and unmodified

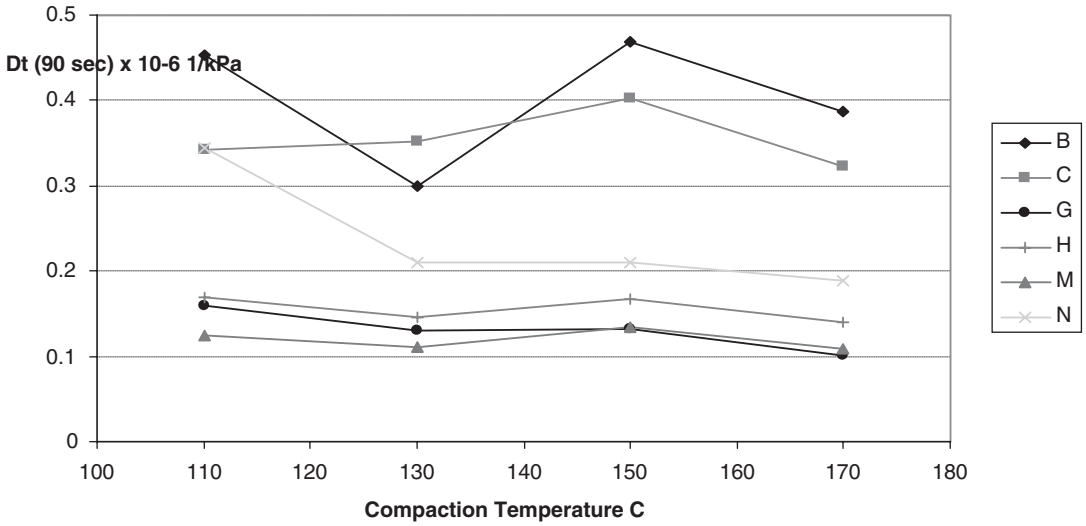

Figure 35. Creep compliance results for modified binders tested at −10°C.

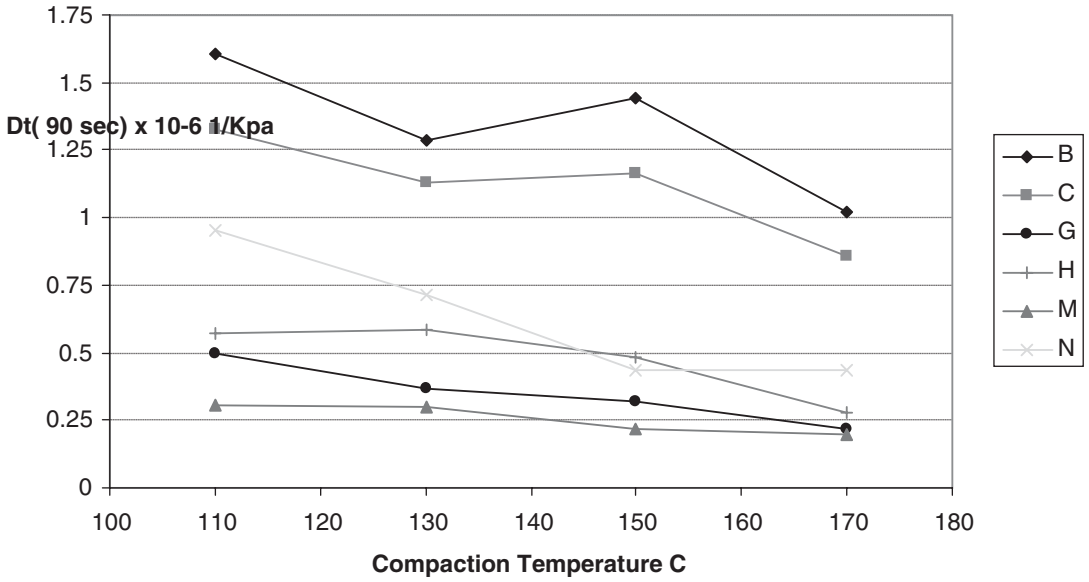

Figure 36. Creep compliance results for modified binders tested at 0°C.

binders respectively, it can be seen that the compliance drops substantially for some binders, including Binders B, C, and N of the modified binder set, and Binders E, D, O, and I for the unmodified binders. These binders are the ones with the lowest low temperature grades. This indicates that the binders with the lowest low temperature PG grades are more susceptible to a loss of compliance due to overheating.

An ANOVA of creep compliance at −20°C with all binders confirmed that compaction temperature and binder ID are statistically significant factors on compliance results. This analysis is shown in Table 31. As the data in Table 32 and Table 33 show, the same is true at the other creep compliance temperatures. However, the magnitude of the F-statistic for compaction temperature relative to the F-statistic for Binder ID is much greater for the test results at 0°C, which indicates that the creep compliance test at this temperature is more sensitive to the compaction temperature. Therefore, compaction temperature does have a significant effect on low temperature prop-

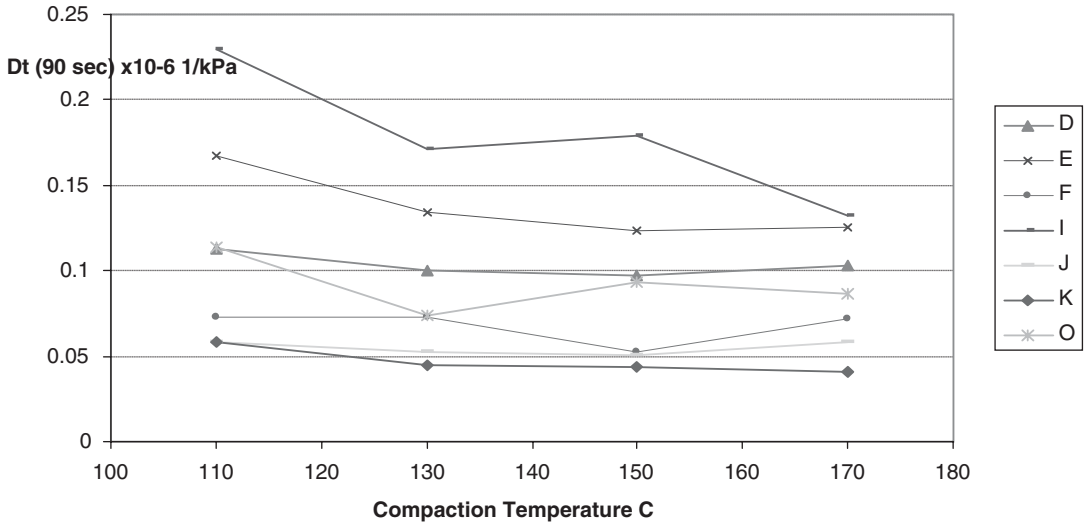

Figure 37. Creep compliance results for unmodified binders tested at −20°C.

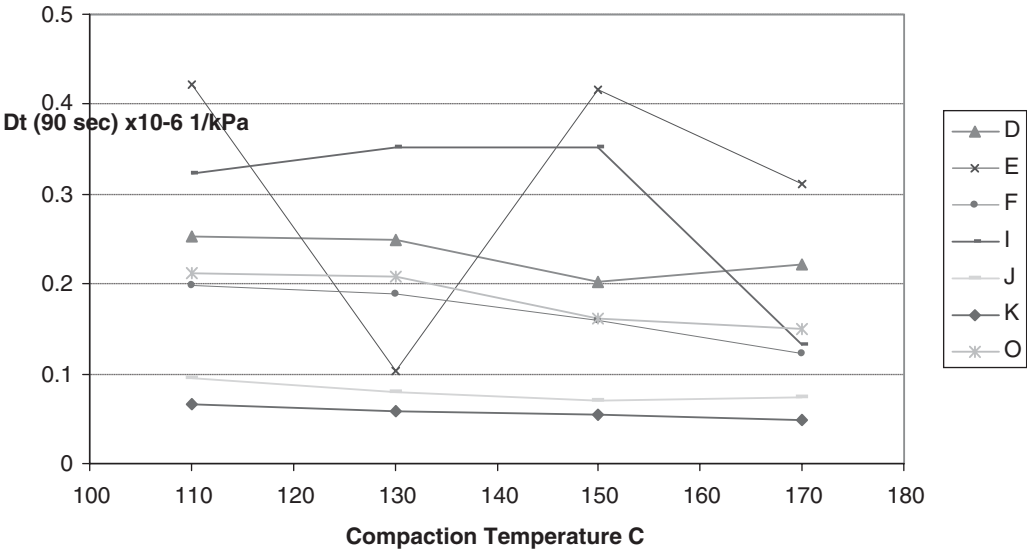

Figure 38. Creep compliance results for unmodified binders tested at −10°C.

erties of the mixtures. Increasing the mixing and compaction temperatures can reduce the ability of a mixture to dissipate thermal stresses.

Figure 40 illustrates a relationship between the creep compliance results at 0°C and binder low PG grade and compaction temperature. This graph shows the strong relationship between the low PG grade and creep compliance, but also shows the influence of compaction temperature on this relationship. The main point of this figure is that mixing and compaction temperatures influence the potential for low temperature cracking, but the magnitude of the effect depends on the original low critical temperature of the binder and how hot the mix was heated.

Following the indirect tensile creep tests, the specimens were tested to determine tensile strengths. Tensile strength tests were initially conducted at −20°C. However, a few specimens reached the maximum load cell capacity of the IDT system, so the remaining tests were conducted at −10°C. The tensile strength results are summarized in Table 34.

An ANOVA on this data, shown in Table 35, indicates that the binder ID, compaction temperature, and their interaction have significant effects on the tensile strengths. The

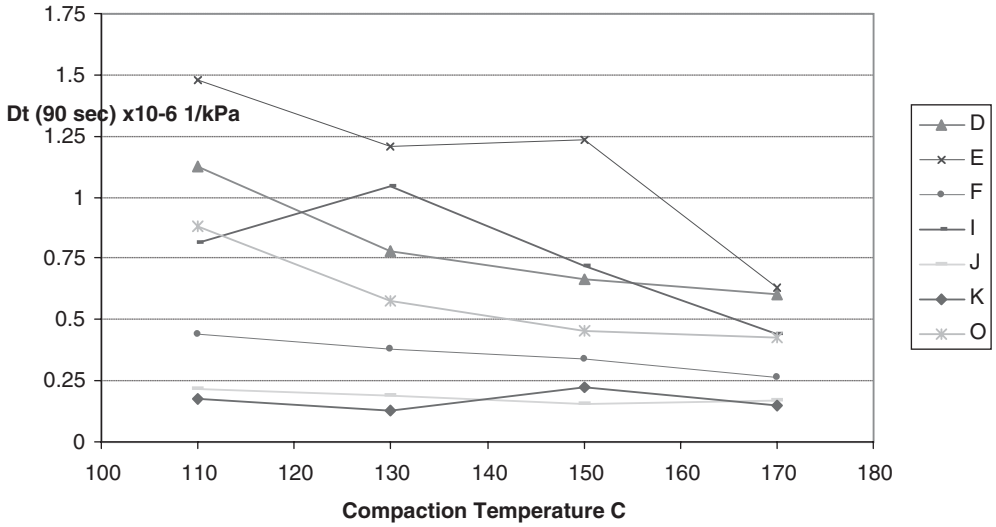

Figure 39. Creep compliance results for unmodified binders tested at 0°C.

Table 31. ANOVA for creep compliance at −20°C.

Factor	Type	Levels	Values
Binder	fixed	13	B,C,D,E,F,G,H,I,J,K,M,N,O
CompT	fixed	4	110,130,150,170

Analysis of Variance for Creep -20, using Adjusted SS for Tests

Source	DF	Seq SS	Adj SS	Adj MS	F	P
Binder	12	0.1006398	0.1006398	0.0083866	42.98	0.000
CompT	3	0.0031606	0.0031606	0.0010535	5.40	0.004
Error	36	0.0070239	0.0070239	0.0001951		
Total	51	0.1108243				

Table 32. ANOVA for creep compliance at −10°C.

Factor	Type	Levels	Values
Binder	fixed	13	B,C,D,E,F,G,H,I,J,K,M,N,O
CompT	fixed	4	110,130,150,170

Analysis of Variance for Creep -10, using Adjusted SS for Tests

Source	DF	Seq SS	Adj SS	Adj MS	F	P
Binder	12	0.570865	0.570865	0.047572	18.66	0.000
CompT	3	0.028798	0.028798	0.009599	3.77	0.019
Error	36	0.091769	0.091769	0.002549		
Total	51	0.691432				

Table 33. ANOVA for creep compliance at 0°C.

Factor	Type	Levels	Values
Binder	fixed	13	B,C,D,E,F,G,H,I,J,K,M,N,O
CompT	fixed	4	110,130,150,170

Analysis of Variance for Creep 0, using Adjusted SS for Tests

Source	DF	Seq SS	Adj SS	Adj MS	F	P
Binder	12	7.08764	7.08764	0.59064	35.14	0.000
CompT	3	0.88120	0.88120	0.29373	17.48	0.000
Error	36	0.60509	0.60509	0.01681		
Total	51	8.57393				

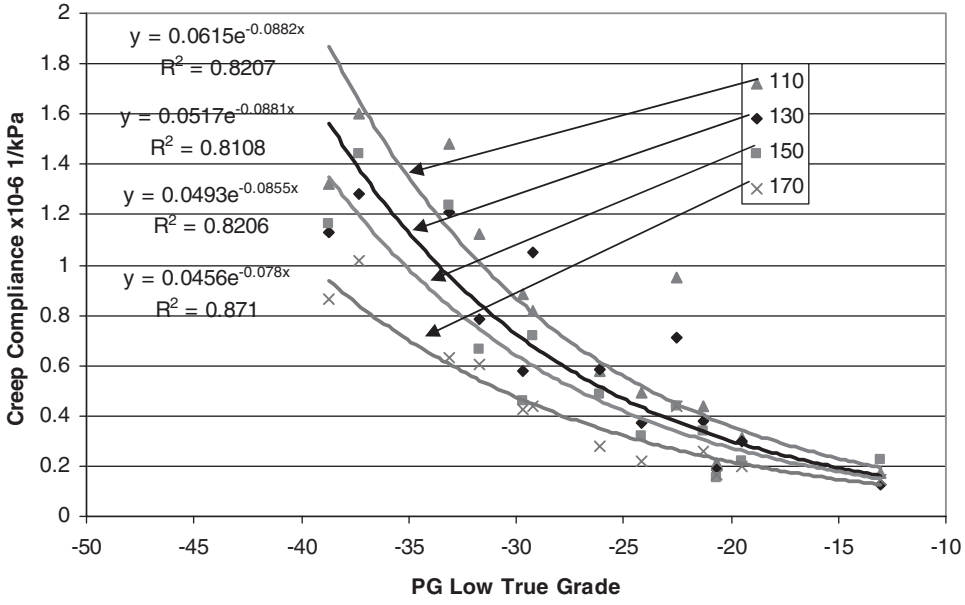

Figure 40. Graph of relationships between low PG grade, compaction temperature, and IDT creep compliance at 0°C.

Table 34. Summary of indirect tensile strengths (MPa).

Test Temp. °C			-20				-10			
Comp. Temp. °C			110	130	150	170	110	130	150	170
Comp. Temp. °F			230	266	302	388	230	266	302	388
M	**85.5 -19.5**	**Avg.**					**3.57**	**3.44**	**3.81**	**3.46**
		St. Dev.					**0.10**	**0.23**	**0.22**	**0.54**
N	**84.3 -25.5**	**Avg.**					**2.67**	**3.20**	**3.04**	**3.12**
		St. Dev.					**0.25**	**0.29**	**0.10**	**0.19**
G	**82.5 -24.2**	**Avg.**	**2.95**	**3.56**	**4.05**	**3.51**				
		St. Dev.	**0.55**	**0.51**	**0.10**	**0.52**				
H	**78.3 -26.1**	**Avg.**					**3.89**	**3.62**	**3.74**	**3.09**
		St. Dev.					**0.15**	**0.34**	**0.39**	**0.82**
C	**75.1 -38.7**	**Avg.**					**2.82**	**2.78**	**2.96**	**3.08**
		St. Dev.					**0.09**	**0.39**	**0.11**	**0.16**
I	71.8 -29.2	Avg.					2.71	2.63	2.64	2.84
		St. Dev.					0.27	0.23	0.21	0.20
B	**69.3 -37.3**	**Avg.**	**2.99**	**4.08**	**3.81**	**3.39**				
		St. Dev.	**0.72**	**0.11**	**0.18**	**0.74**				
F	67.8 -21.3	Avg.					3.26	3.54	3.68	3.82
		St. Dev.					0.21	0.43	0.35	0.17
O	65.6 -29.7	Avg.					2.83	3.14	3.97	3.73
		St. Dev.					0.20	0.39	0.17	0.60
K	65.3 -13.0	Avg.					3.14	3.83	3.74	3.79
		St. Dev.					*	0.07	0.23	**
J	64.3 -20.7	Avg.					3.52	3.31	3.74	3.76
		St. Dev.					0.35	0.28	0.27	0.07
E	60.9 -33.1	Avg.					2.78	2.75	2.75	2.95
		St. Dev.					0.15	0.28	0.29	0.28
D	60.3 -31.7	Avg.					3.43	3.48	3.64	3.49
		St. Dev.					0.57	0.43	0.29	0.25

* only one tensile strength result, ** only two tensile strength results

interaction plot (Figure 41) shows that there were no consistent trends. Compaction temperature seems to have different effects on tensile strengths for the different binders. For example, a few binders show a peak in tensile strength at 130°C or 150°C, others show lower tensile strengths in the middle of the temperature range, and others show tensile strengths increasing throughout the compaction temperature range.

The data were further analyzed for each binder separately to evaluate the significance of compaction temperature. In these separate analyses, only Binders K and O were found to have compaction temperature as a significant effect on tensile strength. For Binder K, a Tukey's multiple comparison ($\alpha = 0.05$) of tensile strengths at the four temperatures showed that the tensile strength at 110°C was significantly lower than for the other temperatures. However, this data set had a very limited number of samples. For Binder O, the tensile strengths at 110°C were significantly lower than the other temperatures, and the tensile strength at 130°C was significantly lower than 150°C, but not significantly different than 170°C. Overall, the tensile strength results varied from binder to binder such that

Table 35. ANOVA for indirect tensile strength at −10°C.

Factor	Type	Levels	Values
Binder	fixed	11	C,D,E,F,H,I,J,K,M,N,O
Temp	fixed	4	110,130,150,170

Analysis of Variance for TS, using Adjusted SS for Tests

Source	DF	Seq SS	Adj SS	Adj MS	F	P
Binder	10	17.87942	16.67716	1.66772	17.74	0.000
Temp	3	1.77062	1.84765	0.61588	6.55	0.000
Mix*Temp	30	6.20140	6.20140	0.20671	2.20	0.002
Error	100	9.40024	9.40024	0.09400		
Total	143	35.25169				

S = 0.306598 R-Sq = 73.33% R-Sq (adj) = 61.87%

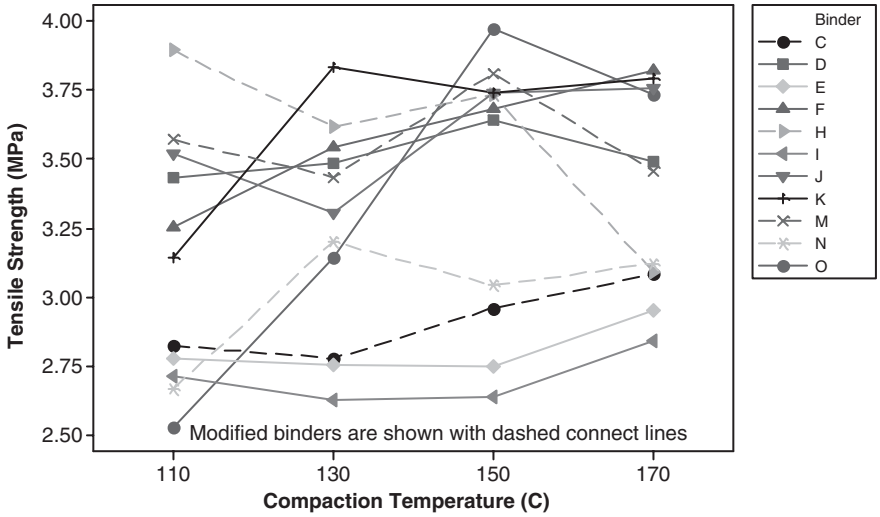

Figure 41. Interaction plot for compaction temperature and binder on tensile strengths at −10°C.

it was not possible to make general conclusions or observations about trends regarding the effect of compaction temperature.

Correlation of Mixing and Compaction Temperatures

A key part of this research was to compare the predicted mixing and compaction temperatures from the candidate binder tests with the results of the mixture experiments. This section presents that analysis using correlations performed with MINITAB release 15 statistical software. The regressions are based on average values from replicate mix tests and binder tests. Outputs included graphical plots of the data, least-squares linear regression equations, 95% confidence intervals for the regressions, the residual error regression S, the coefficient of determination R^2, and the adjusted R^2. An ANOVA table was also generated for each regression, which includes the observed significance level (P-value) for the regression equations. For several correlations, one or two data points were identified as suspected outliers. Discussion of the outliers is presented as part of the analysis associated with the particular correlation. In each case where outlier data is suspected, the correlations are provided both with and without the questionable data.

Figure 42 shows the correlations of the mixing temperatures from the Steady Shear Flow (SSF) method with the mixing temperatures to achieve 98% coating using the bucket mixer. The bucket mixer coating test results for Binder H was not considered reasonable as the predicted temperature to achieve the baseline coating percentage was outside of the experimental range. The regression statistics indicate the SSF mixing temperature explains only about 40% of the variation observed in temperatures needed to achieve the baseline coating percentage with the bucket mixer. Binders that had the largest residuals were O, C, B, and I. The temperatures to achieve good coating for Binders O and C were much higher than predicted by the SSF method and for B and I coating was achieved at temperatures much lower than predicted by the SSF method.

Figure 43 shows a similar set of plots of SSF mixing temperatures versus the mixing temperatures to achieve 89% coating with the pugmill mixer. The regression statistics are somewhat poorer compared with those with the bucket mixer. For this data set, Binder E was considered as a possible outlier since the predicted temperature to achieve the baseline percentage was 222°F (106°C), which seems quite low and is outside of the experimental range.

Figure 44 shows the correlations of mixing temperatures from the Phase Angle method with the coating test results using the bucket mixer. As noted above, the bucket mixer coating test results for Binder H were not considered valid, so these data were removed and the correlations were performed again. The statistics for the regressions in these two plots are poorer than for the SSF method. As with the SSF correlations, the binders that have large residuals include Binders O, C, I, and B. Binder M also has a large residual in the Phase Angle–bucket mixer coating test correlations. This is the binder that includes the Sasobit® wax. The large residual with this binder could indicate that the Phase Angle method is not a good predictor of mixing temperatures for binders with Sasobit®, perhaps because the Phase Angle measurements are made at below temperatures where the Sasobit® wax melts. The poor correlations with O, C, I, and B for both the SSF and the Phase Angle methods is evidence that the problematic data likely arise

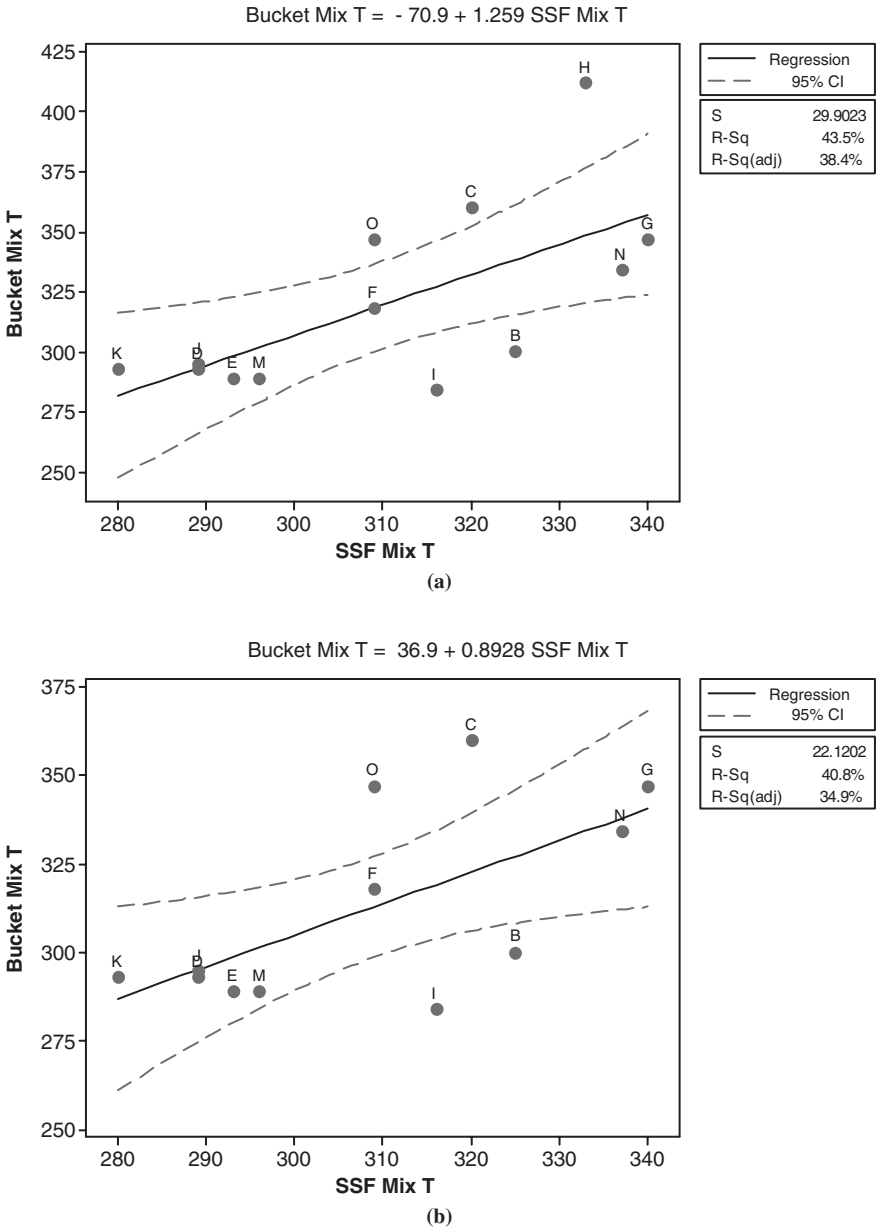

Figure 42. Correlations of the SSF mixing temperature with the bucket mixer temperature for 98% coating: (a) all data; (b) excludes Binder H.

from the bucket mixer coating results rather than the candidate methods for determining mixing and compaction temperatures.

Figure 45 shows the correlations of the Phase Angle method predicted mixing temperatures with the temperatures to achieve the baseline coating percentage in the pugmill mixer. As discussed with the SSF method–pugmill mixer correlation, the coating test results for Binder E in the pugmill were not considered valid. The regression statistics between the Phase Angle method and the pugmill mixer coating results are slightly better than for the SSF method. A summary of correlation statistics is shown in Table 36.

Overall, the correlations between the mixing temperatures from the candidate methods and the coating test results are fairly weak, generally with R^2 values in the range of 30 to 40%. However, the lack of strength of the correlations is likely due more to the coating test results that are based on curve-fitting through data from subjective measurements that lack good repeatability.

Figure 46 and Figure 47 show correlations between the candidate methods mixing temperatures and the midpoints of the mixing temperature range recommended by the binder suppliers. The correlation between the SSF method mixing temperature and the suppliers' recommended mixing temperatures is

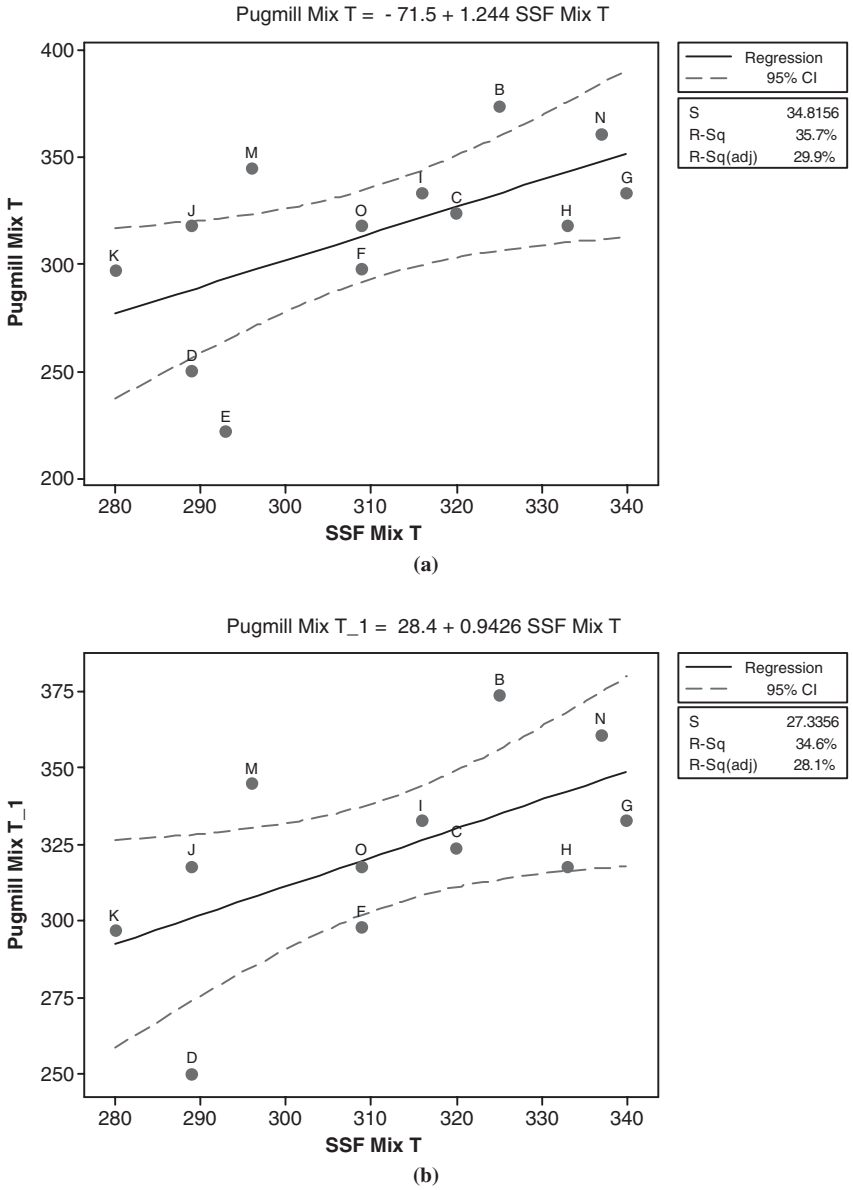

Figure 43. Correlations of the SSF mixing temperature with the pugmill mixer temperature for 89% coating: (a) all data; (b) excludes Binder E.

quite reasonable, with an R^2 of 70%. The correlation of the Phase Angle method mixing temperatures with the suppliers' recommended mixing temperatures is very weak unless the results from Binder M are removed. The issue with the Sasobit® wax in Binder M was noted previously. With this data point removed, the correlation statistics improve considerably, although not as strong as with SSF method. However, it is also important to note that the regression equation between the phase angle method and producers' recommendations was slightly closer to the line of equality than for the SSF method. Overall, these correlations show that both methods provide results generally consistent with field experience and therefore pass a test of reasonableness.

Figure 48 and Figure 49 show the correlations between the workability tests and the results of the candidate methods for determining mixing and compaction temperatures. For these correlations, the temperatures midway between the mixing and compaction temperatures from the candidate methods were used as the independent variable. Although the correlations are weak as indicated by the low correlation coefficients, the regressions were statistically significant (α=0.05). No data were excluded from these correlations. However, most of the scatter is likely due to poor precision of the workability tests. Despite numerous attempts to improve the workability equipment and test method during this study, there is considerable doubt about the validity of the test as an indicator of binder

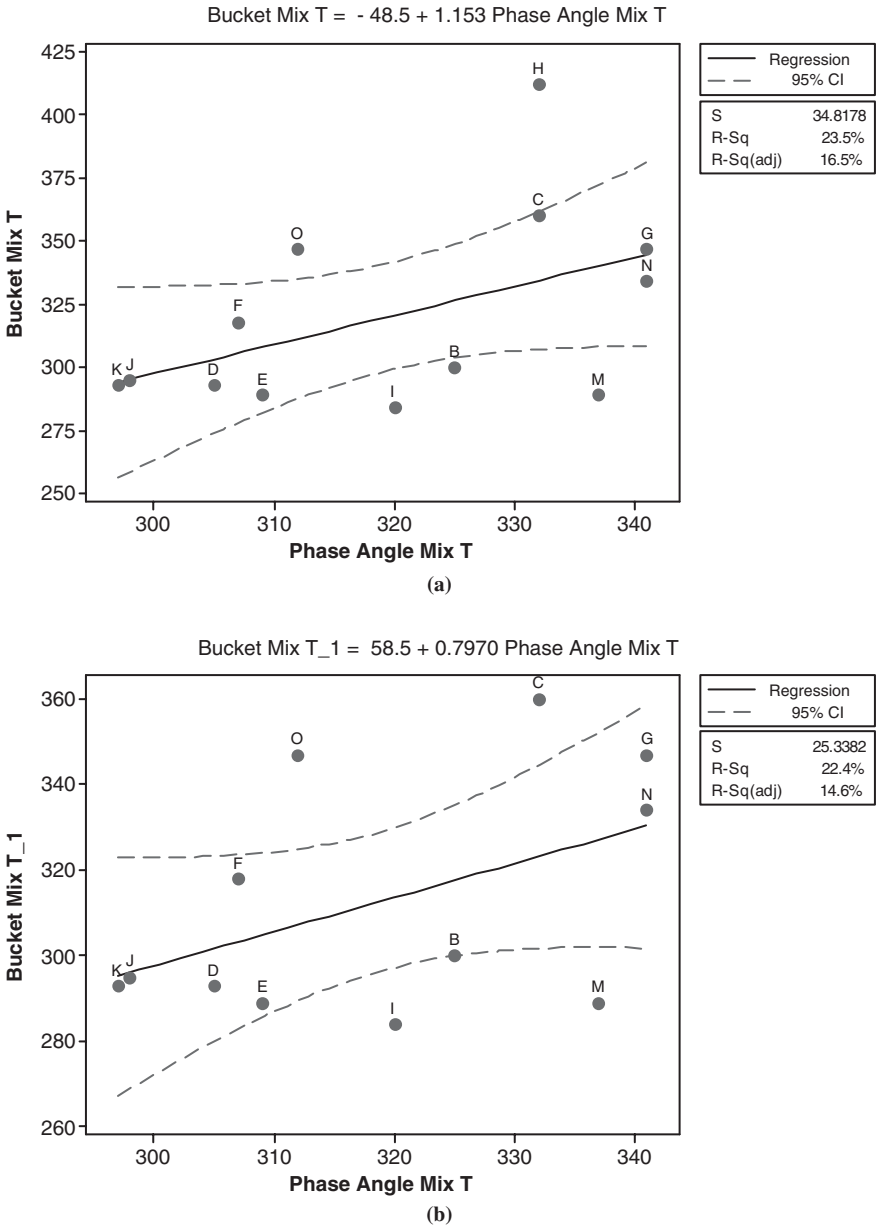

Figure 44. Correlation of Phase Angle Method mixing temperature with the bucket mixer temperature for 98% coating: (a) all data; (b) excludes Binder H.

stiffness on mix workability. The average temperature difference for the duplicate runs on all of the workability tests was 26°F, which is a similar magnitude as the residuals for the correlations.

Correlations between the compaction temperatures predicted by the candidate methods with the results of the compaction tests are shown in Figure 50 and Figure 51. Excluding the data for Binders I and J, both of the candidate methods' compaction temperatures correlate well with the results from the mix compaction tests. Three binders had compaction test results that were outside of the experimental range for the tests: Binders I, J, and N. It is clear from the correlation graphs that the SGC compaction test temperatures for I and J are well above the reasonable range for these binders. Binder N is a heavily modified binder that was expected to require a relatively high temperature to achieve the baseline density level. Its compaction experiment results were just above the highest test temperature used in the compaction experiment.

A summary of the regression statistics for the correlations between the candidate methods and mix test results is shown in Table 36. Also shown are the key statistics from the correlations with the respective midpoints of the binder producers'

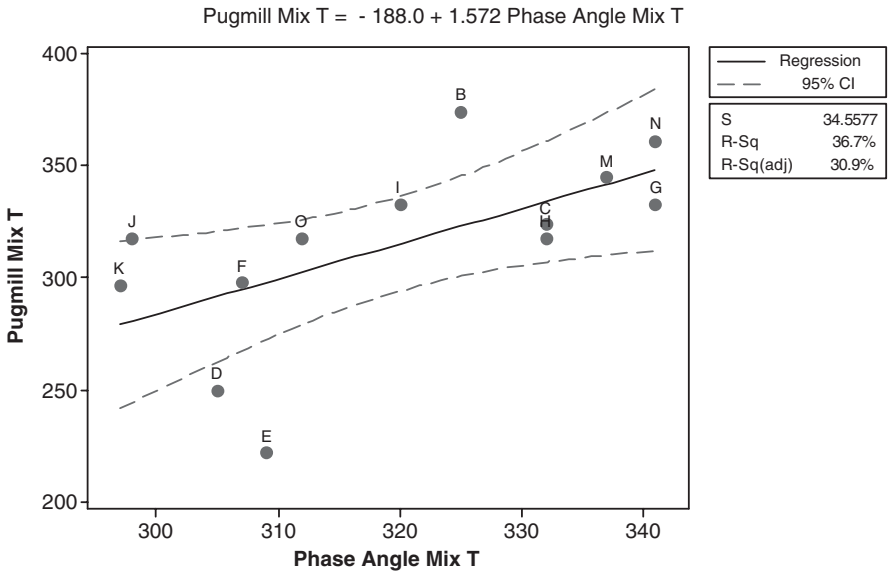

(a)

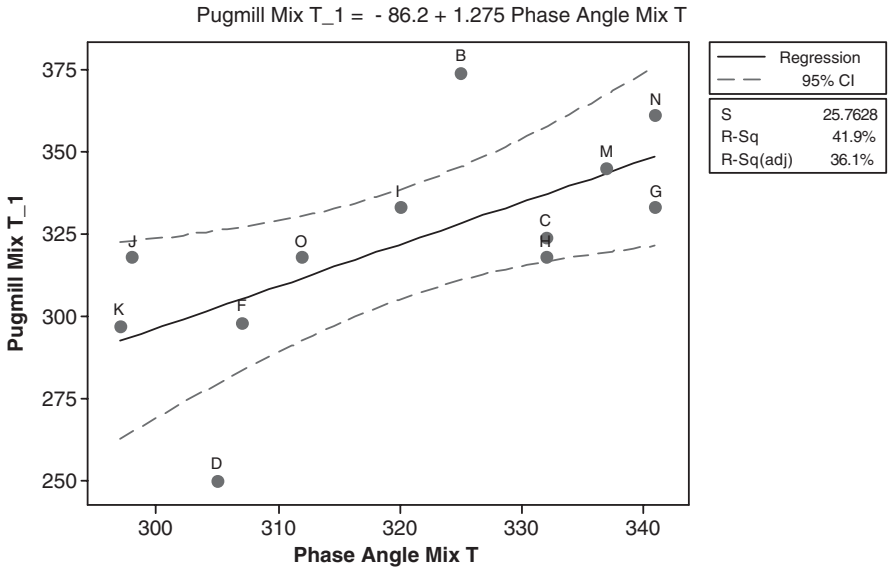

(b)

Figure 45. Correlation of Phase Angle method mixing temperature with the pugmill mixer temperature for 98% coating: (a) all data; (b) excludes Binder E.

Table 36. Summary of correlation statistics.

	Steady Shear Flow			Phase Angle		
Mix Test	Residual Error	R^2	P-value	Residual Error	R^2	P-value
Bucket	22.1	40.8	0.025	25.3	22.4	0.121
Pugmill	27.3	34.6	0.044	25.7	41.9	0.023
Workability	34.0	30.6	0.050	30.5	44.3	0.013
Compaction	18.7	68.4	0.002	16.7	74.8	0.001
Producers' Midpoint	7.8	70.1	0.000	8.8	58.2	0.004

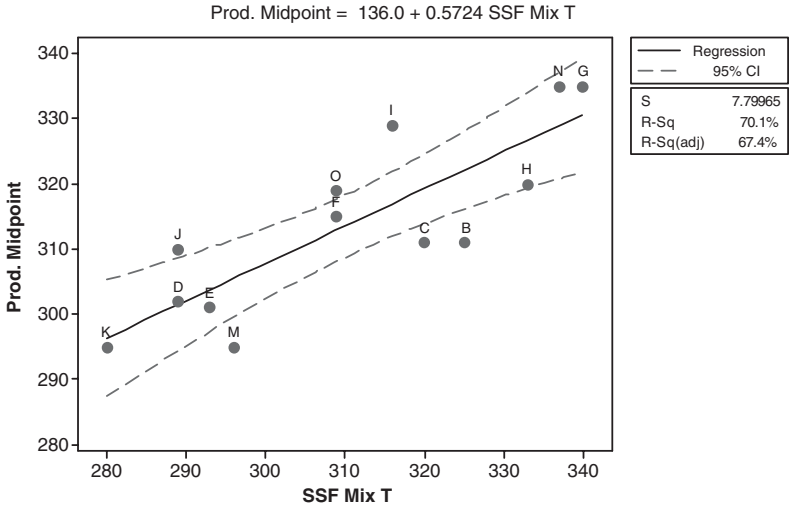

Figure 46. Correlation of the SSF mixing temperature with the midpoint of the binder producers' recommended mixing range.

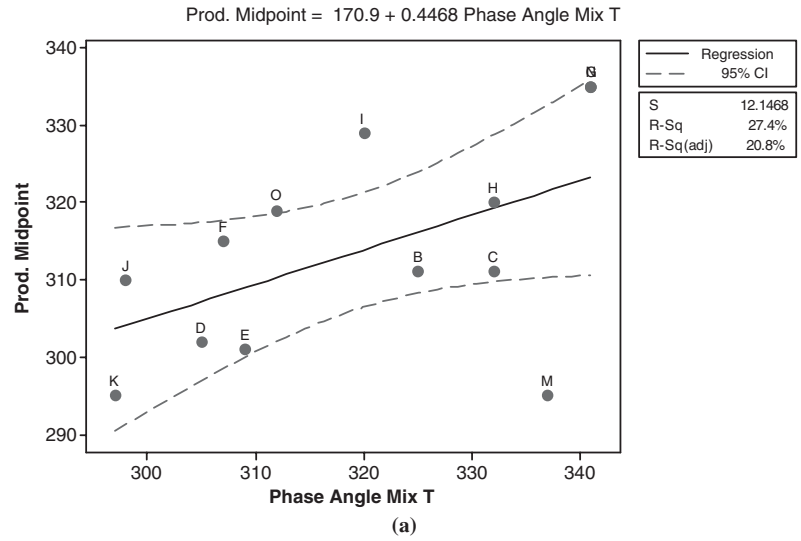

(a)

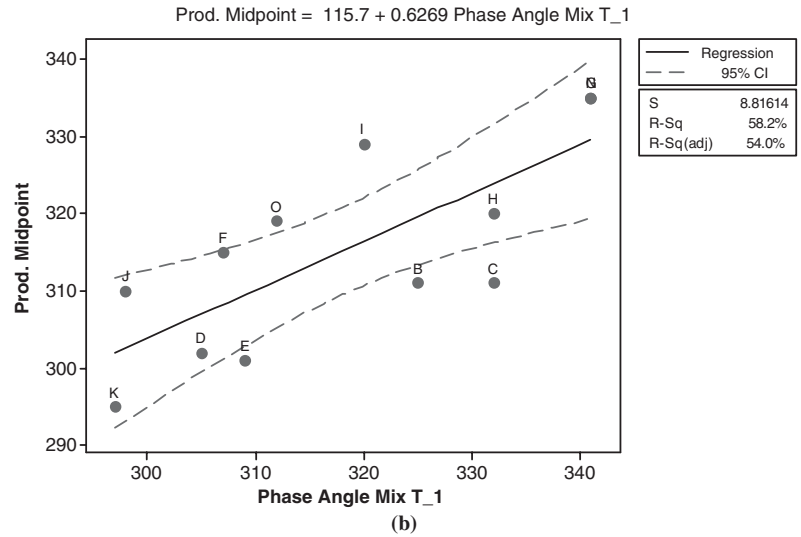

(b)

Figure 47. Correlation of the Phase Angle Method mixing temperature with the midpoint of the binder producers' recommended mixing range: (a) all data; (b) excludes Binder M.

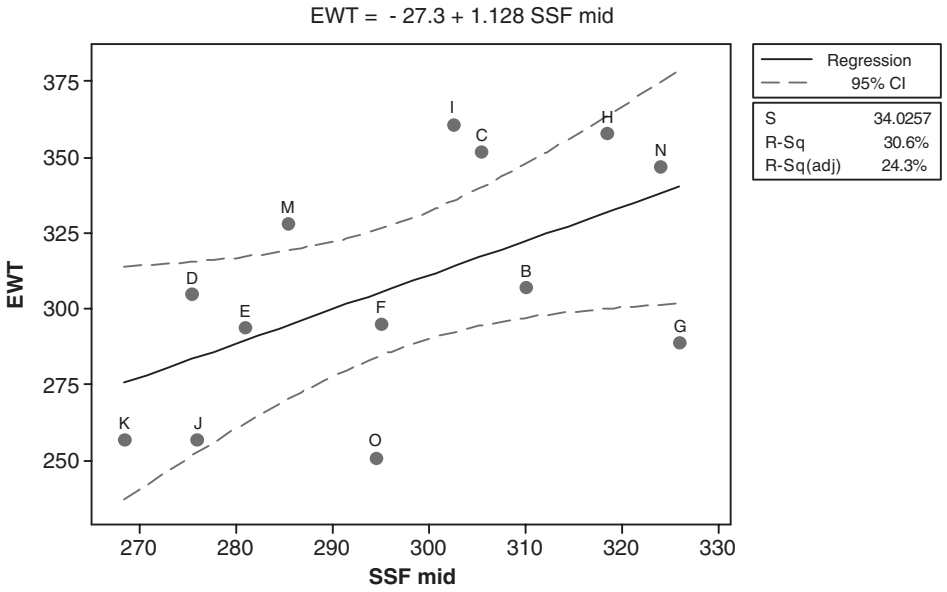

Figure 48. Correlation of SSF mixing and compaction temperature midpoint with workability experiment equivalent torque temperature.

recommended mixing temperatures. These statistics are based on the correlations without suspected outliers, even where the statistics did not improve with these data excluded. Lower P-values indicate the correlation is more significant. A *P*-value of 0.05 or less is generally considered a statistically significant correlation. In general, the correlation statistics are similar for the two methods. The SSF method had better correlation statistics with the bucket mixer coating test results and the producers' recommended mixing temperatures. The Phase Angle method statistics appeared to be slightly better than the other correlations with mix test results.

Statistical analyses were conducted to determine whether the SSF method or the Phase Angle method provided a better overall fit to the experimental data from the mixture tests and the binder producers' recommended mixing temperatures. The analyses used an F-statistic to test the null hypothesis that the residual variances were equal, H_0: $\sigma^2(SSF) = \sigma^2(PA)$, for each regression summarized in Table 36. The F-test is an

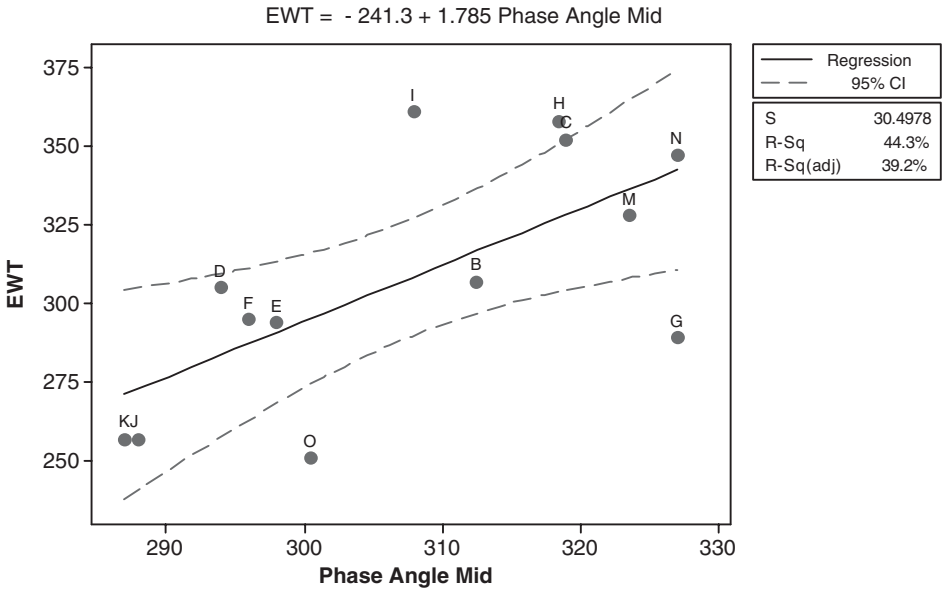

Figure 49. Correlation of Phase Angle method mixing and compaction temperature midpoint with workability experiment equivalent torque temperature.

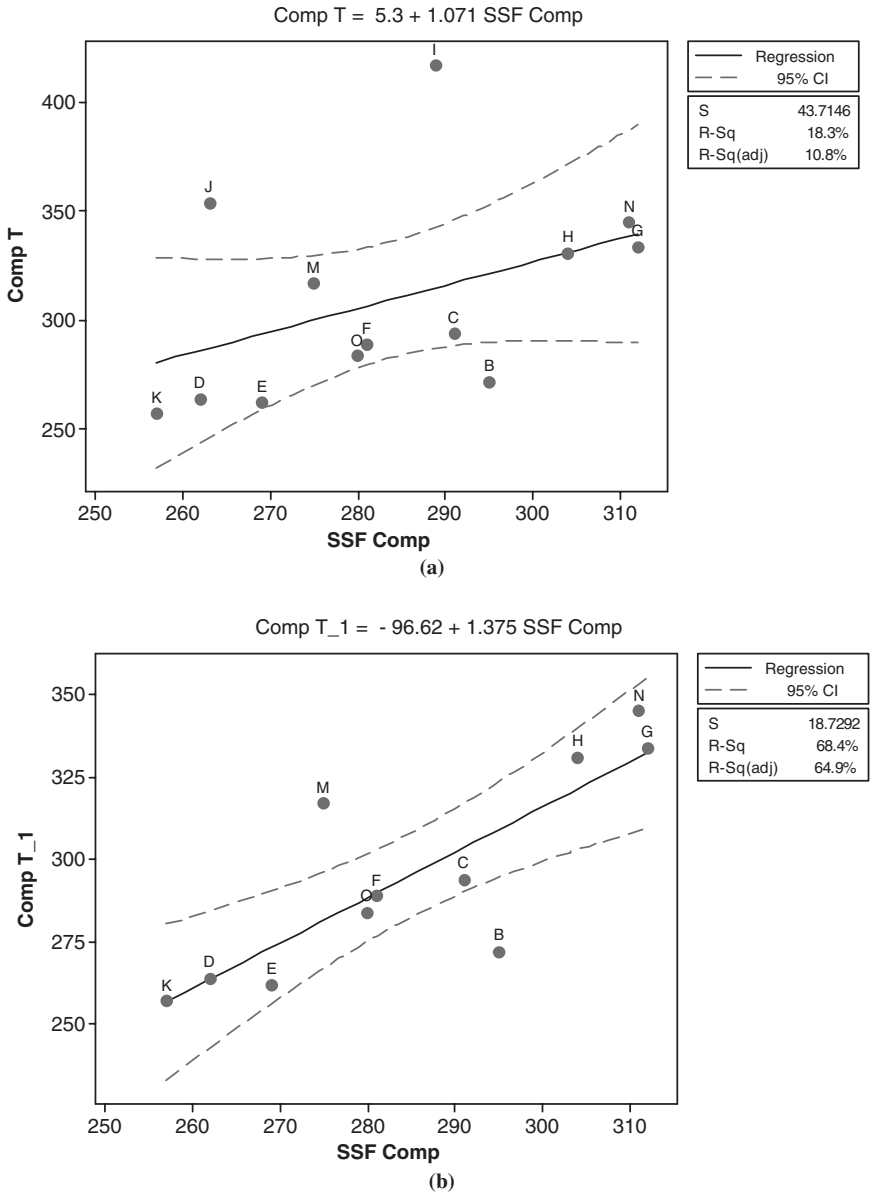

Figure 50. Correlation of the SSF Method compaction temperatures with the compaction experiment equivalent density temperatures: (a) all data; (b) excludes Binders I and J.

approximation because it violates the independence assumption and, therefore, does not possess as much statistical power as the case when the chi-squared random variables are independent. The full analyses are provided in Appendix D.

The analyses indicated that for each of the mix tests, there was not sufficient statistical evidence that either method explained more variability in the experimental data than the other, even when the R^2 values differed by as much as 18.4%, as was the case for the correlations with coating tests results for the bucket mixer. Therefore, it can be concluded that the neither the SSF method nor the Phase Angle method is statistically better in correlating to mixing and compaction temperatures from mixture tests or producers' recommendations.

Comparison of SSF and Phase Angle Methods

Although the candidate methods are based on different binder properties, there are some similarities between the SSF method and Phase Angle method. Both methods use a standard DSR and common parallel plate geometries for testing of the binder; therefore, they have some practical limitations including the test temperatures at which the properties are measured and at which particulate matter begins to have an effect.

Correlations of the mixing and compaction temperatures determined by the two methods, shown in Figure 52 and Figure 53 respectively, further illustrates the similarities. These

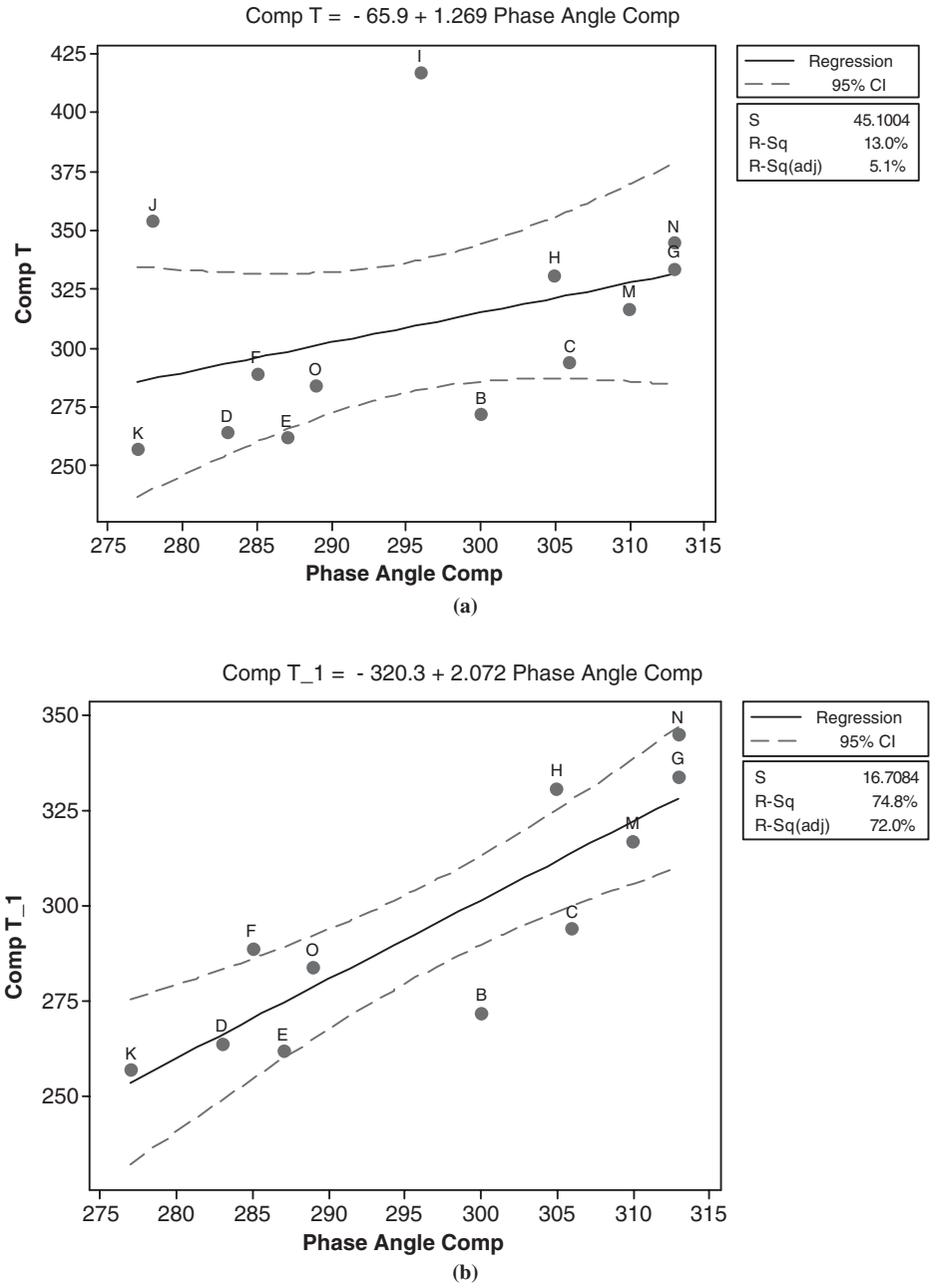

Figure 51. Correlation of the Phase Angle method compaction temperatures with the compaction experiment equivalent density temperatures: (a) all data; (b) excludes Binders I and J.

plots show that the results of the two methods are well correlated, especially when Binder M is removed from the data set. The difference in the results for Binder M may be due to the warm mix asphalt additive, Sasobit®, included in this binder. Sasobit® is a Fischer-Tropsch wax that solidifies in asphalt between 149°F and 239°F (65°C to 115°C). The SSF test temperatures were slightly higher (up to 88°C) compared with test temperatures in the Phase Angle method, which went up to 80°C. It is possible that a phase change of the Sasobit® wax occurred in the temperature range between the two methods, which affected the rheological behavior of the binder and resulted in significantly different mixing and compaction temperatures for Binder M.

Based on the correlation equations, the mixing temperatures from the SSF and Phase Angle methods will be equivalent at 347°F (175°C). At the lower end of the mixing temperature range for typical paving-grade binders, the results of the SSF method will be about 13°F (7°C) lower than the mixing temperature from the Phase Angle method. Similarly, based on the correlation of compaction temperatures from the two

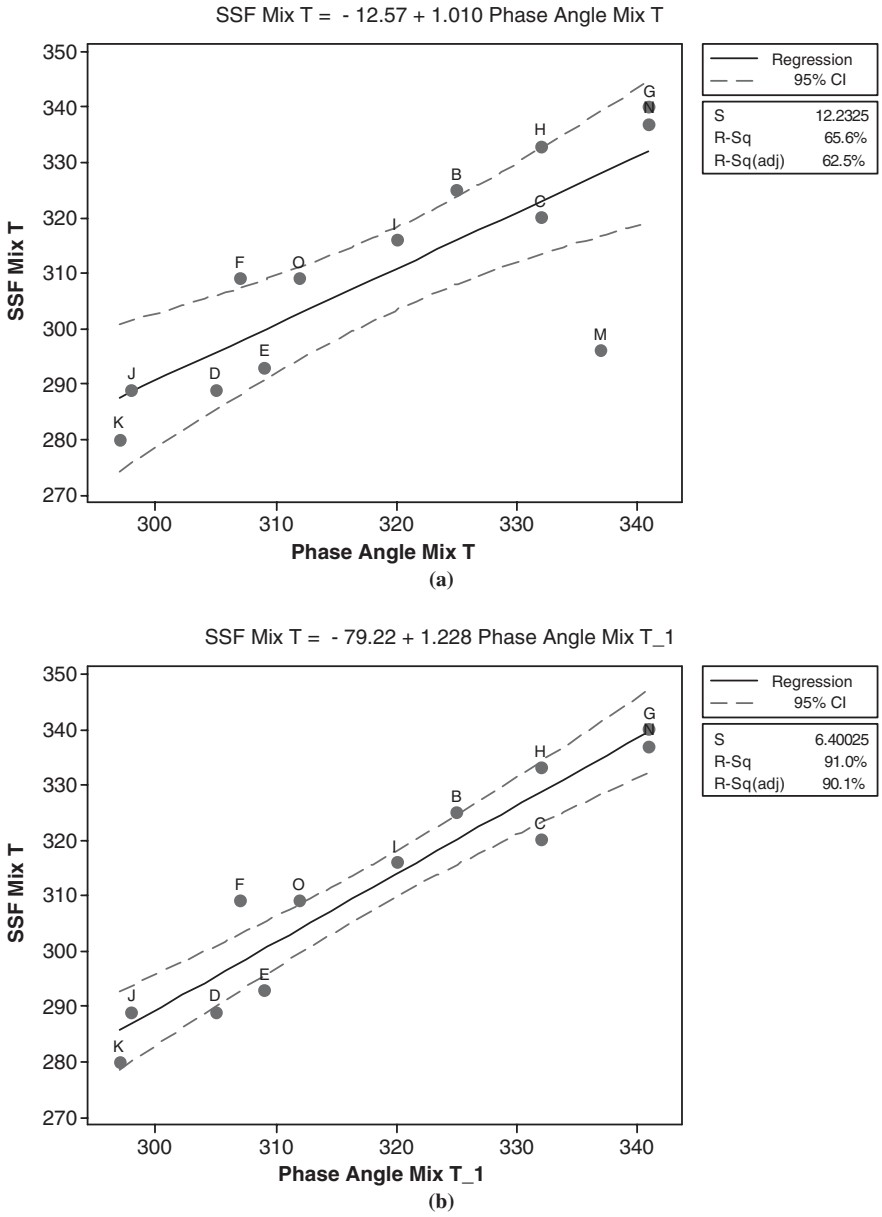

Figure 52. Correlation of mixing temperatures from the SSF Method and the Phase Angle method: (a) all binders, (b) excludes Binder M.

methods, the methods will give equivalent results at 318°F (159°C), which should be the upper end of the range of compaction temperatures. At the lower end of the compaction temperature range for typical paving-grade binders, the results of the SSF method will be about 18°F (10°C) lower than the compaction temperature from the Phase Angle method.

Validation Experiment Results and Analysis

A set of four independent binders were selected at the beginning of the study for a small validation experiment to verify the recommended method. This set of binders included a variety of crude sources, PG grades, and modification types, as shown in Table 37. Since the SSF method and the Phase Angle method had similar correlations with the mix tests and both appear to be viable options for determining mixing and compaction temperatures, both methods were carried forward in the validation experiment.

A summary of the mixing and compaction temperatures determined from the SSF and Phase Angle methods for the validation binders is shown in Table 37. The true grades of each of the validation binders determined by NCAT differed from the grades reported by the producers. Also included in the table are the midpoints of the mixing and compaction temperatures recommended by the respective binder suppliers. Another point of reference is the equiviscous mixing and

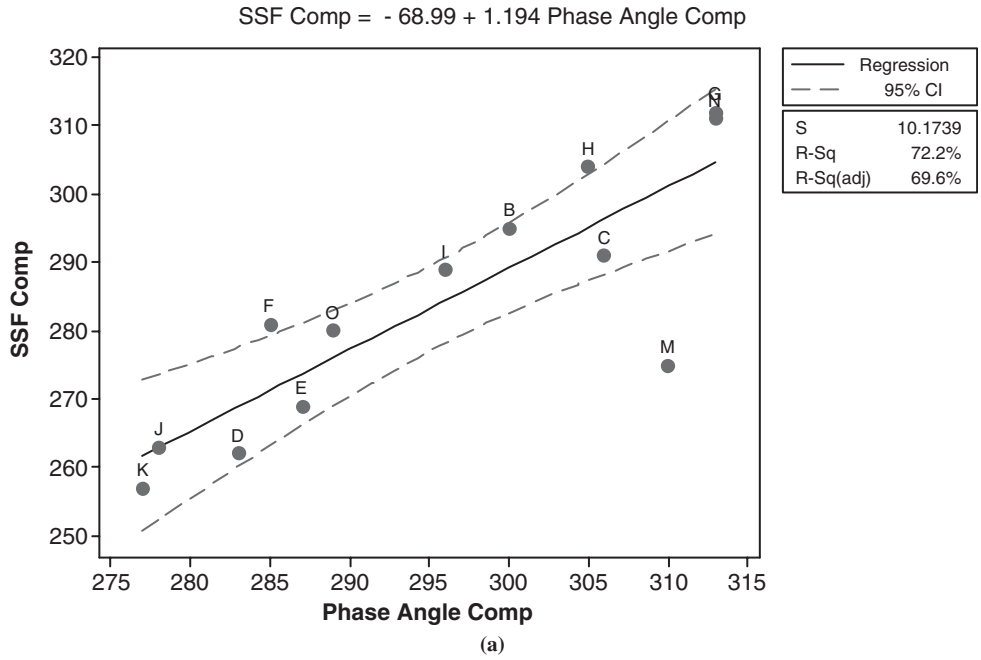

(a)

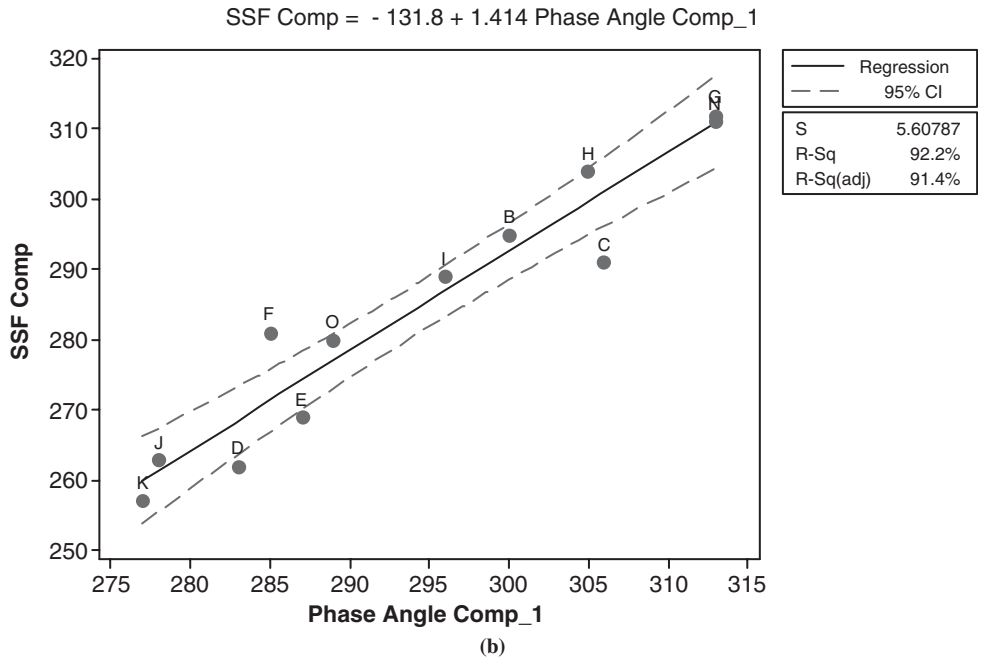

(b)

Figure 53. Correlation of Compaction Temperatures from the SSF Method and the Phase Angle Method: (a) all binders and (b) excludes Binder M.

compaction temperatures for the unmodified Binder Y, which were 333°F and 308°F, respectively.

Overall, the temperatures from the Phase Angle method are lower than for the SSF method, but the differences are not consistent for this set of binders. For Binder Z, the results for the methods were very similar, but for Binder W, the difference between the results of the two methods was 20°F for the mixing temperature. Compared with the producers' recommended mixing and compaction temperatures, the Phase Angle method under predicted the mixing and compaction temperatures for three of the four validation binders. The Phase Angle method also under predicted the mixing and compaction temperatures relative to the equiviscous method for the unmodified binder. The SSF method over predicted mixing temperatures for three of the four binders and over predicted compaction temperatures in just two cases. Both candidate methods over predict mixing and compaction temperatures for Binder X and under predict mixing and compaction temperatures for Binder Z.

Table 37. SSF and Phase Angle method results for validation binders.

Binder I.D.	Binder True Grade	SSF Method		Phase Angle Method		Midpoint of Producer's Recommendation	
		Mixing Temp. (ºF)	Comp. Temp. (ºF)	Mixing Temp. (ºF)	Comp. Temp. (ºF)	Mixing Temp. (ºF)	Comp. Temp. (ºF)
W	**90.0 -17.8**	**358**	**329**	**338**	**311**	**345**	**325**
X	**74.2 -27.9**	**345**	**315**	**338**	**310**	**312**	**282**
Y	73.0 -21.4	325	295	314	291	321	298
Z	**81.9 -20.1**	**327**	**300**	**325**	**300**	**350**	**320**

The suppliers' recommendations for binders are typically based on field experience using aggregate types, gradations, or other variables that may be substantially different than the materials and conditions used in this experiment.

Mixture tests with the validation binders were conducted in the same manner and with the same materials as for the main mixture experiments. Mixture tests with the validation binders included coating tests with both mixer types, workability tests, and compaction tests.

Data from the mix coating tests using the bucket and pugmill mixers for each of the validation binders are shown in Table 38. Following the same approach used for the main coating test experiment, these data were used to predict the mixing temperatures needed to achieve the baseline coating percentages for both mixer types. The results of the coating test experiments with the validation binders are shown in Table 39. It can be seen that the results of the coating tests with the pugmill mixer are reasonable for each of the binders, ranging from 291°F for the unmodified Binder Y to 341°F for the SBS modified Binder W. However, the temperatures for achieving the baseline coating percentage with the bucket mixer are excessive and are extrapolated outside of the temperature range of the experiment for the three modified binders.

Table 40 summarizes the results of the workability tests for the validation binders. Only one sample was tested for each binder. As with the main workability experiment, the regressions from these workability tests were used to estimate the temperature at which the torque was equal to 10 N·m for each binder. These results appear to be reasonable and follow the expected trend that higher PG binders will require a higher temperature to achieve the same workability.

Mix compaction tests with the validation binders followed the same protocol as with the main compaction experiment

Table 38. Results of coating tests with validation binders.

		Percentage of Coated Aggregate Particles by ASTM D2489							
Mixer Type		Pugmill				Bucket			
Mixing Temp. °C		120	140	160	180	120	140	160	180
Mixing Temp. °F		248	284	320	356	248	284	320	356
W	**90.0 -17.8**	**17.7**	**62.2**	**76.4**	**86.1**	**43.9**	**66.5**	**81.7**	**88.6**
X	**74.2 -27.9**	**36.7**	**70.7**	**80.3**	**93.3**	**35.0**	**26.4**	**97.4**	**99.8**
Y	73.0 -21.4	73.7	92.9	92.4	91.0	75.3	83.6	98.7	95.2
Z	**81.9 -20.1**	**36.8**	**79.4**	**85.3**	**92.1**	**27.6**	**44.5**	**73.6**	**98.5**

Table 39. Predicted mixing temperatures for good coating for the validation binders.

ID	True Grade	Pugmill Mixer			Bucket Mixer		
		a	*b*	T for 89% Coating	*A*	*b*	T for 97% Coating
W	**90.0 -17.8**	**4508.4**	**0.0609**	**341**	**174.784**	**0.0413**	**406**
X	**74.2 -27.9**	**1614.4**	**0.0570**	**331**	**30484.3**	**0.0744**	**365**
Y	73.0 -21.4	27.68	0.0373	291	57.00	0.04256	349
Z	**81.9 -20.1**	**6693.6**	**0.0699**	**311**	**9506.3**	**0.0682**	**365**

Table 40. Summary of workability test results for the validation binders.

ID	Workability Regression Equation	R^2	ºC	ºF
W	**$y = -0.0024x^2 - 0.3432x + 20.098$**	**0.94**	**155**	**311**
X	**$y = 0.0021x^2 - 0.9269x + 108.17$**	**0.79**	**150**	**302**
Y	$y = 0.0059x^2 - 1.8786x + 165.73$	0.57	139	282
Z	**$y = 0.0048x^2 - 1.5287x + 136.05$**	**0.86**	**153**	**308**

except that for the validation binders, compaction tests were only performed at the three temperatures: 130°C, 150°C, and 170°C. Table 41 shows the results of the compaction tests for the validation binders. It can be seen from these data that none of the mixes reached the baseline density of 92.9% of Gmm established in the main compaction experiment. This is probably due to a slight adjustment to the SGC internal angle during routine calibration of the machine that took place in the time lag between the main compaction experiment and the validation tests. Therefore, the temperature-density regression was used to estimate the temperature to achieve a density level of 92.0% of Gmm. The compaction temperatures based on this approach seems reasonable for three of the four binders. The predicted compaction temperature for Binder W is outside of the experimental range and appears to be too high.

Table 42 summarizes the differences between results of the mixture tests and the results from candidate methods for each of the validation binders. Since the coating test results with the bucket mixer were so far outside of the experimental range and outside of reasonable limits, they were not included in this analysis. Comparing the absolute differences for the two candidate methods, it can be seen that results with the Phase Angle method agree more closely with the mix tests than the SSF method. However, it also can be seen that many of the differences are substantial for both of the candidate methods. Although these large differences may be considered to be an indication that neither of the candidate methods provides accurate mixing and compaction temperatures, it is even more likely that the results of the mix tests are less reliable than the candidate binder tests.

Table 41. Results of compaction tests with validation binders.

Binder I.D.	Binder True Grade	%Gmm at 25 Gyrations			Regression Equation (T is temperature, °C)	Compaction Temperature for 92.0% Gmm,°F (°C)
		266ºF (130ºC)	302ºF (150ºC)	338ºF (170ºC)		
W	**90.0 -17.8**	**91.5**	**91.8**	**92.1**	**%Gmm = 0.0135T+89.756**	**344 (173)**
X	**74.2 -27.9**	**91.7**	**91.5**	**92.8**	**%Gmm = 0.028T+87.926**	**294 (146)**
Y	73.0 -21.4	91.8	92.4	92.4	%Gmm = 0.014T+90.053	282 (139)
Z	**81.9 -20.1**	**91.8**	**92.3**	**92.3**	**%Gmm = 0.125T+90.213**	**301 (149)**

Table 42. Summary of differences (°F) between mix test results and candidate methods results for the validation binders.

Binder I.D.	SSF Mixing Temp. – Temp. for 89% Coating in Pugmill Mixer	Phase Angle Mixing Temp - Temp. for 89% Coating in Pugmill Mixer	SSF Mix & Comp. Midpoint Temp. - Temp. for Equal Workability	Phase Angle Mix & Comp. Midpoint Temp. - Temp. for Equal Workability	SSF Compaction Temp. - Temp. for 92.0% Gmm	Phase Angle Compaction Temp. - Temp. for 92.0% Gmm
W	**+17**	**-3**	**+33**	**-15**	**-15**	**-33**
X	**+14**	**+7**	**+28**	**+21**	**+21**	**+16**
Y	+34	+23	+28	+13	+13	+9
Z	**+16**	**+14**	**+6**	**-1**	**-1**	**-1**
Σ|Δ|	81	47	95	50	50	59

CHAPTER 4

Conclusions and Recommendations

Summary of Key Findings

The results of the experiments conducted as part of this study have led to the following conclusions.

1. The high shear rate viscosity method does not provide an improvement in selecting mixing and compaction temperatures for modified binders compared with the equiviscous method. The mixing and compaction temperatures determined by the high shear viscosity method are very similar to the temperatures determined by the equiviscous method that are considered too high for modified binders based on general field experience of binder suppliers.
2. Mixing and compaction temperatures determined with the SSF method are substantially lower than the equiviscous mixing and compaction temperatures. The differences between the results are greater for the modified binders. This indicates that many of the modified asphalt binders exhibit shear thinning behavior. However, the SSF method also results in lower mixing and compaction temperatures for unmodified binders; in most cases, the SSF mixing temperatures are more than 10°F lower than the equiviscous mixing temperatures.
3. For modified asphalt binders, the mixing and compaction temperatures determined by the Phase Angle method are also substantially lower and more reasonable than by the equiviscous method. For unmodified binders, comparisons of mixing and compaction temperatures between the Phase Angle method and the equiviscous method were mixed. In some cases, the Phase Angle method yielded temperatures within a few degrees of the equiviscous method results. However, some Phase Angle results were also more than 10°F above or 10°F below the results from the equiviscous method.
4. The results of the SEP test showed that opacity and mass loss from asphalt binders increase with higher temperatures. However, the amount and rate of emissions increase differs among the binders. No links were evident between opacity and binder high grade number, binder low grade number, grade spread, whether the binder was modified, or crude source. Grading of the binders after SEP tests showed that the critical high temperatures and critical low temperatures increased slightly with higher SEP temperatures. Also, the non-recoverable compliance values (Jnr) decrease (i.e., the binders became more elastic) with higher SEP temperatures. However, there was no evidence of degradation of the binders due to exposure at elevated temperatures in the SEP test. The lack of evidence of degradation from the SEP test does not mean that binder degradation is not possible. It is entirely possible that the conditions in SEP test are not sufficiently severe to cause breakdown of polymer modifiers. Although the SEP test may have value in identifying binders with opacity problems, it is not recommended as a test for establishing maximum temperatures for mixing with aggregates.
5. Coating experiment results showed that the binder, mixing temperature, and mixer type significantly affected the coating percentage. However, neither of the lab mixers consistently provided reasonable mixing temperatures for all of the binders. Coating test results with completely dry aggregates and wet aggregates were not significantly different. Foaming of the asphalt was not observed during the tests with the wet aggregates. Correlations between the mixing temperatures from the candidate methods and the coating test results were weak. The poor correlations were likely due to inconsistencies with the subjective coating test.
6. Poor repeatability was also a problem with the workability experiments. This test did not provide dependable results by which to evaluate relationships between temperature and workability of mixes with different binders.
7. Compaction experiments using the SGC indicate that a mixture's aggregate components have a greater affect on compaction behavior than the binder characteristics. How-

ever, when aggregate type and gradation were held constant, the binder ID and compaction temperature significantly affect the mix density at 25 gyrations. Maximum shear ratio was not a useful indicator of compactability.

8. Compaction temperature has a significant effect on low temperature properties of mixtures: lower compaction temperatures resulted in slightly higher creep compliance values. Conversely, aging of the binders due to high mixing temperatures stiffened mixtures (lower creep compliance), which reduces the ability of the pavement to dissipate thermal stresses. The effect of aging was more evident for binders with lower PG grades. In other words, a PGXX-34 is affected more by increases in mixing and compaction temperatures than a PGXX-16.
9. Correlations of the mixing and compaction temperatures determined from the candidate methods with laboratory tests on mixtures for coating and workability were poor. The weak correlations between the binder tests and the mix tests are partially attributable to the poor precision of the coating and workability tests. On the other hand, compaction temperatures from both of the candidate methods correlated well with the results of the laboratory compaction tests. Results of the candidate methods also agree reasonably well with the binder suppliers' recommended mixing temperatures.

Recommendation of a New Method for Determining Mixing and Compaction Temperatures

The objective of this research was to identify or develop a simple, reliable, and accurate procedure for determining mixing and compaction temperatures that is applicable to modified and unmodified binders in HMA. Two candidate procedures, the SSF method and the Phase Angle method, were thoroughly evaluated.

- An advantage of both candidate methods is that they can be set up and performed using existing standard DSR equipment used in most asphalt binder labs in the United States. Limitations of both methods include the restrictions normally applied to parallel plate DSR testing, such as the binder test sample must be homogenous and free of particulate matter (e.g., ground rubber particles) that may interfere with or distort the rheological response of the instrument.
- Both methods also appear to provide reasonable temperatures for mixing and compaction temperatures for a variety of modified and unmodified asphalt binders being used across the United States.
- Correlations of the mixing and compaction temperatures with laboratory coating, workability, and compactability were similar for both methods.

Draft AASHTO format procedures for the SSF method and the Phase Angle method in are included in Appendix C. Mixing and compaction temperatures determined by these methods are only applicable to the laboratory setting for mix design work, quality assurance testing of HMA, and fabricating HMA samples for laboratory performance tests. The mixing and compaction temperatures determined by this method should *not* be used to control plant production or pavement construction temperatures. Greater latitude in mixing temperatures is necessary in the field to allow for different ambient conditions, haul distances, and other mix characteristics that affect coating and compactability. Although excessive temperatures may cause emission problems for some binders, no evidence of this was found in the laboratory work nor did tests demonstrate degradation. At this time, the best guidance for plant mixing temperatures is the EC 101 guidance (*38*).

Recommendations for Further Work

There are several additional key steps that should be considered in order to validate, refine, and eventually implement the use of the SSF and/or Phase Angle methods. Four additional steps are outlined as follows:

1. Independent validation of the methods by asphalt suppliers;
2. Refinement of the SSF and Phase Angle methods;
3. Interlaboratory studies to determine precision information for the new procedures; and
4. Training on the new method(s) for full implementation by the asphalt paving industry.

Independent Validation

The first major step is to validate the SSF and Phase Angle methods with many more asphalt binders in other laboratories. This would logically begin with asphalt suppliers conducting both methods in parallel with grading tests on their current slate of paving grade asphalt products. Simple DSR control and analysis programs to run the tests and analyze results need to be developed and distributed for the variety of DSR's being used in the asphalt industry. To begin this effort, preliminary training on the methods would be necessary. A single organization should be identified to collect the results of this broader field validation effort in an organized fashion. Ideally, an online database would be established to facilitate entry of results from users anywhere in the world. The following list shows basic information that would be useful to gather in such a database:

- Binder supplier.
- Binder PG grade.
- Modification type(s).
- Crude source.

- Location(s) the binder is used (state, region, etc.).
- Supplier's recommended mixing and compaction temperatures.
- Equiviscous mixing and compaction temperatures.
- SSF mixing and compaction temperatures.
- Phase Angle mixing and compaction temperatures.
- Issues with the procedures and/or equipment.
- Comments and observations regarding laboratory mixing and compaction.
- Comments and observations regarding field mixing and compaction.

This information would allow users and researchers to see how well the methods gain acceptance and if problems occur, where and with what sort of binders. A single organization should be responsible for initial training on the methods, establishing the database, trouble-shooting problems, and reporting of the field validation data. This initial field validation effort should take about 18 months.

Refinement of the SSF and Phase Angle Methods

Gerald Reinke, developer of the SSF method, has recently recommended using a higher shear stress of 1000 Pascals compared with the 500 Pascals used in this study. The recommended change is evidently to try to reach a better steady state viscosity for some highly modified binders. Since viscosities of such binders decrease at higher shear stresses (shear thinning behavior), the resulting mixing and compaction temperatures could be expected to be slightly lower for those binders. Reinke's recommended refinement of the SSF method simply adds one additional stress level to the procedure, so it would be relatively easy to analyze the data using both stress levels as part of the independent validation work described earlier.

Although the Phase Angle method developed in this study is simple, reasonable, and innovative, criticisms of the method are (1) that the relationships between phase angle and mixing and compaction temperatures are too empirical; (2) the selection of frequencies at δ=86° seems arbitrary; and (3) the common water-cooled DSRs may not be able to reach the desired phase angle transition region within the temperature range of the water bath. Further research is warranted to explore several possible refinements of the concept. One idea suggested by the AI is to simply perform the frequency sweep testing at only 80°C and find the frequency corresponding to the phase angle at 86°. This could substantially reduce the testing and analysis time. Another path of further study should evaluate the use of the phase angle measurements on aged binders (e.g., RTFO or some other aging protocol) since rheological behaviors of asphalts change at different rates during plant mixing or lab conditioning protocols. Another idea to evaluate would be to change from the parallel plate geometry to a cup and bob geometry in the DSR for the phase angle measurements. This would allow for testing at higher temperature ranges (closer to mixing and compaction temperatures) and examination of the binder behavior at the more fundamental phase angle point of 45° (the point where loss moduli and storage moduli are equal). This analysis would provide more points on the phase angle master curve for analysis of the frequency-temperature relationships for determining mixing and compaction temperatures.

Interlaboratory Studies

Interlaboratory studies are useful for improving test methods and determining repeatability and reproducibility information of the results. A ruggedness study should be conducted on new methods to identify what procedural factors have the greatest influence on the results. The recommended method for conducting a ruggedness study is ASTM C1067, *Standard Practice for Conducting A Ruggedness or Screening Program for Test Methods for Construction Materials.* Steps for developing a ruggedness study include

1. Identify seven procedural factors for the test method;
2. Establish high and low levels for each factor;
3. Design the experiment: normally eight combinations of 14 factor levels (7 factors × 2 levels) with two replicates for each combination;
4. Identify at least three laboratories to participate in the study; and
5. Determine three to five materials that cover the range of materials properties to which the test method is applicable. The selection of the procedural factors should be selected following the independent validation work described above.

For many test methods used in pavement materials analysis, a second interlaboratory study is conducted to establish precision statistics. The recommended procedure for this type of interlaboratory study is ASTM C802, *Standard Practice for Conducting an Interlaboratory Test Program to Determine the Precision of Test Methods for Construction Materials.* However, given that the purpose of either the SSF method or the Phase Angle method would be only to prepare asphalt mixture samples and they would not be used in determining whether a material met a criteria for the purpose of payment, the repeatability and reproducibility statistics are not critical. Alternatively, a more economical way to obtain useful precision information for either of these procedures would be to include it in the AMRL proficiency testing program for asphalt binder testing.

Training

A key final step in implementation of a new method is training on the procedure and getting users to understand how the results should be used. Multiple avenues should be

used for delivery of training on using the Phase Angle method ranging from traditional instructor-led courses with hands on workshops to more contemporary methods like self-paced web-based training. Many technicians can be reached effectively within existing regional and national binder technician certification programs. To aid in these training venues, simple educational materials, such as Powerpoint slides with examples, need to be developed and distributed. Online delivery of training materials is likely to become a very important method for training in the near future. Interactive web-based training content is able to reach a broad audience at any time, with self-paced learning using new media including animation and video.

References

1. Romagosa, H. "The Market for Polymer Modified Asphalts in the USA — 2003 Volumes and Trends," Association of Modified Asphalt Producers, http://www.modifiedasphalt.org/library.asp#past, January, 2003.
2. Fink, D.F. and J.A. Lettier. "Viscosity Effects in the Marshall Stability Test," AAPT 1951.
3. Parker, C.F. "Use of Steel-Tired Rollers," *Highway Research Board Bulletin No. 246,* Highway Research Board, National Research Council, Washington D.C., 1950.
4. Serafin, P.J., L.L Kole, and A.P. Chritz. "Michigan Bituminous Experimental Road: Final Report," AAPT Vol. 36, 1967.
5. *Mix Design Methods for Hot-Mix Asphalt Paving.* Manual Series No. 2, First Edition, The Asphalt Institute, April, 1956.
6. Kiefer, R.W. "The Effect of Compaction Temperature on the Properties of Bituminous Concrete," *American Society for Testing and Materials Special Technical Publication No. 294,* Sixty-third Annual Meeting Papers, 1960.
7. *Mix Design Methods for Asphalt Concrete and Other Hot-Mix Types.* Manual Series No. 2, Second Edition, The Asphalt Institute, February, 1962.
8. Bahri, G.R. and L.F. Rader. "Effects of Asphalt Viscosity on Physical Properties of Asphalt Concrete," *Highway Research Record No. 67,* Highway Research Board, National Research Council, Washington D.C., 1965.
9. Kennedy, T.W., F.L. Roberts, and R.B. McGennis. "Effects of Compaction Temperature and Effort on the Engineering Properties of Asphalt Concrete Mixtures," *ASTM Special Technical Publications 829,* 1984.
10. Crawley, A.B. "An Evaluation of Lower Mixing Temperatures for Bituminous Paving Mixes," MSHD-RD-85-069, Mississippi DOT, 1985.
11. Newcomb, D.E., M. Stroup-Gardiner, and J.A. Epps. "Laboratory and Field Studies of Polyolefin and Latex Modifiers for Asphalt Mixtures," *Polymer Modified Asphalt Binders,* ASTM STP 1108, 1992.
12. Aschenbrener, T. and N. Far. "Influence of Temperature and Antistripping Treatment on the Results from the Hamburg Wheel-Tracking Device, Final Report," CDOT-DTD-R-94-9, Colorado DOT, July 1994.
13. Azari, H., R.H. McCuen, and K.D. Stuart. "Optimum Compaction Temperature for Modified Binders," *Journal of Transportation Engineering,* Vol. 129, Issue 5, September 2003.
14. Bahia, H.U., and D.I. Hanson. "NCHRP Project 9-10 Superpave Protocols for Modified Asphalt Binders," Draft Topical Report (Task 9), prepared for the National Cooperative Highway Research Program, Transportation Research Board, National Research Council, Washington, D.C., May 2000.
15. Huner, M.H., and E.R. Brown. "Effects of Re-Heating and Compaction Temperature on Hot Mix Asphalt Volumetrics," NCAT Report 01-04, National Center for Asphalt Technology, November 2001.
16. McGennis, R.B., R.M. Anderson, D. Perdomo, and P. Turner. "Issues Pertaining to Use of the Superpave Gyratory Compactor," *Transportation Research Record 1543,* Transportation Research Board, National Research Council, Washington, D.C., 1996.
17. De Sombre, R., D.E. Newcomb, B. Chadbourn, and V. Voller. "Parameters to Define the Laboratory Compaction Temperature Range for Hot Mix Asphalt," *Journal of the Association of Asphalt Paving Technologists,* Vol. 67, 1998.
18. Leiva, F., and R.C. West. "Relationships between Laboratory Measured Characteristics of HMA and Field Compactability," *Proceedings, Association of Asphalt Paving Technologists,* Vol. 77, 2008.
19. Willoughby, K.A., J.P. Mahoney, L.M. Pierce, J.S. Uhlmeyer, K.W. Anderson, S.A. Read, S.T. Muench, T.R. Thompson, and R. Moore. "Construction Related Asphalt Concrete Pavement Temperature Differentials," WA-RD 476.1, Washington State Transportation Center, July 2001.
20. Chadbourn, B.A., D.E. Newcomb, V.R. Voller, R.A. De Sombre, J.A. Luoma, and D.H. Timm. "An Asphalt Paving Tool for Adverse Conditions," MN/RC-1988/18, University of Minnesota, June 1998.
21. Roberts, F.L., P.S. Kandhal, E.R. Brown, D.Y. Lee, and T.W. Kennedy. *Hot Mix Asphalt Materials, Mixture Design, and Construction,* Second Edition, NAPA Education Foundation, 1996.
22. *The Asphalt Handbook.* Manual Series No.4, Asphalt Institute, 1989.
23. *Hot-Mix Asphalt Paving Handbook 2000.* Transportation Research Board.
24. Clark, R.G. "Practical Results of Asphalt Hardening on Pavement Life," *AAPT* Vol. 27, 1958.
25. Fink, D.F. "Research Studies and Procedures," *AAPT* Vol. 27, 1958.
26. Serafin, P.J. "Laboratory and Field Control to Minimize Hardening of Paving Asphalts," *AAPT* Vol. 27, 1958.
27. Lottman, R.P., S.K. Sonawala, and M. Al-Habboob. "Change of Asphalt Viscosity During Mixing with Hot Aggregates," *AAPT* VoL. 32, 1963.
28. Airey, G.D., and S.F. Brown. "Rheological Performance of Aged Polymer Modified Bitumens," *Journal of the Association of Asphalt Paving Technologists*, Vol. 67, 1998.

29. Linde, S. and U. Johansson. "Thermo-Oxidative Degradation of Polymer Modified Bitumen," *Polymer Modified Asphalt Binders.* ASTM STP 1108, 1992.
30. Stroup-Gardiner, M., and C. Lange. "Hot Mix Asphalt Smoke and Emissions Potential," presented at the Transportation Research Board 80th Annual Meeting, Washington, D.C., January 2001.
31. Lange, C.R., and M. Stroup-Gardiner. "Quantification of Potentially Odorous Volatile Organic Compounds from Asphalt Binders Using Head-Space Gas Chromatography," *Journal of Testing and Evaluation,* Mar. 2005, Vol. 33, No. 2.
32. Stroup-Gardiner, M., C.R. Lange, and A. Carter. "Quantification of Emission Potential from Asphalt Binders Using Mass Loss and Opacity Measurements," International Journal of Pavement Engineering. (Publication pending, International Journal for Pavement Engineering.)
33. Whiteoak, D. *The Shell Bitumen Handbook*, Shell Bitumen U.K., 1st Ed., 1991.
34. Terrel, R.L., and J.A. Epps. "Using Additives and Modifiers in Hot Mix Asphalt," *Quality Improvement Series 114,* National Asphalt Pavement Association, 1989.
35. Shuler, T., D. Hanson, and R. McKeen. "Design and Construction of Asphalt Concrete Using Polymer Modified Asphalt Binders," *Polymer Modified Asphalt Binders, ASTM* STP 1108, 1992.
36. Shenoy, A. V. "Determination of the Temperature for Mixing Aggregates with Polymer-Modified Asphalt." *International Journal of Pavement Engineering,* Vol. 2, Number 1, 2001.
37. Albritton, G.E., W.F. Barstis, and A.B. Crawley. "Polymer Modified Hot Mix Asphalt Field Trial," FHWA/MS-DOT-RD-99-111, 1999.
38. *Best Management Practices to Minimize Emissions During HMA Construction*, EC 101, Asphalt Pavement Environmental Council (National Asphalt Pavement Association, Asphalt Institute, and State Asphalt Pavement Associations), April 2000.
39. Bahia, H.U., D.I. Hanson, M. Zeng, H. Zhai, M.A. Khatri, and R.M Anderson. *NCHRP Report 459: Characterization of Modified Asphalt Binders in Superpave Mix Design,* Transportation Research Board, National Research Council, Washington, D.C., 2001.
40. Grover, R. "Determining Mixing and Compaction Temperatures of Asphalt Binders Using Zero Shear Viscosity," RMAUPG Binder Subcommittee Meeting, October 8, 2002.
41. Tang, Y., and J. Haddock. Field Testing of the Zero Shear Viscosity Method, 2005 TRB Workshop.
42. Khatri, A., H.U. Bahia, and D. Hanson. "Mixing and Compaction Temperatures for Modified Binders using the Superpave Gyratory Compactor," *Journal of the Association of Asphalt Paving Technologists,* Vol. 70, 2001.
43. Yildirim, Y., M. Soaimanian, and T.W. Kennedy. "Mixing and Compaction Temperatures for Hot Mix Asphalt," University of Texas, Center for Transportation Research, Research Report #1250-5, January 2000.
44. Yildirim, Y., M. Soaimanian, and T.W. Kennedy. "Mixing and Compaction Temperatures for Superpave Mixes," *Journal of the Association of Asphalt Paving Technologists,* Vol. 69, 2000.
45. Reinke, G. "Determination of Mixing and Compaction Temperature of PG Binders Using a Steady Shear Flow Test," presentation made to the Superpave Binder Expert Task Group, http://bridge.ecn.purdue.edu/~spave/Technical%20Info/Meetings/Binder%20ETG%20Sept%2003%20Las%20Vegas,%20NV/Reinke_MIX%20AND%20COMPACTINO%20INFO%20FOR%20ETG%209-15-03.pdf. September 2003.
46. Sudduth, R., G. Baumgardner, and A. Menapace. "Evaluation of the Measurement of the Non-Newtonian Shear and Extensional Components of Viscosity Using a Brookfield Viscometer for Eight Different Modified Asphalts and One Control," 2005.
47. Stuart, K.D. "Methodology for Determining Compaction Temperatures for Modified Asphalt Binders," FHWA-RD-02-016, Federal Highway Administration, 2002.
48. Marvillet, J. and P. Bougalt. "Workability of Bituminous Mixes. Development of a Workability Meter," Proceedings, *Association of Asphalt Paving Technologists,* Vol. 48, 1979.
49. Gudimettla, J.M., L.A. Cooley Jr., and E.R. Brown. "Workability of Hot Mix Asphalt," NCAT Report 03-03, National Center for Asphalt Technology, April 2003.
50. Gudimettla, J.M., L.A. Cooley Jr., and E.R. Brown. "Workability of Hot Mix Asphalt," *Transportation Research Record 1891,* Transportation Research Board of the National Academies, Washington, D.C., 2004.
51. Christenson, D.W. and R.F. Bonaquist. *NCHRP Report 530: Evaluation of Indirect Tensile Test (IDT) Procedures for Low-Temperature Performance of Hot Mix Asphalt,* Transportation Research Board of the National Academies, Washington, D.C., 2004.
52. Dalton, F. "Gyratory Shear and Volumetric Mix Design Using the Pine AFG1 Superpave Gyratory Compactor," Report 1999-04, Pine Instrument Company.

APPENDIX A

Responses of Survey on Agency Specifications Regarding Mixing and Compaction Temperatures

Table A1. NCHRP Project 9-39 survey response.

State/Organization	1. Procedure to determine mixing and compaction temperature for unmodified hot mix asphalt?	2. Procedure to determine mixing and compaction temperature for polymer-modified hot mix asphalt?	3. Procedure to determine mixing and compaction temperature for crumb rubber-modified hot mix asphalt?	4. Procedure to determine mixing and compaction temperature for air blown or chemically-modified asphalt ?	5. Are the same procedures used to determine plant production and laydown temperatures?	Comments
Alabama	Temp/visc curves from supplier; based on A.I. method	Supplier's recommendation	N/A	N/A	Set by contractor; <350 °F	
Alaska	Mix @ 276-286°F; Compact @ 259-267°F	Mix @ 325-335°F; Compact @ 305-315°F	Mix @ 325-335°F; Compact @ 305-315°F	N/A	Yes	
Arkansas	T 245/T 312	T 245/T 312; Supplier recommendation	N/A	N/A	Yes	Test for presence/amount of modifier as part of QPL procedure. PG 70-22 & 76-22 w/SB,SBS,SBR
Arizona	T 245/T 312; Use supplier recommendation If mix temperature >325°F or if compaction temperature > 300°F	T 245/T 312; Use supplier recommendation If mix temperature >325°F or if compaction temperature > 300°F	Mixing and compaction temperature both @ 325°F	T 245/T 312	Set by contractor; ≤325°F unless higher temperature recommended by supplier & approved by ADOT	
California	T 49/T 202	T 49/T 202	T 49/T 202	T 49/T 202	Yes	Use Haake viscometer for modified asphalt
Colorado	T 245/T 312	T 245/T 312	N/A	N/A	Yes	
Connecticut	T 245/T 312	Supplier recommendation	N/A	T 245/T 312	Only used as a guide	
Dist. Of Columbia	T 245/T 312	T 245/T 312	T 245/T 312	N/A	Yes	
Delaware	T 245/T 312	Supplier recommendation	N/A	N/A	Set by contractor	
Florida	Set by contractor based on supplier recommendation and contractor experience; ≤315°F	Set by contractor based on supplier recommendation and contractor experience; ≤330°F	Set by FDOT based on lab and field experience; ≤320°F	Set by contractor based on supplier recommendation and contractor's experience	Based on experience	
Georgia	T 245/T 312	Supplier recommendation	N/A	N/A	Yes	
Hawaii	T 245/T 312	N/A	N/A	N/A	Yes	
Idaho	Supplier recommendation	Supplier recommendation	N/A	N/A	Yes	
Indiana	Dense-graded = 300±9°F; Open-graded = 260±9°F	Dense-graded = 300+9°F; Open-graded = 260+9°F	N/A	Must meet appropriate PG spec.	Yes	PG 58-28, 64-28, 70-28, 64-22, 70-22, 76-22
Illinois	Mix@295 ±5°F; Compact@295 ±5°F	Mix@325 ±5°F; Compact@305 ±5°F	N/A	N/A	Supplier recommendation and contractor's experience	
Iowa	Mix and compact @ 275 °F	Mix and compact @ 275 °F	Supplier recommendation	N/A	Yes	
Kansas	Supplier recommendation; <350°F	Supplier recommendation; <350°F	N/A	N/A	Yes	

Table A2. NCHRP Project 9-39 survey response.

State/Organization	1. Procedure to determine mixing and compaction temperature for unmodified hot mix asphalt?	2. Procedure to determine mixing and compaction temperature for polymer-modified hot mix asphalt?	3. Procedure to determine mixing and compaction temperature for crumb rubber-modified hot mix asphalt?	4. Procedure to determine mixing and compaction temperature for air blown or chemically-modified asphalt ?	5. Are the same procedures used to determine plant production and laydown temperatures?	Comments
Kentucky	Based on PG grade & supplier recommendation; for PG 64-22 mix@300 ±5°F, compact @ 265 ±5°F	Based on PG grade & supplier recommendation; for PG 76-22 mix@340 ±5°F, compact@ 310 ±5°F	N/A	N/A	Maintain temperature @plant within ±15°F of approved temperature based on PG grade; @ plant PG 58-22 & 64-22: min=250°F, max=330°F; PG 70-22: min=300°F, max=350°F; PG 76-22: min=310°F, max=350°F	Roadway temp based on PG grade; PG 58-22 & 64-22: min=230°F, max=330°F; PG 70-22: min=275°F, max=350°F; PG 76-22: min=300°F, max=350°F
Louisiana	Supplier recommendation	Supplier recommendation	Supplier recommendation	N/A	Supplier recommendation, but may be adjusted based on ambient temperature, haul distance, etc.	
Maine	AASHTO T 245/T 312	AASHTO T 245/T 312	N/A	AASHTO T 245/T 312	Yes	Supplier recommendation may also be used, but may be adjusted based on ambient temp, haul distance, etc. Typical placement tempeerature 275-325°F
Maryland	AASHTO T 245/T 312	Supplier recommendation	N/A	N/A	Controlled by paving operation based on ambient temperature, haul distance, etc.	
Massachusetts	AASHTO T 245/T 312	Supplier recommendation	AASHTO T 245/T 312	N/A	Yes	
Michigan	Supplier recommendation	Supplier recommendation	Supplier recommendation	Supplier recommendation	Yes	
Minnesota	Supplier recommendation	Supplier recommendation	N/A	Supplier recommendation	Supplier recommendation, but may be adjusted based on ambient temperature, haul distance, etc.	
Mississippi	Temperature/viscosity curves from supplier	Temperature/viscosity curves from supplier	Temperature/viscosity curves from supplier	N/A	Yes	Temp/visc curves verified by AASHTO T 316 per 100,000 gallons
Missouri	Supplier recommendation	Supplier recommendation	N/A	N/A	Yes	
Montana	Supplier recommendation	Supplier recommendation	N/A	Supplier recommendation	Yes	Suppliers generally use T 245/T 312 with allowance for field adjustment
Nebraska	AASHTO T 245/T 312	Supplier recommendation	NDOR Spec - mix=350°F,compact=325°F	N/A	Yes	
Nevada	N/A	Supplier recommendation	N/A	N/A	Yes	Does not use unmodified asphalt
New Hampshire	T 245/T 312	T 245/T 312	N/A	N/A	Yes	
New Jersey	T 245/T 312	Supplier recommendation	N/A	T 245/T 312	Yes	
New Mexico	Supplier recommendation	Supplier recommendation	N/A	Supplier recommendation	Yes	
New York	T 245/T 312	Supplier recommendation	N/A	T 245/T 312	Yes	
North Carolina	T 245/T 312	Supplier recommendation	N/A	N/A	PG 64-22 JMF@ 300°F; PG 70-22 JMF@ 315°F; PG 76-22 JMF@ 335°F	Mix @ plant within ±15°F of JMF; Roadway temperature within +15 to -25°F of JMF
North Dakota	T 245/T 312; Supplier recommendation	T 245/T 312; Supplier recommendation	N/A	N/A	Yes	

Table A3. NCHRP Project 9-39 survey response.

State/Organization	1. Procedure to determine mixing and compaction temperature for unmodified hot mix asphalt?	2. Procedure to determine mixing and compaction temperature for polymer-modified hot mix asphalt?	3. Procedure to determine mixing and compaction temperature for crumb rubber-modified hot mix asphalt?	4. Procedure to determine mixing and compaction temperature for air blown or chemically-modified asphalt ?	5. Are the same procedures used to determine plant production and laydown temperatures?	Comments
Ohio	AASHTO T 245/T 312	Supplier recommendation	N/A	N/A	Supplier recommendation, but adjust as needed	
Oklahoma	Mix @ 325°F, compact @ 300°F	Mix @ 325°F, compact @ 300°F	N/A	N/A	Unmodified- mix @ 305 ± 20°F Compact@ 290°F; Modified- mix @325 ± 20°F Compact @ 300°F	
Oregon	T 245/T 312	Supplier recommendation	N/A	Supplier recommendation	Yes	
Pennsylvania	T 245/T 312	Supplier recommendation	N/A	Supplier recommendation	Maintain temperature within specification value based on PG grade; NAPA EC-101	PG 52-28 @ 240-300°F; PG 58-28 @ 260-310°F; PG 64-22 @ 265-320°F; PG 76-22 @ 280-330°F
Puerto Rico	T 245/T 312	N/A	N/A	N/A	Yes	
Rhode Island	T 245/T 312	T 245/T 312; ≤330 °F	T 245/T 312; ≤330 °F	T 245/T 312	Yes	Typical range = 285-300°F
South Carolina	T 245/T 312	T 245/T 312	T 245/T 312	N/A	Yes	
South Dakota	T 245/T 312	Supplier recommendation	N/A	N/A	Supplier recommendation, but may be increased up to 25°F based on ambient temperature, haul distance, etc.	
Tennessee	T 245/T 312	Supplier recommendation; but ≤340°F	Supplier recommendation; but ≤340°F	N/A	Plant & roadway temperature must be within specified range based on PG Grade	PG 64-22 @ 290-320°F; PG 70-22 @ 320-350°F; PG 76-22 @ 320-350°F; PG 82-22 @ 320-350°F
Texas	Supplier recommendation	Supplier recommendation	Supplier recommendation	Supplier recommendation	Yes	
Utah	T 245/T 312	Supplier recommendation, if available; otherwise based on experience	N/A	Supplier recommendation, if available; otherwise based on experience	Items 1 and 2 generally followed by HMA producer, but may be set by contractor; <335 °F	
Vermont	Supplier recommendation	Supplier recommendation	N/A	N/A	Supplier recommendation, but may be adjusted based on ambient temperature, haul distance, etc.	
Virginia	T 245/T 312	T 245/T 312	N/A	N/A	Yes	
Washington	Supplier recommendation	Supplier recommendation	N/A	N/A	Yes	Suppliers generally use T 245/T 312
West Virginia	T 245/T 312	Supplier recommendation	N/A	N/A	Plant & Roadway temperature must be within ±25 °F of the median temperature from AASHTO T 245/T 312 or recommended by supplier	
Wisconsin	Mix @ supplier recommendation; Compact @ 275 ±5 °F	Mix @ supplier recommend.ation; Compact @ 275 ±5 °F	N/A	Mix @ supplier recommendation; Compact @ 275 ±5 °F	Supplier recommendation	

Table A4. NCHRP Project 9-39 survey response.

State/Organization	1. Procedure to determine mixing and compaction temperature for unmodified hot mix asphalt?	2. Procedure to determine mixing and compaction temperature for polymer-modified hot mix asphalt?	3. Procedure to determine mixing and compaction temperature for crumb rubber-modified hot mix asphalt?	4. Procedure to determine mixing and compaction temperature for air blown or chemically-modified asphalt ?	5. Are the same procedures used to determine plant production and laydown temperatures?	Comments
Wyoming	Based on PG Grade	Based on PG Grade; PG 64-28 and 70-28 are polymer modified	N/A	N/A	Use supplier recommendation for modified asphalt and AASHTO T312 for unmodified	PG 58-28; mix@305, compact@280 PG 64-22; mix@310, compact@285 PG 64-28; mix@315, compact@290 PG 70-28; mix@325, compact@300
Army Corps of Engineers	ASTM D2493	NAPA EC 101 as function of PG Grade	NAPA EC 101 as function of PG Grade	NAPA EC 101 as function of PG Grade	Yes	
British Columbia Min. of Transp & Highways (Canada)	Temperature/viscosity curves from supplier	N/A	N/A	N/A	Do not know	
New Brunswick DOT (Canada)	Supplier recommendation	Supplier recommendation	N/A	Supplier recommendation	Yes	Temperatures vary by supplier and PG grade; Mixing ranges from 290-347 °F; Compaction varies from 257-334 °F
Danish Road Directorate (Denmark)	ASTM D-1559 and experience; Max. temperature legislated	ASTM D-1559 and experience; Max. temperature legislated; Max. mixing tempereature=374 F, Max. compact temperature= 365 F	N/A	N/A	Yes	Maximum temperatures regulated by legislation & Danish Asphalt Industries based on mix type, binder type, etc.; may be lower than by ASTM D-1559 (4.3.1 & 4.3.2)
Central Road Research Institute (India)	ASTM D2493	Own specifications; Binder @ mixing = 330-365 °F, Mix @ plant = 285-320 °F, Mix @ roadway = 265-300 °F	Own specifications; Binder @ mixing = 330-365 °F, Mix @ plant = 285-320 °F, Mix @ roadway = 265-300 °F	Own specifications; Binder @ mixing = 330-365 °F, Mix @ plant = 285-320 °F, Mix @ roadway = 265-300 °F	Yes	
Quebec Min. of Transportation (Canada)	French Procedure LC 25-007; similar to AASHTO T 245/T 312	T 245/T 312; If temperature corresponding to 0.17 Pa·s is >338 F, use maximum mixing range of 313-338 °F	N/A	T 245/T 312; If temperature corresponding to 0.17 Pa·s is >338 F, use maximum mixing range of 313-338 °F	Yes	
Saskatchewan Highways and Transp. (Canada)	T 245/T 312	Supplier recommendation	Based on other agencies and contractor's experience	N/A	Yes	Very little modified asphalt used
N. Y. State Thruway Authority	T 245/T 312	N/A	N/A	N/A	Yes	Uses N. Y. DOT specifications
Ontario Min. of Transportation (Canada)	Supplier recommendation; T 245 / T 312	Supplier recommendation; T 245 / T 312	Supplier recommendation; T 245 / T 312	Supplier recommendation; T 245 / T 312	Yes	Suppliers use AASHTO T 312

Table A5. NCHRP Project 9-39 survey response.

State/Organization	1. Procedure to determine mixing and compaction temperature for unmodified hot mix asphalt?	2. Procedure to determine mixing and compaction temperature for polymer-modified hot mix asphalt?	3. Procedure to determine mixing and compaction temperature for crumb rubber-modified hot mix asphalt?	4. Procedure to determine mixing and compaction temperature for air blown or chemically-modified asphalt ?	5. Are the same procedures used to determine plant production and laydown temperatures?	Comments
Public Works Ministry of Malaysia	ASTM D2493; based on experience 275 °F is widely used for compaction temperature	Supplier recommendation; ASTM D2493	Supplier recommendation; ASTM D2493	N/A	Yes	Prevalent binder is pen grade 80/100; May also use recommendation from NCHRP Report 459
Manitoba Dept. of Transportation (Canada)	ASTM D2493	Supplier recommendation	N/A	ASTM D2493 (Oxidized asphalt only)	Yes	
Australian Dept. of Transport & Regional Services	Optimum mixing = 320-338 °F Maximum compaction = 285-320 °F	Optimum mixing = 320-347 °F Maximum compaction = 302-324 °F	N/A	N/A	Yes	Temperature varies within range given depending on binder class/type.
Chinese Transportation Ministry	Chinese Method T0619/ T 0625 (Similar to AASHTO T 245/T 312)	Heat AC to 325-338 °F; Heat aggregate to 365-428 °F depending on polymer; Maximum temp= 383 °F	N/A	N/A	Placement temperature varies based on binder penetration or modifier; Unmodified minimum=257 °F; Modified minimum=320 °F	Compaction temp. varies based on binder penetration or modifier; Start compaction at temperature not less than: Unmodified=248 °F; Modified=302 °F
Japan Road Association	Similar to AASHTO T245/T 312 but uses temperature at viscosity of 180 ±20 cSt for mixing and temperature at viscosity of 300 ±30 cSt for compaction	Supplier recommendation	Supplier recommendation	Supplier recommendation	Yes	Suppliers compact mix with unmodified binder and determine density. Compact same mix with modified binder over a range of temperatures; determine the temperature that gives same density as unmodified and use as minimum compaction temperature. Add 18 °F to

Metric Conversion Note: °C = (°F - 32) * 5/9

APPENDIX B

Mix Design Data for Base Mix and Other Compaction Experiment Mixes

NCHRP Project 9-39 Mix Design Data

N_{design}: 100 gyrations
Compactor: Pine AFGC125X

Sieve Size	Baseline Mix Granite	Granite Coarse 15% RAP	Granite Fine 15% RAP	Gravel Coarse 15% RAP	Gravel Fine 15% RAP
3/4"	100.0	100.0	100.0	99.9	99.9
1/2"	98.5	98.1	99.1	99.6	99.8
3/8"	84.8	81.3	91.1	88.2	94.8
#4	56.2	47.6	55.6	51.5	64.7
#8	43.9	36.0	40.3	33.8	42.0
#16	33.3	27.1	30.4	23.9	29.1
#30	24.8	19.7	22.7	18.2	21.8
#50	15.5	11.8	14.3	11.9	13.7
#100	8.8	6.1	8.0	8.2	9.2
#200	5.1	3.3	4.5	6.2	6.9
Total AC %	5.1	5.4	5.5	4.7	6.6
Virgin AC %	5.1	4.7	4.8	4.0	5.9
Air Voids %	4.0	4.0	4.0	4.0	4.5
VMA %	15.0	14.6	14.3	11.1	14.3
VFA%	74.2	73.8	70.3	63.3	74.5

RAP Pb % 5.0

Stockpiles	Baseline Mix Granite	Granite Coarse 15% RAP	Granite Fine 15% RAP	Gravel Coarse 15% RAP	Gravel Fine 15% RAP
Labstock Granite	75%	55%	60%		
Granite W-10	25%	30%	25%		
RAP		15%	15%	15%	15%
Blaine Gravel Fine				40%	75%
Blaine Gravel Coarse				45%	10%

Mix Design Binder: NCAT Labstock PG 67-22 (Ergon)

APPENDIX C

Draft AASHTO Standard for Steady Shear Flow and Phase Angle Methods

Note: These draft specifications have been modified for the purpose of inclusion in this report.

Standard Method of Test for

Determining the Laboratory Mixing & Compaction Temperature of Asphalt Binder Using a Dynamic Shear Rheometer (DSR)

Steady Shear Flow Method

AASHTO Designation: X XXX-XX

Standard Method of Test for

Determining the Laboratory Mixing & Compaction Temperature of Asphalt Binder Using a Dynamic Shear Rheometer (DSR)

Steady Shear Flow Method

AASHTO Designation: X XXX-XX

SCOPE

This test method covers the determination of laboratory mixing and compaction temperatures using a steady shear flow test. The steady shear flow test is conducted using the Dynamic Shear Rheometer (DSR) utilizing the rheometers capability to function in constant rotation in one direction.

The values stated in SI units are to be regarded as the standard.

This standard does not purport to address all of the safety concerns, if any, associated with its use. It is the responsibility of the user of this standard to establish appropriate safety and health practices and determine the applicability of regulatory limitations prior to use.

REFERENCED DOCUMENTS

2.1 AASHTO Standards

- M320, PERFORMANCE GRADED ASPHALT BINDER
- T315, DETERMINING THE RHEOLOGICAL PROPERTIES OF ASPHALT BINDER USING A DYNAMIC SHEAR RHEOMETER (DSR)

2.2. ASTM Standard

- D8, TERMINOLOGY RELATING TO MATERIALS FOR ROADS AND PAVEMENTS
- D2493,VISCOSITY-TEMPERATURE CHART FOR ASPHALTS

---

3. TERMINOLOGY

3.1 Definitions:

3.1.1 Definitions of terms used in this practice may be found in ASTM D8, determined from common English usage, or combinations of both.

4. SUMMARY OF TEST METHOD

4.1. A sample of unaged asphalt binder is tested in the DSR using the 25-mm plate geometry with a 0.5-mm gap setting. The sample is tested in flow mode over a range of shear stresses from 0 to 500 Pa at 3 temperatures (76, 82, 88C).

4.2. After testing is completed, the viscosity values at 500 Pa are plotted versus temperature on a log-log scale. From the plot, mixing and compaction temperatures are determined based upon specified viscosity ranges.

5. SIGNIFICANCE AND USE

5.1 This test method is designed to determine the laboratory mixing and compaction temperatures for modified and unmodified asphalt binders.

6. PROCEDURE

6.1. Sample Preparation – The sample for the Steady Shear Flow test is prepared the same as samples for T 315 using the 25-mm plates with the following exceptions as noted in 6.1.1. The temperature control will also follow T 315 requirements.

6.1.1 The test gap for the Steady Shear Flow test will be 0.5 mm. An additional 0.025- mm gap will be added before trimming to allow for creation of the bulge.

6.2. Set the DSR software to perform a steady shear flow test from 50 to 500 Pa, collecting 5 data points for viscosity per log decade.

6.2.1 A 12 second data-sampling period should be used.

6.2.2 Steady state conditions will be met when 3 consecutive viscosity readings vary less than 2%. A maximum test time for each stress level of 12 minutes should be set to ensure that tests won't last interminably.

6.3. *After testing is completed, increase temperature by 6°C and repeat steps 6.1 – 6.3 until the number of desired test temperatures has been reached.*

7. HAZARDS

7.1. Use standard laboratory safety procedures in handling the hot asphalt binder when preparing specimens for this test method.

8. CALCULATION

8.1. Using the results obtained in Section 6, create a log-log plot of Viscosity (Pa-S) at 500 Pa versus Temperature (°C). Information on the construction of viscosity – temperature charts can be found in ASTM D2493.

8.2. Construct a line through the 3 data points on the plot created in section 8.1. Extend the line as necessary to cross mixing and compaction target viscosity ranges.

8.3. Using target ranges of 0.15 to 0.19 Pa-S for mixing and 0.32 – 0.38 Pa-S for compaction, determine the mixing and compaction temperature ranges either visually or using a computer graphing program.

9. REPORT

9.1 Report the following information:

9.1.1 Sample identification;

9.1.2. Test Temperatures, nearest 0.1 °C;

9.1.3. Viscosity at 500 Pa for each test temperature, cP;

9.1.4. Mixing temperature range, nearest °C;

9.1.5. Compaction temperature range, nearest °C;

10. PRECISION AND BIAS

10.1. *Precision* – The research required to develop precision estimates has not been conducted.

10.2. *Bias* – The research required to establish the bias has not been conducted.

11. KEYWORDS

11.1. *Steady Shear Flow; laboratory mixing temperature; laboratory compaction temperature, Dynamic Shear Rheometer (DSR); modified asphalt binder, target viscosity range.*

APPENDIX

X.1. SAMPLE CALCULATIONS

X1.1. Table X1.1 shows a set of test results at 3 temperatures:

Table X1.1 – Steady Shear Flow Test Results

Test Temperature, °C	***Viscosity at 500 Pa, Pa-S***
76.0	*34.1*
82.0	*18.8*
88.0	*10.7*

X.1.2. Figure X1.1 shows the data in Table X1.1 plotted on a log-log Temperature - Viscosity chart:

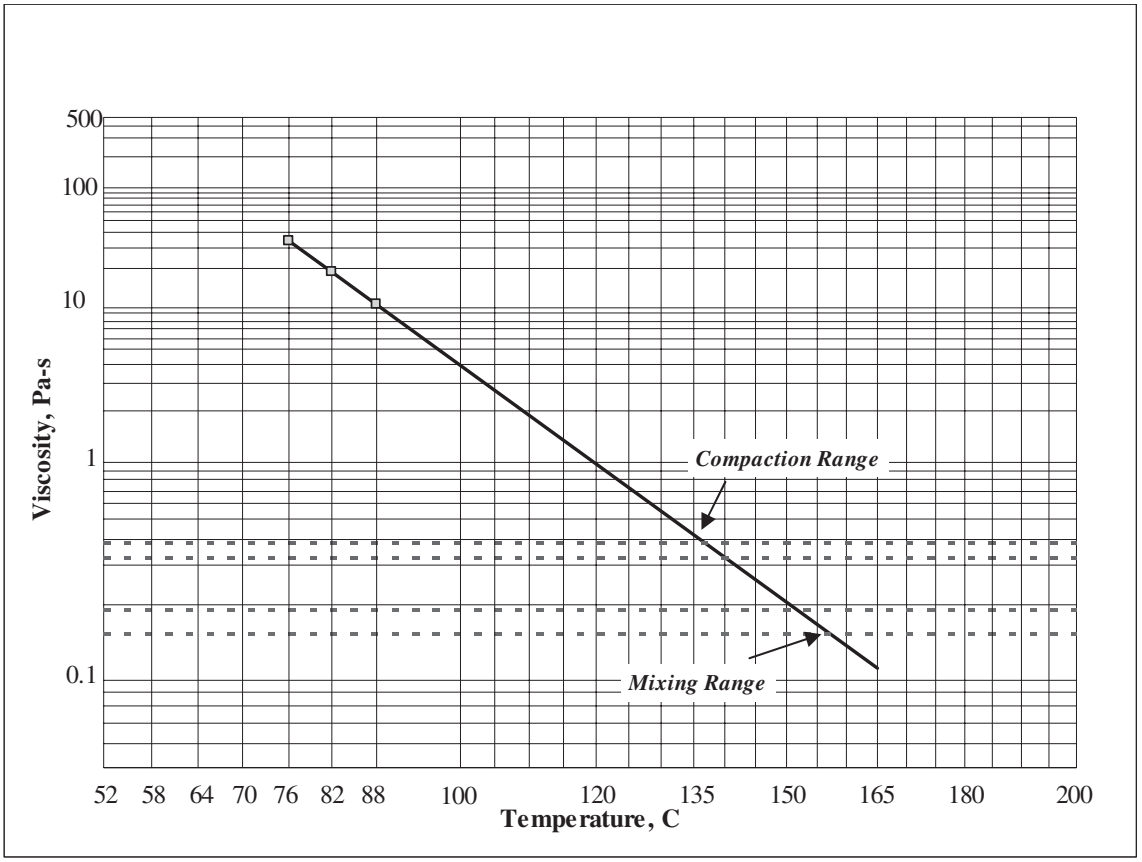

Figure X1.1 – Test Data Plot Showing Viscosity at 500 Pa and 3 Test Temperatures

X.1.3 Using a compaction temperature range of 0.32 – 0.38 Pa-S, the laboratory compaction temperature of this asphalt binder will be 137 – 140°C.

X.1.4. Using a mixing temperature range of 0.15 – 0.19 Pa-S, the laboratory mixing temperature of this asphalt binder will be 152 – 157°C.

Standard Method of Test for

Determining the Laboratory Mixing & Compaction Temperature of Asphalt Binder Using a Dynamic Shear Rheometer (DSR).

The Phase Angle Method.

AASHTO Designation: X XXX-XX

American Association of State Highway and Transportation Officials
444 North Capitol Street N.W., Suite 249
Washington, D.C. 20001

Standard Method of Test for

Determining the Laboratory Mixing & Compaction Temperature of Asphalt Binder Using a Dynamic Shear Rheometer (DSR)

The Phase Angle Method

AASHTO Designation: X XXX-XX

SCOPE

This test method covers the determination of the dynamic shear modulus and phase angle of asphalt binder when tested in dynamic (oscillatory) shear using parallel plate test geometry. It is applicable to asphalt binders having dynamic shear modulus values in the range from 50 Pa to 10 MPa. This range in modulus is typically obtained between 40°C and 150°C at an angular frequency of 0.1 to 100 rad/s. This test method is intended for determining the linear viscoelastic properties of asphalt binders over a range of both frequency & temperature in order to determine a reasonable master curve of the visco-elastic properties of asphalt binder. This master curve will be used to determine the appropriate laboratory mixing & compaction temperatures.

This standard is appropriate for unaged material or material aged in accordance with T 240 and R 28.

Particulate material in the asphalt binder is limited to particles with longest dimensions less than 250µm.

This standard may involve hazardous materials, operations, and equipment. This standard does not purport to address all of the safety problems associated with its use. It is the responsibility of the user of this procedure to establish appropriate safety and health practices and to determine the applicability of regulatory limitations prior to use.

REFERENCED DOCUMENTS

***AASHTO Standards*:**

- M 320, Performance-Graded Asphalt Binder
- R 28, Accelerated Aging of Asphalt Binder Using a Pressurized Aging Vessel (PAV)
- R 29, Grading or Verifying the Performance Grade of an Asphalt Binder
- T 40, Sampling Bituminous Materials
- T 240, Effect of Heat and Air on a Moving Film of Asphalt (Rolling Thin-Film Oven Test)

***ASTM Standards*:**

- C 670, Practice for Preparing Precision and Bias Statements for Test Methods for Construction Materials
- E 1, Specification for ASTM Thermometers
- E 77, Standard Test Method for Inspection and Verification of Thermometers
- E 563, Standard Practice for Preparation and Use of an Ice-Point Bath as a Reference Temperature
- E 644, Standard Test Methods for Testing Industrial Resistance Thermometers
- D 2170, Standard Test Method for Kinematic Viscosity of Asphalts (Bitumens)
- D 2171, Standard Test Method for Viscosity of Asphalts by Vacuum Capillary Viscometer

***Deutsche Industrie Norm (DIN) Standards*:**

- 43760, Standard for Calibrations of Thermocouples

National Cooperative Highway Research Program Report:

- **NCHRP Report xxx, Procedure for Determining Mixing and Compaction Temperatures of Asphalt Binders in Hot Mix Asphalt**

TERMINOLOGY

***Definitions*:**

asphalt binder—*an asphalt-based cement that is produced from petroleum residue either with or without the addition of non-particulate organic modifiers.*

Descriptions of Terms Specific to This Standard:

annealing—*heating the binder until it is sufficiently fluid to remove the effects of steric hardening.*

complex shear modulus (G*)—*ratio calculated by dividing the absolute value of the peak-to-peak shear stress, τ, by the absolute value of the peak-to-peak shear strain, γ.*

calibration—*process of checking the accuracy and precision of a device using NIST-traceable standards and making adjustments to the device where necessary to correct its operation or precision and accuracy.*

dummy test specimen—*a specimen formed between the dynamic shear rheometer (DSR) test plates from asphalt binder or other polymer to measure the temperature of the asphalt binder held between the plates. The dummy test specimen is used solely to determine temperature corrections.*

loading cycle—*a unit cycle of time for which the test sample is loaded at a selected frequency and stress or strain level.*

phase angle (δ)—*the angle in radians between a sinusoidally applied strain and the resultant sinusoidal stress in a controlled-strain testing mode, or between the applied stress and the resultant strain in a controlled-stress testing mode.*

loss shear modulus (G´´)—*the complex shear modulus multiplied by the sine of the phase angle expressed in degrees. It represents the component of the complex modulus that is a measure of the energy lost (dissipated during a loading cycle).*

storage shear modulus (G´)—*the complex shear modulus multiplied by the cosine of the phase angle expressed in degrees. It represents the in-phase component of the complex modulus that is a measure of the energy stored during a loading cycle.*

parallel plate geometry—*refers to a testing geometry in which the test sample is sandwiched between two relatively rigid parallel plates and subjected to oscillatory shear.*

oscillatory shear—*refers to a type of loading in which a shear stress or shear strain is applied to a test sample in an oscillatory manner such that the shear stress or strain varies in amplitude about zero in a sinusoidal manner.*

linear viscoelastic—*within the context of this specification refers to a region of behavior in which the dynamic shear modulus is independent of shear stress or strain.*

portable thermometer—*is an electronic device that consists of a temperature detector (probe containing a thermocouple or resistive element), required electronic circuitry, and readout system.*

reference thermometer—*a NIST–traceable liquid-in-glass or electronic thermometer that is used as a laboratory standard.*

temperature correction—*difference in temperature between the temperature indicated by the DSR and the test specimen as measured by the portable thermometer inserted between the test plates.*

thermal equilibrium—*is reached when the temperature of the test specimen mounted between the test plates is constant with time.*

thermal gradient- *temperature inequality throughout the test specimen due to the poor thermal conductivity of or poor stability of the temperature control device. These inequalities are typically from top of specimen to bottom of specimen and/or from center of specimen to edge of specimen. Thermal gradients can cause errors in the reporting of the specimen's modulus & phase angle.*

thermal hysteresis- *where the modulus of the specimen at temperature X differs depending on whether the specimen is heated to temperature X or cooled to reach temperature X.*

verification—*process of checking the accuracy of a device or its components against an internal laboratory standard. It is usually performed within the operating laboratory.*

steric hardening—*see molecular association.*

molecular association—*a process where associations occur between asphalt binder molecules during storage at ambient temperature. Often called steric hardening in the asphalt literature, molecular associations can increase the dynamic shear modulus of asphalt binders. The amount of molecular association is asphalt specific and may be significant even after a few hours of storage.*

Isotherms – *equation or curve on a graph representing he behavior of a material at a constant temperature*

Isochrones – *equation or curve on a graph representing he behavior of a material at a constant frequency*

Frequency Sweep – *is an oscillatory test performed within the linear visco-elastic region of a sample where the variable is frequency and the temperature is held constant.*

Master curve – *when several frequency curves (isotherm) determined at different temperatures are shifted, each one according to its individual shift factor, to a reference temperature and presented together in one diagram afterwards, the result is the so-called master curve.*

Black space – *is a graphic representation of phase angle variation with respect to complex modulus from isotherm done at different temperatures.*

SUMMARY OF TEST METHOD

This standard contains the procedure used to measure the complex shear modulus (*G) and phase angle (δ) of asphalt binders using a dynamic shear rheometer and parallel plate test geometry.**

The standard is suitable for use when the dynamic shear modulus varies between 50 Pa and 10 MPa. This range in modulus is typically obtained between 40 and 150°C at an angular frequency range of 0.1 to 100 rad/s, dependent upon the grade, test temperature, and conditioning (aging) of the asphalt binder.

Testing is required at multiple temperatures to acquire phase angle values between 87 degrees and 75 degrees. Generally, this can be obtained using 3 temperatures, although more can be used.

The required temperatures to test the sample will depend on the Performance Grade (PG) of the binder. Lower PG binders will be tested at lower temperatures while higher PG binders will be tested at higher temperatures. All grades will be tested at 80°C. The chart in Table 1. below provides a guide to temperature selection.

Table 44—Temperature testing schedule

Temperature	Nominal PG value								
°C	46	52	58	64	70	76	82	88	94
40	xx	xx	xx						
50	X	X	X	xx	xx				
60	X	X	xx	X	xx	xx			
70	xxx	xxx	X	X	X	xx	xx		
80	X	X	X	X	X	X	xx	xx	xx
90			xxx	xxx	X	X	X	xx	xx
100					xxx	X	X	X	X
110					xxx	xxx	X	X	
120						xxx	xxx	X	X
130						xxx	xxx	xxx	xxx
140							xxx	xxx	X
									xxx

xx	May be required to achieve a phase angle of 75 degrees
xxx	May be required to achieve a phase angle of 88 degrees

Test specimens 1 mm thick by 25 mm in diameter are formed between parallel metal plates. During testing, one of the parallel plates is oscillated with respect to the other at pre-selected frequencies and rotational deformation

amplitudes (strain control) (or torque amplitudes (stress control)). The required stress or strain amplitude depends upon the value of the complex shear modulus of the asphalt binder being tested. The required amplitudes have been selected to ensure that the measurements are within the region of linear behavior.

The test specimen is maintained at the test temperature to within ± 0.1°C by positive heating and cooling of the upper and lower plates or by enclosing the upper and lower plates in a thermally controlled environment or test chamber. In either case, the sample must be immersed in a bath of either forced air or flowing water to provide heat transfer with minimal thermal gradients and eliminate the potential of thermal hysteresis.

Oscillatory loading frequencies using this standard can range from 0.1 to 100 rad/s using a sinusoidal waveform. The complex modulus (G^*) and phase angle (δ) are calculated automatically as part of the operation of the rheometer using proprietary computer software supplied by the equipment manufacturer.

4.6. Results obtained from the testing must combined to create a master curve. This master curve will be compiled using the time-temperature-superposition principle with a reference temperature set to 80°C. Rheometer manufacturer's as well as other 3rd party software modeling providers offer automated software to perform this function.

SIGNIFICANCE AND USE

The mixing process of hot mix asphalt requires the binders to adequately coat the aggregate to a uniform film thickness. The asphalt binder exhibits differing mechanical (visco-elastic) properties at different temperatures. Knowing the binders visco-elastic properties enables the proper selection of temperature where these visco-elastic behaviors enable adequate mixing and coating of the aggregate.

The compaction process of hot mix asphalt requires the binder to move under compaction in order to achieve the proper pavement density. Knowing the binders visco-elastic properties enables the proper selection of temperature where these visco-elastic behaviors enable proper compaction to occur.

A series of frequency sweeps are performed by the rheometer at several temperatures in an automated fashion. The data collected is then automatically processed to produce a time-temperature-superposition master curve of the binder at the reference temperature of 80°C.

From the master curve, the frequency where the binder transitions from viscous (newtonian) behavior to visco-elastic (non newtonian) behavior provides information relating to the required temperature needed to adequately mix

or compact the asphalt binder. The phase angle is used to identify the transition frequency where the phase angle equals 86 degrees.

Through a simple mathematical algorithm, this value of frequency is processed to both a mixing & compaction temperature.

APPARATUS

***Dynamic Shear Rheometer (DSR) Test System*—A dynamic shear rheometer test system consisting of parallel metal plates, an environmental chamber, a loading device, and a control and data acquisition system.**

Test Plates—*Metal test plates made from stainless steel or aluminum with smooth ground surfaces. A set of 25.00 ± 0.05 mm in diameter (Figure 1). The base plate in some rheometers is a flat plate. A raised portion, a minimum of 1.50 mm high, with the same radius as the upper plate is required. The raised portion makes it easier to trim the specimen and may improve test repeatability.*

> **Note 1**—To get correct data, the upper and lower plates should be concentric with each other. At present there is no suitable procedure for the user to check the concentricity except to visually observe whether or not the upper and lower plates are centered with respect to each other. The moveable plate should rotate without any observable horizontal or vertical wobble. This operation may be checked visually or with a dial gauge held in contact with the edge of the moveable plate while it is being rotated. There are two numbers that determine the running behavior of a measuring system: centricity (horizontal wobble) and runout (vertical wobble). Typically, wobble can be seen if it is greater than ± 0.02 mm. For a new system, a wobble of ± 0.01 mm is typical. If the wobble grows to more than ± 0.02 mm with use, it is recommended that the instrument be serviced by the manufacturer.

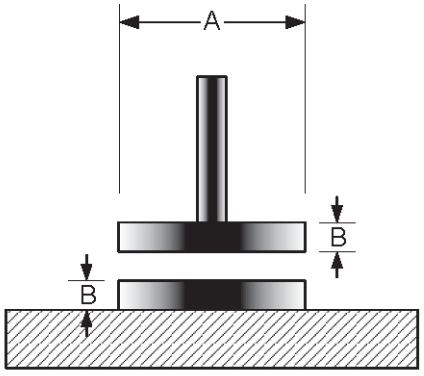

Dimension	25-mm Nominal
A	25 ± 0.05 mm
B	≥ 1.50 mm

Figure 1—Plate Dimensions

Environmental Chamber—*A chamber for controlling the test temperature, by heating (in steps or ramps), or cooling (in steps or ramps), to maintain a constant specimen environment. The medium for heating and cooling the specimen in the environmental chamber shall not affect asphalt binder properties. The temperature in the chamber may be controlled by the circulation of fluid such as water, conditioned forced gas such as air or nitrogen, surrounding the sample. The environmental chamber and the temperature controller shall control the temperature of the specimen, including thermal gradients within the sample, to an accuracy of ±0.1°C. The chamber shall completely enclose the top and the bottom plates to minimize thermal gradients.*

> **Note 2**—A circulating bath unit separate from the DSR which pumps the bath fluid through the test chamber may be required if a fluid medium is used.

Temperature Controller—A temperature controller capable of maintaining specimen temperatures within ± 0.1°C for test temperatures ranging from 40 to 100°C. In some cases with highly polymer modified asphalt binder will require temperatures up to 140°C.

Internal Temperature Detector for the DSR—A platinum resistance thermometer (PRT) mounted within the environmental chamber as an integral part of the DSR and in close proximity to the fixed plate, and with a resolution of 0.1°C (see Note 3). This thermometer shall be used to control the temperature of the test specimen between the plates and shall provide a continuous readout of temperature during the mounting, conditioning, and testing of the specimen.

> **Note 3**—Platinum resistance thermometer (PRTDs) meeting DIN Standard 43760 (Class A) or equal are recommended for this purpose. The PRTD shall be calibrated as an integral unit with its respective meter or electronic circuitry.

Loading Device—*The loading device shall apply a sinusoidal oscillatory load to the specimen over a frequency range of 0.10 to 100.0 ± 1%. The loading device shall be capable of providing either a stress controlled or strain controlled load. If the load is strain controlled, the loading device shall apply a cyclic torque sufficient to cause an angular rotational strain accurate to within 100 μ rad of the strain specified. If the load is stress controlled, the loading device shall apply a cyclic torque accurate to within 10 μN·m of the torque specified. Total system compliance at 100 N·m torque shall be less than 2 mrad/N·m. The manufacturer of the device shall provide a certificate certifying that the frequency, stress, and strain are controlled and measured with an accuracy of one percent or less in the range of this measurement.*

Control and Data Acquisition System—*The control and data acquisition system shall provide a record of temperature, frequency, deflection angle, and torque. Devices used to measure these quantities shall meet the accuracy*

requirements specified in Table 2. In addition, the system shall calculate and record the shear stress, shear strain, complex shear modulus (G) and phase angle (δ). The system shall measure and record G*, in the range of 100 Pa to 10 MPa, to an accuracy of 1.0 percent or less and the phase angle, in the range of 0 to 90 degrees, to an accuracy of 0.1 degrees.*

Table 2—Control and Data Acquisition System Measurement Requirements

Function	Minimum Accuracy Value or Range
Temperature	0.01°C Resolution ± 0.1 °C Stability ± 0.1 °C Gradients throughout sample 40 to 150 °C Range
Frequency	to 100 rad/sec Range 1% Resolution / Accuracy 0.1 degree Phase Angle Measurement
Torque	10 nN·m Resolution 10μ to 10mN·m Range
Deflection angle	1 μrad

***Specimen Mold (Optional)*—The overall dimensions of the silicone rubber mold for forming asphalt binder test specimens may vary but the thickness shall be greater than 5 mm. If the mold is a single sample mold, the following dimensions have been found suitable: For a 25-mm test plate with a 1-mm gap, a mold cavity approximately 18 mm in diameter and 2.0 mm deep.**

***Specimen Trimmer*—A specimen trimmer with a straight edge at least 4 mm wide.**

***Wiping Material*—Clean cloth, paper towels, cotton swabs, or other suitable material as required for wiping the plates.**

***Cleaning Solvents*—Mineral oil, citrus-based solvents, mineral spirits, toluene, or similar solvent as required for cleaning the plates. Acetone for removing solvent residue from the surfaces of the plates.**

***Reference Thermometer*—Either a NIST-traceable liquid-in-glass thermometer(s) or NIST–traceable electronic thermometer shall be maintained in the laboratory as a temperature standard. This temperature standard shall be used to verify the portable thermometer (Section 9.3).**

Liquid-in-Glass Thermometer—*NIST-traceable liquid-in-glass thermometer(s) with a suitable range and subdivisions of 0.1°C. The thermometer(s) shall be a partial immersion thermometer(s) within an ice point and shall be calibrated in accordance with ASTM E 563.*

Optical Viewing Device (Optional)—An optical viewing device for use with liquid-in-glass thermometers that enhances readability and minimizes parallax when reading the liquid-in-glass reference thermometer.

Electronic Thermometer—*An electronic thermometer that incorporates a resistive detector (see Note 3) with an accuracy of ± 0.05°C and a resolution of 0.01°C. The electronic thermometer shall be calibrated at least once per year using a NIST–traceable reference standard in accordance with ASTM E 77.*

***Portable Thermometer*—A calibrated portable thermometer consisting of a resistive detector, associated electronic circuitry, and digital readout. The thickness of the detector shall be no greater than 2.0 mm such that it can be inserted between the test plates. The reference thermometer (see Section 6.6) may be used for this purpose if its detector fits within the dummy specimen as required by Section 9.4.1 or 9.4.2.**

HAZARDS

Standard laboratory caution should be used in handling the hot asphalt binder when preparing test specimens.

PREPARATION OF APPARATUS

Prepare the apparatus for testing in accordance with the manufacturer's recommendations. Specific requirements will vary for different DSR models and manufacturers.

Inspect the surfaces of the test plates and discard any plates with jagged or rounded edges or deep scratches. Clean any asphalt binder residue from the plates with an organic solvent such as mineral oil, mineral spirits, a citrus-based solvent, or toluene. Remove any remaining solvent residue by wiping the surface of the plates with a cotton swab or a soft cloth dampened with acetone. If necessary, use a dry cotton swab or soft cloth to ensure that no moisture condenses on the plates.

Mount the cleaned and inspected test plates on the test fixtures and tighten firmly.

Select the testing temperature according to the grade of the asphalt binder or according to the preselected testing schedule (see Note 4). Allow the DSR to reach a stabilized temperature within ± 0.1°C of the test temperature.

> **Note 4**—M 320 and R 29 provide guidance on the selection of test temperatures.

With the test plates at the test temperature or the middle of the expected testing range, establish the zero gap level (1) by manually spinning the moveable plate, and while the moveable plate is spinning, close the gap until the removable plate touches the fixed plate (The zero gap is reached when the plate stops spinning completely.), or, (2) for rheometers with normal force transducers, by closing the gap and observing the normal force and after

establishing contact between the plates, setting the zero gap at approximately zero normal force.

> **Note 5—The frame, detectors, and fixtures in the DSR can change dimension with temperature causing the zero gap to change with changes in temperature. Adjustments in the gap are not necessary when measurements are made over a limited range of temperatures. The gap should be set at the test temperature or, when tests are to be conducted over a range of temperatures, the gap should be set at the middle of the expected range of test temperatures. If the instrument has thermal gap compensation, the gap may be set at the first test temperature instead of the middle of the range of test temperatures. Follow manufacturer's recommendations for specific instrument model procedures to ensure accurate from testing over a range of temperatures.**

Once the zero gap is established as per Section 8.5, move the plates apart to approximately the test gap and preheat the plates. Preheating the plates promotes adhesion between the asphalt binder and the plates, especially at the intermediate grading temperatures.

To preheat 25-mm plates, bring the test plates to the test temperature or the lowest test temperature if testing is to be conducted at more than one temperature. Move the plates apart and establish a gap setting of 1.05 mm for the 25-mm diameter test specimens.

> **Note 6**—In order to obtain adequate adhesion between the asphalt binder and the test plates, the plates must be preheated. Preheating is especially critical when the silicone mold is used to prepare the asphalt binder for transfer to the test plates. When the direct placement method is used, as long as the test plates are immediately brought in contact with the asphalt binder, the heat carried with the asphalt binder improves adhesion. The preheating temperature needed for proper adhesion will depend on the grade and nature of the asphalt binder and the test. For highly modified asphalt binders only, higher preheat temperatures may be used.

VERIFICATION AND CALIBRATION

Verify the DSR and its components at least every six months and when the DSR or plates are newly installed, when the DSR is moved to a new location, or when the accuracy of the DSR or any of its components is suspect. Four items require verification—test plate diameter, DSR torque transducer, portable thermometer, and DSR test specimen temperature. Verify the DSR temperature transducer before verifying the torque transducer.

***Verification of Plate Diameter*—Measure the diameters to the nearest 0.01 mm. Maintain a log of the measured diameters as part of the laboratory quality control plan so that the measurements are clearly identified with specific plates. If the plates are not within tolerance, they must not be used.**

Note 7—An error of ± 0.05 mm in the diameter of the plate results in a 0.8 percent error in the complex modulus for the 25-mm plate. For the 8-mm plate, errors in diameter of ± 0.01, ± 0.02, and ± 0.05 mm give respective errors in complex modulus of 0.5, 1.0, and 2.5 percent.

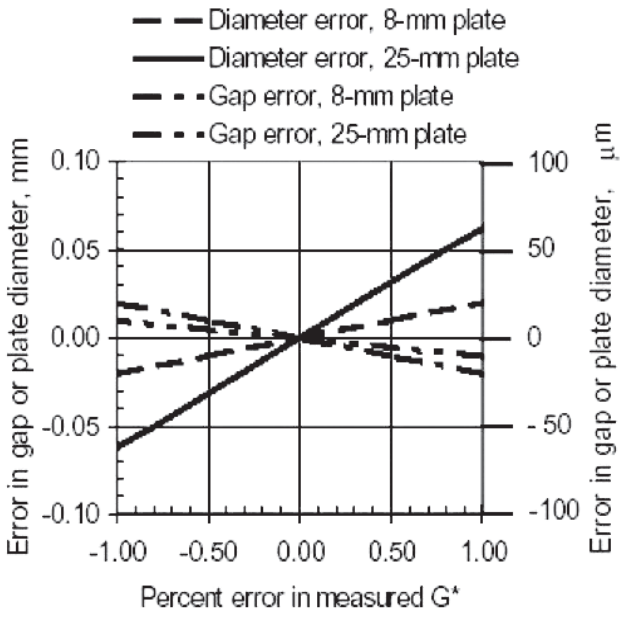

Figure 2—Effect of Error in Gap or Plate Diameter

***Verification of Portable Thermometer*—Verify the portable thermometer (used to measure the temperature between the test plates), using the laboratory reference thermometer. If the reference thermometer (Section 6.6) is also used as a portable thermometer to measure the temperature between the test plates, it shall be meet the requirements of Section 6.7. Electronic thermometers shall be verified using the same meters and circuitry (wiring) that are used when temperature measurements are made between the plates.**

Recommended Verification Procedure— *Bring the reference thermometer into intimate contact with the detector from the portable thermometer and place them in a thermostatically controlled and stirred water bath (Note 8). Ensure that de-ionized water is used to prevent electrical conduction from occurring between electrodes of the resistive temperature sensitive element. If de-ionized water is not available, encase the reference thermometer and the detector of the portable thermometer into a waterproof plastic bag prior to placement into the bath. Obtain measurements at intervals of approximately 6°C over the range of test temperatures allowing the bath to come to thermal equilibrium at each temperature. If the readings of the portable thermometer and the reference thermometer differ by 0.1°C or more, record the difference at each temperature as a temperature correction, and maintain the corrections in a log as part of the laboratory quality control program.*

Note 8—A recommended procedure for the high temperature range is to use a stirred water bath that is controlled to ± 0.1°C such as the viscosity bath used for ASTM D 2170 or D 2171. For a low temperature bath, an ice bath or controlled temperature bath may be used. Bring the probe from the portable thermometer into contact with the reference thermometer, and hold the assembly in intimate contact. A rubber band works well for this purpose. Immerse the assembly in the water bath, and bring the water bath to thermal equilibrium. Record the temperature on each device when thermal equilibrium is reached.

Note 9—If the readings from the two devices differ by 0.5°C or more, the calibration or operation of the portable thermometer may be suspect, and it may need to be recalibrated or replaced. A continuing change in the temperature corrections with time may also make the portable thermometer suspect.

Test Specimen Temperature Correction—**Thermal gradients within the rheometer can cause differences between the temperature of the test specimen and the temperature indicated by the DSR thermometer (also used to control the temperature of the DSR). The DSR thermometer shall be checked at an interval no greater than six months. When these differences are 0.1°C or greater, determine a temperature correction by using a thermal detector mounted in a silicone rubber wafer (Section 9.4.1) or by placing asphalt binder (dummy sample) between the plates and inserting the detector of the portable thermometer into the asphalt binder (Section 9.4.2).**

Method Using Silicone Rubber Wafer—*Place the wafer between the 25-mm test plates, and close the gap to bring the wafer into contact with the upper and lower plate so that the silicone rubber makes complete contact with the surfaces of the upper and lower plates. If needed, apply a thin layer of petroleum grease or anti-seize compound to completely fill any void space between the silicone rubber and the plates. Complete contact is needed to ensure proper heat transfer across the plates and silicone rubber wafer. Determine any needed temperature correction as per Section 9.4.3.*

Note 10—Anti-seize compound available by that name at hardware and auto supply stores is much less apt to contaminate the circulating water than petroleum grease.

Note 11—The currently available silicone wafer is 2 mm thick and slightly greater than 25 mm in diameter.

Method Using Dummy Test Specimen—*The dummy test specimen shall be formed from asphalt binder or other polymer that can be readily formed between the plates. Mount the dummy test specimen between the test plates, and insert the detector (probe) of the portable thermometer into the dummy test specimen. Close the gap to the test gap (1 mm for 25-mm plates and 2 mm for 8-mm plates) keeping the detector centered vertically and radially in the dummy test specimen. Heat the plates as needed to allow the dummy test specimen to completely fill the gap between the test plates. It is not necessary to trim the dummy test specimen but avoid excessive material around the edges of the plates. Determine any needed temperature correction as per Section 9.4.3.*

Note 12—Silly putty can leave a residue of silicone oil on the surfaces of the plates, and for this reason, its use as a dummy specimen is not recommended.

Determination of Temperature Correction—*Obtain simultaneous temperature measurements with the DSR thermometer and the portable thermometer at 6°C increments to cover the range of test temperatures. At each temperature increment, after thermal equilibrium has been reached, record the temperature indicated by the portable thermometer and the DSR thermometer to the nearest 0.1°C. Temperature equilibrium is reached when the temperature indicated by both the DSR thermometer and the portable thermometer do not vary by more than 0.1°C over a five minute time period. Obtain additional measurements to include the entire temperature range that will be used for measuring the dynamic shear modulus.*

Plot Correction versus Specimen Temperature—*Using the data obtained in Section 9.4, prepare a plot of the difference between the two temperature measurements versus the temperature measured with the portable thermometer (see Figure 3). This difference is the temperature correction that must be applied to the DSR temperature controller to obtain the desired temperature in the test specimen between the test plates. Report the temperature correction at the respective test temperature from the plot and report the test temperature between the plates as the test temperature. Alternatively, the instrument software may provide these temperature corrections automatically.*

Note 13—The difference between the two temperature measurements may not be a constant for a given rheometer but may vary with differences between the test temperature and the ambient laboratory temperature as well as with fluctuations in ambient temperature. The difference between the two temperature measurements is caused in part by thermal gradients in the test specimen and fixtures.

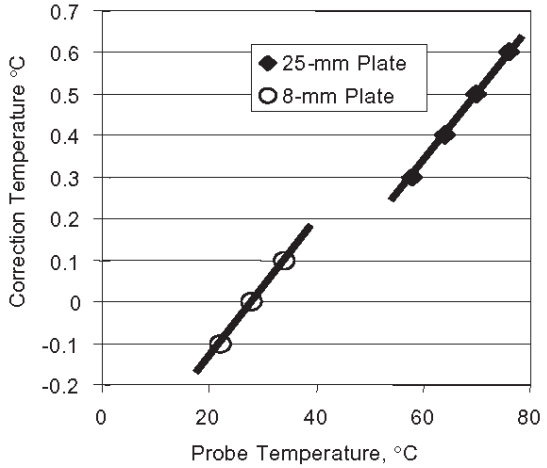

Figure 3—Determination of Temperature Correction

***Verification of DSR*—Verify the accuracy of the torque transducer and angular displacement transducer.**

Note 14—A newly installed or reconditioned instrument should be verified on a weekly basis using the procedures in Section 9.5 until acceptable verification has been demonstrated. Maintaining the data in the form of a control chart where the verification measurements are plotted versus calendar date is recommended (see Appendix X2).

Verification of Torque Transducer—*Verify the calibration of the torque transducer a minimum of once every six months using a reference fluid or manufacturer-supplied fixtures when the calibration of the torque transducer is suspect or when the dynamic viscosity, as measured for the reference fluid, indicates that the torque transducer is not in calibration.*

Verification of Torque Transducer with Reference Fluid—The complex viscosity measured with the DSR shall be within three percent of the capillary viscosity as reported by the manufacturer of the reference fluid; otherwise, the calibration of the torque transducer shall be considered suspect. Compare the fluid reported viscosity to the instrument reported complex viscosity (η^*). Alternately, calculate the complex viscosity from the complex modulus (G^*) divided by the angular frequency in rad/s. Recommended practice for using the reference fluid is given in Appendix X3.

Note 15—A suitable reference fluid is available from Cannon Instrument Company as Viscosity Standard Number N2700000SP.

Verification of Torque Transducer with Fixtures—Verify the calibration of the torque transducer using the manufacturer-supplied fixtures in accordance with the instructions supplied by the manufacturer. Suitable manufacturer-supplied fixtures are not widely available. If suitable fixtures are not available, this requirement shall be waived.

Verification of Angular Displacement Transducer—*If manufacturer-supplied fixtures are available, verify the calibration every six months or when the calibration of the DSR is suspect. If suitable fixtures are not available, this requirement shall be waived.*

If the DSR cannot be successfully verified as per Section 9.5, it shall not be used for testing in accordance with this standard until it has been successfully calibrated by the manufacturer or other qualified service personnel.

PREPARING SAMPLES AND TEST SPECIMENS

***Preparing Test Samples*—If unaged binder is to be tested, obtain test samples according to T 40.**

Anneal the asphalt binder from which the test specimen is obtained by heating until sufficiently fluid to pour the required specimens. Annealing prior to testing

removes reversible molecular associations (steric hardening) that occur during normal storage at ambient temperature. Do not heat the binder above a temperature of 163°C. Cover the sample, and stir it occasionally during the heating process to ensure homogeneity and to remove air bubbles. Minimize the heating temperature and time to avoid hardening the sample.

Note 16—For neat asphalt binders, minimum pouring temperatures that produce a consistency equivalent to that of SAE 10W30 motor oil (readily pours but not overly fluid) at room temperature are recommended. Heating unaged asphalt to temperatures above 135°C should be avoided; however, with some modified asphalts or heavily aged binders, pouring temperatures above 135°C may be required.

Cold material from storage containers must be annealed prior to usage. Structure developed during storage can result in overestimating the modulus by as much as 50 percent.

***Preparing asphalt binderTest Specimens*—Zero the gap as specified in Section 8. Carefully clean and dry the surfaces of the test plates so that the specimen will adhere to both plates uniformly and strongly. Bring the chamber to the starting test temperature or the beginning of the range (see Note 6) when using 25-mm specimens. This requirement is to preheat the upper and lower plates to allow specimen adhesion to both plates. Prepare a test specimen using one of the methods specified in Section 10.3.1, 10.3.2, or 10.3.3.**

Transfer asphalt binder to one of the test plates through pouring (Section 10.3.1), direct transfer (Section 10.3.2), or by use of a silicone mold (Section 10.3.3).

Note 18—Direct transfer or pouring are the preferred methods because the test results are less likely to be influenced by steric hardening than with the silicone mold method. Direct placement and direct pouring result in higher asphalt binder temperatures when the plates and asphalt binder are brought into contact, improving adhesion. For this reason, it is also important to bring the asphalt binder and plates into contact promptly after pouring or direct placement.

Pouring—*Only when using rheometers that are designed for removal of the plates without affecting the zero setting, remove the removable plate and, while holding the sample container approximately 15 mm above the test plate surface, pour the asphalt binder at the center of the upper test plate continuously until it covers the entire plate except for an approximate 2-mm wide strip at the perimeter (see Note 19). Wait only long enough for the specimen to stiffen, to prevent movement, and then mount the test plate in the rheometer for testing.*

Note 19—An eye dropper or syringe may be used to transfer the hot asphalt binder to the plate.

Direct Transfer—*Transfer the hot binder to one of the plates using a glass or metal rod, spatula, or similar tool. Immediately after transferring the hot binder to one of the plates, proceed to Section 10.4 to trim the specimen and form the bulge.*

Note 20—A small, narrow stainless steel spatula of the type used to weigh powders on

an analytical balance has been found suitable for transferring the hot binder. When using a rod, form a mass of sufficient size to form the test specimen by using a twisting motion. The twisting motion seems to keep the mass on the rod in control. A 4- to 5-mm diameter rod is suitable.

Silicone Mold—*Pour the hot asphalt binder into a silicone rubber mold that will form a pellet having dimensions as required in Section 6.2. Allow the silicone rubber mold to cool to room temperature. The specimen may be mounted to either the upper or lower plate. To mount the specimen to the lower plate, remove the specimen from the mold and center the pellet on the lower plate of the DSR. To mount the specimen to the upper plate, center the specimen still in the silicone rubber mold, on the upper plate. Gently press the specimen to the upper plate and then carefully remove the silicone rubber mold leaving the specimen adhered to the upper plate.*

The filled mold should be cooled at room temperature by placing the mold on a flat laboratory bench surface without chilling. Cooling to below room temperature results in an unknown thermal history that may affect the measured values of modulus and phase angle. Cooling may also result in the formation of moisture on the surface of the specimen that will interfere with adhesion of the specimen to the plates.

Note 21—Solvents should not be used to clean the silicone rubber molds. Wipe the molds with a clean cloth to remove any asphalt binder residue. With use, the molds will become stained from the asphalt binder, making it difficult to remove the binder from the mold. If sticking becomes a problem, discard the mold.

Note 22—Some binder grades cannot be removed from the silicone mold without cooling. Materials such as PG 52-34, PG 46-34, and some PG 58-34 grades do not lend themselves to being removed from the mold at ambient temperatures. If the binder specimen cannot be removed from the mold without cooling, the direct transfer or pouring method may be used, or the filled mold may be chilled in a freezer or refrigerator for the minimum time needed to facilitate demolding the specimen.

***Trimming Test Specimen*—Immediately after the specimen has been placed on one of the test plates as described above, move the test plates together until the gap between the plates equals the testing gap plus the gap closure required to create the bulge. (See Section 10.5 for gap closure required to create the bulge.) Trim excess binder by moving a heated trimming tool around the edges of the plates so that the asphalt binder is flush with the outer diameter of the plates.**

Note 23—The trimming tool should be at a temperature that is sufficiently hot as to allow trimming but not excessively hot as to pyrolyse the edge of the specimen.

Note 24—The gap should be set at the starting test temperature (Section 11.1.1) or at the middle of the expected range of test temperatures (Section 11.1.2). See Note 5 for guidance on setting the gap. Typically, reliable test results may be obtained with a single sample using temperatures within 12°C of the temperature at which the gap is set.

***Creating Bulge*—When the trimming is complete, decrease the gap by the amount required to form a slight bulge at the outside face of the test specimen. The gap required to create a bulge is rheometer specific and depends upon factors such as the design of the rheometer and the temperature difference between the trimming temperature and test temperature. Recommended closure values for creating the gap are 0.05 mm for the 25-mm plate. A recommended practice for verifying the gap closure required to produce an appropriate bulge is given in Appendix X4.**

Note 25—The complex modulus is calculated with the assumption that the specimen diameter is equal to the plate diameter. If the binder forms a concave surface at its outer edges this assumption will not be valid and the modulus will be underestimated. The calculated modulus is based upon the radius of the plate raised to the fourth power. A slight bulge equal to approximately one-quarter of the gap is recommended. A procedure for determining the closure required to form an acceptable gap is given in Appendix X4.

PROCEDURE

Program the DSR to perform a frequency sweep from 0.1 rad/sec to 100 rad/s, 10 points per decade logarithmically spaced, use a strain of 12% (or as needed to ensure all the testing is within the linear region for the sample tested). Testing should begin at the lowest frequency and increment up to the highest frequency.

Program the DSR to perform the series of isotherms. Set the rheometer to perform the frequency sweep defined in 11.1 to be performed at multiple temperatures starting from the lowest temperature to be tested and incremented up to the highest temperature. The range of temperatures to be selected should produce resulting phase angle data, at a minimum, from 88 degrees or more through at least 75 degrees or less. Generally, this can be achieved with 3 temperatures although, there is no problem using more temperatures to achieve this range. Temperatures of 40°C, 50°C, 60°C, 70°C, 80°C, 90°C, 100°C are the most common to use. However, some highly modified binders may require higher temperatures to achieve phase angles near 90 degrees. Likewise, some unmodified binders may require lower temperatures to achieve phase angle near 75 degrees (Refer to section 4.4 for temperature selection).

Set the rheometer to have a thermal equilibrium time for each temperature to ensure the sample achieves thermal equilibrium with thermal gradients of no more than ± 0.1°C throughout the sample and free from thermal hysteresis. (refer to appendix X12 to determine appropriate time to achieve thermal equilibrium)

Note 26—It is impossible to specify a single equilibration time that is valid for DSRs produced by different manufacturers. The design (fluid bath or air oven) of the environmental control system and the starting temperature will dictate the time required

to reach the test temperature. The method for determining the correct thermal equilibration time is described in Appendix X12.

Note 27—The gap should be set at the starting test temperature (Section 11.1.1) or at the middle of the expected range of test temperatures (Section 11.1.2). See Note 5 for guidance on setting the gap. Typically, reliable test results may be obtained with a single sample, 25-mm plate, using temperatures within 12°C of the temperature at which the gap is set.

Set the temperature controller to the desired test temperature, including any offset as required by Section 9.4.4. Allow the temperature indicated by the RTD to come to the desired temperature. The test shall be started only after the temperature has remained at the desired temperature ± 0.1°C for long enough to ensure the sample is completely at thermal equilibrium. . (refer to appendix X12 to determine appropriate time to achieve thermal equilibrium)

When conducting test; 1) start testing at the lowest frequency and increase to the highest frequency 2) start the temperature from the lowest temperature and increase to the highest temperature.

The data acquisition system specified in Section 6.1.4 automatically calculates *G and δ from test data acquired when properly activated to generate isotherms for each frequency sweep at each temperature.**

Initiate the testing immediately after preparing and trimming the specimen. The testing at subsequent temperatures should be done as quickly as possible to minimize the effects of molecular associations (steric hardening) or sample edge failure that can cause changes in reported modulus which can occur if the specimen is held in the rheometer for a prolonged period of time. When testing at multiple temperatures all testing should be completed within four hours.

Inspect the sample at the completion of the testing to ensure it has not excessively dripped out of the gap between the plates.

If additional testing is needed to collect the required data and the sample appears intact, it can be used. It is also possible to remove and load a fresh sample for additional testing.

ANALYSIS & INTERPRETATION OF RESULTS

Verification of the linear visco-elastic region.

The dynamic modulus and phase angle depend upon the magnitude of the shear strain; the modulus and phase angle for both unmodified and modified asphalt binder decrease with increasing shear strain outside the linear visco-elastic region of the asphalt sample as shown in Figure 5. A plot such as that shown in Figure 5 can be generated by gradually increasing applied strain amplitude on the sample and

measure the resulting stress, thereby producing a strain sweep results in Figure 5. It is not necessary to generate such sweeps during normal testing; however, such plots are useful for verifying the limits of the linear region.

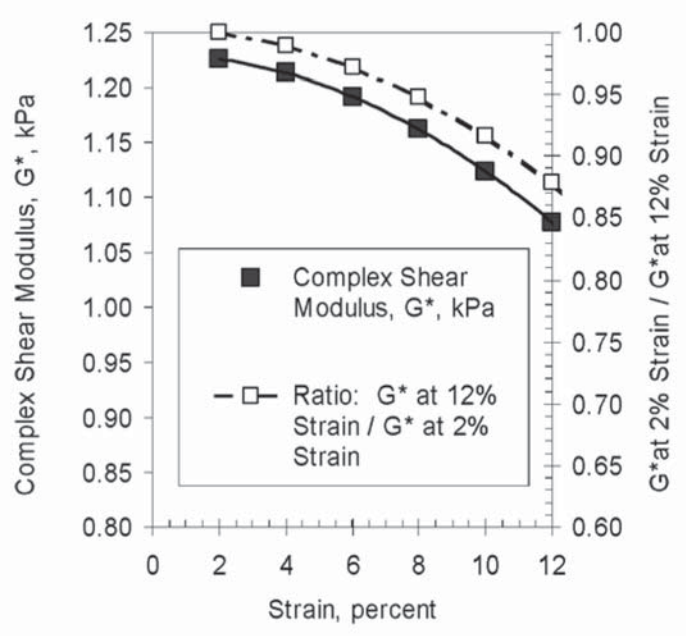

Figure 5—Example of Strain Sweep

A linear region may be defined at small strains where the modulus is relatively independent of shear strain. This region will vary with the magnitude of the complex modulus. The linear region is defined as the range in strains where the complex modulus is 95 percent or more of the zero-strain value.

The shear stress varies linearly from zero at the center of the plates to a maximum at the extremities of the plate perimeter. The shear stress is calculated from the applied or measured torque, measured or applied strain, and the geometry of the test specimen.

Report values of complex shear modulus and phase angle at each temperature obtained by frequency sweep.

Omit all outliers/results where the measured strain and/or stress are outside of the measurable range of the instrument.

Construct graph showing all frequency sweeps results. Graph G & phase angle vs. frequency. (refer to X13)*

Create a master curve of the isotherms at the reference temperature of 80°C. (refer to X14)

Identify from the master curve the frequency where the phase angle (δ) crosses 86 degrees. (refer to X14)

Construct Black space graph by plotting the phase angle vs. complex shear modulus to verify data. (Refer to X15)

A continuous curve on the Black space graph indicates a successful data set has been used to create the master curve. (Refer to X15)

Calculate mixing & compaction temperature from the resulting data from item 12.5.1 in accordance to reference X16.

Use the following equation to determine laboratory compaction temperature in ºF.

$$\textit{Mixing Temperature (ºF)} = 325\omega^{-0.0135} \qquad \textit{(X16)}$$

Where ω *= the frequency in rad/s for the phase angle of 86 degrees as reported from the master curve. 12.2.4*

Use the following equation to determine laboratory compaction temperature in *ºF.*

$$\text{Compaction Temperature (ºF)} = 300\omega^{-0.012} \qquad \textit{(X17)}$$

Where* ω *= the frequency in rad/s for the phase angle of 86 degrees as reported from the master curve. 12.2.4

REPORT

A sample report format is given in Appendix X13. Provide a complete identification and description of the material tested including name, code, and source.

Describe the instrument used for the test including the model number and type of temperature control (ie, wet fluid immersion, dry forced gas, dry radiant, dry directly heated plates).

The strain and stress levels specified in Tables 2 and 3 have been selected to ensure a common reference point that has been shown to be within the linear region for plain and modified asphalt binders. Some systems may not be linear within this region. When this situation is observed report the modulus at the recommended stress or strain levels but report that the test conditions were outside the linear region.

For each test, report the following:

Test plate diameter, nearest 0.1 mm and test gap, nearest 1μ*m;*

Test temperature, nearest 0.1°C, for the reported frequency of 13.4.3;

Frequency (to the nearest 10%), rad/s as derived from the master curve for Phase Angle of 86 degrees;

Strain amplitude, nearest 0.01 percent, for the reported frequency of 13.4.3
Complex modulus (G) corresponding to the phase angle of 86 degrees, kPa to three significant figures;*

Binder PG grade

Mix Temperature to the nearest degree, ^{o}F ;

Compaction Temperature to the nearest degree, ^{o}F.

PRECISION AND BIAS

***Precision*—Criteria for judging the acceptability of dynamic shear results obtained by this method are given in Table 4.**

Single-Operator Precision (Repeatability) — *Have not been determined as of yet.*

Multi-laboratory Precision (Reproducibility) — *Have not been determined as of yet.*

***Bias*—No information can be presented on the bias of the procedure because no material having an accepted reference value is available.**

KEYWORDS

Dynamic shear rheometer; DSR; complex modulus; phase angle, asphalt binder; mix, mix temperature; compaction, compaction temperature; casola method, tts, time temperature superposition., NCHRP 9-39

APPENDIXES

X1. TESTING FOR LINEARITY

X1.1. *Scope*:

X1.2. This procedure is used to determine whether an asphalt binder exhibits linear or non-linear behavior at the testing temperature, e.g., 40, 50, 60, 70, 80, or 90°C. The determination is based on the change in complex shear modulus at 10 rad/s when the strain is increased from 2 to 20 percent.

X1.3. *Procedure*:

X1.4. Verify the DSR and its components in accordance with Section 9 of this standard.

X1.5. Prepare the DSR in accordance with Section 10 of this standard.

X1.6. Prepare a test specimen for testing with 25-mm plates as per Section 11 of this standard. Select the test temperature for the binder in question.

X1.7. Determine the complex shear modulus at 2 and 12 percent strain following the test procedure described in Section 12 except as noted below. Always start with the lowest strain and proceed to the next larger strain.

X1.8. *Strain Controlled Rheometers*—If the software provided with the DSR will automatically conduct tests at multiple strains, program the DSR to obtain the complex shear modulus at strains of 2 to 20 percent in 2% increments. If this automatic feature is not available, test by manually selecting strains of 2, 4, 6, 8, 10, 12, 14, 16, 18 and 20 percent strain.

X1.9. For stress controlled rheometers, compute the starting stress based on the complex shear modulus, G^*, and shear stress, τ, as determined at the upper grading temperature during the grading of the binder. At this temperature the complex modulus, G^*, will be greater than or equal to 1.00 kPa and the shear stress, τ, will be between 0.090 and 0.150 kPa (see Table 2). Calculate the starting stress as τ /6.00 kPa. Increase the stress in five increments of τ /6.00 kPa.

Note X1.1—Sample calculation: Assume a PG 64-22 asphalt binder with G^* = 1.29 kPa at 64°C and τ. = 0.135 kPa. The starting stress will be 1.35kPa/6 = 0.225 kPa. Test at 0.225, 0.450, 0.675, 0.900, 1.13, and 1.35 kPa, starting with 0.225 kPa.

X1.10. *Plot of Complex Modulus Versus Strain*—Prepare a plot of complex shear modulus versus percent strain as shown in Figure 5. From the plot, determine the complex shear modulus at 2 and 12 percent strain.

X1.11. *Calculations*:

X1.12. Calculate the modulus ratio as the complex shear modulus at 12 percent strain divided by the complex shear modulus at 2 percent strain.

\

X1.13. *Report*:

X1.14. *Report the following*:

X1.15. Complex shear modulus (G*) to three significant figures,

X1.16. Strain, nearest 0.1 percent,

X1.17. Frequency, nearest 0.1 rad/s, and

X1.18. The ratio calculated by dividing the modulus at 12 percent strain by the modulus at 2 percent strain.

X1.19. *Data Interpretation*:

X1.20. The measurement was performed in the non-linear range of the material if the modulus ratio as calculated in Section X1.11 is < 0.900 and linear if ≥ 0.900. If the measurement does indicate the linear region to be other than 12%, the maximum strain within the linear region may be used.

X2. CONTROL CHART

X2.1. *Control Charts*:

X2.2. Control charts are commonly used by various industries, including the highway construction industry, to control the quality of products. Control charts provide a means for organizing, maintaining and interpreting test data. As such, control charts are an excellent means for organizing, maintaining, and interpreting DSR verification test data. Formal procedures based on statistical principles are used to develop control charts and the decision processes that are part of statistical quality control.

A quality control chart is simply a graphical representation of test data versus time. By plotting laboratory measured values for the reference fluid in a control chart format, it is easy to see when:

X2.2.1. The measurements are well controlled and both the device and the operator are performing properly.

X2.2.2. The measurements are becoming more variable with time, possibly indicating a problem with the test equipment or the operator.

X2.2.3. The laboratory measurements for the fluid are, on the average above or below the target (reference fluid) value.

Many excellent software programs are available for generating and maintaining control charts. Some computer-based statistical analysis packages contain procedures that can be used to generate control charts. Spreadsheets such as Microsoft's Excel can also be used to generate control charts and, of course, control charts can be generated manually. (See Table X3.1 as an example print-out).

X2.3. *Care in Selecting Data*:

X2.3.1 Data used to generate control charts should be obtained with care. The idea of randomness is important but need not become unnecessarily complicated. An example will show why a random sample is needed—a laboratory always measures the reference fluid at the start of the shift or workday. These measurements could be biased by start-up errors such as a lack of temperature stability when the device is first turned on. The random sample ensures that the measurement is representative of the process or the material being tested. Said another way, a random sample has an equal chance of being drawn as any other sample. A measurement or sample always taken at the start or end of the day, or just before coffee break, does not have this chance.

X.3 Example

X3.1. The power of the control chart is illustrated in Table X3.1 using the verification data obtained for the DSR. Other DSR verification data suitable for a quality control chart presentation includes measurements for determining the temperature correction, calibrating the electronic thermometer, and maintaining data from internally generated asphalt binder reference samples. For this example, the reported viscosity for the reference fluid is 271 Pa-s; hence, the calculated value for G^* is 2.71 kPa. This value for G^* is labeled as "G^* from Reference Fluid" in Figure X3.1. The laboratory should obtain this value on average if there is no laboratory bias.

Table X3.1—Sample Test Data

Week	Measured G^*, kPa
1	2.83
2	2.82
3	2.77
4	2.72
5	2.69
6	2.72
7	2.77
8	2.75
9	2.71
10	2.82
11	2.66
12	2.69
13	2.75
14	2.69
15	2.73
16	2.77
17	2.72
18	2.67
19	2.66
20	2.78
21	2.74
22	2.69
Average	2.73
Std. Dev.	0.051
CV %	1.86

X3.2. *Comparison of 22-Week Laboratory Average for G* with Value Calculated from Reference Fluid:*

X3.2.1. The 22-Week average of the laboratory measurements is labeled as "22-Week Laboratory Average" in Figure X3.1. Over the 22 weeks, for which measurements were made, the average was 2.73 kPa. This value compares favorably with the calculated reference value, 2.71 kPa, differing on the average by only 0.7 percent. There appears to be little laboratory bias in this data.

X3.3 *Comparison of CV of Laboratory Measurements with Round Robin CV*:

X3.3.1. From a previous round robin study, the within laboratory standard deviation (d1s) for the fluid was reported as 0.045 (CV = 1.67 percent). The 22-week standard deviation for the measured values of G^* is 0.051 CV = 1.86 percent), as compared to 0.045 (CV =1.67 percent) reported from the round robin. However, it should be pointed out that the 22-week CV, 1.86 percent, also includes day-to-day variability, a component of variability not included in the round-robin d1s value. Based on this information the variability of the laboratory measurements are acceptable.

X3.4 *Variability of Measured Values*:

X3.4.1 In Figure X3.1, the value of G^* calculated from the reference fluid is shown as a solid line. Also shown are two dotted lines that represent the G^* calculated from the reference fluid ± 2 d1s where d1s is the value from the round robin. The calculated reference value for the fluid is 2.71 kPa, and the standard deviation is 0.045. Thus, a deviation of 2 d1s gives values of:

$$2.71\text{kPa} \pm (2)\,(0.045) = 2.80\text{ kPa}, 2.62\text{ kPa} \qquad (X3.1)$$

If the laboratory procedures are under control, the equipment is properly calibrated, and there is no laboratory bias, 95 percent of the measurements should fall within the limits 2.62 kPa and 2.80 kPa. Laboratory measurements outside this range are suspect, and the cause of the outlier should be investigated. The outlier may be the result of either testing variability or laboratory bias. The measurement from Week 10 in Figure X3.1 falls outside the ±2 d1s limits and is cause for concern such that testing procedures and verification should be investigated.

If a measurement deviates from the target, in this case G^* from the reference fluid, by more than ±3 d1s, corrective action should be initiated. The ±3 d1s limits 99.7 percent of the measured values if the laboratory procedures are under control and the equipment is properly calibrated.

X3.5. *Trends in Measured Value:*

X3.5.1 The control chart can also be used to identify unwanted trends in the data. For example, from weeks one to five, a steady decrease in the measured value is observed. This is cause for concern and the reason for the trend should be investigated. More sophisticated rules for analyzing trends in control charts can be found elsewhere.

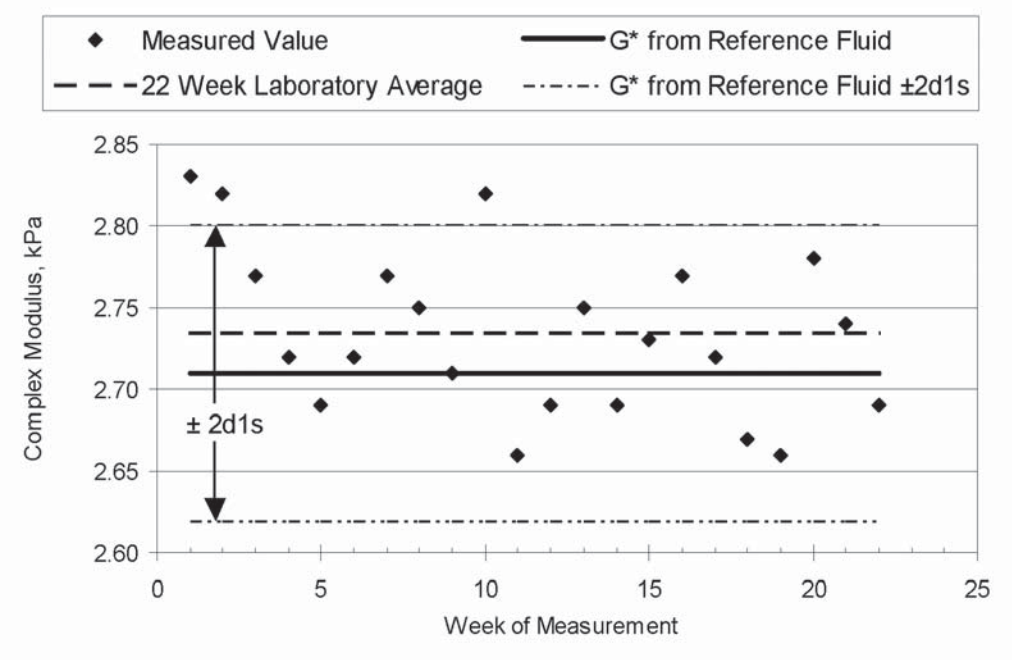

Figure X3.1—Control Chart

X4. USE OF REFERENCE FLUID

X4.1. *Source of Reference Fluid:*

X4.2. An organic polymer produced by Cannon Instrument Company as Viscosity Standard N2700000SP has been found suitable as reference fluid for verifying the calibration of the DSR. The viscosity of the fluid, as determined from NIST–traceable capillary viscosity measurements, is approximately 270 Pa-·s at 64°C. However, the viscosity of the fluid varies from one lot to the next. The lot-specific viscosity is printed on the label of the bottle.

X5. CAUTIONS IN USING REFERENCE FLUID

X5.1 Some items of caution when using the reference fluid are:

X5.1.1 The fluid cannot be used to verify the accuracy of the phase angle measurement.

X5.1.2. The fluid must not be heated as heating can degrade the fluid causing a change in its viscosity.

X5.1.3 The fluid should be used for verification only after the DSR temperature measurements are verified.

X5.1.4. The fluid cannot be used to calibrate the torque transducer. The manufacturer or other qualified service personnel using a calibration device designed specifically for the rheometer should perform the calibration. These calibration devices are typically not available in operating laboratories.

X5.1.5. When tested at 10 rad/s, the reference fluid should only be used at 64°C and above. At lower temperatures, the fluid is viscoelastic; hence, the viscosity, η, reported on the certificate by Cannon will not match the complex viscosity $\eta^* = G^*/10$ rad/s determined from the measurement.

X5.1.6. Bubbles in the fluid will have a dramatic effect on the measured value of G^*. The fluid in the bottle should be free of bubbles and care must be taken not to introduce bubbles when preparing test specimens. Recommended procedures for preparing test specimens are given in Section X6.

X6. RELATIONSHIPS BETWEEN OSCILLATION (DYNAMIC SHEAR) AND STEADY FLOW (STEADY SHEAR). CALCULATION OF G* FROM STEADY-STATE VISCOSITY MEASUREMENTS AND CALCULATION FROM G' TO N1.

X6.1. Among the different methods for converting between dynamic and steady-state viscosity of polymers, the most popular and most successful is the so-called Cox-Merz empirical rule. The rule leads, in simplified terms, to the following approximation.

$$G^*/\omega = \eta^*$$
$$\eta \sim \eta^* \quad [\text{where } \omega = \dot{\gamma}] \qquad (X6.1)$$

where:

G^* = the complex modulus in Pa,
ω = the angular frequency in radians/s, in oscillation
η^* = the complex viscosity as measured in oscillation, in Pa.s.
N_1 = Normal Force in N, generated in shear

$\dot{\gamma}$ = the angular velocity in s^{-1}
η = the shear rate independent capillary viscosity as reported by the supplier of the reference fluid (and steady shear viscosity as measured in the DSR)
G' = the storage modulus in Pa

For this rule to apply the measurements must be in the viscous region where the phase angle approaches 90 degrees. The value of the complex modulus is then simply 10 times the value of the capillary viscosity. For example, if the capillary viscosity is 270,000 mPa-s the complex modulus is:

G^*, kPa ≈ (270,000 mPa•s)(1 kPa/1,000,000 mPa) (10 rad/s) = 2.70 kPa•rad *(X6.2)*

The reference fluid behaves as a viscous fluid at 64°C and above and provides very accurate estimates of G^* above 64°C. At temperatures below 58°C the fluid gives incorrect values for G^* with the error increasing as the temperature departs from 64°C. At 64°C and above G^* divided by the frequency in radians per second should be no more than three percent different than the viscosity printed on the bottle label. If this is the case, then the torque calibration should be considered suspect.

- $N_1 = 2(G')$ [where $\omega = \dot{\gamma}$] Is the elastic relationship when testing between dynamic shear and steady shear where the angular frequency is equal to the angular velocity.

X7. METHODS FOR TRANSFERRING THE FLUID TO THE TEST PLATES

X7.1. Three different methods are recommended for transferring the fluid to the test plates:

X7.2. The glass rod method (Section X7.1), the spatula method (Section C4.3), and a direct method where a removable test plate is held in direct contact with the fluid in the bottle (Section C4.4).

X7.3. *Glass Rod Method (Figure X7.1)*:

X7.3.1 In this method, a glass rod is inserted into the fluid and rotated (Step 1) while in the fluid. Continue rotating the rod, and pull it slowly from the fluid (Step 2) carrying a small mass of the fluid with the rod. Touch the mass to the plate (Step 3) to transfer the fluid to the plate. See Figure X7.1.

Figure X5.1 (Figure not included)—Using a Glass Rod to Place the Reference Fluid on the Plate

X7.4. *Spatula Method (Figure X7.2)*:

X7.5. When carefully used a spatula may be used to transfer the fluid. Special care must be taken not to trap air as the material is scooped from the bottle, Step 1. Smear the mass on the spatula onto the plate (Step 2) and cut the mass from the spatula by drawing the spatula across the edge of the plate (Step 3). This method appears to be the most difficult to implement and is the least recommended of the three methods.

Figure X7.2 (Figure not included)—Using a Spatula to Place the Reference Fluid on the Plate

X7.6 *Direct Touch Method (Figure X7.3)*—If the rheometer is equipped with plates that may be removed and reinstalled without affecting the gap reference, remove one of the plates and touch the surface of the plate to the surface of the fluid in the bottle (Step 1). Pull the plate from the bottle, bringing a mass of the fluid along with the plate (Step 2). Invert the plate and allow the fluid to flow out into a mushroom shape (Step 3).

Figure X7.3 (Figure not included)—Direct Touch Method to Place the Reference Fluid on the Plate

Proceed immediately to Section 10.5 to trim the reference fluid specimen and form the bulge.

Proceed with testing the reference fluid specimen as described in Section 11.

X8. SELECTION OF GAP CLOSURE TO OBTAIN BULGE

X8.1. *Need for Accurate Measurement of Specimen Diameter:*

X8.2. The accuracy of the DSR measurements depends upon an accurate measurement of the diameter of the test specimen. The diameter of the test specimen is assumed equal to the diameter of the test plates. For this reason, the trimming of excess binder and the final closure of the gap to produce a slight bulge in the test specimen are critical steps in the DSR test procedure. When the gap is closed to its final dimension, the bulge must be of sufficient size to compensate for any shrinkage in the binder and consequently avoiding a concave surface as shown in Figure X8.1. The diameter of the test specimen in Figure X8.1 approaches d, rather than d', the diameter of the plate. The modulus, G^*, is calculated according to the following equation:

$$|G^*|=(2h/\pi r^4)\cdot(\tau/\Theta) \qquad (X8.1)$$

where:

G^*	=	Complex modulus
τ	=	Torque applied to test specimen
h	=	Thickness of test specimen
Θ	=	Angular rotation, radians
r	=	radius of test plate

Figure X8.1 (Figure Not Included)—Concave Surface Resulting from Insufficient Closure after Trimming

Figure X8.2 (Figure Not Included)—Proper Bulge

X8.3 According to Equation X8.1, the modulus depends upon the radius (or diameter) raised to the fourth power. Therefore, a small concavity in the outer surface of the test specimen, as shown in Figure X8.1, will have a large effect on the measured modulus because the actual specimen diameter will be less than the plate diameter. For a given amount of concavity, the effect on the measured modulus is greater for the 8-mm plate than the 25-mm plate. A more desirable result is a slight bulge as illustrated in Figure X8.2. Shear stresses are not transferred directly from the plate to the overhanging binder; therefore, the effect of a slight bulge on the measured modulus is much less than a slight concavity. It should be noted that errors in the diameter of the test specimen do not affect the measured values of the phase angle.

X9. RECOMMENDED GAP CLOSURE VALUES

X9.1 Recommended values for the gap closure required to form a bulge at the test temperature similar to the bulge illustrated in Figure X8.2 are given in Section 10.5 as 50 μm and 100 μm for the 25-mm and 8-mm plates, respectively. Although these values may be appropriate for many rheometers, they may not be appropriate for all rheometers. The applicability of these values to a specific rheometer may be determined by preparing a test specimen using the recommended closure and observing the shape of the bulge after the final closure of the gap and after the test specimen is at the test temperature. If the recommended closure values do not give an appropriate bulge, the recommended closure values should be adjusted as appropriate.

Proper and improper bulges are shown in Figures X10.1 through X10.3. A magnifying glass is useful for examining the shape of the bulge. Regardless of the closure required to produce a desirable bulge, the actual gap should be used in the calculations.

X10. FACTORS AFFECTING BULGE DEVELOPMENT

X10.1 A number of factors can affect the bulge formed at the test temperature. These include:

X10.2. The amount of closure used to create the bulge.

X10.3. The difference in temperature between the trimming temperature, the temperature at which the bulge is created, and the test temperature.

X10.4. Thermal expansion-contraction characteristics of the rheometer.

X10.5. Thermal contraction and expansion of the asphalt binder.

A concave surface is more likely to form at the intermediate temperatures, than at the upper test temperatures (8-mm plate rather than the 25-mm plate). In fact, at the higher test temperatures excessive material can be squeezed from the plates as shown in Figure X10.3. This situation should also be avoided and may require gap closures somewhat less than the recommended values.

Figure X10.1—Good Bulge Size

Figure X10.2—Concave Bulge

Figure X10.3—Oversized Bulge

X11. DETERMINATION OF TIME TO THERMAL EQUILIBRIUM

X11.1.1 *Reason for Determining Time Required to Obtain Thermal Equilibrium:*

X11.1.2 After the test specimen has been mounted in the DSR, it takes some time for the asphalt binder between the test plates to reach thermal equilibrium. Because of thermal gradients within the test plates and test specimen, it may take longer for the test specimen to come to thermal equilibrium than the time indicated by the DSR thermometer. Therefore, it is necessary to experimentally determine the time required for the test specimen to reach thermal equilibrium.

X11.1.3. The time required to obtain thermal equilibrium varies for different rheometers. Factors that affect the time required for thermal equilibrium include:

X11.1.4. Design of the rheometer and whether air or liquid is used as a heating-cooling medium; water has roughly 25 times more thermal conductivity to that of air. Air conductivity is improved by increasing the velocity of air flow.

X11.1.5. Difference between ambient temperature and the test temperature, different when testing below room temperature, and above room temperature,

X11.1.6. Difference in temperature between the trimming and test temperature, and

X11.1.7. Plate size, different for the 8-mm and 25-mm plate.

X11.2. It is not possible to specify a single time as the time required to obtain thermal equilibrium. For example, thermal equilibrium of the asphalt sample is reached much quicker with liquid-controlled rheometers than with air-cooled rheometer. This requires that the time to thermal equilibrium be established for individual rheometers, typical trimming and testing temperatures, and testing conditions.

X12. METHOD TO DETERMINE THE TIME REQUIRED TO OBTAIN THERMAL EQUILIBRIUM FOR BOTH THE DSR & THE SAMPLE

X12.1.1. The time to reach thermal equilibrium is the time required to reach a constant modulus regardless of heating to that temperature or cooling down to that temperature. Typically, this time will be greater than the time for the DSR reports on its display reading for temperature to be stable. The asphalt sample heats and cools much slower then the response of the environmental chamber. Thus, it is important to determine the precise time required for a DSR to achieve thermal equilibrium for the asphalt sample.

X12.2. As a guide, safe values which can be used with most modern are as follows. Rheometers using a total fluid immersion principle of the sample in water will require a minimum of 3 minutes from the time the chamber stabilizes within ±0.1°C. A forced gas oven will require a minimum of 60 minutes from the time the chamber stabilizes within ±0.1°C. Refer to the manufacturer for specific help to determine the required time to stabilize the

sample for accurate asphalt measurements for specific DSR model. Dry directly heated plates or oven chambers employing radiant heating or not pre-conditioned gas may take significantly longer then 60 minutes to achieve thermal equilibrium on the asphalt sample with acceptable thermal gradients.

X12.3. The following procedure can be used to determine the appropriate time required to achieve sample thermal equilibrium for a specific DSR.

X12.3.1 A reliable estimate of the time required for thermal equilibrium can be obtained by monitoring the DSR temperature and the complex modulus of a sample mounted between the test plates. Because the modulus is highly sensitive to temperature, it is an excellent indicator of thermal equilibrium. The following procedure is recommended for establishing the time to thermal equilibrium:

X12.3.2. Mount a binder sample in the DSR and trim in the usual manner. Create a bulge and bring the test chamber or fluid to the test temperature.

X12.3.3. Operate the DSR in a continuous mode at 10 rad/s using an unmodified asphalt binder sample—one that does not change modulus with repeated shearing. If testing at grade temperature use 10% strain. If testing at other then grade temperature, use the smallest strain value that gives good measurement resolution.

X12.3.4. Perform a series of temperature steps, each held for at least 2000 seconds, while recording the modulus at 30 s time intervals. These steps should approach the nominal temperature from heating and cooling in order to identify any thermal hysteresis within the sample. Results should be displayed on a plot of the modulus versus time (Figure X12.1). As the example in Figure X12.1, the temperature profile was 70°C, 76°C, 70°C, 64°C, 70°C, 76°C, 70°C. Results as shown in Figure X12.1. can be graphed as an overlay of G* to permit the comparison of the 70°C results of modulus as shown in (Figure X12.2). Where the G* data for 70°C overlay defines the instrument's time to reach thermal equilibrium. In this example, the time to thermal equilibrium is reported as 0.6k seconds (600 seconds).

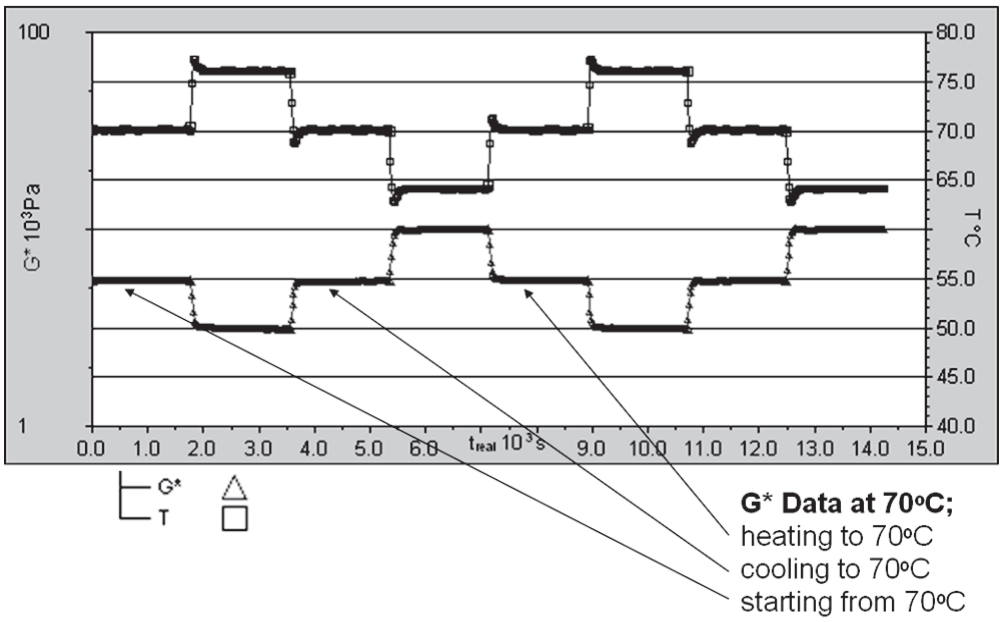

Figure X12.1—Results of the test to determine a DSR's temperature performance

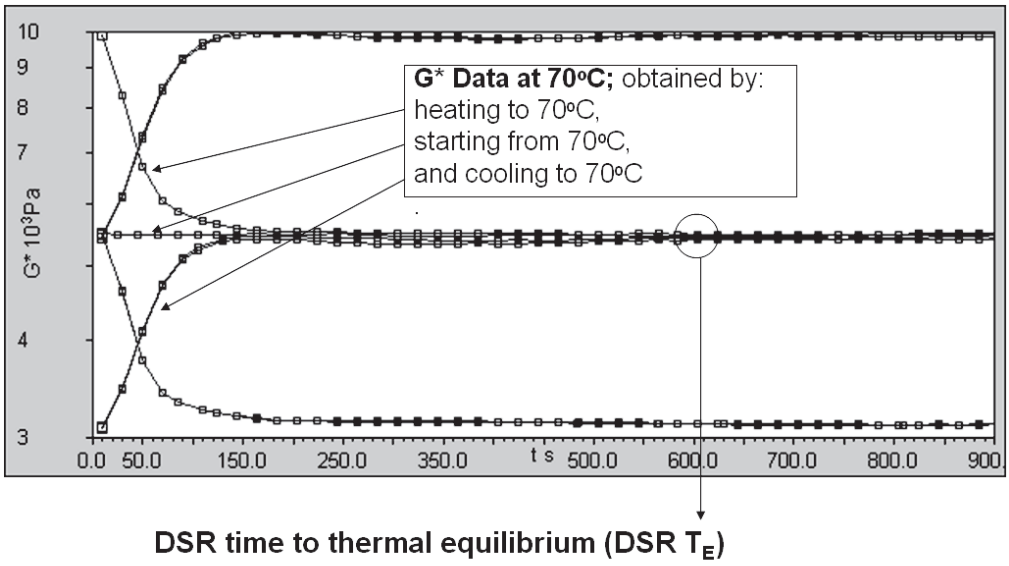

Figure X12.2—Comparison of Modulus at 70C; Thermal equilibrium reached where the center G* values agree (at about 500sec in this example)

X12.3.5. By approaching the nominal temperature from both heating and cooling, enables the identification of actual Thermal Equilibrium from the effects of apparent thermal hysterisis. Thermal hysteresis is the effect of the inefficient thermal conductivity of the environmental chamber in which the sample core or sample edge contains greater then the required ±0.1°C thermal gradient over the time permitted to achieve thermal equilibrium The appearance of thermal equilibrium may be mistaken for the slow response of the asphalt to change temperature as asphalt is a poor thermal conductor. This effect is obvious in **Figure X12.3.** Given longer time to achieve thermal equilibrium the amount of thermal hysteresis should reduce.

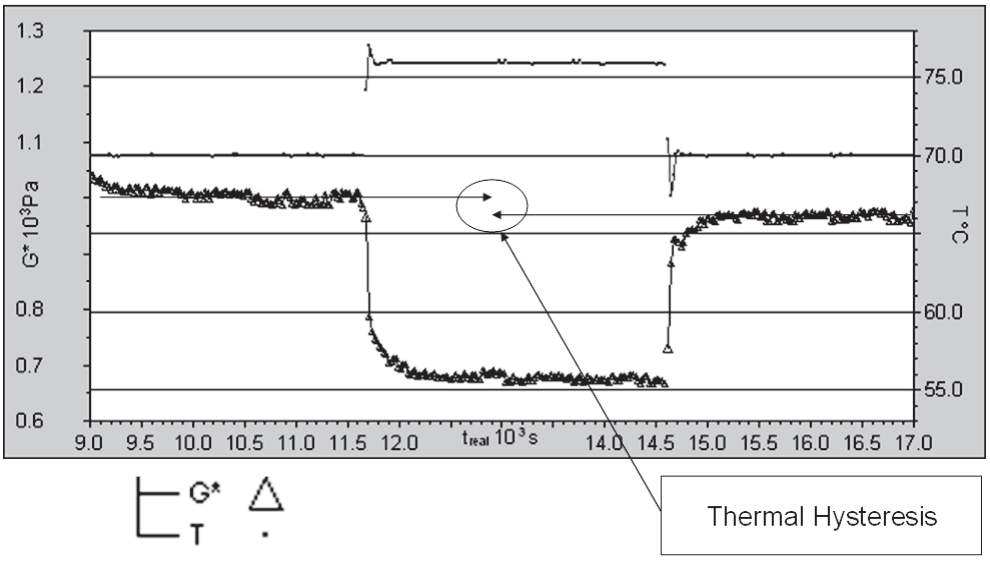

Figure X12.3—Identifying Thermal Hysteresis; G* does not recover post.

X12.3.6. Once the DSR's time to thermal equilibrium has been identified, a small buffer time of 2 minutes should be added as a conditioning period to the testing programmed time for equilibrium. From the example of **Figure X12.3**., where the DSR's time to thermal equilibrium is 600 seconds (DSR T_E), and the additional conditioning buffer of 120 seconds gives the total time to use for testing as 720 seconds. Testing thermal equilibrium (Sample T_E would be 720 seconds (12min), as shown in (**Figure X12.4**.).

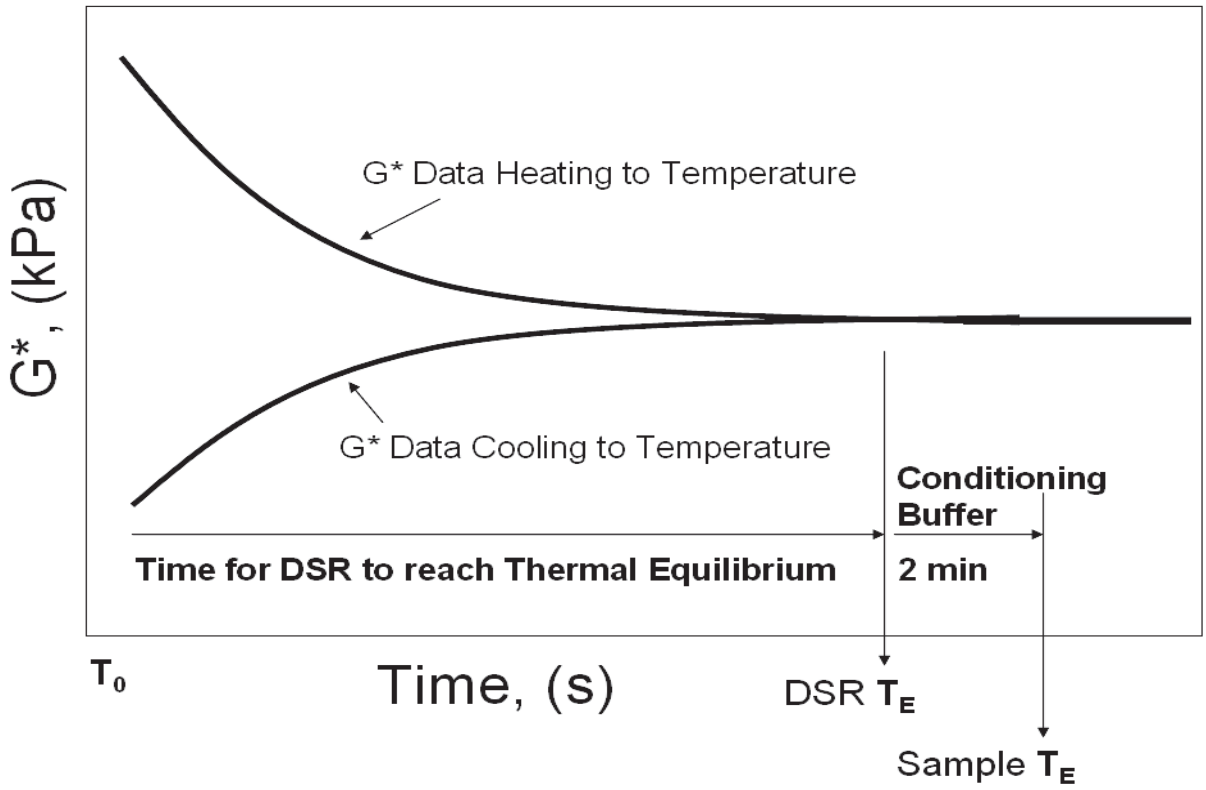

Figure X12.4—Identifying the Sample time for Thermal Equilibrium

X12.4. Because the time required to reach thermal equilibrium can vary with the test temperature and testing conditions, the time to thermal equilibrium should be established separately for any new testing protocol. Once the time to thermal equilibrium has been established, it does not have to be repeated unless the test conditions change.

X13. EXAMPLE OF FREQUENCY SWEEP ISOTHERMS

X13.1 Graph of G* and phase angle for each of the individual frequency sweeps at each temperature on a single graph (Figure X13.1)

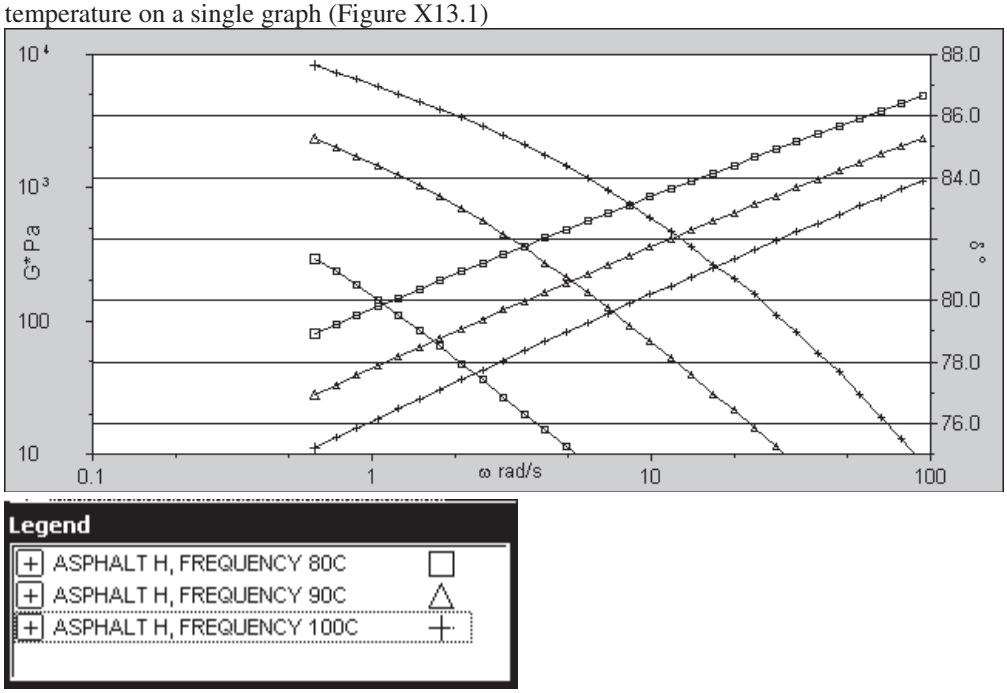

Figure X13.1-Graph of frequency sweeps for each temperature.

X14. EXAMPLE OF MASTER CURVE AT 80°C AND DETERMINATION OF FREQUENCY WHERE THE PHASE ANGLE IS EQUAL TO 86 DEGREES.

X14.1. Display of Isotherms (Figure X14.1) The example in Figure X14.1 shows 4 sets of isotherms for an asphalt binder.

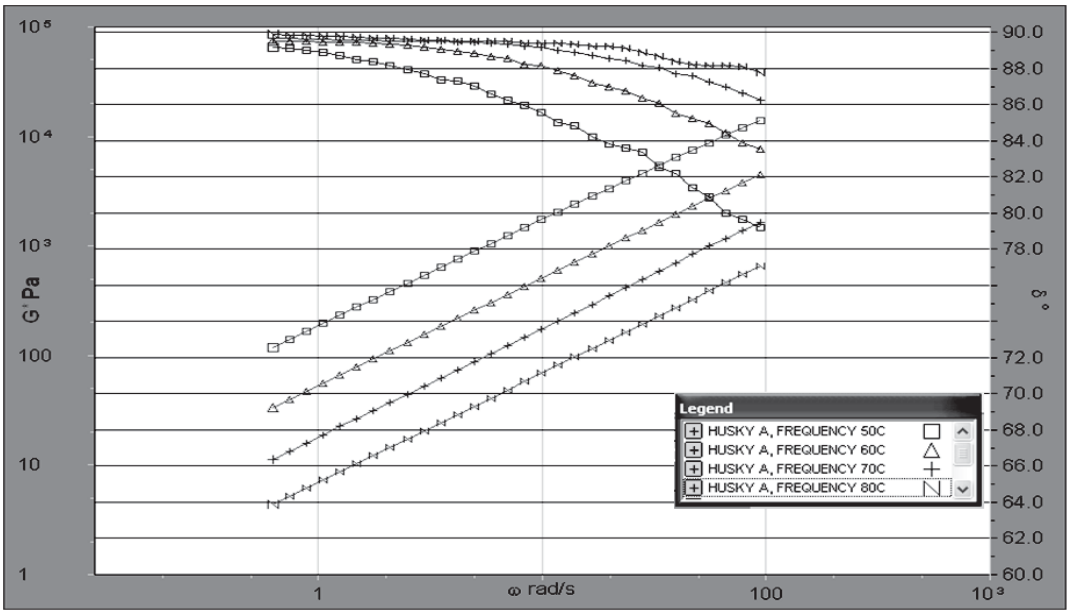

Figure X14.1- Graph of Isotherms.

X14.2. Performing the Time Temperature Superposition model to the data using a reference temperature of 80°C would produce the master curve shown in Figure X14.2.

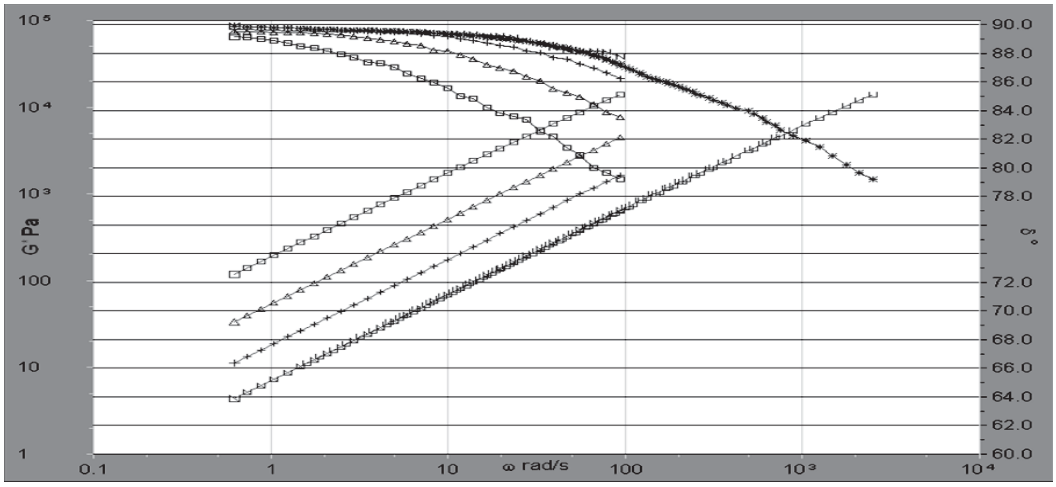

Figure X14.2.- Master Curve created to an 80°C reference from isotherms.

X14.3. From the master curve, identify the phase angle of 86 degrees and determine the frequency at which it occurs (Figure X14.3). Most modern DSRs provide features within their software in which enables the operator the ability to identify specific points from the graph or table. In the event the exact value is not provided, interpolate between the two nearest points bracketing the 86 degree value. The exactness required for the reporting of frequency in this process is ±10%. Small errors in reporting have little to no effect on the final determination of both mixing & compaction temperature.

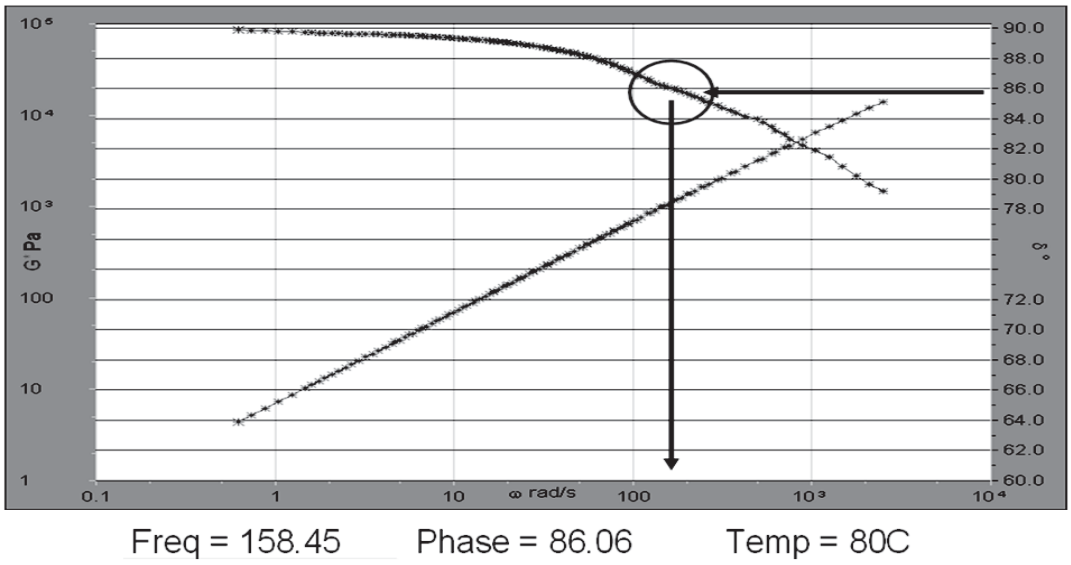

Figure X14.3- Determination of Frequency at a phase angle of 86 degrees from the master curve

---

X15. VERIFICATION OF MASTER CURVE WORKING DATA BY USING BLACK SPACE DIAGRAM

X15.1 A good example of a Black Space diagram where there is shown a continuous curve exhibited in the results (Figure X15.1). This is where there are not obvious discontinuities.

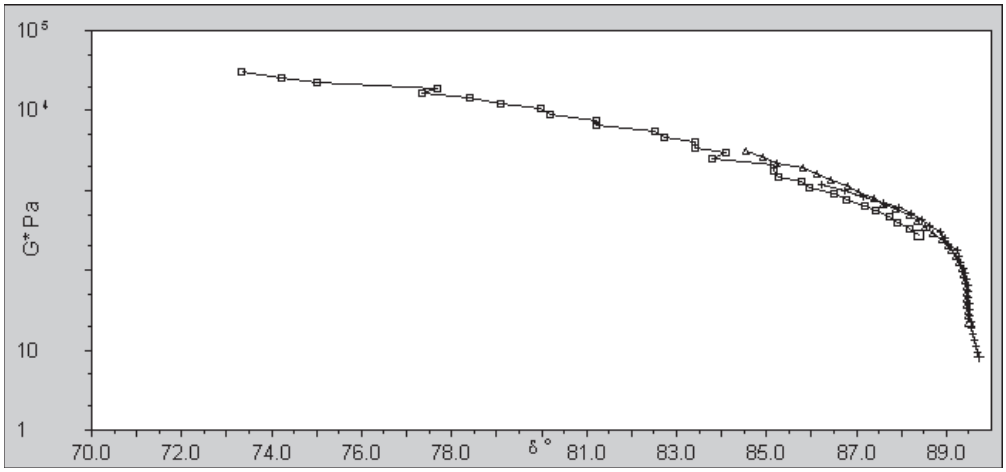

FIGURE X15.1- Good example of Black Space diagram

X15.2. A poor example of a Black Space diagram, where there are obvious discontinuities in the results (Figure X15.2). In the case of a poor Black Space, the data should be retested with particular attention to ensuring all the data are collected in the linear visco-elastic region by ensuring the correct strains are applied properly to all frequencies and that the temperatures are correct for each frequency tested. (Figure X15.2)

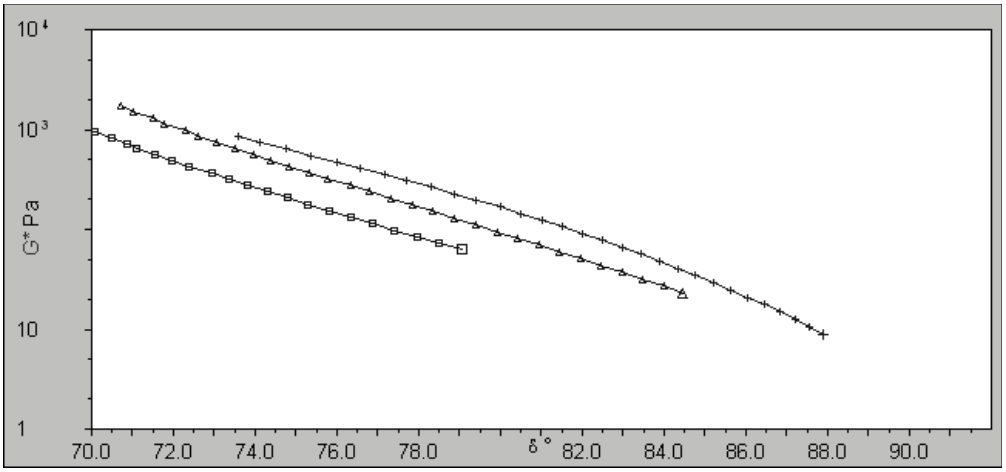

FIGURE X15.2- Poor example of Black Space diagram

X16. DETERMINATION OF LABORATORY MIXING TEMPERATURE

X16.1. Use the following equation to determine laboratory compaction temperature in *ºF*.

$$Mixing\ Temperature\ (ºF) = 325\omega^{-0.0135} \qquad (X16)$$

Where ω = *the frequency in rad/s for the phase angle of 86 degrees as reported from the master curve. 12.2.4*

X17. DETERMINATION OF LABORATORY COMPACTION TEMPERATURE

X17.1. Use the following equation to determine laboratory compaction temperature in *ºF*.

$$Compaction\ Temperature\ (ºF) = 300\omega^{-0.012} \qquad (X17)$$

Where ω = *the frequency in rad/s for the phase angle of 86 degrees as reported from the master curve. 12.2.4*

X18. SAMPLE REPORT

Header Information:

Item	Data Group 1	Item	Data Group 2
Operator's Name:	24 Alpha-Numeric	Date of Test (dd/mm/yy):	__/__/__
Test Specimen ID No.:	18 Alpha	Time of Test (hr:min):	__:__
Project ID No.:	12 Alpha-Numeric	DSR Manufacturer:	12 Alpha-Numeric
File Name:	12 Alpha-Numeric	DSR Model:	12 Alpha-Numeric
Sample Grade:	12 Alpha-Numeric	DSR Serial Number Or Other Identifying ID No.:	18 Alpha-Numeric
Frequency, rad/s for Phase Angle of 86 degrees at a temperature of 80°C	0.000	Software Version:	12 Alpha-Numeric
Mix Temperature, °F	000		
Compaction Temperature, F	000		

X19. REFERENCES

X19.1. Anderson, D. A. and M. Marasteanu. "*Manual of Practice for Testing Asphalt Binders in Accordance with the Superpave PG Grading System.*" The Pennsylvania Transportation Institute, The Pennsylvania State University, PTI 2K07, November 1999 (Revised February 2002).

X19.2. Wadsworth, H., ed. *Handbook of Statistical Methods for Engineers and Scientists.* McGraw-Hill, New York, NY, 1990.

X19.3. Anderson, D. A., C. E. Antle, K. Knechtel, and Y. Liu. *Interlaboratory Test Program to Determine the Inter- and Intra-Laboratory Variability of the SHRP Asphalt Binder Tests*. FHWA, 1997.

X19.4. Cox, W. P. and E. H. Merz. Correlation of Dynamic and Steady Flow Viscosities, *Journal of Polymer Science*, Volume 28, 1958, pp. 619–622.

X19.5. West, R. Procedure for Determining Mixing and Compaction Temperatures of Asphalt Binders in Hot Mix Asphalt, *NCHRP Report XXX*, 2008.

APPENDIX D

Statistical Analyses of the Steady Shear Flow and Phase Angle Methods

Results from Regression Analyses

This section describes a statistical analysis to determine if either the Steady Shear Flow method or the Phase Angle method provides a better fit to experimental data from the mixture tests and the producers' recommendations for mixing temperature.

Given below are the Minitab outputs for regressions between the bucket mixing temperature (BuckMixT) and the Steady Shear Flow Mixing Temperature (SSFMT), and between bucket mixing temperature (BuckMixT) and the Phase Angle Mixing Temperature (PAMT).

Regression Analysis: BuckMixT versus SSFMT

```
The regression equation is
BuckMixT = 37 + 0.893 SSFMT                                    (1)

12 cases used, 1 cases contain missing values

Predictor    Coef   SE Coef     T      P
Constant     36.9    105.1   0.35   0.733
SSFMT      0.8928   0.3399   2.63   0.025


S = 22.1202   R-Sq = 40.8%   R-Sq(adj) = 34.9%

Analysis of Variance

Source          DF    SS      MS     F      P
Regression       1  3375.9  3375.9  6.90  0.025
Residual Error  10  4893.0   489.3
Total           11  8268.9
```

Regression Analysis: BuckMixT versus PAMT

```
The regression equation is
BuckMixT = 58 + 0.797 PAMT
     (2)

12 cases used, 1 cases contain missing values

Predictor    Coef   SE Coef      T      P
Constant     58.5    149.8    0.39  0.705
PAMT       0.7970   0.4697    1.70  0.121

S = 25.3382   R-Sq = 22.4%   R-Sq(adj) = 14.6%

Analysis of Variance

Source          DF      SS      MS     F      P
Regression       1  1848.7  1848.7  2.88  0.121
Residual Error  10  6420.2   642.0
Total           11  8268.9
```

In order to ascertain that the two regressors, SSFMT and PAMT, explain the same amount of variation in Buck-Mix Temperature, we first note that Neter's test for equality of two fatigue curves is not applicable because Neter's test requires that the two curves describe mixes from two different mixtures. Clearly, the two models: BuckMixT = 37 + 0.893SSFMT, and BuckMixT = 58 + 0.797PAMT, have the same response variable, namely Buck-Mix-Temperature, and hence are not from two different mixtures.

However, it is widely known in statistical literature that the ratio

$$\frac{\chi^2_{\nu_1}/\nu_1}{\chi^2_{\nu_2}/\nu_2},$$

has the Fisher's F sampling distribution, where $\nu_1 = n_1 - 1$ is the *df* of the chi-square in the numerator and $\nu_2 = n_2 - 1$ is the *df* of the chi-square in the denominator, but the two chi-squared random variables must be stochastically independent. Form ANOVA theory, it is well known that $(SS_{Error}/\sigma^2_{\epsilon})/\nu_2$ has a

chi-square sampling distribution with error degrees of freedom equaling ν_2. The σ_ϵ^2 represents the process error variance. That is, for model (1), which describes Buck-Mix Temperature versus SSFMT,

$\frac{\mathbf{SS(Residual\ Error)_{SSFMT}} / \sigma_\epsilon^2}{\mathbf{10}}$ has the χ_{10}^2 sampling distribution, and similarly for model (2) we have another χ_{10}^2, but unfortunately the two chi-squared are not independent because the responses, Buck-Mix-Temperature, are the same for both models. The following test is at the very best an approximation, because it violates the independence assumption, and does not possess as much statistical power as the case when the two chi-squared random variables are independent. To this end, the ratio

$$\frac{\mathbf{SS(Residual\ Error)_{PAMT}} / (\mathbf{10}\sigma_\epsilon^2)}{\mathbf{SS(Residual\ Error)_{SSFMT}} / (\mathbf{10}\sigma_\epsilon^2)}$$

has very roughly an F-distribution with 10 degrees of freedom for the numerator and 10 for the denominator. That is to say,

$$F_{10,10} \cong \frac{\mathbf{SS(Residual\ Error)_{PAMT}} / (\mathbf{10}\sigma_\epsilon^2)}{\mathbf{SS(Residual\ Error)_{SSFMT}} / (\mathbf{10}\sigma_\epsilon^2)} =$$

$$\frac{\mathbf{MS(Residual\ Error)_{PAMT}}}{\mathbf{MS(Residual\ Error)_{SSFMT}}}$$

$F_{10,10} \cong$ 642.0/489.3 = 1.3121 (*P-value* $\cong$ 2*0.337883 $\cong$0.676; the multiplier 2 is needed because the hypothesis H_0: $\sigma^2_{PAMT} = \sigma^2_{SSFMT}$ is 2-sided.) Because, the $F_{0.30,10,10}$ =1.406, we may draw a tenuous conclusion that there is not sufficient statistical evidence that SSFMT explains more variability in Buck-Mix-Temp that does PAMT, even if the model R-Sq for SSFMT is 40.8%, while R-Sq for PAMT is only 22.4%. Note that even if we set the type I error rate as high as 60% for the above 2-sided test of equality of two residual variances, we still cannot reject H_0: $\sigma^2_{PAMT} = \sigma^2_{SSFMT}$. Further, the following correlation matrix

from Minitab clearly shows that the two regressor variables SSFMT and PAMT are highly correlated (r = 0.810 with a *P-value* = 0.001.)

Correlations: SSFMT, PAMT, BuckMixT

	SSFMT	PAMT
PAMT	0.810	
	0.001	
BuckMixT	0.639	0.473
	0.025	0.121

Cell Contents: Pearson correlation
P-Value

In conclusion, it should be noted that perhaps the two regressors, SSFMT and PAMT**,** explain different amount of variation in Buck-Mix-Temp from a practical standpoint, but due to the small sample sizes (12 to 13) the practical differences cannot be detected from statistical standpoint.

We now perform the same analyses for Pugmill Mixing Temperature (PugMixT). The Minitab regression outputs are given below.

Regression Analysis: PugMixT versus SSFMT

```
The regression equation is
PugMixT = 28 + 0.943 SSFMT
      (3)

12 cases used, 1 cases contain missing values

Predictor    Coef  SE Coef     T      P
Constant     28.4    128.0  0.22  0.829
SSFMT      0.9426   0.4096  2.30  0.044

S = 27.3356   R-Sq = 34.6%   R-Sq(adj) = 28.1%

Analysis of Variance

Source          DF       SS      MS     F      P
Regression       1   3958.6  3958.6  5.30  0.044
Residual Error  10   7472.3   747.2
Total           11  11430.9

Unusual Observations

Obs  SSFMT  PugMixT     Fit  SE Fit  Residual  St Resid
  3    289   250.00  300.81   12.26    -50.81     -2.08R

R denotes an observation with a large standardized residual.
```

Regression Analysis: PugMixT versus PAMT

```
The regression equation is
PugMixT = - 86 + 1.27 PAMT
      (4)

12 cases used, 1 cases contain missing values

Predictor    Coef  SE Coef      T      P
Constant    -86.2    152.2  -0.57  0.584
PAMT       1.2745   0.4743   2.69  0.023

S = 25.7628   R-Sq = 41.9%   R-Sq(adj) = 36.1%

Analysis of Variance

Source          DF       SS      MS     F      P
Regression       1    4793.7  4793.7  7.22  0.023
Residual Error  10    6637.2   663.7
Total           11   11430.9

Unusual Observations

Obs  PAMT  PugMixT     Fit  SE Fit  Residual   St Resid
  3   305   250.00  302.55   10.48    -52.55     -2.23R

R denotes an observation with a large standardized residual.
```

$F_{10,10} \cong$ 663.7/747.2= 0.888; $F_{0.60,10,10}$ = 0.848, showing that the F_0-statistic = 0.888 is not significant at the 80% level. The *P-value* $\cong$ 2*0.4275 = 0.855, and 0.4275 = Pr($F_{10,10} \leq$ 0.888).

Correlations: SSFMT, PAMT, PugMixT

```
           SSFMT     PAMT
PAMT       0.810
           0.001

PugMixT    0.588    0.648
           0.044    0.023

Cell Contents: Pearson correlation
               P-Value
```

It should be noted that because of positive correlations amongst SSFMT, PAMT, and PugMixT, the $MS_{RESIDUALS}$ from models (3) and (4), in all likelihood, would

tend to be closer to each other than the required case of independence if the two variables SSFMT and PAMT were independent. Hence, the F-test at best is very conservative (larger *P-value*) than if an exact test could be performed.

The Minitab output for Equivalent Workability Temperature (EWT) is given below.

Regression Analysis: EWT versus SSFmid

```
The regression equation is
EWT = - 27 + 1.13 SSFmid

Predictor    Coef   SE Coef      T      P
Constant    -27.3    152.4    -0.18  0.861
SSFmid     1.1276   0.5119     2.20  0.050

S = 34.0257   R-Sq = 30.6%   R-Sq(adj) = 24.3%

Analysis of Variance

Source          DF     SS    MS     F      P
Regression       1    5617  5617  4.85  0.050
Residual Error  11   12735  1158
Total           12   18352
```

Regression Analysis: EWT versus PAMid

```
The regression equation is
EWT = - 241 + 1.78 PAMid

Predictor     Coef   SE Coef      T     P
Constant   -241.3     186.0   -1.30  0.221
PAMid      1.7849    0.6041    2.95  0.013

S = 30.4978   R-Sq = 44.3%   R-Sq(adj) = 39.2%

Analysis of Variance

Source          DF       SS      MS      F      P
Regression       1     8121.0  8121.0  8.73  0.013
Residual Error  11    10231.3   930.1
Total           12    18352.3
```

Correlations: SSFmid, PAMid, EWT

```
         SSFmid   PAMid
PAMid     0.830
          0.000

EWT       0.553   0.665
          0.050   0.013

Cell Contents: Pearson correlation
               P-Value
```

$F_{11,11} \cong$ 930.1/1157.73 = 0.803; $F_{0.65,11,11}$ = 0.788, showing that the F_0-statistic = 0.803 is not significant at the 70% level. The *P-value* $\cong$ 2*0.361 = 0.723, and 0.361= Pr($F_{11,11} \leq$ 0.803).

The Minitab output for Compaction Temperature is given below.

Regression Analysis: CompT versus SSFCompT

```
The regression equation is
CompT = - 96.6 + 1.37 SSFCompT

11 cases used, 2 cases contain missing values

Predictor    Coef   SE Coef      T      P
Constant   -96.62    89.06    -1.08  0.306
SSFCompT   1.3745   0.3116     4.41  0.002

S = 18.7292   R-Sq = 68.4%   R-Sq(adj) = 64.9%

Analysis of Variance

Source          DF      SS      MS      F      P
Regression       1   6823.5   6823.5  19.45  0.002
Residual Error   9   3157.0    350.8
Total           10   9980.5
Unusual Observations

Obs  SSFCompT   CompT     Fit   SE Fit   Residual  St Resid
  1       295  272.00   308.86    6.42    -36.86     -2.10R
 11       275  317.00   281.37    6.48     35.63      2.03R

R denotes an observation with a large standardized residual.
```

Regression Analysis: CompT versus PACompT

```
The regression equation is
CompT = - 320 + 2.07 PACompT

11 cases used, 2 cases contain missing values

Predictor    Coef  SE Coef      T      P
Constant   -320.3    119.1  -2.69  0.025
PACompT    2.0724   0.4007   5.17  0.001

S = 16.7084   R-Sq = 74.8%   R-Sq(adj) = 72.0%

Analysis of Variance

Source          DF      SS      MS      F      P
Regression       1   7468.0  7468.0  26.75  0.001
Residual Error   9   2512.5   279.2
Total           10   9980.5
```

Correlations: SSFCompT, PACompT, CompT

```
            SSFCompT   PACompT
PACompT       0.850
              0.000

CompT         0.827     0.865
              0.002     0.001

Cell Contents: Pearson correlation
               P-Value
```

$F_{9,9} \cong$ 270.2 /350.8= 0.7702; $F_{0.65,9,9}$ = 0.7676, showing that the F_0-statistic = 0.7702 is not significant at the 70% level. The *P-value* $\cong$ 2*0.3518 = 0.7036, and 0.3518= Pr($F_{9,9} \leq$ 0.7702).

The Minitab output for the Producers' Recommended Mixing Temperature is given below.

Regression Analysis: Prod.Midpoint versus SSFMT

```
The regression equation is
Prod.Midpoint = 136 + 0.572 SSFMT

Predictor    Coef   SE Coef     T      P
Constant   136.00    35.07    3.88  0.003
SSFMT      0.5724   0.1128    5.08  0.000

S = 7.79965   R-Sq = 70.1%   R-Sq(adj) = 67.4%

Analysis of Variance

Source          DF      SS      MS      F      P
Regression       1   1567.6   1567.6  25.77  0.000
Residual Error  11    669.2     60.8
Total           12   2236.8
```

Regression Analysis: Prod.Midpoint versus PAMixT1

```
The regression equation is
Prod.Midpoint = 116 + 0.627 PAMixT1

12 cases used, 1 cases contain missing values

Predictor    Coef  SE Coef     T      P
Constant   115.73    53.56  2.16  0.056
PAMixT1    0.6269   0.1681  3.73  0.004

S = 8.81614   R-Sq = 58.2%   R-Sq(adj) = 54.0%

Analysis of Variance

Source          DF      SS      MS      F      P
Regression       1  1081.0  1081.0  13.91  0.004
Residual Error  10   777.2    77.7
Total           11  1858.2
```

Correlations: SSFMT, PAMixT1, Prod.Midpoint

```
                      SSFMT        PAMixT1
PAMixT1               0.954
                      0.000

Prod.Midpoint         0.837          0.763
                      0.000          0.004

Cell Contents: Pearson correlation
               P-Value
```

$F_{10,11} \cong$ 77.7/60.8 = 1.278; $F_{0.70,9,9}$ = 1.3846, showing that the F_0-statistic = 1.278 is not significant at the 60% level. The *P-value* $\cong$ 2*0.3454 = 0.6907, and 0.3454= Pr($F_{10,11} \geq$1.278).

In summary, none of the above tests for equality of two residual variances were significant even at the 50% level (the minimum 2-sided *P-value* =0.676). Because all the tests were very conservative (due to positive correlation), even if we do not multiply the Pr. Level of the 2-sided tests by 2, the smallest P-value would be 0.338, which is not significant at an $\alpha = 0.25$.

Abbreviations and acronyms used without definitions in TRB publications:

AAAE	American Association of Airport Executives
AASHO	American Association of State Highway Officials
AASHTO	American Association of State Highway and Transportation Officials
ACI–NA	Airports Council International–North America
ACRP	Airport Cooperative Research Program
ADA	Americans with Disabilities Act
APTA	American Public Transportation Association
ASCE	American Society of Civil Engineers
ASME	American Society of Mechanical Engineers
ASTM	American Society for Testing and Materials
ATA	Air Transport Association
ATA	American Trucking Associations
CTAA	Community Transportation Association of America
CTBSSP	Commercial Truck and Bus Safety Synthesis Program
DHS	Department of Homeland Security
DOE	Department of Energy
EPA	Environmental Protection Agency
FAA	Federal Aviation Administration
FHWA	Federal Highway Administration
FMCSA	Federal Motor Carrier Safety Administration
FRA	Federal Railroad Administration
FTA	Federal Transit Administration
HMCRP	Hazardous Materials Cooperative Research Program
IEEE	Institute of Electrical and Electronics Engineers
ISTEA	Intermodal Surface Transportation Efficiency Act of 1991
ITE	Institute of Transportation Engineers
NASA	National Aeronautics and Space Administration
NASAO	National Association of State Aviation Officials
NCFRP	National Cooperative Freight Research Program
NCHRP	National Cooperative Highway Research Program
NHTSA	National Highway Traffic Safety Administration
NTSB	National Transportation Safety Board
PHMSA	Pipeline and Hazardous Materials Safety Administration
RITA	Research and Innovative Technology Administration
SAE	Society of Automotive Engineers
SAFETEA-LU	Safe, Accountable, Flexible, Efficient Transportation Equity Act: A Legacy for Users (2005)
TCRP	Transit Cooperative Research Program
TEA-21	Transportation Equity Act for the 21st Century (1998)
TRB	Transportation Research Board
TSA	Transportation Security Administration
U.S.DOT	United States Department of Transportation